INVESTIGATING IMMUNE RESPONSES IN PERITONEAL ADIPOSE TISSUES DURING HELMINTH INFECTION AND CANCER METASTASIS

By

CHIAMAKA IJEOMA CHIDOMERE

A thesis submitted to the University of Birmingham

For the Degree of DOCTOR OF PHILOSOPHY

Institute of Immunology and Immunotherapy

College of Medical and Dental Sciences

University of Birmingham

June 2021

UNIVERSITY OF BIRMINGHAM

University of Birmingham Research Archive
e-theses repository

This unpublished thesis/dissertation is under a Creative Commons Attribution 4.0 International (CC BY 4.0) licence.

You are free to:

Share — copy and redistribute the material in any medium or format

Adapt — remix, transform, and build upon the material for any purpose, even commercially.

The licensor cannot revoke these freedoms as long as you follow the license terms.

Under the following terms:

Attribution — You must give appropriate credit, provide a link to the license, and indicate if changes were made. You may do so in any reasonable manner, but not in any way that suggests the licensor endorses you or your use.

No additional restrictions — You may not apply legal terms or technological measures that legally restrict others from doing anything the license permits.

Notices:

You do not have to comply with the license for elements of the material in the public domain or where your use is permitted by an applicable exception or limitation.

No warranties are given. The license may not give you all of the permissions necessary for your intended use. For example, other rights such as publicity, privacy, or moral rights may limit how you use the material.

Unless otherwise stated, any material in this thesis/dissertation that is cited to a third-party source is not included in the terms of this licence. Please refer to the original source(s) for licencing conditions of any quotes, images or other material cited to a third party.

ABSTRACT

Visceral adipose tissues (VATs) within the peritoneal cavity harbour tertiary lymphoid structures known as fat associated lymphoid clusters (FALCs). These are highly vascularized; contain stromal, innate and adaptive immune cells which respond to inflammation and infection. However, FALCs are also reported to be frequent sites for metastatic tumour formation. Therefore this thesis aimed to investigate the role of VAT FALCs (namely mesenteric and omental FALCs) in mediating immune responses during helminth infection and cancer metastasis. Initial characterisation of immune cell subsets within VAT FALCs showed a marked Th2 cytokine environment which was more prominent in the omentum. Using the intestinal helminths, *Heligmosomoides polygyrus* and *Schistosoma mansoni,* we found that VAT FALCs responded to localised infections by supporting ILC2 and T cell proliferation, activation and expression of Th2 cytokines. Meanwhile, in the MC38 colon cancer model, we observed rapid and preferential localisation of tumour cells to VAT FALCs which was accompanied by the recruitment of Tregs, myeloid cells and the likely translocation of IL-33 to the stromal cell cytoplasm. However, prophylactic peritoneal inflammation reduced tumour burden and prevented tumour homing to FALCs, suggesting the manipulation of these structures to induce anti-tumour responses. Similarly, metastatic omentum from patients with high grade serous ovarian cancer was significantly infiltrated by immunosuppressive cells, with effector cells skewed towards a less activated phenotype, compared to healthy omentum. Together, these findings therefore highlight the dual, but paradoxical role of VAT FALCs during helminth infection and peritoneal cancer metastasis.

DEDICATION

I dedicate this PhD thesis to my phenomenal parents, Dr Okey and Mrs Ndidi Chidomere.

You have been my pillar of support throughout my life.

I am eternally grateful for the sacrifices, endless prayers, wise counsel, and for encouraging me to always aim for the best.

You both are an inspiration to me, and I hope I continue to make you proud.

ACKNOWLEDGEMENTS

Firstly I would like to return all glory to God almighty who has been my source of comfort and sustenance all through this PhD programme.

A million thanks to my supervisor Dr Jorge Caamaño for all his unquantifiable help, patience, courage and commitment in guiding me, as well as developing trust and confidence in me over these 4 years. Additionally, I remain as grateful to Dr David Withers for his dedication as a co-supervisor, especially his valuable advice and support all through this journey.

Thirdly, a heartfelt thanks to our collaborators at AstraZeneca, Gianluca Carlesso and Alison Humbles who have also been instrumental in the success of this project. I truly appreciate every feedback, counsel and financial support provided.

I'd also like to say a special thanks to the whole of the fourth floor of the IBR, as well as the undergraduate and post-graduate students I have supervised. Their cooperation, kindness and patience have helped in moulding me; working with them has been a blessing and so enjoyable.

Massive thanks to my family and wonderful friends who have consistently believed in me and cheered me on during challenging periods to the end.

Finally, I appreciate all the technicians and IT staff within the college for their great support.

TABLE OF CONTENTS

CHAPTER 1: INTRODUCTION 13
1.1 The Immune System 14
1.1.1 Innate and Adaptive Immunity Overview 14
1.1.2 Innate Immunity and Pattern Recognition Receptors 14
1.1.3 Cells of the Innate Immune System 17
1.1.4 Cells of the Adaptive Immune System 19
1.1.5 Introducing Secondary and Tertiary Lymphoid Organs 28
1.2 Adipose Tissue and Tertiary Lymphoid Structures 29
1.2.1 Structure, Function and Types of Adipose Tissues 29
1.2.2 Fat Associated Lymphoid Clusters (FALCs) 32
1.2.3 Stromal Cells in Lymph Node and FALC Formation 35
1.2.4 Innate Lymphoid Cell (ILC) Development 40
1.2.5 ILC2 Regulation and Role in Maintaining Adipose Tissue Homeostasis. 46
1.3 Immune Responses to Helminth Infections 51
1.3.1 Helminth Infections: Introducing *Heligmosomoides polygyrus* and *Schistosoma mansoni* 51
1.3.2 ILC2s and *Heligmosomoides polygyrus* Infection 53
1.3.3 Immune Responses to *Schistosoma mansoni* 57
1.4 Peritoneal Cancer Metastasis 59
1.4.1 The Tumour Microenvironment 59
1.4.2 Understanding Peritoneal Tumour Metastasis: Colon and Ovarian Cancers 64
1.4.3 Role of IL-33 in Colon and Ovarian Cancers 67
1.4.4 Current Therapy for Treatment of Metastatic Colon and Ovarian Cancers 70
1.5 Project Aims and Objectives 73
CHAPTER 2: MATERIALS AND METHODS 74
2.1 Mice 75
2.2 Human Subjects 75
2.3 Murine Experiments 76
2.3.1 Infection of mice with *Heligmosomoides polygyrus* 76
2.3.2 Infection of mice with *Schistosoma mansoni* 76

2.3.3 Inoculation of mice with MC38 77
2.4 Enzymatic Digestion of Tissues 77
2.4.1 Isolation of cells from murine and human adipose tissue 78
2.4.2 Isolation of cells from murine small intestine 78
2.4.3 Isolation of cells from murine mesenteric lymph nodes 79
2.5 Flow Cytometry Staining 80
2.5.1 Staining of murine samples 80
2.5.2 Staining of human samples 81
2.5.3 *Ex vivo* stimulation for intracellular cytokine analysis 81
2.6 Whole-Mount and Immunofluorescence Staining of Murine and Human Adipose Tissues. 84
2.7 Statistical Analysis 86
CHAPTER 3: IMMUNE CELL CHARACTERISATION IN PERITONEAL ADIPOSE TISSUES 87
3.1 Introduction 88
3.2 Immune Cell Composition in Visceral Adipose Tissues at Homeostasis 91
3.2.1 Comparing FALC composition between visceral adipose tissues 91
3.2.2 Analysis of lymphoid and myeloid subsets within visceral adipose tissues 94
3.3 Chemokine and Cytokine Expression of Type 2 ILCs within Visceral Adipose Tissues . 103
3.3.1 ILC2 chemokine receptor expression in visceral adipose tissues differs from mLN 103
3.3.2 ILC2s in visceral adipose tissues produce IL-5 at homeostasis 107
3.3.3 *Ex vivo* stimulation of ILC2s leads to increased expression of IL-5 and IL-13 in visceral adipose tissues 111
3.4 Summary 115
3.4.1 Understanding the Composition of Visceral Adipose FALCs at Steady State 115
3.4.2 Phenotypic and Functional Characterisation of Visceral Adipose FALCS at Steady State 117
CHAPTER 4: IMMUNE RESPONSES IN PERITONEAL ADIPOSE TISSUES DURING HELMINTH INFECTION 122
4.1 Introduction 123
4.2 Investigating the Phenotype of Effector ILC2s during *Heligmosomoides polygyrus* Infection 126

4.3 *In Vivo* Responses to *Heligmosomoides polygyrus* Infection 133

4.4 Investigating the Role of IL-33 in Mediating ILC2 and CD4 T Cell Responses within Visceral Adipose Tissues following *Heligmosomoides polygyrus* infection 142

4.4.1 ILC2 responses within visceral adipose tissues of *Il33*$^{-/-}$ mice are not significantly affected following *H. poly* infection. 146

4.4.2 CD4 T cell responses within visceral adipose tissues of *Il33*$^{-/-}$ mice are not significantly affected following *H. poly* infection 153

4.5 Investigating the Role of Visceral Adipose Tissues during *Schistosoma mansoni* infection 157

4.6 Summary 176

4.6.1 Immune Responses in Peritoneal Adipose Tissues during *H. Poly* Infection 176

4.6.2 Immune Responses in Peritoneal Adipose Tissues during *S. Mansoni* Infection .. 184

CHAPTER 5: INVOLVEMENT OF FALCs IN PERITONEAL CANCER METASTASIS 189

5.1 Introduction 190

5.2 MC38 Murine Colon Cancer Model 191

5.3 Human Cancer Metastasis – Ovarian Cancer 210

5.4 Summary 229

5.4.1 The immune landscape of metastatic tumours in visceral adipose tissues 229

CHAPTER 6: DISCUSSION 239

CHAPTER 7: APPENDIX 253

7.1 The Role of Visceral Adipose Tissues during *Schistosoma Mansoni* Infection (See Chapter 4.5) 254

7.2 Peritoneal Cancer Metastasis (See Chapter 5.3) 256

REFERENCES 258

LIST OF FIGURES

Figure 1.1: Antigen presentation via major histocompatibility (MHC) molecules.....21
Figure 1.2: Differentiation of T cells 27
Figure 1.3: A diagrammatic representation of Fat Associated Lymphoid Clusters.....39
Figure 1.4: Development of innate lymphoid cells 44
Figure 1.5: ILC activation and effector function 45
Figure 1.6: ILC2s in adipose tissue metabolism.....50
Figure 1.7: ILC2-derived IL-4 supports Th2 cell differentiation during *Heligmosomoides polygyrus* infection 56
Figure 1.8: The tumour microenvironment is a complex interplay of immune and stromal cell components.....63
Figure 1.9: Anatomical location of the murine omentum and mesenteries, as well as human omentum.....71
Figure 3.1: Evaluating the differences in FALC numbers between visceral adipose tissues....92
Figure 3:2: Gating strategy to identify lymphoid immune cell subsets within visceral adipose tissue FALCs 95
Figure 3.3: Assessing lymphoid immune cell populations within visceral adipose tissue FALCs at homeostasis.....97
Figure 3.4: Gating strategy to identify myeloid immune cell subsets within visceral adipose tissue FALCs 99
Figure 3.5: Assessing myeloid immune cell populations within visceral adipose tissue FALCs at homeostasis.....101
Figure 3.6: Assessing ILC2 subsets based on CCR8 and CCR9 expression, between visceral adipose tissues and mLN at homeostasis.....104
Figure 3.7: Assessing *in vivo* IL-5 production by ILC2s in visceral adipose tissues at homeostasis.....108
Figure 3.8: Assessing cytokine production by ILC2s in visceral adipose tissues following *ex vivo* stimulation 112
Figure 4.1: Gating strategies to identify Ki67 expression within ILC2 CCR8/CCR9 subsets ...128
Figure 4.2: Proliferation within ILC2 CCR8 and CCR9 subsets in visceral adipose tissues following *H. poly* infection.....131
Figure 4.3: Gating strategy to identify activation and *in vivo* IL-4 production by ILC2s and CD4 T cells 134
Figure 4.4: Assessing *in vivo* ILC2 responses in visceral adipose tissues of B6.4get mice following *H. poly* infection.....138
Figure 4.5: Assessing *in vivo* CD4 T cell responses in visceral adipose tissue of B6.4get mice following *H. poly* infection.....140
Figure 4.6: IL-33 can be detected on FALC stromal cells using *Il33*$^{+/Citrine}$ reporter mice.....144

Figure 4.7: Gating strategies to identify ILC2s, CD4 T cells and Tregs between WT and *Il33*$^{-/-}$ mice following *H. poly* infection 147
Figure 4.8: Assessing ILC2 responses in visceral adipose tissues of *Il33*$^{-/-}$ mice following *H. poly* infection 151
Figure 4.9: Assessing CD4 T cell responses in visceral adipose tissues of *Il33*$^{-/-}$ mice following *H. poly* infection 155
Figure 4.10: *S. mansoni* worms are visible within the mesenteric vasculature at D49 post infection 158
Figure 4.11: Assessing ILC2 responses in visceral adipose tissues following *S. mansoni* infection 161
Figure 4.12: Analysis of T cell responses in visceral adipose tissues following *S. mansoni* infection 168
Figure 4.13: Assessing cytokine profile of T cells in visceral adipose tissues following *S. mansoni* infection 174
Figure 5.1: Assessing the tumour burden within mesenteric and omental FALCs following MC38 injection 194
Figure 5.2: Analysis of lymphoid subsets in visceral adipose tissues following MC38 injection 196
Figure 5.3: Analysis of myeloid subsets in visceral adipose tissues following MC38 injection 204
Figure 5.4: IL-33 is translocated to the cytoplasm of FALC stromal cells following MC38 injection 208
Figure 5.5: Analysis of lymphoid cell subsets in human metastatic omentum from high-grade serous ovarian cancer patients 212
Figure 5.6: Gating strategy to identify cytokine and PD1 expression by lymphoid cell subsets in human metastatic omentum from high-grade serous ovarian cancer patients 216
Figure 5.7: Assessing the cytokine production and PD1 expression of lymphoid cell subsets in human metastatic omentum from high-grade serous ovarian cancer patients 220
Figure 5.8: Analysis of macrophage subsets in human metastatic omentum from high-grade serous ovarian cancer patients 223
Figure 5.9: Assessing PDL1 expression by macrophage subsets in human metastatic omentum from high-grade serous ovarian cancer patients 226
Figure 7.1: Assessing CD4 T cell responses in visceral adipose tissue of mice *following S. mansoni* infection 254
Figure 7.2: Assessing IL-13 production by CD4 T cells in human metastatic omentum from high-grade serous ovarian cancer patients 256

LIST OF TABLES

Table 2.1: List of murine antibodies used for flow cytometry 82
Table 2.2: List of human antibodies used for flow cytometry 83
Table 2.3: Antibodies used during immunofluorescence staining of murine and human adipose tissues.....85

LIST OF ABBREVIATIONS

AAMs	Alternatively Activated Macrophages
APCs	Antigen Presenting Cells
AT(s)	Adipose Tissue(s)
BAT	Brown Adipose Tissue
BECs	Blood Endothelial Cells
CAFs	Cancer Associated Fibroblasts
CD3i	Internal CD3
Cercs	Cercariae
CCL	Chemokine Ligand
CCR	CC Chemokine Receptor
CLP	Common Lymphoid Progenitor
CTLs	Cytotoxic T cells
CXCL	C-X-C Chemokine Ligand
DAPI	4',6-Diamidino-2-Phenylindole Dihydrochloride
DC	Dendritic Cell
EDTA	Ethylenediaminetetraacetic Acid
FALCs	Fat Associated Lymphoid Clusters
FCS	Foetal Calf Serum
FDC	Follicular Dendritic Cell
Foxp3	Forkhead Box P3
FRC	Fibroblastic Reticular Cell
GATA3	GATA Transcription Factor Family Member 3
Gp38	Podoplanin
HGSOC	High-grade Serous Ovarian Cancer
H. poly	*Heligmosomoides polygyrus*
HFD	High-fat Diet
ICAM-1	Intercellular Adhesion Molecule 1
Ig	Immunoglobulin
IFN	Interferon
IL	Interleukin
IL- 4Rα	Interleukin 4 Receptor α
IL-7Rα	Interleukin 7 Receptor α
ILCs	Innate Lymphoid Cells
ILC1/2/3	Group 1/2/3 Innate Lymphoid Cell
iNKT	Invariant Natural Killer T cell

iNOS	Inducible Nitric Oxide
ip	Intraperitoneal
LEC	Lymphatic Endothelial Cells
Lin	Lineage
LTD_4	Leukotriene D 4
LTi	Lymphoid Tissue Inducer Cell
LTo	Lymphoid Tissue Organiser Cell
LTα1β2	Lymphotoxin Alpha 1 Beta 2
LTβR	Lymphotoxin Beta Receptor
mAb	Monoclonal Antibody
MAdCAM-1	Mucosal Vascular Addressin Cell Adhesion Molecule 1
MHC I/II	Major Histocompatibility Complex Class One/Two
(m)LN	(Mesenteric) Lymph Node
MSCs	Mesenchymal Stromal Cells
NACT	Neoadjuvant Chemotherapy
NF-κB	Nuclear factor κB
NK	Natural Killer Cells
NKT	Natural Killer T cell
N.brasiliensis	*Nippostrongylus brasiliensis*
PAMPs	Pathogen-Associated Molecular Patterns
PRRs	Pattern Recognition Receptors
RA	Retinoic Acid
RORγt	Retinoic Acid Receptor -Related Orphan Receptor Gamma T
RPMI	Roswell Park Memorial Institute
SI	Small Intestine
SLOs	Secondary Lymphoid Organs
STAT6	Signal Transducer And Activator Of Transcription 6
SVF	Stroma-Vascular Fraction
TAMs	Tumour Associated Macrophages
TANs	Tumour Associated Neutrophils
TCR	T Cell Receptor
T-bet	T Box Transcription Factor
Th1/2	T-Helper Cell Type 1/2
TILs	Tumour Infiltrating Lymphocytes
TLOs	Tertiary Lymphoid Organs
TLRs	Toll Like Receptors
TME	Tumour Microenvironment
TNF	Tumour Necrosis Factor
Tregs	Regulatory T cells
TSLP	Thymic Stromal Lymphopoietin
UCP-1	Uncoupling Protein 1
VAT(s)	Visceral Adipose Tissue(s)
VCAM-1	Vascular Cell Adhesion Molecule 1
WAT(s)	White Adipose Tissue(s)
WHO	World Health Organisation

CHAPTER 1: INTRODUCTION

1.1 The Immune System

1.1.1 Innate and Adaptive Immunity Overview

The immune system is a complex network of lymphoid cells, organs, humoral factors and cytokines with an essential function in defending the host against invasion from disease causing pathogenic organisms. The pathogenicity of the organisms as well as the integrity of the host defence dictate the success of disease (Parkin and Cohen, 2001). In addition, the ability of the immune system to distinguish ''self'' from ''non-self'' is central to mounting an effective immune response that is both specific and selective to the invading pathogen, and not the host's own tissues, which could result in autoimmunity (Chaplin, 2010).

In its broadest sense, the immune system can be divided into two categories, which are reflections of the speed and specificity of the immune response; they include the rapid but non-specific innate, and the slower-acting yet more specific adaptive immunity. The innate immune system is highly conserved with its presence known in all multicellular organisms as well as the use of receptors that are ancient in their lineage (Medzhitov and Janeway, 1997). Innate responses are therefore encoded by genes in the host's germline that recognise microbial pathogens, while adaptive responses are encoded by gene elements that undergo somatic rearrangement into antigen-binding molecules (Chaplin, 2010), an elaborate process that can only be achieved by vertebrates.

1.1.2 Innate Immunity and Pattern Recognition Receptors

Innate immune recognition of foreign molecules is mediated by a set of ancestral germline-encoded proteins expressed by both immune and non-immune cells known as Pattern Recognition Receptors (PRRs). These recognise conserved structures found on pathogens called pathogen-associated molecular patterns (PAMPs) and in certain instances, damage-

associated molecular patterns (DAMPs) which are molecules released by damaged cells (Amarante-Mendes et al., 2018). PRRs can be classified into families and include Toll-like receptors (TLRs), C-type lectin receptors (CLRs), nucleotide-binding oligomerisation domain (NOD)- Leucine Rich Repeats (LRR) – containing receptors (NLRs), the retinoic acid-inducible gene 1 (RIG-1)-like receptors (RLRs) and the absent in melanoma 2 (AIM2)-like receptors (ALRs). TLRs and CLRs can be further categorised as membrane-bound receptors, present on the cell surface or on endocytic compartments, while RLRs, NLRs and ALRs are classified as unbound intracellular receptors owing to their cytoplasmic location (Brubaker et al., 2015). Interaction between PAMPs on pathogens, with innate immune cells expressing PRRs, induces pro-inflammatory and antimicrobial responses that coordinate early host responses to help contain or eliminate the infectious agent, as well as costimulatory signals that shape and prime adaptive responses (Amarante-Mendes et al., 2018).

Following its identification in the late 1990's, TLRs emerged as one of the most studied PRRs (Mogensen, 2009). These are type I transmembrane proteins comprising of 10 members (TLR1-TLR10) in humans and 12 (TLR1-TLR9, TLR11-TLR13) in mouse, expressed by immune cells such as dendritic cells (DCs) and macrophages but also stromal cells including fibroblast and epithelial cells. Depending on the PAMP being recognised, TLRs can be further sub-divided, with TLR1/2/4/6 recognising microbial membrane components such as lipids, while TLR3/7/8/9 recognise nucleic acids derived from bacteria and viruses, as well as self-nucleic acids. More specifically, PAMPs including peptidoglycans, zymosan and lipoproteins are engaged by TLR2 along with TLR1 or TLR6, lipopolysaccharides (LPS) on the surface of gram-negative bacteria by TLR4 and bacterial flagellin by TLR5. Double-stranded- small interfering- and self-RNAs are sensed by TLR3, single-stranded RNA by TLR7, with TLR10 recognising

influenza A virus (Kawasaki and Kawai, 2014, Mogensen, 2009). The intracellular signalling and enzymatic cascade that ensues post TLR engagement requires sorting and signalling adaptors, include the utilisation of the TIR-domain-containing adaptors, such as MyD88, and TRIF, and lead to the activation of transcription factor nuclear factor κB (NF-κB), interferon regulatory factors (IRFs) and mitogen-activated protein (MAP) kinases. This eventually culminates in the induction of inflammatory cytokines, chemokines and type 1 interferons (IFNs) that defend the host against microbial infection (Kawasaki and Kawai, 2014).

CLRs recognise a range of microorganisms; Dectin-1 and Dectin-2 are well characterised CLRs expressed by DCs, monocytes, macrophages, and neutrophils. In contrast to TLRs these are type II transmembrane proteins, with Dectin-1 activated by β-glucans found in the fungal cell wall, but also the yeast cell wall extract – zymosan, which is also composed largely of β-glucan. This induces a number of cytokines shown to be dependent on activation of the caspase-recruitment domain 9- B-cell lymphoma 10 (CARD9-Bcl-10) pathways in myeloid cells (Hara et al., 2007). Meanwhile, Dectin-2 was shown to recognise fungal α-mannans and subsequently promote T-helper 17 (Th17) differentiation important in host defence against *Candida albicans* (Saijo et al., 2010).

RLRs sense cytoplasmic Double stranded viral RNA molecules while NLRs are important in sensing intracellular microbes and danger signals (Mogensen, 2009), and finally the ALRs are a recently characterised TLR responsible for both positively and negatively regulating the type 1 IFN in response to cytosolic DNA binding (Nakaya et al., 2017).

1.1.3 Cells of the Innate Immune System

The innate immune system comprises of physical barriers such as the skin or mucosal epithelium, as well as chemical and cellular defences. It serves as an immediate first-line attack against the invading pathogen and in most cases is sufficient to clear the infection. Recognition by preformed antimicrobial peptides is the initial activity the pathogen must survive; one such important component being the complement cascade that leads to opsonisation of bacteria by antibodies and subsequently the direct killing of bacteria, as well as the induction of inflammatory responses. However upon breaching such a barrier, a number of cytokines and chemokines are released as a result of tissue damage/stress, leading to the recruitment and activation of phagocytic cells as well as local inflammation that ultimately result in an ''induced'' (or activated) innate immune system (Kellie and Al-Mansour, 2017).

Very early stages of infection are characterised by the recruitment of phagocytes; polymorphonuclear leukocytes known as neutrophils can respond within minutes, followed by mononuclear macrophages that can mature from circulating monocytes. Both cells engulf organisms into membrane-bound vesicles (phagosomes) that develop into phagolysosome through the fusion of phagosomes with intracellular vesicles. Within this compartment reactive oxygen species or highly toxic proteins and enzymes such as lysozyme mediates the killing of the pathogen (Kellie and Al-Mansour, 2017, Parkin and Cohen, 2001). In addition, the expression of PRR by these innate cells – as discussed above – necessitates their activation. Similarly, DCs phagocytose foreign molecules following recognition of PAMPs, process the pathogens' proteins and display the resulting peptides on their surface in the context of major histocompatibility complex (MHC) molecules. In response to chemokines,

DCs migrate to secondary lymphoid organs (SLOs) such as lymph nodes (LN) and spleen, present these peptides on their surface in the context of peptide-MHC complexes to naive lymphocytes and, together with the interaction between costimulatory molecules on DCs (such as CD40, CD80/86) and cognate ligand/receptors on lymphocytes (CD40L, CD28 respectively), induce activation of these lymphocytes (Clark et al., 2000, Pennock et al., 2013). As such DCs are specialised antigen presenting cells (APCs) that importantly bridge innate and adaptive immune responses.

Unlike macrophages and neutrophils described above, eosinophils are granulocytic cells that do not phagocytose cells. Rather they are involved in protecting the host against parasitic infections following binding of their high (FcεRI) and low (FcεRII) affinity receptors to immunoglobulin-E (IgE) coated parasite, and subsequently release eosinophil-derived molecules onto the surface of these organisms (Nutten et al., 1997, Parkin and Cohen, 2001). They also have roles in promoting allergic reactions. In addition it is now recognised that beyond these classical functions, eosinophils are involved in a number of regulatory functions in multiple tissues (Wen and Rothenberg, 2016), one of which includes the regulation of visceral adipose tissue and maintenance of metabolic homeostasis, discussed further in chapter 1.2.

Intracellular infections such as viruses and tumour cells are targeted by cytolytic natural killer (NK) cells, either through the binding of NK immunoglobulin receptors (FcR) to antibody-coated targets cells that express pathogen or tumour derived antigens. A second mechanism of action involves NK inhibitory receptors that detect levels of MHC Class I (MHC I) on target cells. Downregulation or absence of MHC I on virus-infected or tumour target cells signal the NK cell to lyse the target cell via the release of perforins and granzymes that

lead to cell death. Normal, healthy cells however express MHC I and are thus spared from apoptosis by contributing to self-tolerance of NK cells. In addition, NK cells are capable of producing a number of cytokines such as IFN–γ and chemokines that go on to modulate the function of other innate and adaptive immune cells (Paul and Lal, 2017).

Tissue resident mast cells and basophils are important during allergic reactions. Briefly, these cells express FcR that have high affinity for IgE; as such, allergen exposure and binding to IgE leads to crosslinking of FcR that results in rapid degranulation and release of bioactive molecules (e.g histamine) as well as membrane derived factors such as prostaglandins and tumour necrosis factor-α (TNF-α) that induce local inflammatory responses (Kellie and Al-Mansour, 2017).

1.1.4 Cells of the Adaptive Immune System

The constant evolution of microbes via mutations that eventually leads to resistance against innate immune defences necessitates the continual evolution and adaptation of the immune system in order to fight back – enter the adaptive immune system, characterised by specificity, discrimination between self and non-self and the development of immunological memory. Clonal selection of lymphocytes, in particular T lymphocytes (T cells) and B lymphocytes (B cells) are also a major feature of the adaptive immune system, with targeted effector responses driven by antigen-specific receptors expressed by these cells (Parkin and Cohen, 2001).

Progenitor T cells originate in the bone marrow and migrate to the thymus to undergo development and maturation. They then emerge from the thymus as naïve T cells that recirculate through the blood, lymph and secondary lymphoid organs such as the spleen and LNs. (Wherry and Masopust, 2016). During maturation, T cells acquire the T cell receptor

(TCR), a multi-protein complex composed of either alpha/beta ($\alpha\beta$) chains (comprises ~90%-95% of subsets) or a smaller subset of gamma/delta ($\gamma\delta$) chains. In addition, the association of invariant accessory proteins including CD3$\gamma\varepsilon$, CD3δ and CD3ζ, enable signal transduction following binding of the TCR to peptide-MHC complexes. The $\alpha\beta$-TCR recognises linear peptide antigens that have been processed and presented in a complex with MHC I or MHC II molecules. $\alpha\beta$-T cells can differentiate into $CD4^+$, $CD8^+$ T cells as well as a smaller subset of CD4/CD8 double negative, NK1.1 expressing cells known as NKT cells, which instead recognise glycolipids presented by CD1d molecules. The differentiation of naïve T cells into activated effector cells requires the combined effort of the TCR/CD3 complex with peptide-MHC complex and the participation of costimulatory molecules such as CD28 on T cell and CD80/86 on the APC – without which anergy occurs, as well as the involvement of cytokines that mediate clonal expansion. In particular, CD4 T cells associate with MHC II, while CD8 T cells associate with MHC I (figure 1.1). Such activation eventually induces downstream signalling cascades involving protein kinases and G-coupled proteins, which result in lymphocyte proliferation and differentiation into lineage-specific and functionally distinct subsets. (Wherry and Masopust, 2016, Cano and Lopera, 2013).

Figure 1.1: Antigen presentation via major histocompatibility (MHC) molecules

A) During MHC II antigen presentation, antigen presenting cells (APCs) such as dendritic cells (DCs), macrophages, B lymphocytes and innate lymphoid cells (ILCs) capture exogenous antigens via endocytic vesicles. Antigens are then processed in the early endosomal compartment resulting in peptides that are loaded onto MHC II molecules. Peptide-MHC complex is expressed on the cell surface where it can be recognised by the T cell receptor (TCR) of CD4 T cells. Interaction between costimulatory molecules such as CD40L-CD40 and CD28-CD80/86 leads to CD4 T cell activation.

B) Nearly all nucleated cells (except red blood cells) can express MHC I and therefore have the potential to present endogenous peptides following infection. As such endogenous antigens derived from the cytosol of the target cell are processed within the proteasome. The resulting peptides are transported via transport associated proteins to the endoplasmic reticulum and loaded onto MHC I molecules. Peptide-MHC complex is transferred to the cell surface where it can be recognised by CD8 T cells via its T cell receptor (TCR). Binding of CD28 with CD80/86 delivers a costimulatory signal that leads to CD8 T cell activation.

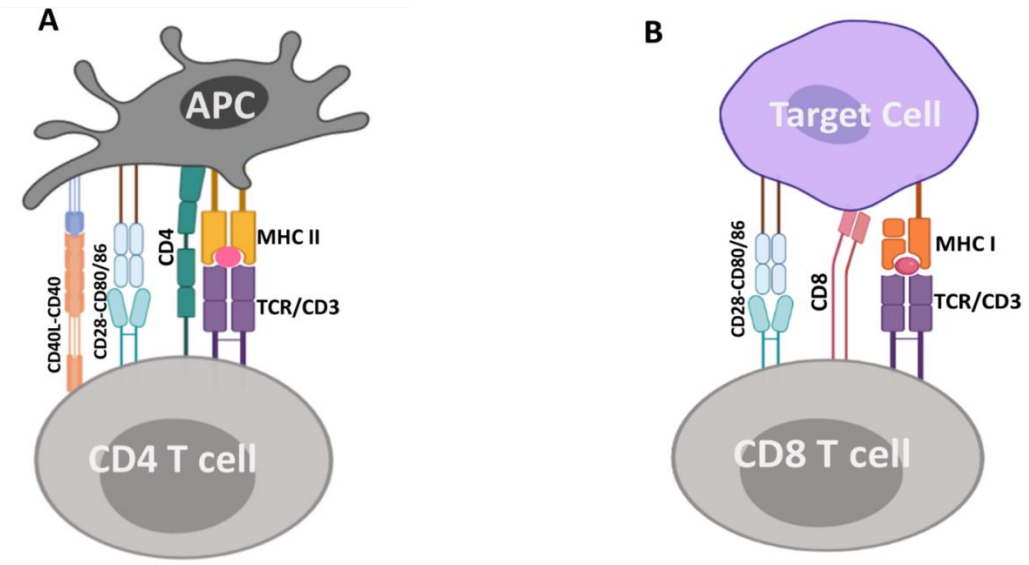

CD4 T cells can further differentiate into T helper (Th) cells that function in producing cytokines as well as stimulating B cells for antibody production. The most common and well-known subsets include Th1, Th2, Th17 and regulatory T cells (Tregs) - figure 1.2. Newer helper subsets have also been reported including Th9, Th22 and T follicular helper cells (Tfh) (Cano and Lopera, 2013); however for the purpose of this project the former four subsets will be discussed further.

Th1 differentiation is induced by interleukin (IL)-12, IL-18, or type 1 IFNs which are secreted by macrophages and DCs following activation by viruses and intracellular bacteria, as well as in conjunction with the master regulator T box transcription factor (T-bet), which not only enhances IFN-γ production but supresses Th2 and Th17 development. In response, Th1 cells produce IL-2 and IFN-γ that help in driving clonal expansion of CD8 T cells. Extracellular pathogens such as parasites and allergens drive Th2 responses, via induction cytokines such as IL-2, IL-4, IL-25 and IL-33 generated by eosinophils, mast cells and NKT cells. The transcription factor STAT6 is activated by these cytokines and in turn upregulates the expression of master regulator GATA transcription factor family member 3 (GATA3). A plethora of Th2 cytokines are released as a result and include IL-4, IL-5, IL-9, IL-10, IL-13. In addition, Th2 cells can induce class switching of immunoglobulins to IgE mediated by IL-4, lead to eosinophilia within the lungs and intestine via IL-5, and through IL-4 and IL-13 cause the production of mucus by goblet cells and drive airway hyper-responsiveness in allergic diseases. Th17 cells are activated by IL-21, IL-22, IL-23 and transforming growth factor (TGF)-β. Its master transcription factor, Retinoic acid receptor-related orphan receptor gamma T (RORγT), is induced by autocrine production of IL-21 along with TGF-β. Its effector cytokines include IL-17A, IL-17F, IL-6, IL-9, IL-21, IL-22 and TNF-α, and are associated with response to

extracellular bacterial or fungal infections. Together with TNF-α, IL-17 can also drive inflammation. (Cano and Lopera, 2013, Luckheeram et al., 2012). Finally, Tregs are important in maintaining immune homeostasis. These cells express the master regulator Forkhead Box P3 (Foxp3) and high amounts of IL-2Rα chain (also known as CD25). Natural or thymic-derived Tregs (nTregs) develop due to high avidity of self-peptide-MHC II complexes and IL-2 receptor signalling, while inducible or peripheral Tregs (iTregs) develop from naïve T cells following antigenic stimulation during tolerogenic conditions, such as high levels of TGF-β, retinoic acid (RA) and suboptimal costimulation of T cells. Immunosuppressive cytokines produced by Tregs include IL-10 and TGF-β, the latter leading to a positive feedback loop of Treg stimulation, while the expression of molecules such as CTLA-4 enable the successful suppression of DCs following interaction with CD80/CD86 binding partners (Plitas and Rudensky, 2016). As such Tregs are able to suppress inflammation by limiting CD4 or CD8 T cell and NK cell activation, prevent the development of autoimmune diseases, induce tolerance to allogenic transplants, but unfortunately, also counteract anti-tumour responses in the tumour microenvironment (TME) (Cano and Lopera, 2013).

When activated, CD8 T cells develop into cytotoxic T cells (CTLs) that mediate the destruction of cells infected by intracellular pathogens, as well as tumour cells (figure 1.2). This differentiation is enabled by the recognition of antigens in the presence of IFN-α, IFN-β and IL-12. Subsequently, cytotoxic T cells release IFN-γ and TNF-α, but also generate cytolytic granules which contain perforins and granzymes capable of lysing target cells directly. CD8 T cells similarly to Th1 cells are controlled by T-bet as well as the transcription factor Eomesodermin (Eomes) (Pennock et al., 2013).

B cells originate and mature in the bone marrow; while in this organ, they undergo splicing and recombination events involving rearrangement of variable (V), diversity (D), and joining (J) segments of the heavy chain locus mediated by recombination activating genes (RAG) 1/2, as well as V and J gene segments within the light chain locus, to produce an IgM-expressing immature B cell (LeBien and Tedder, 2008). A selection process occurs next, necessary for eliminating any B cells that are strongly self-reactive, while allowing weakly self-reactive cells to enter the periphery. Mature, but naïve B cells are attracted by chemokines such as CXCL13 in a CXCR5-dependent manner to SLOs, primarily the LNs and spleen. They can then encounter either small soluble antigens presented by APCs or large intact antigens, to generate short-lived immune responses, or form germinal centres where affinity maturation and development of memory B cells occur (Merlo and Mandik-Nayak, 2013). As well as serving as antigen receptors, immunoglobulins can be secreted into the extracellular space by plasma cells to bind and neutralise pathogens. Five classes or isotypes of antibodies exist; IgM is usually the first antibody secreted, and its initial production leads to activation of the complement cascade. Class switch recombination and somatic hypermutation leads to production of IgG (involved in opsonisation, and antibody-dependent-cell-mediated cytotoxicity), IgA (which protects mucosal surfaces), and IgE (involved in responses against parasitic infections, but also in mediating allergic reactions); while IgD is expressed on transitional B cells via alternative splicing of mRNA (Merlo and Mandik-Nayak, 2013). In addition to mediating the humoral immune response through their production of antibodies, B cells can regulate cellular immune responses. They function as APCs that interact with both CD4 and CD8 T cells via B cell expression of respective MHC II and MHC I, as well as their expression of costimulatory molecules such as CD40 (Hoffman et

al., 2016). Furthermore, a subset known as Bregs have been reported to modulate immune response via their secretion of IL-10 (Yanaba et al., 2008), while other B cells acquire the capacity to produce inflammatory cytokines including IFN-γ, TNF-α and IL-17, that can subsequently impact the phenotype of CD4 T cells. Lastly, B cells are also needed for the proper development of the secondary lymphoid architecture, as well as in the formation of ectopic (or tertiary) lymphoid structures during chronic inflammation (Hoffman et al., 2016). One of the defining features of adaptive immunity is its ability to generate 'memory', thereby enabling a quicker and more robust response following a secondary challenge. Distinct classes of antigen specific memory B cells exist; while IgM memory B cells enter the germinal centre reaction, IgG memory B cells differentiate into plasma cells. During B-T cell interactions within SLOs, some proliferating B cells are destined to become germinal centre-dependent and germinal centre-independent memory B cells, both of which can occur during T cell-dependent responses. In addition, T cell-independent memory B cells (B1) can also be generated (Kurosaki et al., 2015); these B1 cells are observed abundantly in the peritoneal cavity, and upon activation can migrate to the spleen where they rapidly secret IgM into the circulation to mediate protection from infection (Ha et al., 2006). Similarly, a pool of memory T cells persists once the primary response is over, which compared to their naïve counterparts can access both SLOs and peripheral tissues thereby enabling a quicker response. In their broadest sense, two subtypes for both CD4 and CD8 T cells exist: central- and effector-memory T cells. While the former are more proliferative post antigen encounter, the latter are characterised by rapid effector responses e.g. IFN-γ and granzyme production, but are less proliferative (Pennock et al., 2013). With subsets of memory B and T cells able to last for decades, being highly sensitive to antigenic stimulation, and in the case

of T cell memory, having a low dependence on costimulatory molecules, these cells are therefore vital players to the adaptive arm of the immune system.

Figure 1.2: Differentiation of T cells

Following pathogen invasion, antigen presenting cells (APCs) such as dendritic cells (DCs) sense pathogen associated molecular patterns (PAMPs) expressed by a range of microbes, process, and present pathogen-derived antigens on their cell surface in the context of MHC complexes. T cells via their TCR recognise peptide-MHC complex (see figure 1.1.) and along with the resulting cytokine milieu and participation of costimulatory molecules differentiate into effector T cell subsets. These subsequently release specific cytokines, to promote pathogen-specific clearance, but also amplify the immune response by feeding back into the cytokine milieu.

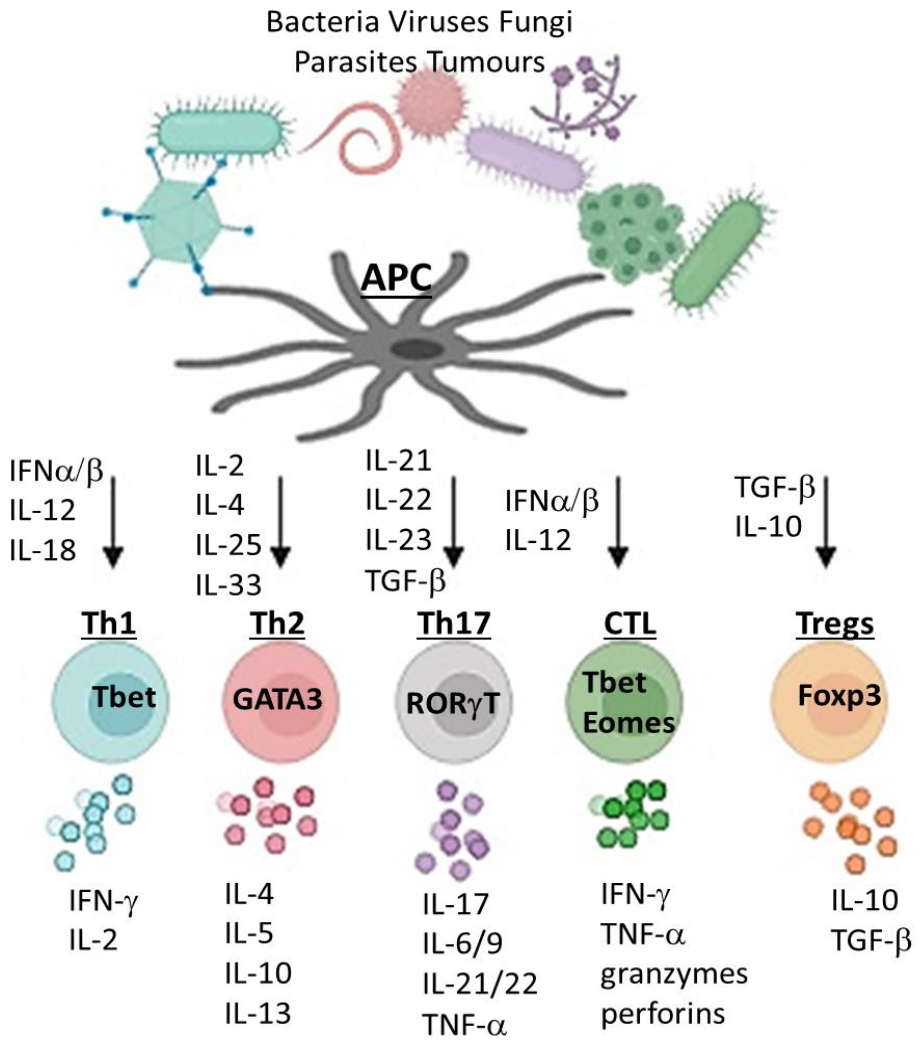

1.1.5 Introducing Secondary and Tertiary Lymphoid Organs

The mammalian immune system harbours organised sites known as lymphatic organs that promote the accumulation of lymphoid cells. Primary lymphoid organs such as the bone marrow and thymus are sites for B and T cell development as discussed in section 1.1.4. SLOs include the LNs, spleen, Peyer's patches, mucosal lymphoid tissues as well as less anatomically defined structures including, isolated lymphoid follicles and bronchus-associated lymphoid tissues (Randall et al., 2008). These structures form during embryogenesis or in early post-natal period at predetermined locations, aided by interactions between haematopoietic, stromal and endothelial cells, and provide the conducible microenvironment to support lymphocyte activation and differentiation into effector cells (Buettner and Lochner, 2016).

Lymphoid structures separate from the traditional SLOs have also been observed in various tissues in both mice and humans (Jones et al., 2016, Lochner et al., 2011). These structures referred to as tertiary lymphoid organs (TLOs), as well as ectopic lymphoid-like structures (ELSs) and ectopic lymphoid follicles (ELFs) are complex aggregates of leukocytes and specialized stromal cells. Examples of such include fat-associated lymphoid clusters (FALCs), a focus of this project, but also mucosa-associated lymphoid tissues (MALT), such as cryptopatches (CP), and induced nasopharynx-associated lymphoid tissue (iNALT), (Barone et al., 2016). TLOs are reported to develop in tissues affected by non-resolving chronic inflammation resulting from infection, cancer, chronic allograft rejection and autoimmunity (Jones et al., 2016). Physiological TLOs not associated with pathology also exist; these develop in response to the presence of microbiota (Buckley et al., 2015). Unlike SLOs, TLOs

are not encapsulated; rather form in response to inflammatory stimuli, with some tissues being more prone to developing TLOs (Jones et al., 2016, Mitsdoerffer and Peters, 2016).

1.2 Adipose Tissue and Tertiary Lymphoid Structures

1.2.1 Structure, Function and Types of Adipose Tissues

Adipose tissue (AT) is a loose connective tissue consisting of cells known as adipocytes whose primary role is to store triglycerides (fat) and excess energy. Throughout life, pre-adipocytes of mesenchymal origin differentiate into mature adipocytes. AT can be broadly divided into white- (WAT) and brown (BAT) adipose tissue. WAT is distributed widely throughout the body, composed of spherical adipocyte cells which vary in size depending on the size of the single lipid droplet stored in them (Saely et al., 2012). The primary metabolic role of WAT is to store energy via the synthesis of fatty acids in a process known as lipogenesis, stimulated by high carbohydrate and glucose intake. Conversely, lipolysis - the breakdown of fat (or energy reserves) also occurs in AT during times of metabolic stress including fasting or prolonged exercise (Coelho et al., 2013). WAT can be located subcutaneously or viscerally, the latter of which can be found within peritoneal adipose tissues such as the mesentery and omentum (Lai and Leung, 2010). As such it offers mechanical protection to several organs and muscle groups by softening and absorbing the impact of shocks, and allowing muscle bundles to slide appropriately on one another while keeping their functional integrity intact (Coelho et al., 2013). Images of murine mesenteries attached to the SI as well as the omentum have been obtained from previous reports - (Moro et al., 2015) and (Berberich et al., 2008) respectively, and are depicted in figures 1.9A

and 1.9B respectively to show the anatomical location of these tissues. In addition, during cold stress a type of WAT known as beige or “brite” fat can provide thermal insulation following the induction of uncoupling protein 1 (UCP-1) expression (Luo and Liu, 2016). Brown adipose tissue (BAT) on the other hand is present at birth and abundant in new-borns or small mammals, becoming less prominent during adulthood. Consisting of triglycerides as multiple small vacuoles that vary in diameter, it houses large and numerous spherical-shaped mitochondria, with greater level of vascularisation compared to WAT (Saely et al., 2012). This high mitochondrial density therefore allows BAT to specialise in thermogenesis, owing to the expression of UCP-1 within these mitochondria. When activated, UCP-1 drives ATP synthesis that in turn stimulates the respiratory chain. Heat is then produced due to the combustion of available substrate and distributed throughout the body via the circulation (Harms and Seale, 2013).

Beyond these functions, AT is known to have dynamic capabilities, acting as an endocrine organ to synthesize biologically active compounds involved in metabolic homeostasis but also in disease pathology. Such compounds include leptin and adiponectin, which were among the first adipokines to be discovered. The leptin peptide which belongs to the IL-6 family of cytokines is expressed mainly by AT and commonly referred to as a satiety hormone owing to its role in regulating food intake and increasing energy expenditure. Subcutaneous AT synthesizes greater levels of leptin compared to visceral adipose tissue (VAT). It also functions in modulating glucose metabolism, lipid oxidation, reward circuitry for feeding and in adipocyte apoptosis (Coelho et al., 2013). Adiponectin which is related to complement 1q family is secreted exclusively from AT (Coelho et al., 2013). Its effects include enhancing insulin sensitivity, cardiovascular protection, and anti-inflammatory

properties (Luo and Liu, 2016). Other adipokines which can be altered during different physiological conditions and aid the body in adapting have also been discovered including but not limited to TNF-α, IL-6, resistin, monocyte chemoattractant protein 1 and Fibroblast growth factor 21 (Hui and Feng, 2018, Luo and Liu, 2016).

AT consists of other cells within the stromal-vascular fraction (SVF), which comprises of blood cells, endothelial cells, immune cells and pre-adipocytes (Coelho et al., 2013). Accumulation of immune cells including classically activated (M1) macrophages, type 1/3 innate lymphoid cells (ILC1/3), Th1 cells, neutrophils, mast cells and CD8 T cells and their associated cytokines results in a pro-inflammatory environment. During obesity for example, adipocytes enlarge, and there is increased expression of harmful adipokines such as the pro-inflammatory proteins, TNF-α, IFN-γ and IL-6, which give rise to a state of chronic low-grade inflammation (Emanuela et al., 2012). Such inflammation is thought to be a key player in the development of obesity-associated diseases, particularly insulin resistance and type 2 diabetes (Ferrante, 2007, Greenberg and Obin, 2006). Early studies by Hotamisligil and colleagues showed that in obese mice compared to lean animals, mRNA expression of the pro-inflammatory cytokine TNF, was at least 5-10-fold higher in the AT of different mouse models of obesity, which also exhibited signs of insulin resistance (Hotamisligil et al., 1993). Macrophages were later reported to correlate with increased BMI and adipocyte size (Cinti et al., 2005), leading to increased interest in the role of this immune cell during obesity. It was then shown that during obesity, AT macrophages could switch from their protective anti-inflammatory M2 phenotype to acquire a pro-inflammatory M1 phenotype characterised by inducible nitric oxide (iNOS), TNF and IL-6 (Lumeng et al., 2007, Seijkens et al., 2014), the latter two affecting insulin resistance directly (Seijkens et al., 2014). In

contrast, homeostasis within lean fat tissue is maintained by an anti-inflammatory environment characterised by alternatively activated M2 macrophages (or AAMs), ILC2s, Th2 cells, Tregs, eosinophils, and their associated cytokines including IL-4, IL-5, IL-10 and IL-13 (Chalubinski et al., 2016). Taken together these indicate that AT immune cells have critical roles in regulating tissue homeostasis.

1.2.2 Fat Associated Lymphoid Clusters (FALCs)

In human and mice, secondary lymphoid tissues such as LNs are associated closely with ATs; however, VATs within the peritoneal cavity have also been reported to harbour novel TLOs known as FALCs. These structures were initially observed as clusters of lymphocytes present along the blood vessels of mouse mesenteries, as well as in human mesentery. FALC clusters were shown to be in direct contact with the surrounding ATs, and ranged between 100-500µm in size, and in number from 5-50 clusters per mesentery, with numbers increasing with age (Moro et al., 2010). Subsequent, studies by our group gained further insights into the formation of these clusters, revealing FALCs to be highly vascularised hubs that form on a network of stromal cells that express the alarmin IL-33. Furthermore, these clusters were observed to be present on mucosal surfaces such as omental, gonadal, mesenteric, mediastinal and pericardial fat in a heterogeneous manner, with the omentum having the highest number of clusters and gonadal fat having the least (Bénézech et al., 2015). Structurally, FALCs resemble omental milky spots, lymphoid aggregates first described in the omentum of rabbits by Von Recklinghausen as white spots (Von. Recklinghausen, 1863). However as no distinct differences are found between omental milky spots and FALCs in the mesenteries, gonadal or mediastinal fat (Cruz-Migoni and Caamaño, 2016), the author shall refer to them collectively as FALCs except when reporting instances where other researchers

have chosen to make this distinction. Phenotypically, FALCs were shown to contain ILC2s, $CD3^+$ T cells and $B220^+$ B cells (Moro et al., 2010), with later studies confirming the presence of other immune cells including macrophages (Bénézech et al., 2015), neutrophils (Buscher et al., 2016, Jackson-Jones et al., 2019) and resident memory T cells (Trms) (Han et al., 2017). The large proportions of B1 cells contained in FALCs are recruited by CXCL13 produced by FALC stromal cells (Bénézech et al., 2015) and supported by ILC2 production of IL-5 (Moro et al., 2010). A schematic of FALC structure is shown in figure 1.3.

Increased demand for localized immune responses is achieved by the development of TLOs (Neyt et al., 2012); FALCs/milky spots in particular provide a second line of defence within the body cavities namely mucosal surfaces, by conferring protection against infection and inflammation, regulation of microbiota as well as in the generation of antibody mediated responses. While mediastinal and pericardial FALCs mediate responses within the pleural cavity, omental and mesenteric FALCs mediate those within the peritoneum (Bénézech and Jackson-Jones, 2019). The development of such antibody mediated responses is facilitated by B-rich clusters within FALCs. It was shown that antigenic challenge with NP-Ficoll could sufficiently induce B1 and B2 cell proliferation within FALCs, IgM and IgG production and class switching, while immunisation with NP-ovalbumin led to antigen-specific B cells and germinal centre-like B cells (Bénézech et al., 2015), thereby highlighting that FALCs were able to initiate T-independent and T-dependent immune responses. In addition, mediastinal and pericardial FALCs were found to respond to pleural nematode infection as well as acute lung inflammation. Following infection with *Litomosoides sigmodontis* or *Altenaria alternata*, FALC B-cells initiated IgM secretion at the site of infection and subsequently differentiated into plasma cells. Furthermore, IL-33 receptor signalling contributed indirectly to pleural B1

cell activation; specifically, IL-33 produced by FALC stromal cells acted on IL-33 responsive cells particularly ILC2s, leading to IL-5 secretion which is an important growth factor for B1 cells (Jackson-Jones et al., 2016). However unlike the observations reported by Jackson-Jones et al., more recently, mediastinal FALCs were reported to contribute to the progression of lung disease rather than its amelioration (Elewa et al., 2018). Following the induction of lung inflammation by bleomycin, mediastinal FALCs were found to increase in size characterised by the recruitment of B cells, granulocytes, and proliferating cells. In addition, lymph vessels and high endothelial venules were more abundant in FALCs as well as in the lungs of bleomycin-treated compared to control group suggesting that these may be routes of cellular infiltration into FALCs and into the lungs (Elewa et al., 2018).

Further studies have also shown FALCs to be a reservoir of resident memory T cells (Trms) (Han et al., 2017). Mesenteric and gonadal WAT were observed to contain an abundant population of CD4 and CD8 T cells, with a proportion of these cells being effector, central and resident memory T cells. Parabiosis experiments further confirmed the presence of bona fide, non-recirculating Trms within the mesenteries. Importantly, increased numbers and proportions of IFN-γ producing CD8 and CD4 T cells following *Toxoplasma gondii* parasitic infection, as well as of tetramer-specific T cells post-infection with the bacterial pathogen *Yersinia pseudotuberculosis*, was noted in the mesenteries therefore highlighting this AT as a site for accumulation of pathogen-specific T cells following different infections. Additionally Trms in WAT could also confer protection against a secondary lethal challenge to *Yersinia pseudotuberculosis,* with FALC numbers in mesenteries, FALC CD8 T cells as well as tetramer-specific T cells found to increase significantly. (Han et al., 2017).

Meanwhile earlier experiments by Rangel-Moreno et al. tested the ability of omental FALCs (or milky spots as the authors referred to them) to independently support immune responses to peritoneal antigens. Indeed, researchers found that B cell responses to these antigens could be generated in mice in the absence of conventional lymphoid organs, mediated instead by omental milky spots filled with B cells clusters and PNAd-expressing high endothelial venules, indicating that blood circulation could serve as a route for immune cell recruitment. In addition, other T cell-dependent B cell responses including somatic hypermutation, limited affinity maturation and isotype class switching were found to be mediated by omental milky spots, as well as the recruitment of effector T cells from other locations and the support of T cell responses (Rangel-Moreno et al., 2009).

1.2.3 Stromal Cells in Lymph Node and FALC Formation

Stromal cells are the connective tissue cells associated with a specific organ, with one of the most studied being mesenchymal stromal cells (MSCs) which are present in the bone marrow, adipose and other tissues. MSCs can differentiate into different stromal cell types, including muscle cells, adipocytes, osteoblasts, fibroblasts and also self-renew (Keating, 2006). Furthermore, the formation of SLOs and TLOs (with a particular focus on LN and FALCs) are governed by immune-stromal cell interactions that are essential to the successful development of these structures.

LNs develop in parallel with lymphatic vascularisation. Located at vascular junctions, LNs are encapsulated structures that contain an outer cortex which harbour B cells and follicular dendritic cells (FDCs), paracortical regions containing T cells and DCs as well as an inner medullary region where macrophages can be found. They collect lymph and cellular contents via afferent lymphatic vessels that can then be transported into the LN cortex or move via

the subscapular sinus to exit via the efferent lymphatics. In addition, lymphocytes and antigens can enter LNs via an arteriole and into the parenchyma region through high endothelial venules that express adhesion molecules including mucosal-associated adhesion molecule 1 (MAdCAM-1) as well as chemokines CCL19 and CCL21 (Ruddle and Akirav, 2009). As such, by providing an environment for the efficient interaction between APCs and lymphocytes, LNs importantly initiate, support and resolve immune responses as well as aid in maintaining tolerance (Hirosue and Dubrot, 2015). LN stromal cells also play a role by providing specific signals and growth factors needed for the movement, migration, maturation and survival of lymphocytes, as well as the organization of specific areas in this tissue that facilitate the interactions between immune cells (Bénézech et al., 2012). One of the initial steps in LN formation is the clustering of haematopoietic lymphoid tissue inducer (LTi) cells with non-haematopoietic stromal cells via the interaction of lymphotoxin-β-receptor (LTβR) on the latter, with the lymphotoxin-αβ ligand on LTi's, leading to their differentiation into lymphoid tissue organiser (LTo) cells (Brendolan and Caamano, 2012). Van de pavert and colleagues showed chemokine CXCL13 induced by neuron–derived RA to be important in the recruitment of LTi cells to the LN anlage (van de Pavert et al., 2009). However, the origin of the lymphoid tissue stromal cells involved in this clustering process was still unknown until Bénézech and colleagues revealed that AT surrounding the developing LN contained adipocyte precursors capable of differentiating into lymphoid tissue stromal cells. The researchers showed that upon receiving positive LTβR signalling, adipocyte precursors downregulated adipogenesis, while promoting increased expression of LN stromal cell markers ICAM-1 and VCAM-1 (Bénézech et al., 2012). Mature LTo cells are also known to be VCAM-1^{+} ICAM-1^{+} MAdCAM-1^{+} with the ability to produce chemokines

including CXCL13, CCL19 and CCL21 that mediate the recruitment of LTi cells in the embryo as well B and T cells in developed lymphoid tissues (Brendolan and Caamano, 2012). Lymphoid tissue stromal cells can be further sub-divided into fibroblastic reticular cells (FRCs) which associate with the T-cell zone; FDCs residing in the B-cell zone and a third subset under the subscapular sinus known as the marginal reticular cells (MRCs) (Koning and Mebius, 2012). Flow cytometric analysis of LN single cell suspensions have shown that four stromal populations can be identified based on differential expression of stromal markers podoplanin (Gp38) and CD31. They include, $CD31^{+}$ blood endothelial cells (BECs), $Gp38^{+}$ FRCs, $CD31^{+}Gp38^{+}$ lymphatic endothelial cells (LECs) and a $CD31^{-}Gp38^{-}$ large double negative population (Bénézech et al., 2012, Koning and Mebius, 2012). These populations were also found to be present in AT, as well as a $Gp38^{int}CD31^{-}$ population (Bénézech et al., 2012), thereby suggesting that the stromal component of FALCs likely resembles that seen in SLOs in regard to its composition, compartmentalisation and likely its function.

Indeed, the local inflammatory microenvironment comprising of signals from stromal cells and resident immune cells are shown to govern TLO development. The conversion of resident and/or inflammatory stromal cells towards a lymphoid tissue stroma like-phenotype is one of the key steps in TLO development. Interactions between chemokines secreted by stromal cells and their receptors expressed by leukocytes also influence tissue ontogeny. Unlike SLOs, TLO formation is not dependent on ILC3s/LTi cells. Instead, TLOs are associated with ectopic expression of cytokines and homeostatic lymphoid chemokines (Buckley et al., 2015), two of which, lymphotoxin alpha (LTα) and CXCL13 have been reported in the development of FALCs and the structurally similar, omental milky spots. LTis express the nuclear hormone receptor RORγt, as such these cells are lacking in $Rorc^{-/-}$ mice. However

well-developed milky spots with large B cell follicles can still be observed in Rorc$^{-/-}$ mice (Rangel-Moreno et al., 2009). Omental milky spots were instead found to be either absent or smaller in size within Lta$^{-/-}$ and Cxcl13$^{-/-}$ mice, with absent B cell areas. CXCL13 was not found to be controlled by LTα owing to its normal expression amongst other chemokines found within Lta$^{-/-}$ mice. In addition, researchers went on to show via immunofluorescence staining, CXCL13 expression in a reticular pattern and primarily in areas surrounding B cell follicles suggestive of stromal cells. Further analysis clarified that B cell areas of milky spots lacked central FDCs, rather were surrounded by reticular networks of CD11b^{+} cells which were likely macrophages. A role for CXCL13 in the recruitment and retention of B1 cells has also been reported in FALCs. However, FALC number and composition in *Lta*$^{-/-}$, *Rorc*$^{-/-}$ mice as well as strains deficient in LTβR (*Ltbr*$^{-/-}$), was found to be identical to their wild type controls (Bénézech et al., 2015). Therefore, as well as confirming the independence of LTi/ILC3s in FALC formation, lymphotoxin-α–LTβR is also not needed. Instead, postnatal formation of FALCs was found to be partly regulated by TNF-receptor signalling and the presence of commensal flora, as shown by the reduced number and size of FALCs in *Tnfrsf1a*$^{-/-}$*Tnfrsf1b*$^{-/-}$ mice as well as in germ-free mice. In addition, new FALCs could arise following the development of peritoneal inflammation. This was shown to be dependent on the interaction between TNF on myeloid cells and TNFR on stromal cells, as well as IL-4Rα signalling, with IL-4 and IL-13 provided by CD1d-restricted NKTs orchestrating FALC formation (Bénézech et al., 2015).

Figure 1.3: A diagrammatic representation of Fat Associated Lymphoid Clusters

FALCs are clusters of immune cells associated with adipocytes in mucosal surfaces. These clusters form on a network of stromal cells that express the alarmin IL-33 and are highly vascularized local hubs that contain stromal, innate, and adaptive immune cells.

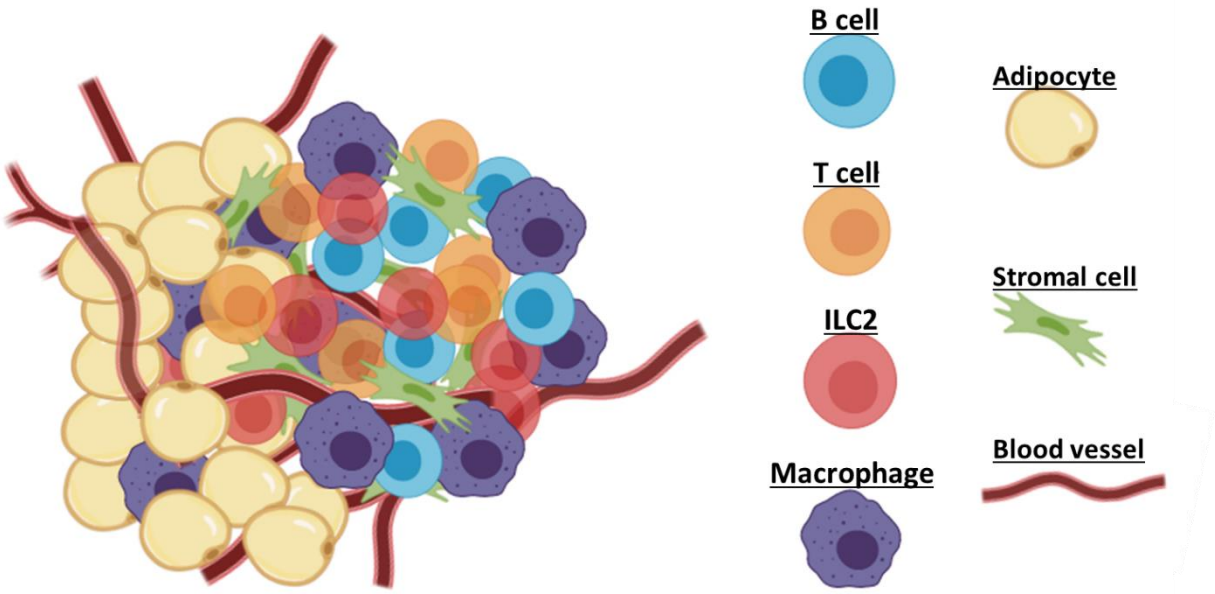

1.2.4 Innate Lymphoid Cell (ILC) Development

FALCs are rich in ILC2s (Moro et al., 2010); a group of immune cells belonging to the innate lymphoid cell (ILC) family. Being the most recently discovered of immune cells, the identification of ILCs were reported by 12 independent research groups as novel types of non-T and non-B lymphocytes before their re-designation as ILCs (Vivier et al., 2016). ILCs can be classified into two main lineages based on their distinct cytokine expression profiles and the transcription factors controlling their development and function. These are: cytotoxic ILCs which include NK cells, and cytokine-producing helper subsets which include ILC1, ILC2 and ILC3 with lymphoid tissue inducer (LTi) cells constituting a subpopulation of ILC3s (Eberl et al., 2015, Artis and Spits, 2015).

All ILCs as well as lymphocytes develop from the common lymphoid progenitor (CLP) (Diefenbach et al., 2014), however the development of NK cells, helper ILCs as well as LTi cells, but not B or T cells, were all found to be dependent on the expression of the transcriptional inhibitor of DNA binding 2 (Id2) (Yokota et al., 1999, Moro et al., 2010, Cherrier et al., 2012), thereby suggesting the existence of a common innate lymphoid progenitor (CILP) downstream of the CLP. Indeed ILC lineages express high levels of Id2 compared to naïve B and T cells (Diefenbach et al., 2014). CILPs then give rise to the NK cell precursor and a separate lineage of $Id2^{+}$IL-7r$\alpha^{+}\alpha4\beta7^{+}$ population known as common helper innate lymphoid progenitors (or CHILPs). The transcription factor NFIL3 was reported to be required for the differentiation of both the NK lineage (Kamizono et al., 2009) but also the generation of early ILC progenitors, owing to the loss of CHILP populations in NFIL3-deficient mice (Diefenbach et al., 2014). In contrast, helper ILC subpopulations but not NK cells have also been reported to be dependent on the GATA3 transcription factor for their

differentiation, taking effect between CILP and CHILP stage of ILC differentiation (Vivier et al., 2018). Subsequently, CHILPs differentiate into either lymphoid tissue inducer progenitors (LTiPs) that under the influence of RORγT, thymocyte selection-associated high mobility group box (TOX) protein and Id2, differentiate into LTi cells. Alternatively, Id2 high CHILPs expressing the transcription factor promyelocytic leukemia zinc finger (PLZF) can also give rise to the innate lymphoid cell precursors (ILCPs) that finally differentiate into ILC1, ILC2 and ILC3 (Vivier et al., 2018) – figure 1.4. Notch signalling has also been attributed to play some role in the generation of ILC lineages, with several studies reporting of the reduced presence of ILC1s, ILC2s and NKP46^{+} ILC3s, as well as LTi cells during defective notch signals (Lee et al., 2011, Yang et al., 2013a, Cherrier et al., 2012). Given their common ancestry with CLPs, ILCs thereby share the developmental origin, and many of the phenotypic characteristics and functions of T cells. However, ILCs do not express antigen specific receptors (Eberl et al., 2015, Hazenberg and Spits, 2014) and are largely tissue resident cells, preferentially found at barrier surfaces (Diefenbach et al., 2014). ILCs are instead activated by stress signals, microbial compounds and the cytokine milieu of the surrounding tissue, and once activated are able to regulate the developing adaptive immune response directly through major MHC II and indirectly through regulating DCs (Eberl et al., 2015).

Focusing specifically on helper ILCs, ILC1s are non-cytotoxic lineage negative (Lin-) cells that produce IFN-γ, TNF-α and require the transcription factor T-bet for their development (Hazenberg and Spits, 2014, Artis and Spits, 2015). ILC1s are important in immunity to intracellular bacteria and parasites (Artis and Spits, 2015). ILC2s produce type 2 cytokines including IL-4, IL-5, IL-9, and IL-13, as well as the epidermal growth factor receptor ligand, amphiregulin. ILC2s are dependent on GATA3 for their development and function, and

mediate anti-helminth immunity, allergic inflammation and tissue repair, but also promote type 2 inflammation (Artis and Spits, 2015). Finally, ILC3s produce IL-17A, IL-17F, IL-22, granulocyte macrophage colony-stimulating factor and TNF – depending on the stimulus. They are involved in antibacterial immunity, chronic inflammation or tissue repair and along with their subpopulation of LTi cells, depend on RORγT for development with the latter needed for the formation of LNs and Peyer's patches during embryonic development (Diefenbach et al., 2014) – figure 1.5. As a result of their cytokine expression, helper ILCs are therefore said to represent the innate counterparts of CD4 Th cells, with ILC1s, ILC2s, and ILC3s, representing Th1, Th2, and Th17 respectively, while NK cells are considered to be the innate counterparts of cytotoxic CD8 T cells (Eberl et al., 2015).

Despite having distinct lineages, developmental pathways and function, plasticity amongst the ILC subsets have been reported, mediated by the combined action of polarising signals that activate cognate cytokine receptors and transcription factors of the responding ILC subset (Vivier et al., 2018). IL-1β has been noted to induce low expression of T-bet on ILC2s as well as of IL-12Rβ2 thereby enabling their response to IL-12 and subsequent conversion to an ILC1 phenotype capable of producing IFN-γ, yet retaining co-expression of GATA3 as well as transcription of IL-5 and IL-13 genes (Ohne et al., 2016). This plasticity which was also observed in tissues of patients with chronic obstructive pulmonary disease or chronic rhino-sinusitis (Bal et al., 2016, Silver et al., 2016) could however be reversed by IL-4 (Bal et al., 2016). In addition, IL-17 producing ILC2s referred to as inflammatory ILC2s (iILC2s), driven by systemic injection of IL-25 (Huang et al., 2015) and later shown to also be dependent on Notch signalling (Zhang et al., 2017a) have been described. These KLRG-1^{hi} iILC2s also expressed intermediate levels of RORγt and as such could transform into ILC3-like cells either

in response to fungal infection with C*andida albicans* or under Th17 polarising conditions (Huang et al., 2015). More recently IL-1β, IL-23 and TGF-β have been shown to drive trans-differentiation of ILC2s into IL-17 ILC3s in the nasal polyps of cystic fibrosis patients, which in turn function in inducing IL-8 and neutrophil recruitment. Similar to other studies IL-4 was found to prevent this conversion as well as vitamin D3, with the latter suppressing IL-23 signalling pathways (Golebski et al., 2019). A regulatory ILC subset was also defined in the gut; induced during inflammation, these ILCregs were found to secret IL-10 that suppressed ILC1 and ILC3, as well as TGF-β that helped maintain and expand the pool of ILCregs during intestinal inflammation (Wang et al., 2017b). A similar ILC2 population has been noted in the murine lung, with IL-2 and IL-33 as well as challenge with allergens found to promote the development of these IL-10 producing ILC2 population (Seehus et al., 2017). Earlier confirmation of ILC plasticity was shown by Vonarbourg and colleagues who used genetic lineage tracing and adoptive transfer experiments to reveal that the gradient of RORγT expression could determine the phenotype and function of IL-22 producing LTi-like cells (i.e ILC3s). In short, reduced RORγT expression was responsible for driving the conversion of ILC3s into IFN-γ producing NK1.1^{+}NKP46^{+} ILC1s (Vonarbourg et al., 2010); this was further shown to involve the upregulation of T-bet via cues from IL-23 and commensal bacteria (Klose et al., 2013), as well as via the regulation of Notch signalling (Rankin et al., 2013, Chea et al., 2016). In reverse, differentiation of specific human ILC1 subsets namely CD127^{+} ILC1s into ILC3s can occur in the presence of IL-23 and IL-2, is dependent on RORγT and is enhanced by IL-1β, and RA. This is a reversible process, with high CD14^{+} DC concentrations driving ILC3 to ILC1 polarisation such as is seen in the gut of Crohn's disease patients (Bernink et al., 2015).

Figure 1.4: Development of innate lymphoid cells

All lymphocytes including ILCs develop from the common lymphoid progenitor (CLP), that are dependent on high levels of inhibitor of DNA binding 2 (Id2) and are IL-7rα responsive, giving rise to common innate lymphoid progenitors (CILPs). CILPs develop into two separate lineages; cytotoxic ILCs (i.e NK cell precursors) as well as the common helper innate lymphoid progenitors (CHILPs), a process dependent on nuclear factor IL-3 inducer (NFIL3). In addition, helper ILCs but not NK cells require GATA3 for their development. CHILPs further differentiate into lymphoid tissue inducer progenitors (LTiPs) driven by RORγT, thymocyte selection-associated high mobility group box protein (TOX) protein and Id2. CHILPs under the influence of PLZF can also give rise to innate lymphoid precursors (ILCPs) that subsequently differentiate into ILC1, ILC2 and ILC3 subsets driven by the indicated transcription factors. Runt-related transcription factor 3 (RUNX3); RAR-related orphan receptor α (RORα); transcription factors T cell factor 1 (TCF-1); Aryl hydrocarbon receptor (AHR).

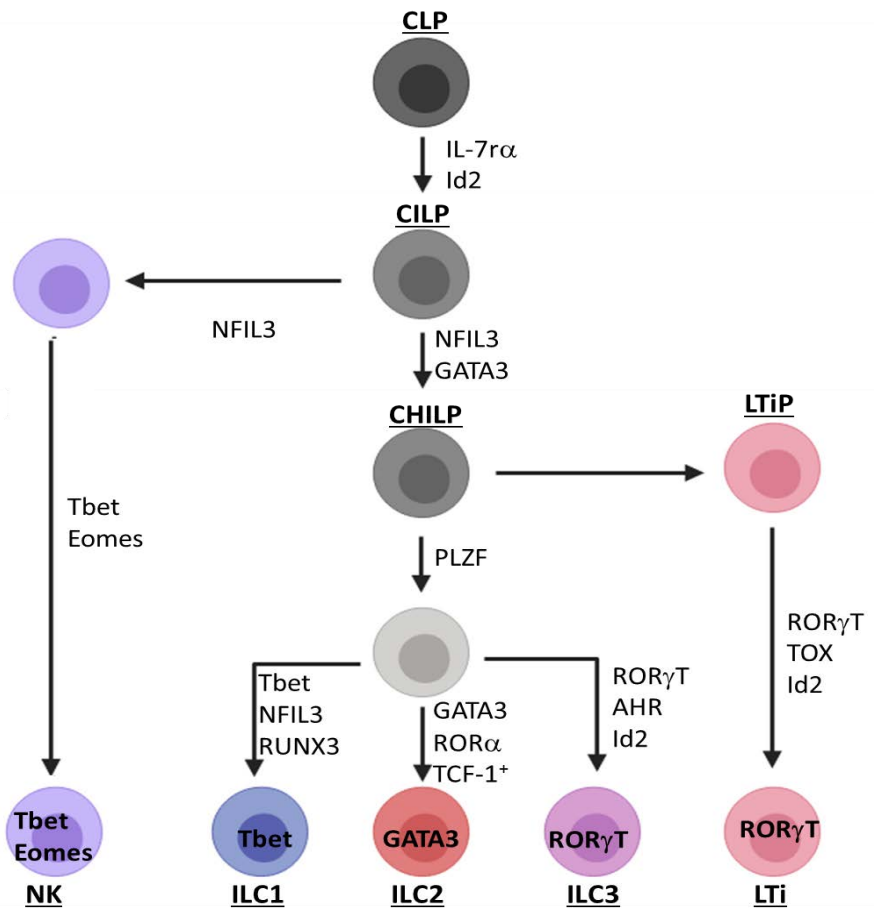

Figure 1.5: ILC activation and effector function

Innate lymphoid cells (ILCs) are grouped based on their expression of transcription factors. Owing to their lack of antigen specific receptors, ILCs become activated by induction cytokines present within their local environment; in response, specific subsets go on to produce their corresponding effector cytokines responsible for driving a number of immune functions.

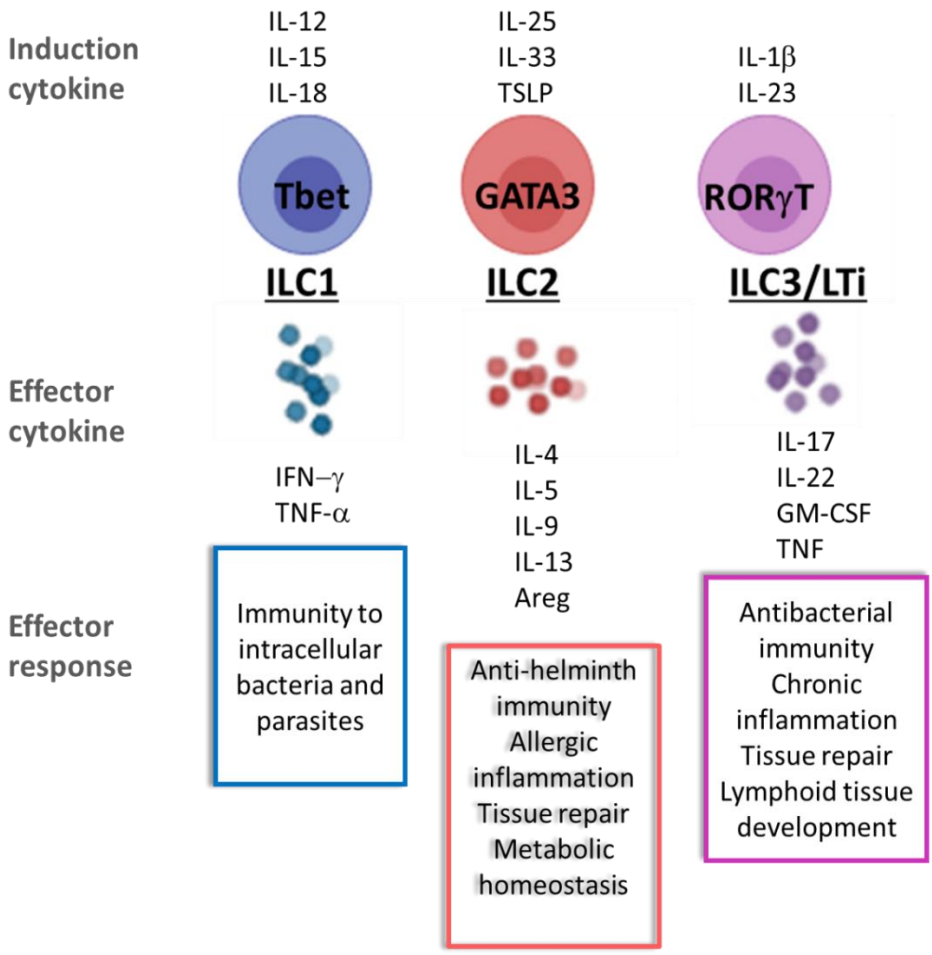

1.2.5 ILC2 Regulation and Role in Maintaining Adipose Tissue Homeostasis.

ILC2s, previously known as 'innate helper type 2 cells', 'natural helper cells' or 'nuocytes' react to epithelium-derived cytokines IL-25, IL-33 and thymic stroma lymphopoietin (TSLP), basophil-derived IL-4 and products of the arachidonic acid pathway in response to epithelial injury, parasitic infection and allergens (Eberl et al., 2015). Having been identified at various sites including secondary lymphoid and non-lymphoid tissues (Withers, 2016), ILC2s are said to be located appropriately (or ''poised'') for their function (M. Webb and D. Tait Wojno, 2017). Flow cytometric analysis during one of the initial discoveries of these cells revealed that ILC2s expressed c-Kit, Sca-1 and IL-7Rα but were negative for lineage markers (CD3ε, TCRβ, TCRδ, CD4, CD5, CD8α, CD11c, CD19, B220, NK1.1, Gr-1, Mac-1, FcεRIα and Ter119) thereby hinting that they belonged to a new lymphocyte lineage (Moro et al., 2010). Mouse ILC2s also express the IL-33 receptor ST2 though this is tissue dependent; moreover peripheral blood human ILC2s lack ST2, instead human blood and tissue ILC2s more selectively express the prostaglandin D2 receptor CRTH2 as well as C-type lectin-like receptor CD161 (Vivier et al., 2018). Moreover, ILC2s are capable of expressing Th2 cytokines IL-4, IL-5 and IL-13 as well as Th2 related genes Maf, Gata3, Junb and STAT6. In addition, stimulation of ILC2 with PMA and ionomycin results in significant production of IL-2, IL-4, IL-5, IL-6, GM-CSF and moderate levels of IFN-γ. Finally, IL-33 combined with IL-2 and IL-25 also leads to large amounts of IL-5 and IL-13 production (Moro et al., 2010); all characteristics now known to be features that identify ILC2s. In mice ILC2s have been identified in mesenteric lymph nodes, spleen, intestine, liver, FALCs, skin (Nausch and Mutapi, 2018), and recently in the thymus (Jones et al., 2018). While in humans they are shown to be in the

nasal polyphs, tonsils, GI tract, FALCs, peripheral blood, lung and skin (Nausch and Mutapi, 2018).

Beyond the role of epithelial cytokines other ILC2 regulators exist, most notable the role of lipid mediators which along with ILC2s, are coincidently increased in tissues of patients with several diseases including asthma, atopic dermatitis and chronic rhino-sinusitis (Doherty and Broide, 2018). In particular, lipid derived leukotrienes have been identified. Leukotriene D4 (LTD_4) was reported to induce the production of IL-4, IL-5 and IL-13 by ILC2s *in vitro*, as well the *in vivo* production of IL-5, both mediated via the cysteinyl leukotriene receptor CysLT1R expressed on ILC2s. ILC2 accumulation and proliferation was also observed to be augmented by LTD_4 following allergen challenge with *Alternaria* species (Doherty et al., 2013). Later studies which also reported of a non-redundant role for LTB_4 in cooperating with IL-33 to activate lung ILC2s, further revealed that such cysteinyl leukotrienes functioned by activating calcium/calcineurin/nuclear factor of activated T cells (NFAT) translocation into the nucleus of ILC2s and its subsequent activation (von Moltke et al., 2016). Given that TCR signalling in Th2 cells also involves NFAT pathway, this finding further demonstrates the parallels of ILC2s and Th2 cells. Meanwhile, in humans, ILC2s identified in the peripheral blood of healthy and asthmatic patients were shown to respond to mast-cell derived prostaglandin D2 leading to their subsequent release of IL-13, with a syngeneic effect observed in the presence of IL-25 and IL-33 (Barnig et al., 2013), thereby further integrating eicosanoids in the induction of ILC2 responses particularly during airway inflammation and lung pathologies.

Multiple studies have highlighted an association between metabolism, obesity and altered ILC responses. Regulation of VAT and metabolic homeostasis depends on a repertoire of immune cells, one being eosinophils (Molofsky et al., 2013). Tregs, invariant natural killer T

cells (iNKTs), eosinophils and AAMs have housekeeping functions in lean subjects such as promoting insulin sensitivity and metabolic homeostasis within VAT (Molofsky et al., 2013, Schipper et al., 2012). Moreover, recruitment and retention of these immune cells depend on different cytokines, chemokines and integrins. Molofsky and colleagues went on to demonstrate the requirement of IL-5 for the maintenance of mice VAT eosinophils, which are also needed to sustain AAMs (Molofsky et al., 2013). ILC2s were observed to be the crucial source of IL-5, with cytokine expression studies revealing the predominance of IL-5^{+} ILC2s within the VAT, where eosinophils and AAMs also reside. Moreover, loss of ILC2s resulted in significant decrease in basal adipose AAM, while IL-5 deficiency led to increased obesity and insulin resistance during high-fat diets, as well as profound reduction in VAT eosinophils. According to the researchers these losses lead to a decline in oxidative metabolism and energy expenditure, thereby resulting in increased adiposity and metabolic impairment with IL-33 shown to be the induction cytokine responsible for ILC2 production of IL-5 and IL-13 and subsequent downstream effects (Molofsky et al., 2013) - figure 1.6.

BAT as described earlier is the main site for thermogenesis in mammals owing to its high expression of UCP-1 containing mitochondria (Harms and Seale, 2013). WAT whose main role is to store chemical energy can also develop clusters of adipocytes that express UCP-1. Such adipocytes, also known as beige cells are reported to have thermogenic capacity (Harms and Seale, 2013) when stimulated by cyclic AMP (Wu et al., 2012). Interestingly, ILC2s are shown to promote beiging (the expression of UCP-1 in adipocytes in WAT) in humans and mice (Brestoff et al., 2015). Following the identification of ILC2 populations in abdominal subcutaneous WAT of non-obese human donors, the authors went on to use IL-33 deficient mice to reveal the importance of this cytokine in maintaining ILC2s, and in

preventing development of spontaneous obesity. Methionine-enkephalin peptides which are produced by ILC2s and directly act on adipocytes were reported to be partly responsible for ILC2-dependent beiging (Brestoff et al., 2015) as shown in figure 1.6. Similarly, another report showed that ILC2 activation by IL-33 could sufficiently promote the growth of functional beige fat in thermoneutral C57BL/6J mice (Lee et al., 2015). This was demonstrated by the significant increase in UCP-1 expression in the subcutaneous WAT of these mice upon IL-33 administration. The mechanism for this was attributed to the activation of IL-4Rα signalling in PDGFRα^+ (platelet derived growth factor receptor alpha) adipocyte precursors (or bipotential cells) by ILC2, as well as eosinophil-derived type-2 cytokines, and thus, the subsequent proliferation and commitment of these bipotential cells to the beige fat lineage (Lee et al., 2015) – figure 1.6.

Figure 1.6: ILC2s in adipose tissue metabolism

ILC2s have been reported to be involved in regulating metabolic homeostasis within adipose tissues. ILC2-derived IL-5 is needed for the maintenance of visceral adipose tissue eosinophils, that in turn produce IL-4 and IL-13, both involved in polarising macrophages to their alternatively activated phenotype, that maintain housekeeping functions through the actions of catecholamine's such as norepinephrine (NE). These eosinophil-derived type-2 cytokines can additionally activate IL-4Rα expressing PDGFRα$^+$ (platelet derived growth factor receptor alpha) adipocyte precursors, leading to the commitment and proliferation of these adipocyte precursors to beige adipocytes. Furthermore, the endogenous opioid-like peptide methionine-enkephalin (MetEnk) produced by ILC2s in response to IL-33, may act directly on white adipose tissue (WAT) to cause accumulation of uncoupling protein-1 (UCP1$^+$) beige adipocytes.

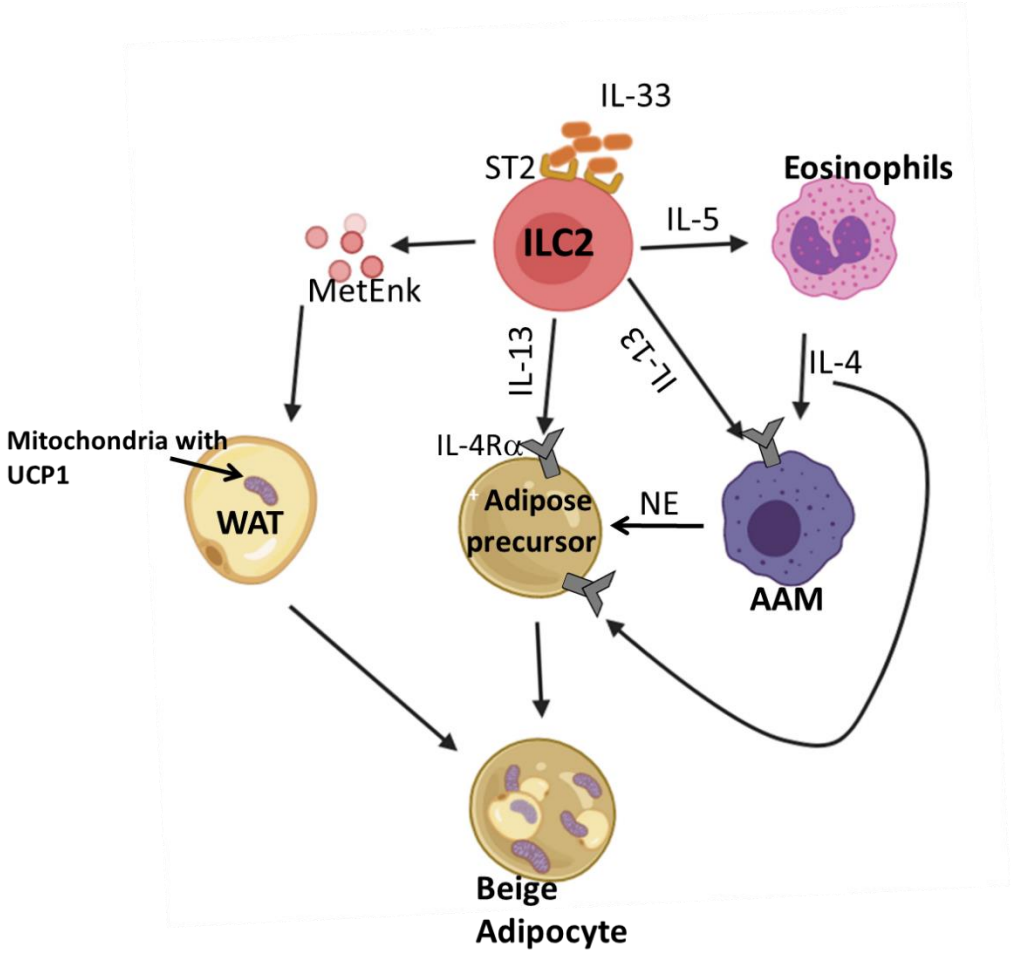

1.3 Immune Responses to Helminth Infections

1.3.1 Helminth Infections: Introducing *Heligmosomoides polygyrus* and *Schistosoma mansoni*

Helminths are parasitic worms that can be classed into two major phyla: the nematodes (or roundworms) which include intestinal worms (also called soil-transmitted helminths), filarial worms and onchocerciasis; and platyhelminthes (or flatworms) that include the trematodes such as schistosomes, and tape worms (also known as cestodes) (Hotez et al., 2008). Infections caused by intestinal helminths and schistosomes pose a major global problem, accounting for one of the most common infectious agents in developing countries, and attributing to high rates of morbidity in both humans and livestock (Reynolds et al., 2012). Furthermore, these infections can impede the mental and physical growth of children as well as their educational progress, as such become detrimental to economic development (Hotez et al., 2006). Helminths have also co-evolved with and become well adapted to their definitive host (Maizels et al., 2012). Nonetheless different model organisms exist that can be used to study mechanisms of immunity to helminths as well as of resistance by these parasites.

Heligmosomoides polygyrus (H. poly) is a naturally occurring intestinal nematode in wild mice. Infection begins with its infective L_3 larvae ingested by feco-oral transmission or administered in a laboratory setting by oral gavage. Within 24 hr of ingestion, its larvae penetrates through the wall of the small intestine (SI) to the submucosa where they undergo two molts, before returning to the gut lumen as adult worms by approximately day 8 (Johnston et al., 2015). Adult worms feed on intestinal tissue, coil around SI villi, and by day 10, mate and produce eggs that are then excreted in the faeces. Eggs hatch in the

external environment, producing larvae and undergoing two molts to become infective L_3, thereby continuing their life cycle (Reynolds et al., 2012). Immune response to *H. poly* is characterised by a strongly polarised type 2 response induced initially by innate immune cell derived IL-4, IL-5, and IL-13 (Urban et al., 1991b, Finkelman et al., 1997, M. Webb and D. Tait Wojno, 2017). Adaptive immunity then provides Th2 effector cell population that minimises pathology with contributions from the B cell compartment (Maizels et al., 2012). However *H. poly* can also exert immunomodulatory functions via a number of mechanisms including the expansion of Tregs, inhibiting DC responsiveness to stimulation and IL-33 blockade (Johnston et al., 2015), thereby conferring its resistance to host immune responses, and enabling the establishment of chronic infections in susceptible host that can persist for decades (M. Webb and D. Tait Wojno, 2017). Due to its close resemblance to highly-prevalent human hookworms and intestinal nematodes of livestock (Maizels et al., 2012), *H. poly* is therefore useful in understanding host-parasite interactions.

Schistosoma mansoni (S. mansoni) is one of the three most common parasitic blood flukes that can infect humans leading to schistosomiasis, a chronic and tropical lethal disease infecting hundreds of millions of people annually (Pearce and MacDonald, 2002). The schistosome life cycle involves a mammalian host as well as secondary snail vectors. The infectious larvae known as cercariae (cerc for short) enter human host via the skin and migrate through the body's tissues and through the blood circulation as schistosomula that grow into schistosomes and adult worms. Adult worms reside in specific locations depending on the type of schistosome species (Nelwan, 2019). In particular, *S. mansoni* adult worms are located deep within the mesenteric vasculature of the large or small intestine, where they acquire nutrients from the blood needed for their growth, maturation and egg production.

Following mating, about 300 eggs can be produced daily by each worm pair; eggs then migrate from the mesenteric vessels, through the intestinal wall and are released into the external environment through urine or faeces. Eggs can then hatch in fresh water to infect their successive snail vectors (Costain et al., 2018). Similar to *H. poly*, schistosomes largely induce polarised Th2 responses; however the manifestation of *S. mansoni* can occur in two fold. Early stages which occur within 4-5 weeks post infection is characterised by an acute disease with a mixed, low level Th1/Th2 response, and occurs prior to the appearance of eggs in the faeces. While chronic diseases (which include intestinal, hepatointestinal and hepatosplenic forms) occur later in the *S. mansoni* life cycle, from the point of egg production at ~5-6 weeks post infection and are characterised by more prolonged Th2 responses and angiogenesis (Costain et al., 2018). Schistosomes can thrive in their host for many years with some individuals developing life-threatening illness such as hepatosplenic schistosomiasis (Pearce and MacDonald, 2002).

1.3.2 ILC2s and *Heligmosomoides polygyrus* Infection

Primary infection with *H. poly* leads to IL-5 production (Finkelman et al., 1997); in addition IL-4, IL-5, IL-10 and IL-13 release from lamina propia (LP) mononuclear cells and SLOs following *H. poly* infection has been observed (Rausch et al., 2008, Setiawan et al., 2007). IL-4, IL-5 and IL-13 are associated with B cell activation and expression of IgE and IgG1 (M. Webb and D. Tait Wojno, 2017). Elevated serum IgE along with increased mucosal mast cells and eosinophilia are components of type 1 immediate hypersensitivity typically induced by helminths (Urban et al., 1991b). However Urban and colleagues revealed that treating *H. poly* infected mice with anti-IL-4 monoclonal antibody (mAb) or a combination of anti-IL-4 and anti-IL-5 significantly reduced the rise in serum IgE production. Furthermore, later

studies by the same group reported that WT and SCID (severe combined immunodeficiency disorder) mice infected with *H. poly* had considerable reduction in egg production following an IL-4/anti-IL-4 mAb complex (IL-4c), which maintained *in vivo* activity of IL-4 significantly longer compared to IL-4 alone. Authors further found that such effects could be abolished using an IL-4R blocking mAb (Urban et al., 1995). These studies thereby highlighted the importance of IL-4 in contributing to immune mechanisms that prevented the fecundity and survival of adult nematodes in infected mice.

However, it was not until years later that ILC2s were found to be the key *in vivo* source of IL-4 during Th2 immune responses to *H. poly* (Pelly et al., 2016). By infecting WT C57BL/6J mice with *H. poly*, researchers not only showed the increased expression of IL-33 as well as Th2 cytokines IL-4, IL-5 and IL-13, but also the expansion of ILC2s in the SI and mLNs, and CD4 Th2 cells as early as 5 days post infection. This therefore demonstrated the early activation of both innate and adaptive type 2 response during *H. poly* infection. Next, using IL-4-GFP reporter mice which correlated with IL-4 protein secretion, activated ILC2s were found to transcribe IL-4-GFP (as well as IL-2 protein) with numbers increasing significantly following *H. poly* infection. Moreover, naïve T-cells differentiated into IL4-GFP^{+} Th2 cells when cultured with supernatant from *H. poly* elicited ILC2s. These results therefore suggested that ILC2-derived IL-4 could drive Th2 differentiation with IL-2 needed for optimal differentiation *in vitro* (Pelly et al., 2016). However, ILC2s were only observed to provide partial protection from *H. poly,* owing to the large number of worms persisting even after the expansion of ILC2s with IL-2:anti-IL-2 cytokine complex (i.e. IL-2c treatment). Thus, it was proposed that ILC2s may be supporting development of the adaptive immune response to *H. poly* instead. Furthermore, LTD_4 was found to be important for the release of

IL-4 by ILC2s. As mast cells are an important source of LTD_4, researchers went on to propose a model of action whereby mast cells activated by tissue damage-associated IL-33, released LTD_4 that subsequently activated ILC2s (Pelly et al., 2016), likely mediated via the receptor CysLT1R whose expression on lung ILC2s had been previously discovered (Doherty et al., 2013). The resulting secretion of IL-4 could thereby drive Th2 differentiation (Pelly et al., 2016) - figure 1.7. Apart from IL-4 production, ILC2-derived IL-5 and IL-13 mediate eosinophil recruitment and goblet cell hyperplasia respectively, both of which are critical to helminth expulsion (M. Webb and D. Tait Wojno, 2017), thereby underpinning the importance of ILC2s, which through their accumulation and production of Th2 cytokines promote early responses to *H. poly* at the site of infection.

Figure 1.7: ILC2-derived IL-4 supports Th2 cell differentiation during *Heligmosomoides polygyrus* infection

During *H. poly* infection, tissue damage induces the release of IL-33 that activates mast cells through its interaction with the ST2 receptor. In response, mast cells release leukotriene D4 (LTD_4) which stimulates ILC2s to secret IL-4, thereby promoting Th2 differentiation.

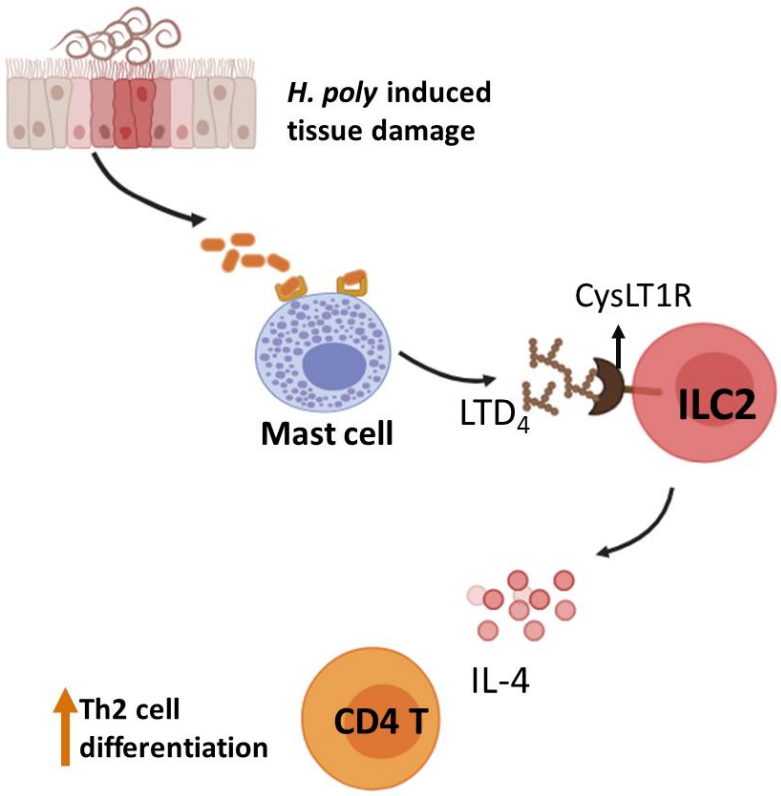

1.3.3 Immune Responses to *Schistosoma mansoni*

The antigenic potential of schistosomes is attributed to the eggs laid by female worms rather than the adult parasites themselves. During their transit to the external environment a large number of eggs become lodged in the liver, intestine or bladder of the definitive host, where they induce granuloma formation via the action of proteolytic enzymes, generate extracellular matrix (ECM) and cause proliferation of fibroblasts (Costain et al., 2018, McManus et al., 2020).

Inflammatory granulomas that encapsulate parasitic eggs are highly organised structures and characterised by AAMs, eosinophils, mast cells, Th2 cells and associated Th2 cytokines, as well as an ECM component (Costain et al., 2018), reaching a peak response by week 7-8 (Pearce and MacDonald, 2002). Findings by Jankovic and colleagues showed that mice lacking IL-4Rα and as such are unresponsive to IL-4 and IL-13, failed to induce characteristic egg-induced pathology and fibrosis, instead developing smaller granulomas with diminished eosinophil and mast cell content, despite normal T cell infiltration (Jankovic et al., 1999), which suggested that active signalling through IL-4Rα was needed to support granuloma formation. Studies employing macrophage/neutrophil-specific IL-4Rα deficient mice went on to show alternative macrophage (but not neutrophil) activation to be impaired during acute schistosomiasis accompanied by enhanced mortality due to liver and intestinal damage, sepsis, and increased Th1 cytokine and NOS-2 activity (Herbert et al., 2004). This thereby highlighted the importance of IL-4 and IL-13 in driving macrophages towards an anti-inflammatory M2 phenotype, and the need of these immune cells for the resolution of egg-induced inflammation and repairing damaged tissues, also confirmed in other reports (Barron and Wynn, 2011). Nonetheless, over time granulomas acquire a fibrotic ECM

mediated by the action of IL-13 (Fallon et al., 2000); in excessive amounts this can prevent blood flow through the liver, leading to portal hypertension (Gause et al., 2003), thereby labelling the once protective granuloma a double-edged sword.

The acute stage of *S. mansoni* infection is dominated by a Th1 response (Pearce and MacDonald, 2002), triggered primarily by larval antigens (Pearce et al., 1991). Very early studies revealed the presence of Th1 cytokines, IFN-γ and IL-2 in splenic supernatants of mice infected with either *S. mansoni* worm or egg antigens, that persisted up to 6 weeks post infection, with no input from Th2 cytokines (Grzych et al., 1991). Further studies went on to also reveal that the induction in Th2 responses from week 6-8 post infection coincided with the downregulation of IFN-γ and IL-2 (Pearce et al., 1991), suggesting a transition to different CD4 subsets, and also shown to be driven by egg deposition (Grzych et al., 1991). Similarly, in humans with acute schistosomiasis, high levels of IL-6, IFN-γ and TNF-α are detected in the PBMC supernatant as well as elevated levels of serum TNF-α in majority of patients, compared to those with chronic disease (de Jesus et al., 2002). In contrast individuals with chronic disease present with higher levels of IL-4 mRNA, and IL-5 in PBMC supernatants stimulated with soluble worm antigenic preparations (Araújo et al., 1996), while having low levels of IFN-γ (de Jesus et al., 2002). IL-4 and IL-5 are associated with the induction of IgE and eosinophil production respectively, both important in protection against re-infection (Colley and Secor, 2014).

Downregulation of Th1 responses is likely to be mediated by the immunosuppressive cytokine IL-10. Using *in vitro* experiments Sher and colleagues successfully demonstrated the suppression of IFN-γ by IL-10 produced in large amounts by schistosome-infected mice (Sher et al., 1991), as further observed by others (de Jesus et al., 2002, Flores Villanueva et al.,

1993) and also in human studies (King et al., 1996). However while IL-10 is responsible for controlling acute inflammation, it has been shown to be redundant in the down-modulation of hepatic granuloma formation during the chronic stage of disease (Wynn et al., 1998) thereby suggesting the involvement of other immune regulators. Indeed, other mechanisms including antibodies, immune complexes, adherent macrophage-like cells, Tregs and TGF-β, and anti-idiotypic responses have been implicated in modulating pathologies associated with schistosomiasis disease progression (Colley and Secor, 2014).

1.4 Peritoneal Cancer Metastasis

1.4.1 The Tumour Microenvironment

Tumours are highly complex and heterogeneous structures, consisting of diverse interactions between malignant and non-malignant cells; the latter of which include activated fibroblasts, immune cells, adipocytes, the ECM, neuroendocrine cells, epithelial cells, blood and lymphatic endothelial cells, which collectively are known as the tumour microenvironment (TME – figure 1.8) (Lawler, 2009, Wei et al., 2020). Furthermore the involvement of cytokines, chemokines, growth factors, inflammatory and matrix remodelling enzymes that surround these cells (Balkwill et al., 2012) along with physical and chemical factors such as fibrosis, low pH and hypoxia add another layer of complexity to the TME (Wei et al., 2020). According to Wang and colleagues ten major characteristics of cancer exist; unlimited multiplication, escape from growth suppression, evading apoptosis, promoting invasion and metastasis, enhanced angiogenesis, maintaining proliferative signalling, elimination of cell energy limitation, escape from immune destruction, increased genomic instability and

mutation, and tumour enhanced inflammation (Wang et al., 2017a). Indeed the cellular and non-cellular components of the TME contribute to tumorigenesis, the acquisition of these characteristics, and subsequent tumour progression as well as drug resistance (Guo and Deng, 2018).

A plethora of immune cells are enriched within the TME, recruited and activated by cytokines and chemokines secreted by cells also within the TME. These include tumour infiltrating lymphocytes (TILs) such as CD8 CTLs, Th1 cells and NK cells, that collectively with M1 macrophages and APCs (namely DCs) mediate anti-tumour effects. Conversely, other immune cells can facilitate tumour cell intravasion and the formation of pre-metastatic niches (Lawler, 2009, Wei et al., 2020). Myeloid cells, in particular macrophages, make up a large proportion of tumour-associated leukocytes and have been reported to promote multiple aspects of tumour progression, including angiogenesis, metastasis, cancer cell proliferation and invasion, and as such immune evasion (Kiss et al., 2018). These are often referred to as tumour associated macrophages (TAMs) and have an IL-12^{low} IL-10^{high} immunosuppressive phenotype and express a number of markers including mannose receptor (CD206), and scavenger receptor class A (SR-A, also known as CD204, or CD163). Their presence in the TME is often associated with poor prognosis (Balkwill et al., 2012). Similarly, tumour associated neutrophils (TANs), while more controversial, are observed to promote angiogenesis, tumour growth and metastasis as well as ECM remodelling in response to ectopic secretion of IL-8 by tumour cells (De Larco et al., 2004). Another inhibitory myeloid population known as myeloid-derived suppressor cells (MDSCs) exists. Though their surface makers often overlap with those used in characterising monocytes and neutrophils, MDSCs have more potent T cell suppressive capacity, promote the polarisation

of macrophages to a TAM-like phenotype and can differentiate into TAMs themselves (Balkwill et al., 2012, Kiss et al., 2018). Of the CD4 T cell subsets, Tregs are well known to promote cancer progression through contact-dependent and independent mechanisms including production of suppressive cytokines TGF-β and IL-10, expression of inhibitory receptors and immune checkpoint molecules (e.g. PD-1 CTLA-4,) and the induction of tolerogenic DCs (Chaudhary and Elkord, 2016).

Stromal cells have also been implicated in the progression and maintenance of cancers. Fibroblasts represent the dominant portion of the stroma in the TME and of these, a subpopulation of activated fibroblasts known as cancer associated fibroblasts (CAFs) or myo-fibroblasts arise in cancerous wounds and remain continually activated (Guo and Deng, 2018, Wang et al., 2017a). They are reported to promote tumour invasion and metastasis via their secretion of cytokines and growth factors including CXCL12, IL-6, vascular endothelial growth factor A (VEGFA), and promote ECM remodelling (Guo and Deng, 2018). However CAFs are highly heterogonous and plastic, as such reported to also have tumour suppressive effects (Wei et al., 2020).

It is becoming increasingly evident that AT plays a role in cancer progression, most likely supported by the fact that increased obesity has been associated with increased risk and aggressiveness of certain cancers as well as cancer related mortality (Lengyel et al., 2018). Firstly, obese AT is associated with a chronic pro-inflammatory microenvironment as a result of pro-inflammatory proteins such as IFN-γ, IL-1β and TNF-α, that favour tumour cell motility, invasion, metastasis as well as the self-renewal capability of cancer stem cells (Gilbert and Slingerland, 2013). Secondly, adipose cells secrete more than 50 different cytokines, chemokines and hormone-like factors, whose levels become altered during

obesity. In particular the disruption of normal adipocyte maturation causes increased leptin secretion from accumulated pre-adipocytes, while adiponectin levels decrease (Gilbert and Slingerland, 2013), leading to altered leptin/adiponectin ratio that can promote cancer cell proliferation as is reported for breast cancer (Grossmann et al., 2010). Furthermore, mesenchymal stromal cells of WAT known as adipocyte stromal cells (ASCs) which are abundant in WAT and proliferate in obesity, migrate to tumours where they can lead to proliferation of adjacent cancer cells, and secret chemokines that recruit immune cells with tumour promoting roles (Lengyel et al., 2018). ASCs are also noted to promote angiogenesis, and can themselves differentiate into cancer associated cells, such as fibroblasts that promote tumour proliferation (Wang et al., 2017a). More importantly to our project, peritoneal ATs are reported to be frequent sites of tumour metastasis and adipocytes have been noted to actively aid in this process as is discussed in the next sections.

Figure 1.8: The tumour microenvironment is a complex interplay of immune and stromal cell components

The interactions between multiple cellular and non-cellular components that occur within the TME. Dendritic cell (DC); natural killer (NK cell); cancer associated fibroblast (CAF); extra cellular matrix (ECM).

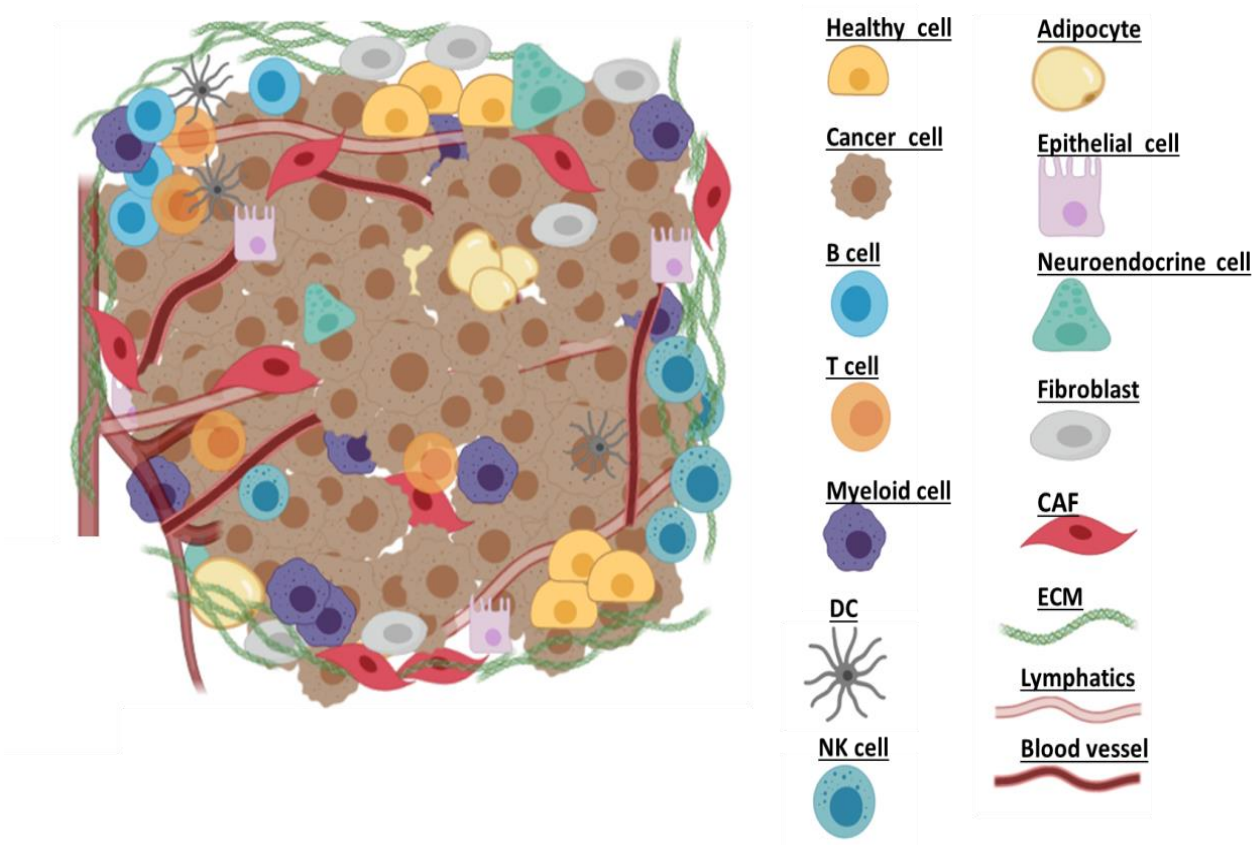

1.4.2 Understanding Peritoneal Tumour Metastasis: Colon and Ovarian Cancers

Colon and ovarian cancer patients as well as animal models for these diseases have revealed that tumour cells often localise to the peritoneal cavity, forming metastasis in omental and mesenteric FALCs/milky spots (Gerber et al., 2006). Such metastatic dissemination can occur via direct intraperitoneal seeding, in which cells dissociate from the primary tumour, become transported throughout the abdomen via the natural flow of the peritoneal fluid and attach to peritoneal surfaces (Lee et al., 2018, Gerber et al., 2006). Indeed, the notion that peritoneal cells and particulates could passively enter the omentum had been noted by other studies (Rangel-Moreno et al., 2009). Though immune aggregates within the omentum appear to be the preferential site of tumour attachment, the peritoneal ligament, mesenteries and together with the omentum all serve as boundaries and conduits for disease spread (Healy and H Reznek, 1998).

Colon cancer is the third most common occurring cancer and is ranked second in terms of cancer mortality, with over 1.8 million new cases in 2018 for instance (Bray et al., 2018, Rawla et al., 2019). It is a multistep adenoma-carcinoma sequence resulting from gene mutations that is further promoted by activating mutations of oncogenes and inactivating mutations of tumour suppressor genes (Brenner et al., 2014). Microsatellite and chromosomal instability, epigenetic mutations and environmental factors can contribute further to carcinogenesis (Tabuso et al., 2017). The peritoneum is reported to be the second most common site for colon cancer metastasis resulting in poor patient prognosis (Aoyagi et al., 2014). In animal models intraperitoneal (ip) injection of a CC531 colon cancer cell line into rats led to the spread of tumour cells throughout the abdominal cavity as early as 3 days post injection, residing on the mesenteries and becoming concentrated in omental milky

spots, with the latter being completely replaced by tumour cells (Lopes Cardozo et al., 2001). Adipose secreted factors such as lipid metabolites and adipokines are likely to mediate colon cancer proliferation. Using a three dimensional collagen gel culture system, isolated mature adipocytes and pre-adipocytes from leptin deficient or WT mice were found to support the growth of a number of colon cancer cells lines *in vitro*. This was partially dependent on leptin with higher levels of this adipokine observed to have more potent proliferative effects on colon cancer cells (Amemori et al., 2007). Within the TME chemokines readily released by the host immune cells or cancer cells can further impact on cancer metastasis and progression. CXCL13-CXCR5 signalling for instance has been implicated in colon cancer metastasis. CXCL13 is a B cell attracting chemokine which binds the cognate receptor CXCR5. CXCL13 was not only found to stimulate the growth of human colon cancer cell lines in a dose dependent manner, but also their migration and invasion, via its upregulation of metalloproteinase – essential factors involved in the metastasis of colon cancer. In addition, a range of human colon cancer cell lines were observed to express CXCR5 – with the SW620 cell line having the highest. However, knockdown of CXCR5 by siRNA inhibited the growth, migration and invasion of colon cells (Zhu et al., 2014), thereby highlighting the role of the CXCL13-CXCR5 interaction in promoting colon cancer metastasis.

Ovarian cancer is the third most common gynaecologic cancer, accounting for the highest mortality rate, with majority of patients diagnosed with advanced-stage disease (Kurnit et al., 2021, Momenimovahed et al., 2019). Carcinomas can originate from the surface of the ovarian epithelium, the fallopian tube epithelium and the mesothelium-covered surfaces of the peritoneal cavity (Lengyel, 2010). While intraperitoneal seeding of ovarian cancer cells does occur, alternative routes of metastasis exist, owing to the presence of circulating

tumour cells in the omental vasculature (Pradeep et al., 2014). Researchers showed that ovarian cancer cells could spread hematogenously (i.e. carried via the blood) with a selective preference for the omentum. This was found to be dependent on ErbB3-neuregulin 1 (NRG1) axis. ErbB3 which is a member of the epidermal growth factor receptor family was found to be overexpressed on ovarian cancer cells, and induced tumour localisation to the omentum which expressed higher levels of the partner ligand NRG1 compared to other tissues (Pradeep et al., 2014). Furthermore, the vasculature within omental and mesenteric immune aggregates display unique characteristics that promote tumour localisation. Using the ID8 ovarian tumour cell line, ip injection of tumour cells was found to result in selective and abundant tumour growth within mice omentum, along with smaller foci within the mesenteries compared to the absence of tumours at other sites examined including liver, lungs and kidneys (Gerber et al., 2006). This further highlighted the peritoneum as a selective site of attachment as well as for transport of tumour cells. In addition, gene array analysis of omental immune aggregates revealed the expression of CD105 on associated blood vessels (Gerber et al., 2006). CD105 is expressed on proliferating endothelial cells undergoing angiogenesis and has been reported to mark the formation of newly formed tumour vessels in the prostate (Wikström et al., 2002), suggesting a possible similar role in ovarian cancer. In support of this, collagen IV indicative of neovascularization (i.e vascular sprouting) could be detected on vessels in the immune aggregates but not in areas outside, as well as the proangiogenic gene VEGFA (Gerber et al., 2006), further indicating the pro-angiogenic state of vessels within these aggregates. Later studies by the same group again using ID8 ovarian cell line, report that VCAM-1^{+} mesothelial cells may be involved in

initiating adhesion of tumour cells, further mediated by the network of collagen I fibres found to overlay omental immune aggregates (Sorensen et al., 2009).

Meanwhile, others have shown that primary human omental adipocytes themselves promote homing of ovarian cancer cells. Here the secretion of the adipokine IL-8 (Nieman et al., 2011), a pro-inflammatory cytokine implicated in angiogenesis, proliferation and survival of cancer cells due to its activation of multiple intracellular signalling pathways (Waugh and Wilson, 2008), was found to attract cancer cells. In addition, omental and peritoneal adipocytes were shown to provide fatty acids to ovarian tumours via lipolysis and β-oxidation, thereby acting as an energy source that fuelled tumour growth (Nieman et al., 2011). Finally, recruitment of neutrophils which mobilised into the abdominal cavity through high endothelial venules in omental milky spots was also reported to be an essential step that occurred before the colonisation of the immune aggregates by ovarian cancer cells. In particular, inflammatory factors including IL-8, monocyte chemoattractant protein-1, CXCL1 and CXCL2 derived from the tumour led to extruded chromatin fibres described as 'neutrophil extracellular traps'. This phenomenon appeared prior to metastasis in murine models and in early-stage ovarian cancer patients, with traps observed to bind ovarian cancer cells, thereby promoting metastasis (Lee et al., 2018).

1.4.3 Role of IL-33 in Colon and Ovarian Cancers

As mentioned in previous chapters, FALC stromal cells express a number of chemokines and cytokines, one of which being IL-33, a cytokine that signals through the ST2 receptor, and can also function as an alarmin in response to tissue damage and/or stress. While the involvement of IL-33/ST2 in cancer formation has been reported by different authors, these have included both protective and detrimental effects.

In a model of invasive colon cancer using the MC38 colon cancer cell line, elevated IL-33 expression was found to correlate to high liver metastasis, suggesting a possible similar role of IL-33 in peritoneal metastasis. Tumour-derived IL-33 was also shown to drive MDSCs and macrophage recruitment leading to remodelling of the TME (Zhang et al., 2017b). Using a different murine model known as $APC^{min/+}$ mice - an animal model of human colon cancer whereby mutations occur in the adenomatous polyposis coli tumour suppressor gene, leading to multiple intestinal neoplasia – increased IL-33 expression in the gut epithelium was observed to enhance tumour development. This was facilitated via IL-33-mediated expansion of $ST2^{+}$ Tregs, increased Th2 cytokine milieu as well as the activation of AAMs in the colon (He et al., 2017), all characteristics known to be tumour-enhancing. More recent studies have further revealed that ST2 upregulation on Tregs induced by IL-33 leads to phenotypic changes in Tregs, causing them to become more activated and migratory, and hence home to tumours. Additionally, Tregs inhibited Th17 differentiation and prevented CD8 T cell accumulation in murine colon (Pastille et al., 2019). IL-33 expression can also be observed in colorectal cancer patients, both in blood and tumour lesions (He et al., 2017, Pastille et al., 2019); thereby suggesting similar mechanisms could exist in humans. Indeed others have observed the expression of IL-33 specifically in vascular endothelial cells and tumour cells in human colon cancer, which associated with poor patient survival and increased metastasis (Fang et al., 2017).

IL-33 activation of c-Jun N terminal kinase (JNK) signalling pathways has been implicated in ovarian cancer; compared to normal ovarian tissue and benign tumours, IL-33 and ST2 are significantly upregulated in metastatic ovarian cancers of the epithelial origin (EOCs), accompanied by increased Ki67 expression indicative of tumour cell proliferation, but

reduced patient survival time. Mechanistically, IL-33 signalling increased extracellular signal-regulated kinase (ERK) and JNK phosphorylation, with blockade of these pathways preventing EOC cell migration, invasiveness, proliferation and cell viability (Tong et al., 2016). Other modes of IL-33 tumour promoting effects have been reported to involve the inhibition of apoptosis of ovarian cancer cells through the downregulation of P27, Fas cell surface death receptor and tumour necrosis factor-related apoptosis-inducing ligand receptor 1 (TRAILR1) (Liu et al., 2019). However in the same year, a different laboratory reported of the anti-tumorigenic effects of IL-33, noting that IL-33 overexpression in ID8 mouse EOC cell lines prolonged the survival of immunocompetent mice by reducing infiltration of $CD11b^{+}GR1^{+}$ MDSCs, while promoting increased CD4 and CD8 T cell recruitment (Sekiya et al., 2019). However, this effect was demonstrated in the context of peritoneal carcinomatosis, a common feature of advanced stage EOCs whereby secondary tumours develop within the peritoneal cavity. Likewise, O'Donnell and colleagues showed a negative correlation between tumour grade and an isoform of the IL-33 receptor known as ST2L in human colon tumours. Researchers went on to find that reduced ST2 expression on CT26 murine colon cancer cells enhanced tumour growth *in vivo*, in part contributed by the lack of tumour-expressing IL-33, macrophage chemotactic factors and subsequent reduction in macrophage infiltration (O'Donnell et al., 2015). Taken together, these rather conflicting reports of pro- and anti-tumorigenic effects of IL-33/ST2 signalling highlight the fact that a clear role for this axis in tumour progression remains elusive, as such warrants further investigation.

1.4.4 Current Therapy for Treatment of Metastatic Colon and Ovarian Cancers

Colon and ovarian cancers account for about 7% and 46% of disease causing peritoneal metastasis respectively, with such metastasis often present at advanced or late stages of the disease (Desai and Moustarah, 2020). Usually, complete cytoreductive surgery of primary tumour or metastatic deposits to reduce cancer cell load and hence minimise immunosuppressive tumour burden as well as prevent complications (Bell et al., 2018), in combination with hyperthermic intraperitoneal chemotherapy and systematic chemotherapy are mainstay treatments (Desai and Moustarah, 2020).

For advanced staged colon cancer, palliative chemotherapy which serves to prolong patient survival rather than cure the disease, is often provided, with fluorouracil being the standard drug of choice for over 40 years (Young and Rea, 2000). Fluorouracil is a synthetic fluorinated pyrimidine that acts by causing the replacement of thymidine with fluorinated nucleotide into the DNA, thereby inhibiting DNA replication and leading to cell death (Van der Jeught et al., 2018). However, a shift to combination and/or sequential combination therapy proved to be more efficacious, as newer chemotherapeutic agents such as capecitabine, irinotecan and oxaliplatin were developed (Venook, 2005). Furthermore, target specific therapies have been approved by the FDA, owing to the need for agents that could be directed specifically at processes involved in tumorigenesis and metastasis. These include mAbs such as anti-VEGF (bevacizumab), and a human epidermal growth factor receptor (HER-1/EGFR)-targeted mAb (cetuximab) (Venook, 2005). Yet, such chemo- as well as targeted therapies offer limited increase in overall survival of patients with a less than 10% survival rate in those with stage IV (i.e metastatic) colon cancers, largely due to therapy resistance (Van der Jeught et al., 2018).

Meanwhile in advanced stages of ovarian cancer (noted as International Federation of Gynaecology and Obstetrics (FIGO) II-IV), the standard of care involves primary debulking surgery (PDS) in those whereby complete or optimal cytoreduction can be achieved (i.e. residual lesions <1 cm), as this ensures higher chance for patient survival (van der Burg, 2001). The platinum-based chemotherapy agent such as cisplatin or carboplatin (with or without a taxane e.g. paclitaxel) can then be offered as a post-operative cytotoxic therapy, with combined effect of both seeming to prove more superior (Fotopoulou et al., 2017). In some patients whereby cytoreductive surgery is suboptimal and disease is very advanced, 3-4 cycles of neoadjuvant chemotherapy (NACT) may be performed followed by interval debulking surgery (IDS) (Berek et al., 2018). However, two randomized prospective trails showed that in some patients with stage III or IV ovarian cancer, NACT prior to IDS, did not lead to greater benefit when compared to those receiving PDS (Kehoe et al., 2015, Vergote et al., 2010). Similarly to colon cancer, the addition of bevacizumab to chemotherapy and then as a maintenance therapy is reported to significantly increase progression free survival (Fotopoulou et al., 2017). Nonetheless and again, the survival rate of patients dramatically decreases in advanced stages of ovarian cancer, with the 5-year relative survival ranging from between 30% and 40% at stage III to below 10% at stage IV (Huang et al., 2018b). These statistics therefore continue to prompt the need for more in-depth characterisation of metastatic tumours, as well as the assessment of immune cells within sites of metastasis, such as peritoneal ATs, including their possible re-programming to drive anti-tumour responses.

Figure 1.9: Anatomical location of the murine omentum and mesenteries, as well as human omentum.

A) In mouse, the mesentery (blue lines) is a double layered fold of peritoneum that is attached to the small and large intestine (Int), as well the colon (Moro et al., 2015).

B) Murine omentum (Om) is a thin layer of fat that wraps around the stomach (Stm), and can be attached to the spleen (Spln) and pancreas (Berberich et al., 2008).

C) Human omentum is a significantly large fold of visceral peritoneum that hangs over the abdominal organ.

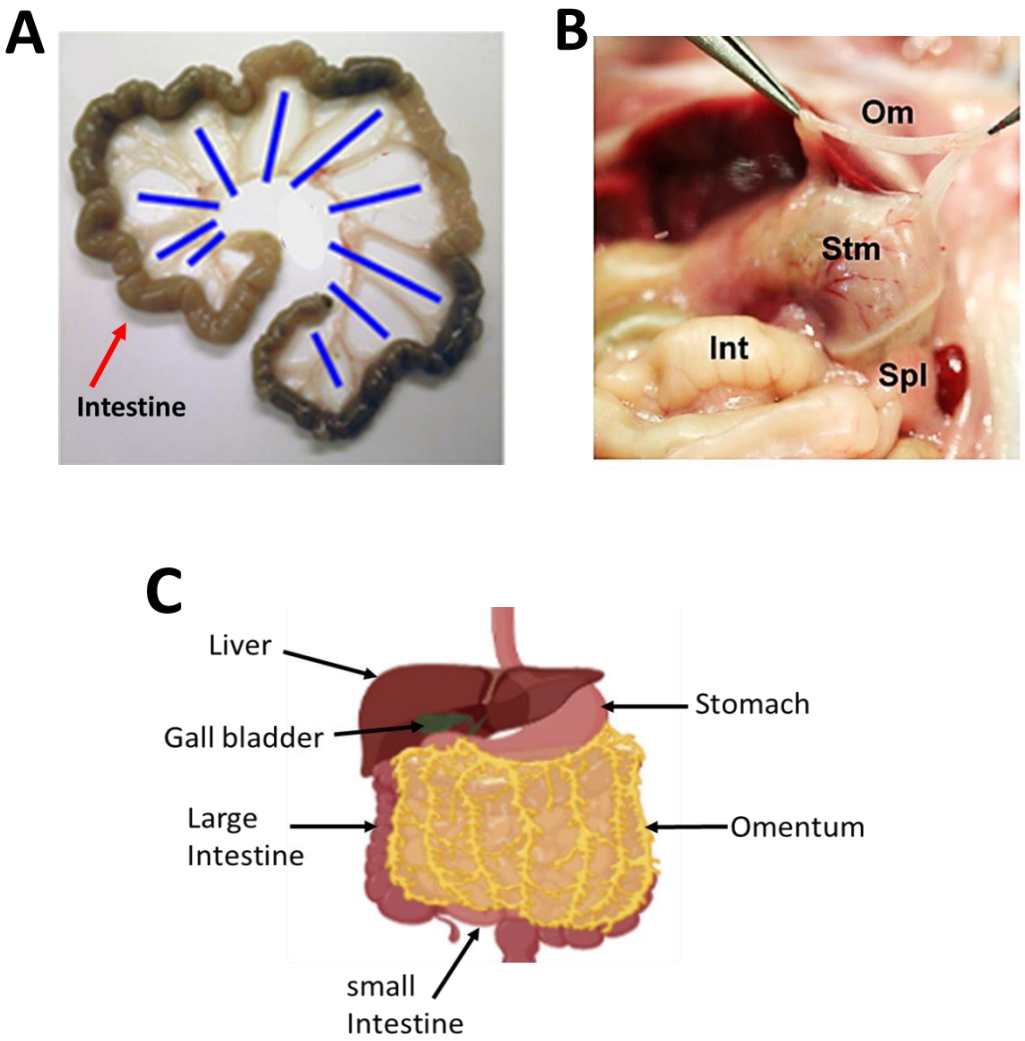

1.5 Project Aims and Objectives

As a dynamic, metabolically active organ, the contribution of AT in the regulation and maintenance of health, as well as its role in disease is being increasingly recognised. Importantly the host of immune cells within this tissue facilitates its diverse functions. Central to our study are the highly vascularised clusters of innate, adaptive and stromal cells within VATs known as FALCs. As such the aim of this project was to investigate the role of VAT FALCs (in particular mesenteric and omental FALCs) in mediating immune responses during two immunologically distinct disease states – helminth infection and cancer metastasis. Therefore, the objectives of this investigation were as follows:

1) To characterise the immune cell composition within VATs at steady state, including the phenotypic and functional profile of immune cells pivotal to our helminth infection model, namely ILC2s.
2) To investigate whether VAT FALCs can respond to helminth infections occurring in their surrounding tissue, by assessing the recruitment of immune cells to VATs, their phenotype and activation status, following infection.
3) To analyse the immune cell composition of VAT FALCs during metastatic tumour formation in murine models of colon cancer, as well in human samples of metastatic high-grade serous ovarian cancer.

CHAPTER 2: MATERIALS AND METHODS

2.1 Mice

All mice used were bred on the C57BL/6J background and maintained within a specific-pathogen free environment at the University of Birmingham Biomedical Services Unit, Birmingham, U.K. *Il33*$^{-/-}$ mice, a knock-in reporter strain carrying the gene encoding Citrine in the *Il33* locus, was received as a kind gift from Prof. A McKenzie, MRC LMB, Cambridge (Hardman et al., 2013). *Il5*$^{tm1.1(Cre)Lky}$ tdtomato (Red5) mice, an IL-5 reporter, in which endogenous *il5* gene has been replaced with tdTomato, thereby resulting in red fluorescence by IL-5 expressing cells, was generated by the Locksley group (Nussbaum et al., 2013). In addition, IL-4-IRES-eGFP (4get) reporter mice on a C57BL/6J background (B6.4get), used in tracking IL-4 expressing cells was also generated by the Locksley group (Mohrs et al., 2001). Finally WT mice were maintained in-house, and experiments conducted according to the Home Office personal licence regulations, as well as the Home Office Project licence of my co-supervisor Dave Withers for the *H.poly* infections.

2.2 Human Subjects

Omental samples were collected from patients with stage III/IV high-grade serous ovarian cancer (HGSOC) at City hospital, Birmingham, U.K, following informed consent according to the institutional tissue collection protocol. Samples included patients who had undergone neoadjuvant chemotherapy (NACT), as well as those who had not received treatment prior to surgery. Control samples were also supplemented via collection of healthy omentum from the Human Biomaterials Resource Centre (HBRC), University of Birmingham. Access to human tissues was approved by the HBRC and NHS REC (HBRC app 18-323 and 11-049) and IRAS 225991. Furthermore, patient information was anonymised and given a sample

identifier number to allow for future identification, and aid in cross-checking for final histology classifications.

2.3 Murine Experiments

2.3.1 Infection of mice with *Heligmosomoides polygyrus*

H. poly L_3 larvae were first counted using a dissecting microscope (Leica), and mice were infected with 200 larvae (or 200 µl PBS for controls) by oral gavage. Mesenteric and omental adipose tissues (ATs), mesenteric lymph nodes (mLN) and small intestine (SI) were harvested 7 days post infection. Worm burden within the intestinal wall were visible under a dissecting microscope (Leica) and thereby counted.

2.3.2 Infection of mice with *Schistosoma mansoni*

This work was done in collaboration with the group of Andrew MacDonald at the University of Manchester, who kindly maintained the parasite life-cycle and carried out infection of the mice. *Biomphalaria glabrata (B. glabrata)* freshwater snails infected with *Schistosoma mansoni (S. mansoni)* were obtained from Professor Karl Hoffmann (Aberystwyth University). *B. glabrata* snails were kept in pond water under a heat lamp for 50 min in order to allow shedding of cercariae from patent *S. mansoni* infected *B. glabrata* snails. Cercariae was then diluted with Lugol's iodine solution at a ratio of 1:1 and counted under a dissection microscope. For infection, C57BL/6J female mice were first anaesthetised with a solution containing 0.01 ml/g of 0.25 ml Domitor (Janssen) and 0.19ml Vetalar (Pfizer) made up in 2.6 ml PBS (Sigma). Next, mice were fastened to a pre-heated pad and their abdomen shaved. A stainless steel ring was then placed onto the shaved abdomen, 200 µl of pond water was added into the ring, followed by the addition of 40 or 180 cercariae into the ring and finally

another 200 µl of pond water, thereby sandwiching the cercariae between the pond water. Cercariae were left on the mice for 30 min to allow penetration; the steel ring and any leftover cercariae were removed and the mice were given subcutaneous injection of 0.1 ml of 0.04 ml antisedan diluted in 0.96ml PBS (Sigma) to awaken them. Once infection was complete mice were observed and weighed 3 times a week, from week 5 onwards. At 49 days post infection mesenteric and omental adipose tissues, as well as mLN were harvested and tissues processed.

2.3.3 Inoculation of mice with MC38

This work was done in collaboration with the group of Tatiana Petrova at the University of Lausanne, Switzerland who kindly conducted the tumour cell injections. Mice were administered 100 µl of Buprenorphine (30 µg/g body weight), intramuscularly in the lower limb for 1 hour to ensure analgesia. Next, intra-peritoneal (ip) injection of 200 µl zymosan (40 µg/g body weight) was given to induce peritoneal inflammation, with control groups receiving 200 µl PBS (D0), followed 3 days later by ip injection of 5 x 10^5 GFP tagged MC38 murine colon cancer cells (D3). Mesenteries and omentum were harvested 10 days post MC38 injection (D13).

2.4 Enzymatic Digestion of Tissues

Firstly, tissues were dissected immediately after culling of mice by schedule 1 cervical dislocation. Gonadal fat, mesenteries (with mLN still intact) and omentum were collected and stored in Rosewell Park Memorial Institute (RPMI)-1640 medium (Life Technologies) supplemented with 2% Foetal calf serum (FCS) (Life Technologies). SI on the other hand was

collected and placed in Hanks Buffered Saline Solution (HBSS) (Sigma-Aldrich) supplemented with 2% FCS. All tissues were stored on ice until processing.

2.4.1 Isolation of cells from murine and human adipose tissue

For murine tissues, mLN were separated from the mesenteric fat under a dissecting microscope (Leica), then transferred to a 6-well plate containing fresh RPMI medium supplemented with 2% FCS, while human omentum was divided into smaller sections. All tissues were then weighed on a laboratory balance (Sartorius), to allow normalisation to tissue weight during statistical analysis. ATs were also examined under the dissecting microscope and any contaminating tissue removed. Following this, ATs were manually disaggregated with single edged razor blades (Fisher Scientific) into tiny pieces and transferred to an enzyme digest mixture consisting of RPMI medium, 2% FCS, 200 µg/ml collagenase P (Roche), 100 µg/ml DNase (Roche), and 800 µg/ml collagenase Dispase (Roche). Digestion was performed in a shaking water bath at 37°C, 120 rpm for 30 min, with samples inverted every 10 min. Digested tissue was then filtered through a nylon mesh filter (John Staniar, 75 microns) into fresh 2% FCS RPMI, and centrifuged at 1700 revolutions per minute (rpm) for 10 min. The oily adipocyte fraction and supernatant was discarded to leave behind the stromal vascular fraction pellet, which was subsequently re-suspended in an appropriate volume of 2% FCS RPMI.

2.4.2 Isolation of cells from murine small intestine

SI was placed on a paper towel soaked in HBSS supplemented with 2% FCS, and excess fat removed. Peyer's patches were also exercised and the SI cut longitudinally down the middle, rinsed in a petri dish containing HBSS/FCS solution and then cut finally into smaller, 1 cm pieces, and placed into 15ml HBSS/FCS solution. SI solution was manually shaken vigorously

and then filtered through nylon mesh (John Staniar, 75 microns), into 15ml pre-warmed solution of HBSS and 2mM EDTA and incubated in a shaker at 37°C, 250-300 rpm for 20 min. After this, SI was filtered and placed in 15 ml of HBSS only, shaken vigorously and then filtered back into fresh 15 ml HBSS/EDTA solution, and incubated in a shaker at 37°C, 250-300 rpm for a further 20 min. SI was then washed in HBSS alone as before, and then incubated with enzyme master mix containing 15 ml 10% FCS RPMI and 1 mg/ml collagenase VIII (Sigma-Aldrich), at 37°C, 250-300 rpm for 10 min, with manual shaking every 5 min. Digested SI was then filtered through 100 µm cell strainers (Greiner Bio-One), rinsed with 5 ml FACS staining buffer (phosphate buffered saline (PBS, Life Technologies), supplemented with 2% FCS and 2mM EDTA), and subsequently filtered through 70 µm strainers (Falcon), and finally centrifuged at 1500 rpm for 5 min.

2.4.3 Isolation of cells from murine mesenteric lymph nodes

Forceps were used to tease apart mLN within 6-well plates. 75 µg /ml DNase (Roche) and 750 µg /ml collagenase Dispase (Roche) was added per well, followed by incubation (without agitation) at 37°C for 20 min, after which 3.75 mM EDTA (Sigma-Aldrich) was added per well. The remaining solution was then filtered through a 70 µm cell strainer (Falcon) into fresh falcon tubes. Residual undigested tissue on the filter was crushed with the end of a 2 ml syringe plunger and the filter was rinsed with fresh FACS buffer twice, followed by centrifugation of sample at 1600 rpm for 5 min. The supernatant was subsequently discarded and the pellet was re-suspended in appropriate volume of FACS staining buffer. About 25% - 35% of mLN was plated per well, using a 96-well plate and the remaining cell suspension was pooled together for use as single colour controls during FACS.

2.5 Flow Cytometry Staining

2.5.1 Staining of murine samples

Single cell suspensions were transferred into 96 well plates, centrifuged at 1700 rpm for 3 min and the supernatant discarded. Cells were incubated first with LIVE/DEAD® fixable Near-IR viability Dye (Invitrogen Life Sciences) diluted at 1/1000 in PBS, for 30 min on ice and in the dark. All subsequent incubation steps were performed in the dark with centrifugation performed at 1700 rpm for 3 min. Cells were then washed twice with PBS; for myeloid cell analysis, cells were incubated with Fc block with purified anti-mouse CD16/32 (eBiosciences) diluted 1/50 in FACS buffer, for 15 min at room temperature. Next, cells were incubated for 30 min on ice with surface stain antibody master mix, made in FACS buffer and required antibodies at 50 µl/sample. When a lineage dump channel was required, all antibodies to be used in the dump channel were of the same fluorochrome. Following incubation, cells were washed twice in FACS buffer, and if intracellular staining was required, all samples were fixed with FoxP3 fixative kit (eBioscience), reconstituted as per manufacturer's instructions, for 30 min. Cells were then washed in the corresponding permeabilisation buffer (eBioscience, 1X, 1: 10 in MQ water). A cocktail of internal antibodies was prepared with the 1X permeabilisation buffer at 50 µl/sample and incubated with samples at room temperature for 30 min. Isotype and/or fluorescence minus one controls (FMOs) were used where appropriate by staining cells with the same antibody cocktail, but without the antibody of interest (in the case of FMOs), or with an isotype antibody added instead. Following incubation with internal antibodies, cells were washed twice in 1X permeabilisation buffer and re-suspended in an appropriate volume of FACS buffer. Finally, samples were filtered through nylon mesh into flow cytometry tubes along with 5 µl of

counting beads (AccuCount Blank Particles 8.0-12.9µm Spherotech) to allow for cell counting. Flow cytometry acquisition was performed on an LSRFortessa X20 (BD Bioscience). Following acquisition, data were analysed via FlowJo Version 10 (Treestar). The list of murine antibodies and dilutions used for flow cytometry are given in table 2.1.

2.5.2 Staining of human samples

For staining of cells isolated from human adipose tissues, the same procedure as in section 2.5.1 was followed with a few exceptions. Firstly, cells were blocked with 5 µl Human BD Fc block (BD Biosciences) prior to addition of LIVE/DEAD® fixable Near-IR viability Dye (Invitrogen Life Sciences). Secondly, incubation of cells with antibody cocktail occurred for 20 min on ice. Thirdly, anti-mouse Ig, κ/Negative control compensation beads (BD Biosciences) was used to optimise compensation settings during FACS. The list of human antibodies and dilutions used for flow cytometry are given in table 2.2.

2.5.3 *Ex vivo* stimulation for intracellular cytokine analysis

For intracellular cytokine analysis, *ex vivo* stimulation was performed prior to FACS staining. Single cell suspensions were transferred to a 24-well plate (Corning) and the volume was made up to 1ml using culture media (RPMI supplemented with 10% FCS, 1% Penicillin-Streptomycin (Sigma-Aldrich) and 1% L-glutamine (Gibco)). To stimulated wells only, phorbol 12-myristate 13-acetate (PMA, 100 µg/ml in DMSO) and Ionomycin (1 mM in DMSO) were added. All wells were incubated at 37°C for 1hr. Brefeldin A at a final concentration of 10 µg/ml was subsequently added to all wells and incubated for a further 3 hr at 37°C. Cells were then transferred to 15 ml centrifuge tubes (Starlab) and the plate washed twice with 2 ml RPMI media. Cells were centrifuged at 1700 rpm for 5 min, the supernatant was

discarded and cell pellet re-suspended in appropriate volume of FACS buffer and transferred to 96-well plates for FACS staining.

Table 2.1: List of murine antibodies used for flow cytometry

Species	Surface / Intracellular	Target Antigen	Fluorophore	Dilution	Clone	Manufacturer
Mouse	**Surface staining**	α-Galactosylceramide (α-gal-cer): For detecting iNKT cells	APC	1:200	PBS-57	NIH Tetramer Core Facility
		CD3e	FITC	1:100	145-2C11	BD Pharmingen
			APC	1:200	145-2C11	eBioscience
			AF700	1:200	17A2	Biolegend
		CD4	BV510	1:300	RM4-5	Biolegend
			BV605	1:300	RM4-5	Biolegend
		CD5	FITC	1:100	53-7.3	BD Pharmingen
			APC	1:200	53-7.3	eBioscience
		CD8	BV711	1:200	53-6.7	Biolegend
		CD11b	FITC	1:300	M1/70	Biolegend
			APC	1:200	M1/70	eBioscience
		CD11c	FITC	1:300	HL3	BD Pharmingen
			APC	1:200	N418	eBioscience
			BV785	1:300	N418	Biolegend
		CD25	BV650	1:200	PC61	Biolegend
		CD45.2	BV786	1:200	104	BD Horizon
			BV605	1:100	104	Biolegend
			BV711	1:300	104	BD Horizon
		CD127 (IL-7Rα)	BV421	1:100	A7R34	Biolegend
			PeCy7	1:75	A7R34	Biolegend
		CD44	BV785	1:200	IM7	Biolegend
		CD45R (B220)	AF700	1:300	RA3-6B2	BD Bioscience
			FITC	1:300	RA3-6B2	BD Pharmingen
			APC	1:300	RA3-6B2	eBioscience

		CD69	Percp-cy5.5	1:100	H1.2 F3	eBioscience
		CCR8	APC	1:50	SA214G2	Biolegend
		CCR9	PE	1:200	eBioCW-1.2	eBioscience
		Killer cell lectin-like receptor G1 (KLRG1)	BV421	1:200	2F1	BD Bioscience
		Major histocompatibility complex class II (MHC class II)	BV510	1:600	M5/144.15.2	Biolegend
		NK1.1	BV650	1:100	PK136	Biolegend
		ST2	Percp710	1:50	DIH9	Biolegend
			PE	1:50	DIH9	Biolegend
Mouse	**Intracellular staining**	CD3 intracellular	AF700	1:100	17A2	Biolegend
		T-bet	APC	1:75	ebio 4B10	eBioscience
		GATA-3	PercP710	1:50	TWAJ	eBioscience
		IL-5	PE	1:50	TRFK5	eBioscience
		IL-13	PE-Cy7	1:50	eBio13A	eBioscience
			Ef660	1:100	eBio13A	eBioscience
		IFN-γ	PE-Cy7	1:100	XMG1.2	eBioscience
		FoxP3	APC	1:100	FJK-16s	eBioscience
			EF450	1:100	FJK-16s	eBioscience
		Ki67	PE-Cy7	1:200	SolA15	eBioscience
		RORγT	PE	1:50	Q31-378	BD Pharmingen
	Secondary antibody	Streptavidin	BV605	1:300	-	Biolegend
		Streptavidin	BV650	1:300	-	Biolegend

Table 2.2: List of human antibodies used for flow cytometry

Species	Surface / Intracellular	Target Antigen	Fluorophore	Dilution	Clone	Manufacturer
Human		CD3	FITC	1:500	UCHT1	Biolegend
			AF700	1:400	HIT39	Biolegend
			BV711	1:300	UCHT1	Biolegend
		CD4	BV605	1:300	OKT4	Biolegend

	Surface staining	CD8	BV711	1:200	SK1	Biolegend
		CD11b	PE	1:400	M1/70	Biolegend
		CD11c	FITC	1:500	3.9	Biolegend
			BV785	1:200	3.9	Biolegend
		CD19	FITC	1:500	HIB19	Biolegend
			BV711	1:300	HIB19	Biolegend
		CD45	BV510	1:300	HI30	Biolegend
		CD56	BV711	1:100	5.1H11	Biolegend
		CD127 (IL-7Rα)	BV421	1:300	A019D5	Biolegend
		CD206	APC	1:100	15-2	Biolegend
		PD-1	Percp-cy5.5	1:100	NAT 105	Biolegend
		PDL1	PE	1:100	29E.2A3	Biolegend
Human	**Intracellular staining**	FoxP3	BV421	1:100	206D	Biolegend
			PE	1:100	206D	Biolegend
		GATA-3	PercP710	1:100	TWAJ	Thermofisher Scientific
		IFN-γ	PE-Cy7	1:200	4S.B3	eBioscience
		IL-13	APC	1:50	JES10-5AD	Biolegend

2.6 Whole-Mount and Immunofluorescence Staining of Murine and Human Adipose Tissues.

ATs were collected in RPMI with 2% FCS, cleaned and weighed using a laboratory balance (Sartorius). Tissues were then fixed in 1 ml (or 1.5 ml for human tissues) of 2% paraformaldehyde (PFA) (Sigma Aldrich) on ice, and placed on a shaker (Luckham Rotatest R100) at 5 rpm for 30 min. All subsequent incubation steps were performed on ice and on the shaker (unless otherwise stated). Following fixation, tissues were washed three times in PBS for 5 min, and then permeabilized with 1X Triton (Sigma Aldrich) for 30 min. After permeabilization, samples were washed three times in PBS, followed by blocking with 10% horse serum in PBS at room temperature and on the shaker for 30 min. Tissues were not washed after blocking. If a biotin conjugated antibody was to be used, an additional blocking

step was performed using an Avidin/Biotin blocking kit (Vector labs) for 15 min at room temperature and on the shaker. Tissues were rinsed briefly between Avidin and Biotin steps. Tissues were then incubated with 500 µl (or 750 µl for human tissues) of primary antibody master mix reconstituted in PBS, and left overnight at 4°C on a gyratory rocker (Stuart) at 30 rpm. Samples were washed three times, and then incubated with a secondary antibody cocktail for 1 hr on ice. This process was subsequently repeated for tertiary antibodies, if needed. Following the final antibody incubation, tissues were incubated with 4', 6-Diamidino-2-Phenylindole Dihydrochloride (DAPI), diluted 1/400 in PBS for 10 min on ice. Tissues were subsequently washed three times and mounted on slides with VectorShield mounting medium (Vector Labs). If FALCs were to be counted, a stereofluorescence microscope (Olympus SZX12) linked to an Olympus C50-60 camera was used to enumerate FALCs and obtain images, prior to mounting tissues. Confocal images of slides were then obtained using the Zeiss LSM 780 Confocal Microscope. The antibodies used for immunofluorescence are listed in table 2.3.

Table 2.3: Antibodies used during immunofluorescence staining of murine and human adipose tissues

Species		Antibody	Conjugate	Dilution	Clone	Manufacturer
Mouse	**Primary antibody**	CD4	Alexa Fluor 647	1:50	RM4-5	BD Pharmingen
		CD45	FITC	1:300	30-F11	eBioscience
		CXCL13	unconjugated	1:200	-	R&D systems
		FoxP3	Biotin	1:100	FJK-16s	eBioscience
		IL-33	Unconjugated	1:200	-	R&D Systems
Human	**Primary antibody**	CD4	Alexa Fluor 594	1:100	RPA-T4	Biolegend
		CD45	FITC	1:100	HI30	Biolegend

		FoxP3	APC	1:50	PCH101	eBioscience
	Secondary antibody	Anti-Fluorescein	Alexa Fluor 488	1:300	-	Life Technologies
		Anti-Green Fluorescent Protein	Alexa Fluor 488	1:200	-	Life Technologies
		Donkey anti-Goat	Alexa Fluor 488	1:200	-	Invitrogen
			Alexa Fluor 555	1:200	-	Invitrogen
		Goat anti-Rabbit	Alexa Fluor 488	1:200	-	Invitrogen
		Nuclear stain	DAPI	1:400	-	Life Technologies

2.7 Statistical Analysis

Following analysis of flow cytometric data using FlowJo Version 10 (TreeStar), raw data was exported into Microsoft Excel for basic quantitative calculations, such as converting cell counts into absolute cell numbers. Data was then transferred to GraphPad Prism version 8 for graphical and statistical analysis. Statistical significance between single variables was determined using an unpaired t test; when analysing two or more variables Kruskal-Wallis test followed by a Dunn's post-hoc was used. Statistical significance is indicated as *$p<0.05$; **$p<0.01$; ***$p<0.001$; p values are not stated for non-significant data.

CHAPTER 3: IMMUNE CELL CHARACTERISATION IN PERITONEAL ADIPOSE TISSUES

3.1 Introduction

Adipose tissue (AT) is a dynamic organ, with physiological and metabolic roles within the host. The majority of human AT is WAT which can be found either beneath the skin (i.e. subcutaneous AT) or surrounding internal organs (i.e. VAT) (Alexopoulos et al., 2014). Both of these differ in numerous characteristics; VAT contains more immune cells, is more metabolically active, as well as being more vascularised and innervated than subcutaneous fat, as such VAT is often associated with increased metabolic and cardiovascular risks (Ibrahim, 2010) as well as a number of medical pathologies (Shuster et al., 2012). Often referred to as abdominal fat due to its presence in the abdominal viscera, VAT is anatomically present mainly in the mesenteries, omentum as well as the gonads, which are ATs of the peritoneal cavity (Ibrahim, 2010, Chau et al., 2014). VAT surrounding other internal organs exists, such as the pericardial and the retroperitoneal fat that surrounds the heart and kidneys respectively (Bjørndal et al., 2011).

Gonadal fat can be found attached to the ovaries and uterus of females (periovarian), and around the testis in males (epidymal) (Bjørndal et al., 2011). It is one of the largest fat depot in rodents, which although initially expands with body weight gain, this expansion is diminished once mice are above a certain threshold weight (van Beek et al., 2015). As such, compared to other VATs such as the mesenteries, gonadal fat is reported to possess limited storage capacities that can subsequently drive the development of metabolic disorders including insulin resistance, liver steatosis as well as the formation of crown-like structures found around necrotic adipocytes (van Beek et al., 2015).

The mesentery is a double layered fold of peritoneum associated with the small and large intestine and the colon; regarded as a contiguous structure, it emerges from the mesenteric

root (i.e. where the mesenteries attaches to the posterior abdominal wall) and fans out to span the intestine from the duodenum to the rectum (Coffey and O'Leary, 2016). Aided by vascular connections within these tissues, the mesentery also supports the intestine preventing it from collapsing into the pelvis and similarly facilitates suspension of the colon (Culligan et al., 2014). Due to its close associations with the intestine, it is therefore likely that the mesenteries can mediate local and systemic responses by sampling intestinal cues. Indeed reports of inflammatory responses generated within mesenteric fat following intestinal inflammation have been described (Karagiannides and Pothoulakis, 2008). Furthermore, in Crohn's disease, bacteria translocation to mesenteries can be observed. Studies using murine models of acute and chronic intestinal inflammation elicited with dextran sulfate sodium, showed mesenteric fat to be infiltrated by immune cells, accompanied by elevated cytokine and adipokine production within this tissue, suggestive of a protective mechanism employed by the mesenteries in response to bacterial translocation (Batra et al., 2012).

The omentum, which is derived from mesothelial cells, is attached to the spleen, stomach, pancreas, and colon. While murine omentum is a thin layer of fat found to wrap the stomach, in humans this tissue is significantly larger, draping over the abdominal organs like an apron (figure 1.9C). In addition, it is a highly vascularised fat depot, containing milky spots/FALCs embedded between adipocytes (Meza-Perez and Randall, 2017). The omentum has been shown to be involved in promoting wound healing, site occlusion and tissue regeneration through the expansion of milky spots, accumulation of growth and angiogenic factors as well as progenitor cells (Litbarg et al., 2007). In addition, it is well known to support immune responses to antigens and particulates that drain from the peritoneal

cavity, and this is largely mediated by the myriad of immune cells housed within these milky spots/FALCs (Rangel-Moreno et al., 2009, Meza-Perez and Randall, 2017).

ILC2s are an abundant immune population found within FALCs; as discussed earlier ILCs as a whole bear close resemblance to Th cells. In order for effector T cells to mediate their function, migration of naïve T cells initially to SLOs and then to target tissues is required, facilitated by the expression of appropriate chemokine receptors at different points during T cell differentiation and activation (Pennock et al., 2013). For instance, naïve T cells migrate from the thymus to SLOs in a CCR7 and CD62L dependent manner; upon T cell priming by antigens these receptors are downregulated and instead a homing receptor switch occurs that upregulates CCR9 and the integrin $\alpha4\beta7$ occurs, enabling T cell migration to the small intestine (Kim et al., 2015). In the same regard progenitor and mature ILCs express homing receptors that dictate their tissue tropism. However and unlike other ILC subsets, ILC2 progenitors begin to express the gut homing receptors, CCR9 and $\alpha4\beta7$ right from the bone marrow and therefore do not undergo a receptor switch within SLOs (Kim et al., 2016). Furthermore, ILC2s express other tissue specific receptors such as in the human skin where a significant proportion of ILC2 express CCR4, CCR10 and cutaneous lymphocyte antigen (CLA) (Salimi et al., 2013). Therefore, to understand the signals that control mature ILC2s during AT cellular migration and function, a previous student from the Caamaño group examined the potential expression of a panel of chemokine receptors on ILC2s, based on their known expression in T cells. This led to the identification of four populations of ILC2s that differentially expressed CCR8 and CCR9 within the gonadal fat, mesenteries as well as the mesenteric LN (mLN) – which was used as a lymphoid tissue comparison. As such further

investigations into these sub-populations as well as their involvement during *H.poly* infection were conducted.

3.2 Immune Cell Composition in Visceral Adipose Tissues at Homeostasis

3.2.1 Comparing FALC composition between visceral adipose tissues

The FALC composition of the different VATs at homeostasis (namely gonadal fat, mesenteries and omentum) were first assessed by enumerating FALCs within these tissues. These clusters of lymphocytes can be identified by immunofluorescence staining using anti-CD45 antibody, as such tissues were isolated from C57BL/6J mice at steady state and stained as whole-mounts. Following enumeration, a stepwise increase in the total number of FALCs was observed from the gonadal fat to the mesenteries to omentum, with the latter observed to have a statistically significant higher number of FALCs compared to the gonadal fat (figure 3.1A). When FALC numbers were adjusted and normalised to take into account the different tissue weights (figure 3.1B), a similar pattern of increase across the three tissues could also be observed.

Figure 3.1: Evaluating the differences in FALC numbers between visceral adipose tissues

The gonadal fat, mesenteries and omentum were isolated from C57BL/6J mice at steady state. Tissues were stained as whole-mounts with FITC conjugated anti-mouse CD45 primary antibody, and amplified with anti-FITC secondary antibody. FALCs were visualised and enumerated using a stereofluorescence microscope as described in materials and methods. Data are representative of two independent experiments whereby n=6. Bars on the graph represent the median value. Statistical significance was determined using Kruskal-Wallis followed by Dunn's multiple comparisons test.

a) Graph comparing the total number of FALCs between the gonadal fat (GF), mesenteries (Me) and omentum (Om).
b) Graph comparing the adjusted number of FALCs per 100 mg tissue between the gonadal fat (GF), mesenteries (Me) and omentum (Om).

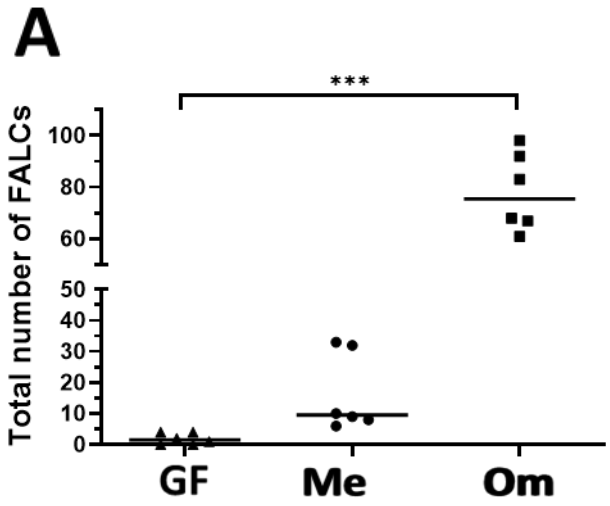
A
***
Total number of FALCs
100
80
60
50
40
30
20
10
0
GF
Me
Om

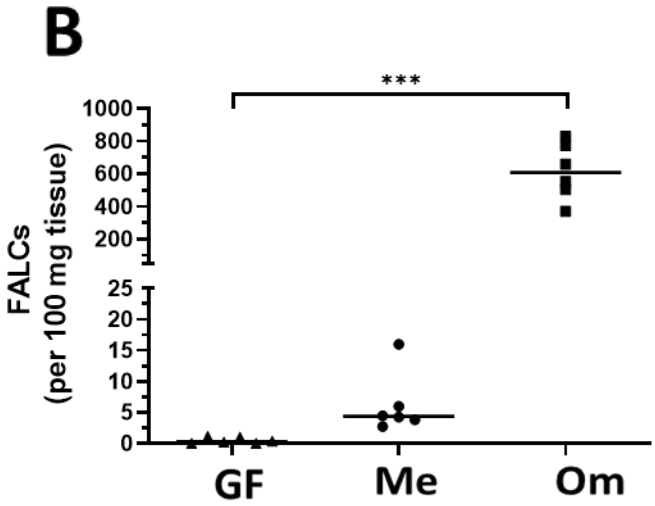
B
***
FALCs
(per 100 mg tissue)
1000
800
600
400
200
25
20
15
10
5
0
GF
Me
Om

Figure 3.1

3.2.2 Analysis of lymphoid and myeloid subsets within visceral adipose tissues

Having established the mesenteries and omentum as VATs with significant numbers of FALCs, a comparison of the immune composition of these tissues at steady state was investigated next. Tissues were enzymatically digested to generate a single cell suspension, which was subsequently stained with antibodies for the detection of lymphoid immune cell subsets via flow cytometry. These included, ILC subsets (ILC1/2/3 - figure 3.2A), B cells, CD4 T and CD8 T cells, NK cells, iNKTs and Tregs (including Foxp3^{+}ST2^{-} and Foxp3^{+}ST2^{+} phenotypes denoted as ST2^{-} and ST2^{+} respectively) – figure 3.2B. The normalised numbers of ILC1s (figure 3.3A), B cells (figure 3.3B), ST2^{-} and ST2^{+} Tregs (figure 3.3C), and iNKTs (figure 3.3D) were statistically significantly higher in the omentum compared to the mesenteries. In addition, normalised numbers of CD4 and CD8 T cells (figure 3.3B) tended to increase in the omentum, though this did not reach statistical significance. Similarly, a slight but non-significant increase in the numbers of NK cells was observed in the omentum compared to the mesenteries – figure 3.3D.

Given the presence of CD11b^{+} myeloid cells reported in FALCs, particularly during peritoneal inflammation (Bénézech et al., 2015), a number of myeloid subsets were also assessed by flow cytometry including conventional DC subsets (cDC1/2s – figure 3.4A), neutrophils, eosinophils, monocytes and macrophages (figure 3.4B). Compared to the mesenteries, the omentum was found to have significantly higher normalised numbers of cDC1s, cDC2s (figure 3.5A), monocytes and macrophages (figure 3.5C), as well as a slight but non-statistically significant increase in the numbers of neutrophils and eosinophils (figure 3.5B).

Figure 3.2: Gating strategy to identify lymphoid immune cell subsets within visceral adipose tissue FALCs

The mesenteries and omentum were isolated from C57BL/6J mice at steady state. Single cell suspension was generated from tissues as described in materials and methods, and lymphoid immune cell subsets were assessed by flow cytometry. Representative FACS plots are shown, whereby n=4-5 for ILC1/2/3s; and n=5 for B cells, T cells, NK cells, iNKTs, $ST2^-$ and $ST2^+$ Tregs, across two independent experiments.

a) FACS plots showing the identification of ILC subsets (ILC1, ILC2, ILC3) within mesenteries (top) and omentum (bottom). Cells have been pre-gated on FSC and SSC followed by live$CD45.2^+$. Lineage (Lin) gate included CD3, CD5, B220, CD11b and CD11c. Numbers on histograms indicate the percentage of $Tbet^+$ ILC1s.
b) FACS plots showing the identification of B cells, T cells, NK cells, iNKTs, $ST2^-$ and $ST2^+$ Tregs within mesenteries (top) and omentum (bottom). Cells have been pre-gated on FSC and SSC followed by live$CD45.2^+$.

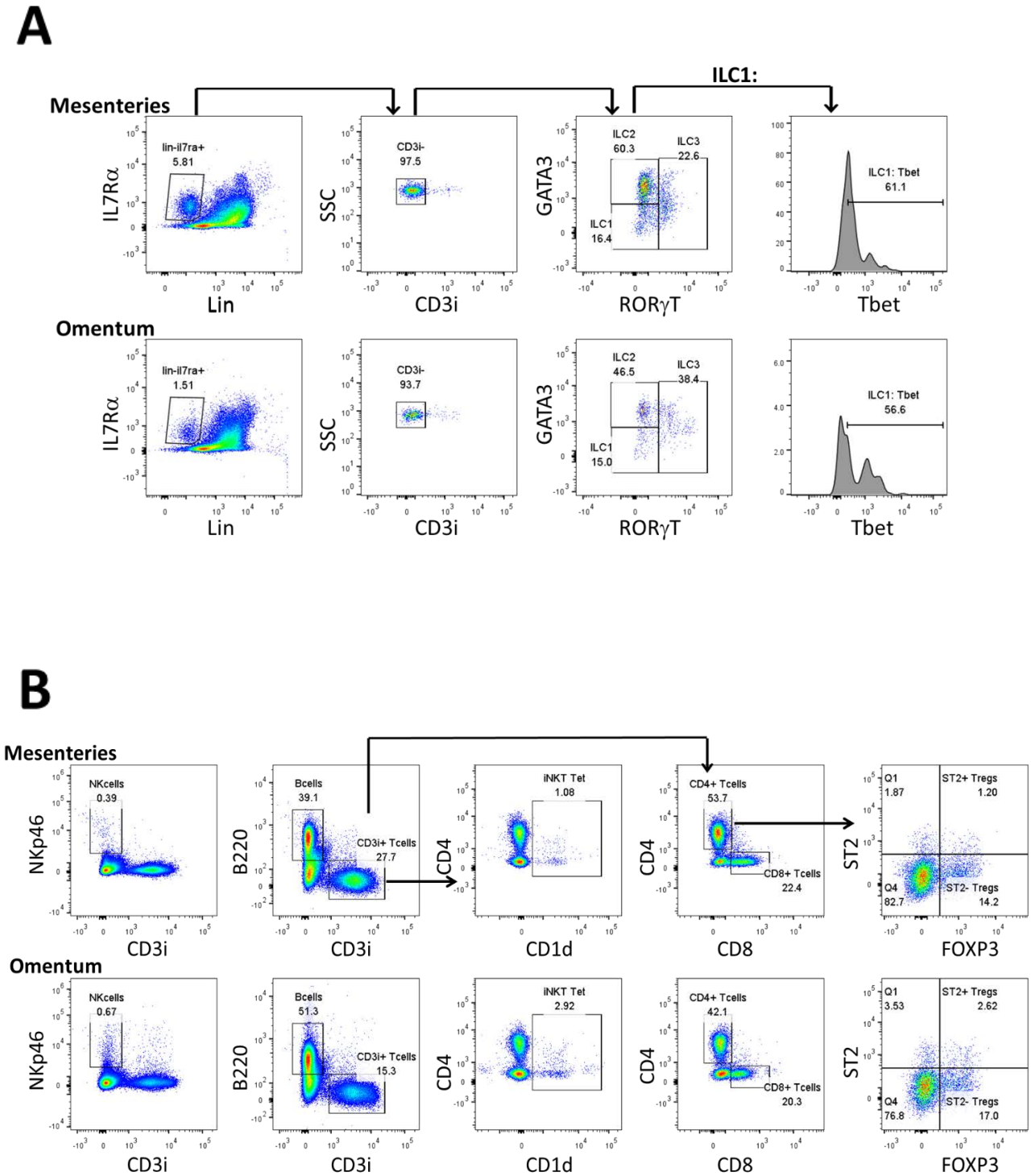
A
ILC1:
Mesenteries
lin-il7ra+
5.81
IL7Rα
Lin
CD3i-
97.5
SSC
CD3i
ILC2
60.3
ILC3
22.6
ILC1
16.4
GATA3
RORγT
ILC1: Tbet
61.1
Tbet
Omentum
lin-il7ra+
1.51
CD3i-
93.7
ILC2
46.5
ILC3
38.4
ILC1
15.0
ILC1: Tbet
56.6
B
Mesenteries
NKcells
0.39
NKp46
CD3i
Bcells
39.1
CD3i+ Tcells
27.7
B220
iNKT Tet
1.08
CD4
CD1d
CD4+ Tcells
53.7
CD8+ Tcells
22.4
CD8
Q1
1.87
ST2+ Tregs
1.20
Q4
82.7
ST2- Tregs
14.2
ST2
FOXP3
Omentum
NKcells
0.67
Bcells
51.3
CD3i+ Tcells
15.3
iNKT Tet
2.92
CD4+ Tcells
42.1
CD8+ Tcells
20.3
Q1
3.53
ST2+ Tregs
2.62
Q4
76.8
ST2- Tregs
17.0

Figure 3.2

Figure 3.3: Assessing lymphoid immune cell populations within visceral adipose tissue FALCs at homeostasis

Unperturbed C57BL/6J mice were culled; mesenteries and omentum were isolated as described in materials and methods. The difference in lymphoid immune cell composition between mesenteric and omental FALCs was assessed. Total number of cells were normalised to weight of individual tissues and represented as number of cells per 100mg of tissue.

Data are representative of two independent experiments with the following sample numbers: ILC1/2/3 (n=4-5); B cells, T cells, NK cells, iNKTs, $ST2^-$ and $ST2^+$ Tregs (n=5). Bars on the graph represent the median value. Statistical significance was determined using Unpaired students t test. *P<0.05, **P<0.01, ***P<0.001 and ****P<0.0001.

a) Graph comparing the adjusted number of ILC1s, ILC2s and ILC3s (left to right) per 100 mg tissue between the mesenteries (Me) and omentum (Om).
b) Graph comparing the adjusted number of B cells, CD4 T and CD8 T cells (left to right) per 100 mg tissue between the mesenteries (Me) and omentum (Om).
c) Graph comparing the adjusted number of $ST2^-$ and $ST2^+$ Tregs (left to right) per 100 mg tissue between the mesenteries (Me) and omentum (Om).
d) Graph comparing the adjusted number of NK cells and iNKTs (left to right) per 100 mg tissue between the mesenteries (Me) and omentum (Om).

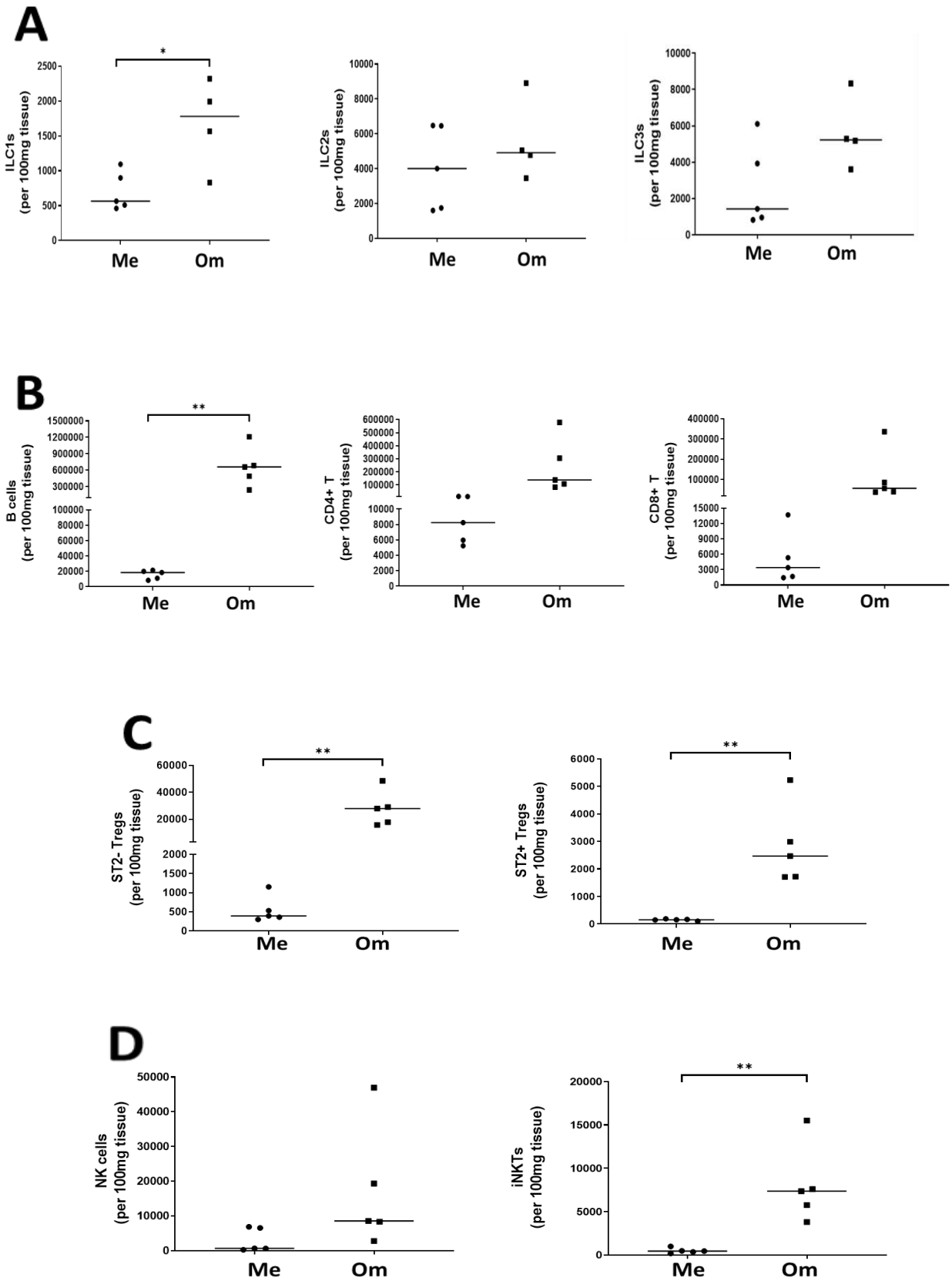
A
ILC1s
(per 100mg tissue)
ILC2s
(per 100mg tissue)
ILC3s
(per 100mg tissue)
Me
Om
B
B cells
(per 100mg tissue)
CD4+ T
(per 100mg tissue)
CD8+ T
(per 100mg tissue)
C
ST2- Tregs
(per 100mg tissue)
ST2+ Tregs
(per 100mg tissue)
D
NK cells
(per 100mg tissue)
iNKTs
(per 100mg tissue)

Figure 3.3

Figure 3.4: Gating strategy to identify myeloid immune cell subsets within visceral adipose tissue FALCs

The mesenteries and omentum were isolated from C57BL/6J mice at steady state. Single cell suspension was generation from tissues as described in materials and methods, and myeloid immune cell subsets were assessed by flow cytometry. Representative FACS plots are shown, whereby n=7 for DCs, and n=6 for neutrophils, eosinophils, monocytes, and macrophages across two independent experiments.

a) FACS plots showing the identification of conventional DC (cDC) subsets (cDC1, cDC2) within mesenteries (top) and omentum (bottom). Cells have been pre-gated on FSC and SSC followed by liveCD45.2^{+}Lin^{-}. Lineage (Lin) gate included CD3, CD19 and Ly6G.
b) FACS plots showing the identification neutrophils, eosinophils, monocytes, and macrophages. Cells have been pre-gated on FSC and SSC followed by liveCD45.2^{+}Lin^{-} CD11c^{-}CD11b^{+}. Lineage (Lin) gate included CD3, CD8 and B220.

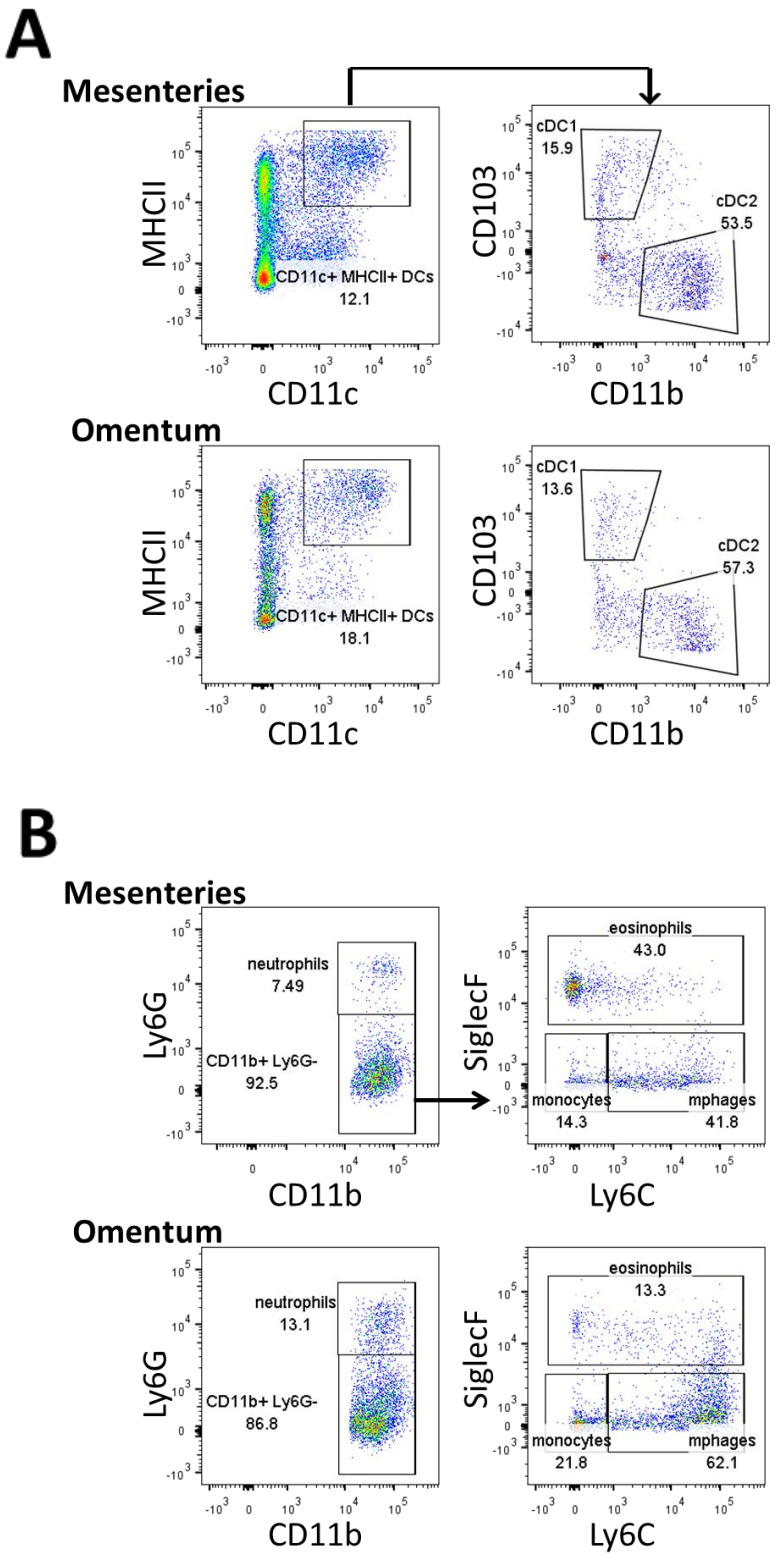
A
Mesenteries
MHCII
CD11c
CD11c+ MHCII+ DCs
12.1
CD103
CD11b
cDC1
15.9
cDC2
53.5
Omentum
MHCII
CD11c
CD11c+ MHCII+ DCs
18.1
CD103
CD11b
cDC1
13.6
cDC2
57.3
B
Mesenteries
Ly6G
CD11b
neutrophils
7.49
CD11b+ Ly6G-
92.5
SiglecF
Ly6C
eosinophils
43.0
monocytes
14.3
mphages
41.8
Omentum
Ly6G
CD11b
neutrophils
13.1
CD11b+ Ly6G-
86.8
SiglecF
Ly6C
eosinophils
13.3
monocytes
21.8
mphages
62.1

Figure 3.4

Figure 3.5: Assessing myeloid immune cell populations within visceral adipose tissue FALCs at homeostasis

Unperturbed C57BL/6J mice were culled; mesenteries and omentum were isolated as described in materials and methods. The difference in myeloid immune cell composition between mesenteric and omental FALCs was assessed. Total number of cells were normalised to weight of individual tissues and represented as number of cells per 100mg of tissue.

Data are representative of two independent experiments with the following sample numbers: DC (n=7); neutrophils, eosinophils, monocytes, and macrophages, (n=6). Bars on the graph represent the median value. Statistical significance was determined using Unpaired students t test. *P<0.05, **P<0.01, ***P<0.001 and ****P<0.0001.

a) Graph comparing the adjusted number of cDC1s and cDC2s (left to right) per 100 mg tissue between the mesenteries (Me) and omentum (Om).
b) Graph comparing the adjusted number of neutrophils and eosinophils (left to right) per 100 mg tissue between the mesenteries (Me) and omentum (Om).
c) Graph comparing the adjusted number of monocytes and macrophages (left to right) per 100 mg tissue between the mesenteries (Me) and omentum (Om).

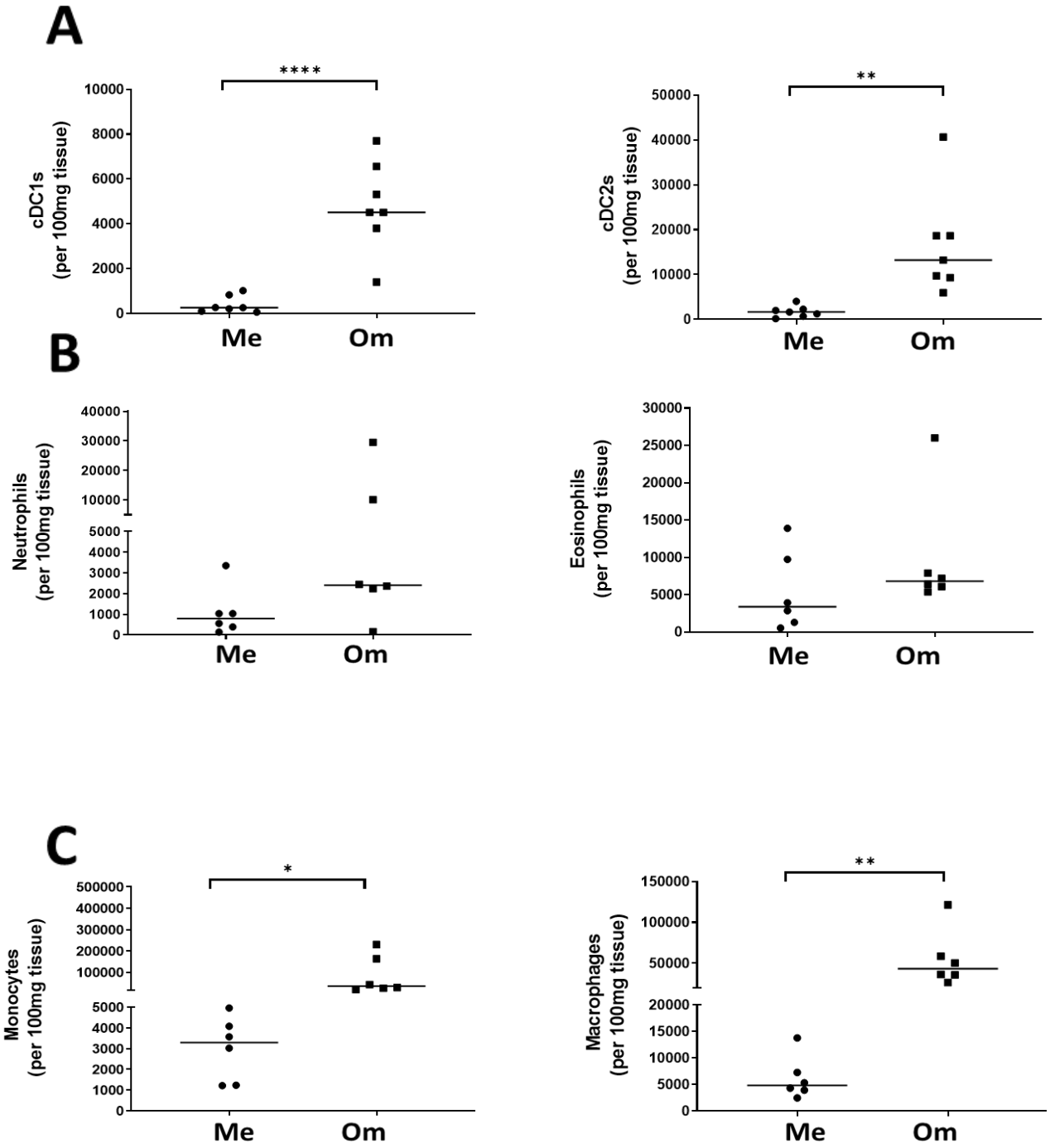
A
****
cDC1s
(per 100mg tissue)
10000
8000
6000
4000
2000
0
Me
Om
**
cDC2s
(per 100mg tissue)
50000
40000
30000
20000
10000
0
Me
Om
B
Neutrophils
(per 100mg tissue)
40000
30000
20000
10000
5000
4000
3000
2000
1000
0
Me
Om
Eosinophils
(per 100mg tissue)
30000
25000
20000
15000
10000
5000
0
Me
Om
C
*
Monocytes
(per 100mg tissue)
500000
400000
300000
200000
100000
5000
4000
3000
2000
1000
0
Me
Om
**
Macrophages
(per 100mg tissue)
150000
100000
50000
20000
15000
10000
5000
0
Me
Om

Figure 3.5

3.3 Chemokine and Cytokine Expression of Type 2 ILCs within Visceral Adipose Tissues

3.3.1 ILC2 chemokine receptor expression in visceral adipose tissues differs from mLN

Previous work within the group had identified sub-populations of ILC2s within the gonadal fat and mesenteries, based on their chemokine receptor expression, designated as $CCR8^+$, $CCR9^+$, $CCR8^+CCR9^+$ and $CCR8^-CCR9^-$. Future plans aimed to further dissect these populations, assessing whether there were differences in proliferation within these ILC2 subsets following *H. poly* infection. However, to establish a working model, boost reliability as well as the authenticity in this and previous results, these findings were first confirmed, and extended to the analysis of the omentum to observe if the same held true for this tissue, with mLN used as a control SLO (figure 3.6A).

At steady state, the proportion of $CCR8^+$ ILC2s was greater in the VATs compared to mLN, with statistical significance observed particularly in the mesenteries (figure 3.6B, top left). On the contrary, $CCR9^+$ ILC2s were found to be significantly higher in mLN compared to both VATs (figure 3.6B, top right). In addition, the proportion of ILC2s co-expressing CCR8 and CCR9 was significantly higher in the mLN compared to the mesenteries and omentum (figure 3.6B, bottom left). Meanwhile, the proportion of $CCR8^-CCR9^-$ double negative ILC2 subsets, tended to increase most in the omentum, compared to other tissues (figure 3.6B, bottom right).

Figure 3.6: Assessing ILC2 subsets based on CCR8 and CCR9 expression, between visceral adipose tissues and mLN at homeostasis

The mesenteries, omentum and mLN were isolated from C57BL/6J mice. Cells were isolated from tissues and chemokine receptor expression on ILC2s was assessed by flow cytometry as described in materials and methods.

Data are representative of two independent experiments whereby n=6. Bars on the graph represent the median value. Statistical significance was determined using Kruskal-Wallis followed by Dunn's multiple comparisons test. *$P<0.05$, **$P<0.01$, ***$P<0.001$ and ****$P<0.0001$.

a) Representative FACS plots comparing ILC2 expression of CCR8 and CCR9, between the mLN (top), mesenteries (middle) and omentum (bottom). Cells have been pre-gated on FSC and SSC followed by liveCD45.2^{+}. Lineage (Lin) gate included CD3, CD5, B220, CD11b and CD11c.

b) Graph comparing the percentage of each individual ILC2 subsets: CCR8^{+} (top left); CCR9^{+} (top right); CCR8^{+}CCR9^{+} (bottom left) and CCR8^{-}CCR9^{-} (bottom right) between mLN, mesenteries (Me) and omentum (Om).

A

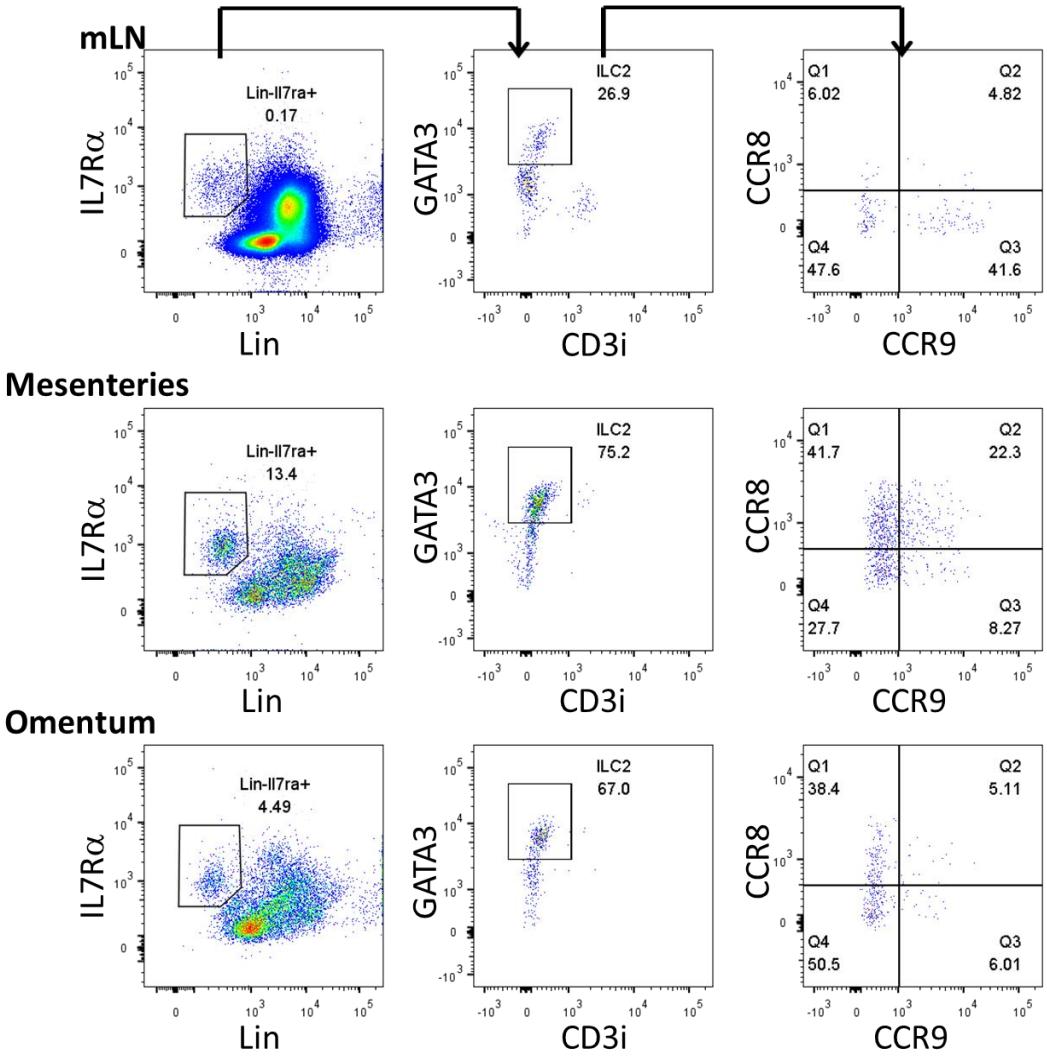
mLN
Lin-Il7ra+
0.17
IL7Rα
Lin
ILC2
26.9
GATA3
CD3i
Q1
6.02
Q2
4.82
Q4
47.6
Q3
41.6
CCR8
CCR9
Mesenteries
Lin-Il7ra+
13.4
ILC2
75.2
Q1
41.7
Q2
22.3
Q4
27.7
Q3
8.27
Omentum
Lin-Il7ra+
4.49
ILC2
67.0
Q1
38.4
Q2
5.11
Q4
50.5
Q3
6.01

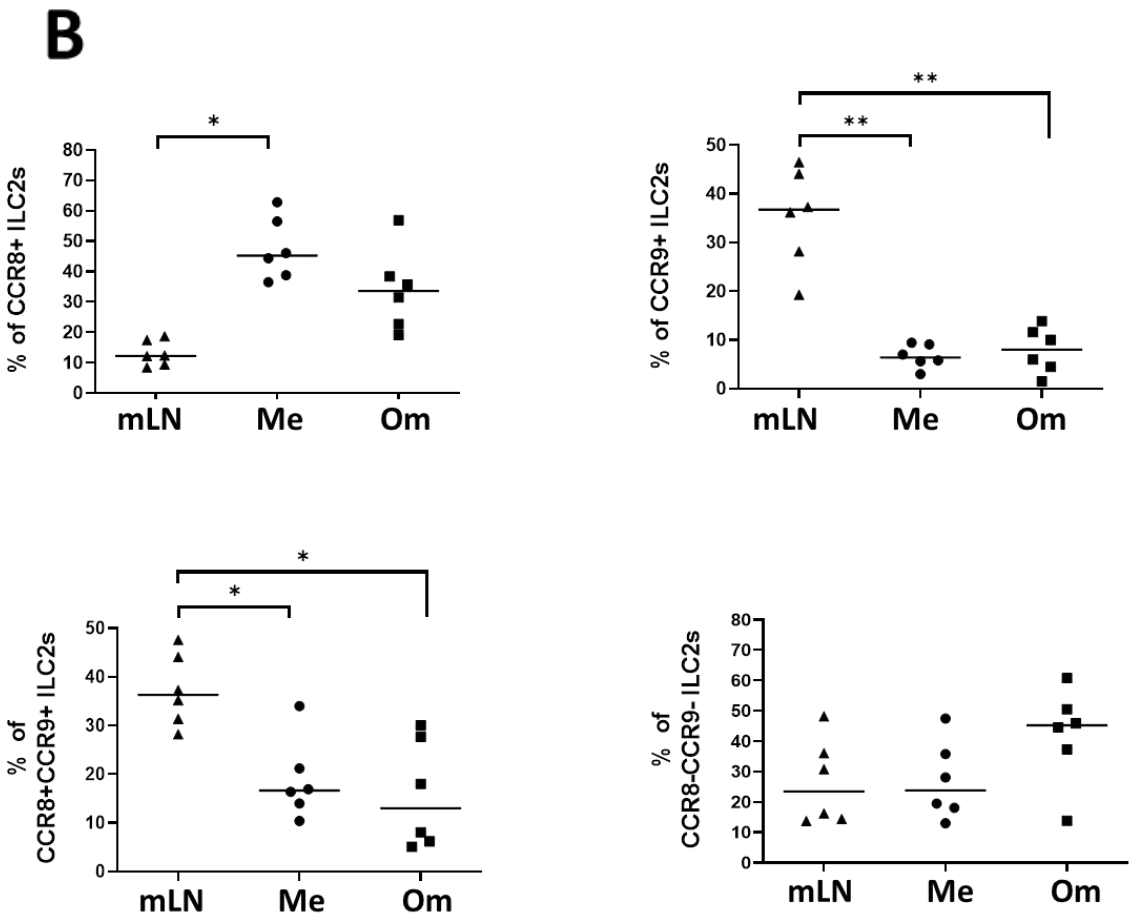
B
% of CCR8+ ILC2s
% of CCR9+ ILC2s
% of CCR8+CCR9+ ILC2s
% of CCR8-CCR9- ILC2s
mLN
Me
Om
*
**

Figure 3.6

3.3.2 ILC2s in visceral adipose tissues produce IL-5 at homeostasis

ILC2s similar to their Th2 counterparts predominantly produce type 2 cytokines as has been shown for a number of peripheral and lymphoid tissue ILC2s (Artis and Spits, 2015). Therefore, VAT ILC2 cytokine expression was assessed using *Il5*$^{tm1.1(Cre)Lky}$ tdtomato (Red5) reporter mice (Nussbaum et al., 2013). ILC2s within the mesenteries, omentum and mLN were isolated at steady state; to avoid loss of reporter signal from cell fixation, ILCs were identified as IL-7Ra^{+}Lin^{-} cells as before, with ILC2s further identified based on their co-expression of the surface markers, KLRG1 and CD25 (Tait Wojno and Beamer, 2018). Compared to WT mice, ILC2s within all tissues examined were found to express IL-5 (figure 3.7A). Furthermore, the percentage of IL-5^{+}ILC2s tended to be higher in the mesenteries and omentum, compared to mLN controls (figure 3.7B, top). A statistically significant increase in the MFI of IL-5 by ILC2s was also observed in the omentum compared to the mLN (figure 3.7B, bottom).

Figure 3.7: Assessing *in vivo* IL-5 production by ILC2s in visceral adipose tissues at homeostasis

The mesenteries, omentum and mLN were isolated from IL-5 reporter (Red5) mice. Single cell suspension was generated and expression of Red5 by ILC2s was assessed by flow cytometry as described in materials and methods. Tissues from WT mice were isolated and used as control for gating of Red5^{+} cells.

Data are representative of two independent experiments whereby n=4. Bars on the graph represent the median value. Statistical significance was determined using Kruskal-Wallis followed by Dunn's multiple comparisons test. *P<0.05, **P<0.01, ***P<0.001 and ****P<0.0001.

a) Representative FACS plots comparing IL-5 (Red5) expression from total ST2^{+} ILC2s in the mLN (top), mesenteries (middle) and omentum (bottom), between WT and Red5 mice. Cells have been pre-gated on FSC and SSC followed by live CD45.2^{+}Lin^{-}IL-7Rα^{+}. Lineage (Lin) gate included CD3, CD5, B220, CD11b and CD11c.
b) Graph comparing the percentage of IL-5^{+}ST2^{+}ILC2s (top) and MFI of IL-5 by ILC2s (bottom) from Red5 mice between mLN, mesenteries (Me) and omentum (Om).

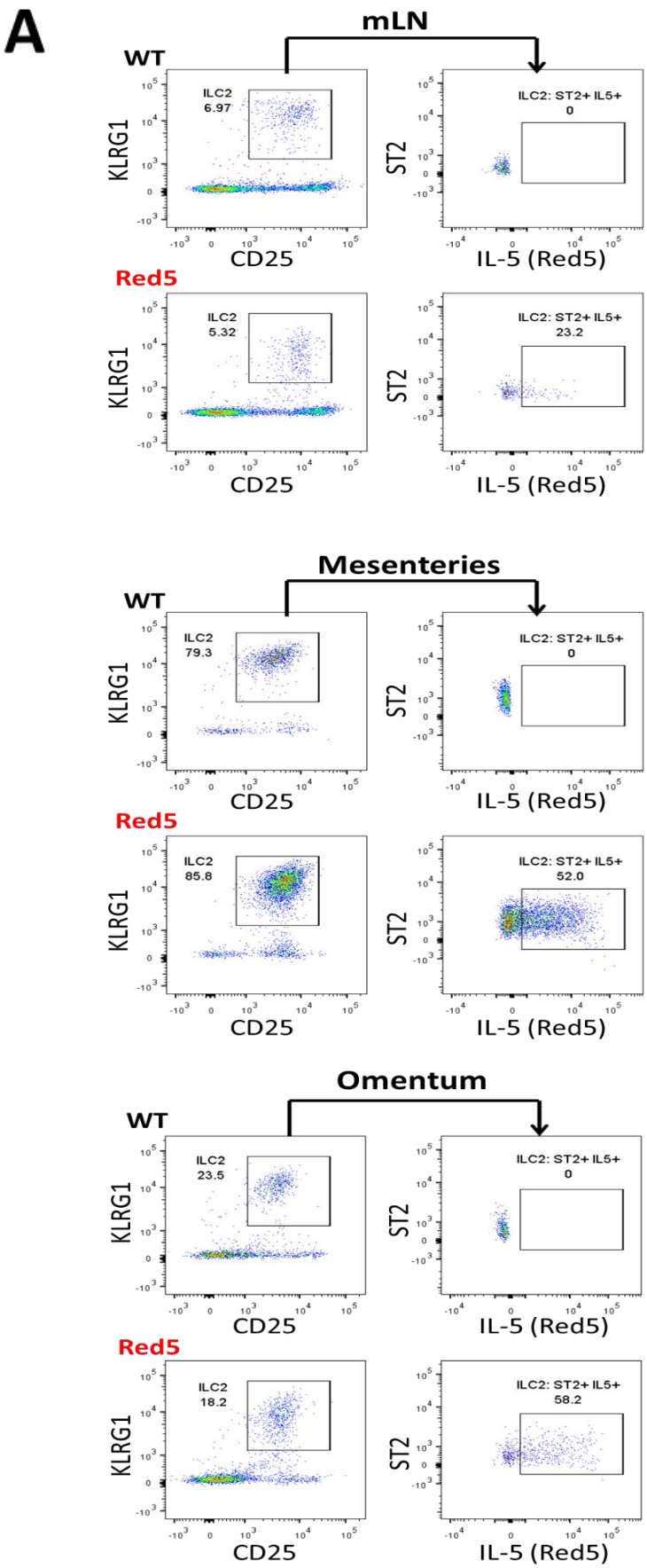
A
mLN
WT
ILC2
6.97
ILC2: ST2+ IL5+
0
KLRG1
ST2
CD25
IL-5 (Red5)
Red5
ILC2
5.32
ILC2: ST2+ IL5+
23.2
Mesenteries
WT
ILC2
79.3
ILC2: ST2+ IL5+
0
Red5
ILC2
85.8
ILC2: ST2+ IL5+
52.0
Omentum
WT
ILC2
23.5
ILC2: ST2+ IL5+
0
Red5
ILC2
18.2
ILC2: ST2+ IL5+
58.2

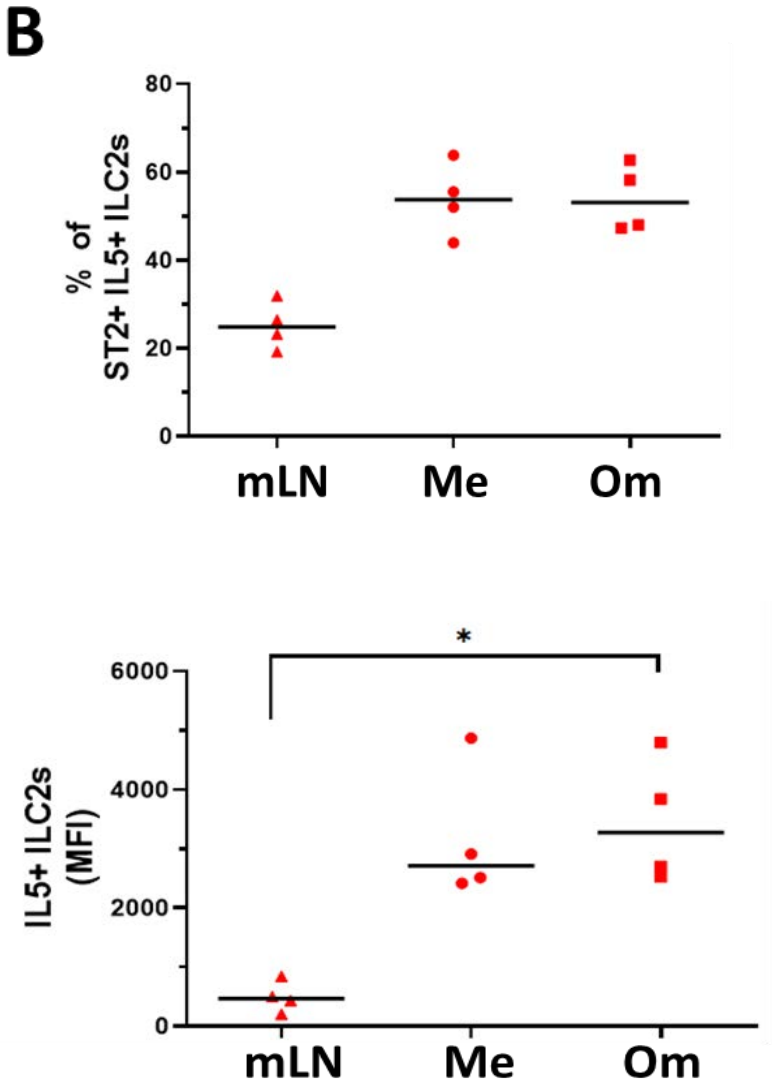
B
% of
ST2+ IL5+ ILC2s
80
60
40
20
0
mLN
Me
Om
*
IL5+ ILC2s
(MFI)
6000
4000
2000
0
mLN
Me
Om

Figure 3.7

3.3.3 *Ex vivo* stimulation of ILC2s leads to increased expression of IL-5 and IL-13 in visceral adipose tissues

Within other sites such as in the SLOs *ex vivo* stimulation of ILC2s can result in significant increase in type 2 cytokine production(Moro et al., 2010). Therefore, to investigate if ILC2s within VAT FALCs responded in a similar manner, single cell suspensions were generated from mesenteries, omentum and mLN. Cells were stimulated *ex vivo* with PMA and ionomycin, with the addition of brefeldin A (BFA) to stop protein export. Unstimulated control cells received BFA only. The difference in IL-5 and IL-13 production between unstimulated and stimulated ILC2s was then examined by flow cytometry (figure 3.8A). Following stimulation, the frequency of IL-13^{+}ILC2s was significantly higher in the mesenteries and omentum (figure 3.8B, middle). In addition, single positive IL-5^{+}ILC2s began to co-express IL-13 post stimulation (figure 3.8A); indeed, a statistically significant increase was observed in the frequency of double positive cytokine expressing (i.e., IL-5^{+}IL13^{+}) ILC2s, which also appeared to be more profound within both VATs compared to the mLN (figure 3.8B, bottom).

Figure 3.8: Assessing cytokine production by ILC2s in visceral adipose tissues following *ex vivo* stimulation

The mesenteries, omentum and mLN were isolated from C57BL/6J mice. Single cell suspension was generated from the tissues and cells were stimulated *ex vivo* with PMA and ionomycin (P/I) as described in materials and methods. Control tissues were not stimulated. The effect of P/I on ILC2 production of Th2 cytokines (namely IL-5 and IL-13) was analysed by flow cytometry.

Data are representative of two independent experiments whereby n=4. Bars on the graph represent the median value. Statistical significance was determined using Unpaired students t test. *P<0.05, **P<0.01, ***P<0.001 and ****P<0.0001.

a) Representative FACS plots showing expression of IL-5 and IL-13 by GATA3^{+}CD3i^{-}ILC2s in mLN (top), mesenteries (middle) and omentum (bottom) between unstimulated and P/I cells. Cells have been pre-gated on FSC and SSC followed by liveCD45.2^{+}Lin^{-}IL-7Rα^{+}. Lineage (Lin) gate included CD3, CD5, B220, CD11b and CD11c.
b) Graph comparing the percentage of IL-5^{+}; IL-13^{+}; and IL-5^{+}IL-13^{+} ILC2s (top to bottom) between unstimulated and P/I cells within the mLN, mesenteries (Me) and omentum (Om).

A

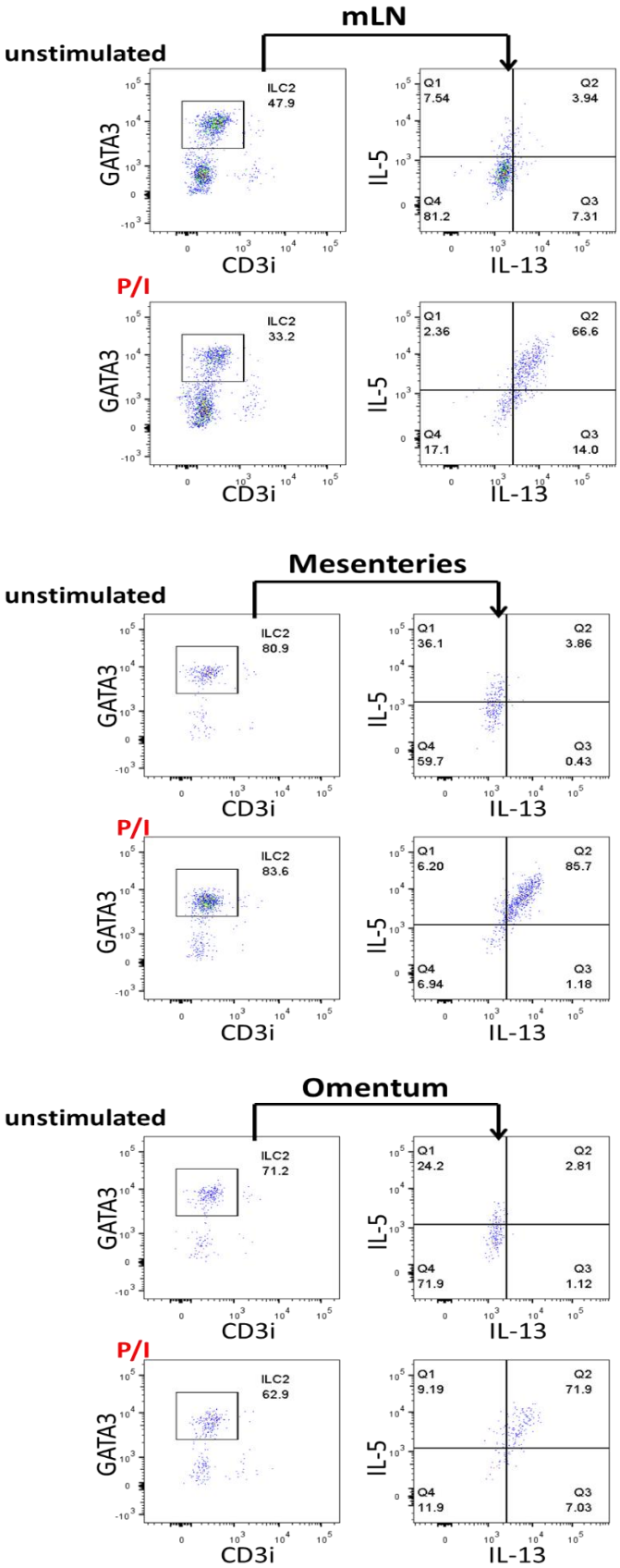
mLN
unstimulated
ILC2
47.9
Q1
7.54
Q2
3.94
Q4
81.2
Q3
7.31
GATA3
CD3i
IL-5
IL-13
P/I
ILC2
33.2
Q1
2.36
Q2
66.6
Q4
17.1
Q3
14.0
Mesenteries
unstimulated
ILC2
80.9
Q1
36.1
Q2
3.86
Q4
59.7
Q3
0.43
P/I
ILC2
83.6
Q1
6.20
Q2
85.7
Q4
6.94
Q3
1.18
Omentum
unstimulated
ILC2
71.2
Q1
24.2
Q2
2.81
Q4
71.9
Q3
1.12
P/I
ILC2
62.9
Q1
9.19
Q2
71.9
Q4
11.9
Q3
7.03

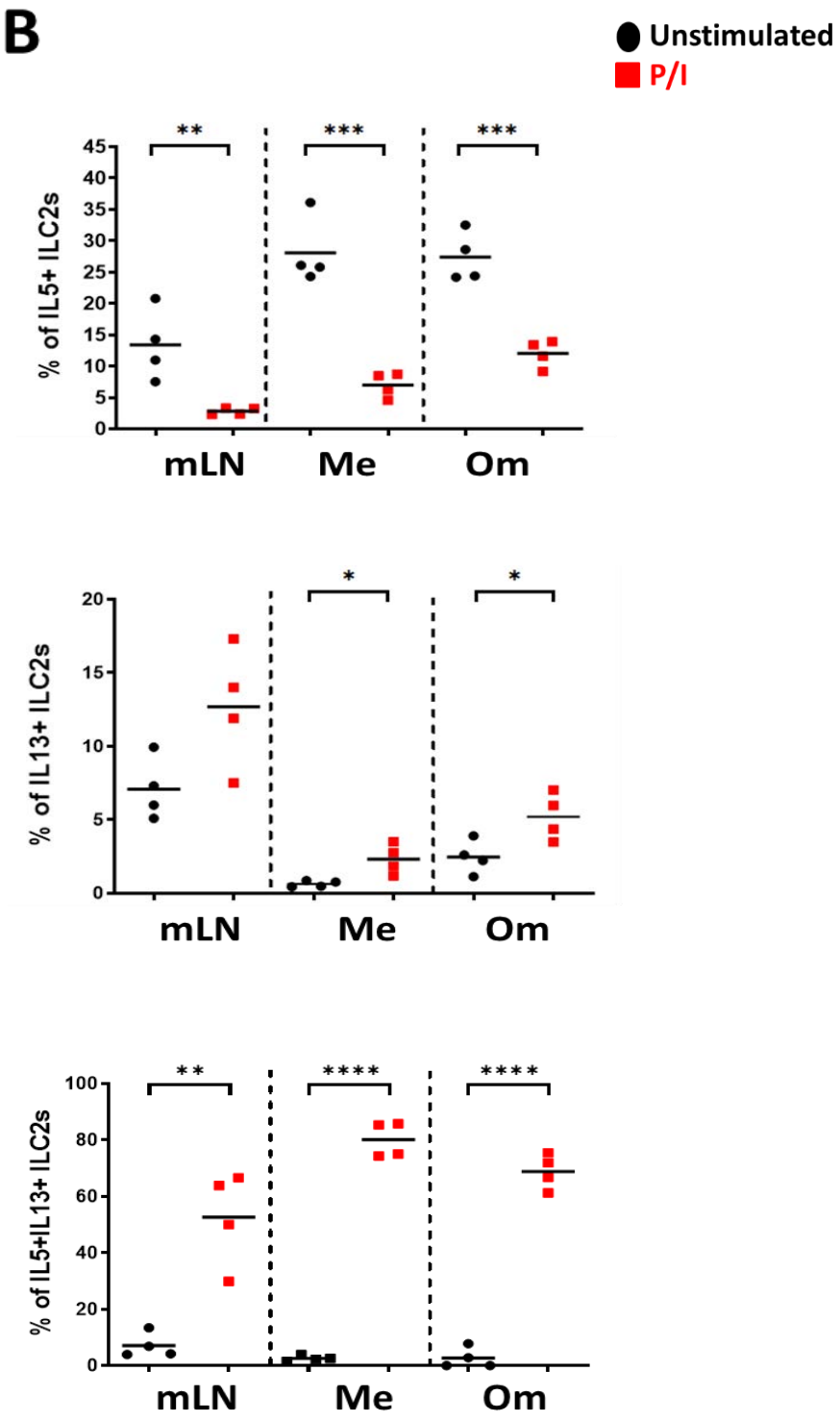
B
Unstimulated
P/I
% of IL5+ ILC2s
45
40
35
30
25
20
15
10
5
0
**
***
***
mLN
Me
Om
% of IL13+ ILC2s
20
15
10
5
0
*
*
mLN
Me
Om
% of IL5+IL13+ ILC2s
100
80
60
40
20
0
**
****
****
mLN
Me
Om

Figure 3.8

3.4 Summary

3.4.1 Understanding the Composition of Visceral Adipose FALCs at Steady State

The distribution of FALCs within ATs associated with mucosal surfaces are reported to be present in a heterogeneous manner (Cruz-Migoni and Caamaño, 2016). As this project focused on VATs of the peritoneal cavity, FALC clusters between three different VATs, the gonadal fat, mesenteries and omentum were first enumerated, to ensure findings recapitulated other published reports. As expected, FALCs were most abundant in the omentum; with gonadal fat having extremely few FALCs (median of less <5 FALCs per 100mg of tissue) as similarly observed by others (Bénézech et al., 2015). As such, it was decided for the purpose of this project - which seeks to understand the role of such lymphoid clusters in contributing to immune responses during different disease contexts - to focus future studies on the mesenteries and omentum, given their significantly greater FALC content.

Given the varied immune cell subsets within these clusters including both lymphoid (Moro et al., 2010) and myeloid subsets (Bénézech et al., 2015, Jackson-Jones et al., 2019), it was next investigated whether the heterogeneity in FALC numbers at homeostasis would also reflect a differential abundance (or lack therefore) in immune cell composition between the mesenteries and omentum. Could the ample presence of these clusters in the omentum for example, skew this tissue towards a certain milieu and what impact would this therefore have on disease pathology? Indeed, significant differences between the VATs examined for several immune cell subsets were observed. As expected, B cells and macrophages were significantly more enriched in the omentum which coincidently had the most number of FALCs, likely reflecting the fact that the serous cavities - of which the peritoneum is amongst - are considered primary sites for B1 cells and macrophages (Bénézech and Jackson-Jones,

2019). Furthermore, FALCs are reported to provide a homeostatic niche for the maintenance and activation of B cells, particularly innate-like B1 and B2 cells (Jackson-Jones and Bénézech, 2018). Notably, FALC ILC2s were shown to be essential in supporting B1 cell self-renewal through their production of IL-5, as well as in inducing IgA secretion by peritoneal B cells *in vitro* (Moro et al., 2010). In addition, the maintenance of AAM is dependent upon ILC2-derived cytokines IL-13 and IL-4, as well as eosinophils, the latter of which is also reliant upon ILC2-derived IL-5 (Molofsky et al., 2013). As shown in figure in 3.1, the omentum contained significantly higher number of FALCs compared to the mesenteries, as such would be expected to also contain increased numbers of immune cells per 100mg tissue as is seen with B cells and macrophages. However, the composition of these FALCs is likely to vary, given the fact that the numbers of other immune cell subsets were observed to be similar between both tissues. For example, the numbers of ILC2s and eosinophils only showed a very modest increase within the omentum, which may further suggest a difference in FALC composition between FALCs of the same tissue, with larger FALCs for example containing more ILC2s, which may compensate for the reduced FALC numbers. In line with this, the author has also observed a heterogeneity in FALC size within the same tissue, in steady state – as has been reported elsewhere (Moro et al., 2010). Other immune populations including CD4 T cells, iNKTs, $ST2^-$ Tregs, $ST2^+$ Tregs and cDC2s were also more abundant in the omentum compared to the mesenteries. Characteristically, these cells are considered to be anti-inflammatory, important in maintaining homeostasis within lean fat tissue through their secretion of type 2 cytokines (Chalubinski et al., 2016), and in the case of cDC2s, Th2 cell differentiation (Gao et al., 2013). This thereby alludes to a type 2, anti-inflammatory profile of FALCs, supported further by the observation by us (unpublished; figure 4.6) and others

(Jackson-Jones et al., 2016) that stromal cells within these clusters express several Th2 cytokines and chemokines, one of them being IL-33, which is involved in inducing type 2 immune responses (Rostan et al., 2015). Interestingly, higher numbers of cytotoxic lymphocytes particularly ILC1s, CD8 T cells and to a lesser extent NK cells, as well cDC1s which aid in activating these cells (Cancel et al., 2019), and monocytes which when recruited to AT can give rise to CD11c^{+} (pro-inflammatory) AT macrophages (Castoldi et al., 2016), were also observed in the omentum. This therefore indicates that while type 2 immune cells may predominate in FALCs, a degree of complexity exists in that these structures can encompass a host of immune cells and are likely to therefore mediate an immune balance that ensures homeostasis is maintained within VATs. It also highlights the potential of these clusters to be dynamic structures that can importantly be manipulated through the enhancement and/or suppression of desired immune subsets, to generate a desired immune response during several disease states.

3.4.2 Phenotypic and Functional Characterisation of Visceral Adipose FALCS at Steady State

The distribution of immune cells between lymphoid and peripheral tissues is regulated by the expression of chemokine receptors, and directed by chemokine gradients, with the latter also mediating lymphocyte development and maturation (Kufareva et al., 2015). Specific ILC2 homing receptors for LNs, spleen (Kim et al., 2015), as well lung, skin and intestine (Kim et al., 2016) have been identified that direct migration of these cells; but further information regarding the dynamics of AT ILC2 chemokine receptor expression is required (Kim et al., 2016, Willinger, 2019). Previous studies within our group provided some insight into the phenotype of VAT ILC2s (particularly within the gonadal fat, and mesenteries), with CCR8 and CCR9 emerging as likely candidates. To further this work, and extend studies to the

omentum, ILC2 expression of CCR8 and CCR9 within the mesenteries, omentum as well as the mLN was examined, first in the steady state and then during infection (the latter is detailed in chapter 4.2).

At homeostasis, significant proportions of ILC2s singly expressing CCR8 were observed within the mesenteries and omentum and found to be even more abundant in these tissues compared to mLNs. This thereby suggested a propensity for $CCR8^{+}$ILC2s to accumulate in VATs compared to lymphoid organs. CCR8 is well known to be expressed on Tregs, $CD4^{+}$ thymocytes, DCs, macrophages and importantly Th2 – but not Th1 cells (Islam et al., 2011). Therefore, with ILC2s being innate counterparts of $CD4^{+}$ Th2 cells (Eberl et al., 2015), the high expression of CCR8 observed on ILC2s within VATs at steady state was not surprising, and further suggested a commonality in the molecular pathways that control tissue distribution and homing of these immune populations. In addition, this observation may allude to CCR8 as a VAT homing receptor. As such to advance this work, it would be interesting to confirm whether CCR8 is upregulated at an ILC2 progenitor stage in the bone marrow as is reported for ILC2 gut homing receptors (Kim et al., 2016), thereby deciphering whether this chemokine receptor directs the migration of ILC2 progenitors to VATs. Such accumulation further suggests the presence of CCR8 ligands within the mesenteries and omentum. Interestingly CCL8, a ligand for CCR8 was previously identified to be upregulated in the epididymal AT of high-fat diet induced and genetically obese mice (Jiao et al., 2009). Additionally, CCL8 was also observed to be expressed by human adipocytes, albeit in response to TNF-α (Tourniaire et al., 2013). Therefore, transcriptional profiling of mesenteric and omental AT via real-time PCR of RNA isolated from these VATs under steady state conditions could be employed to confirm the presence of this as well as other CCR8 ligands.

Meanwhile by employing intravital microscopy, Puttur and colleagues were able to reveal some of the mechanisms regulating the amoeboid-like movement of ILC2s in the lung during allergic airway inflammation. Most relevant to our results, pulmonary ILC2s were also shown to express CCR8 at homeostasis, with IL-33 treatment inducing the upregulation of this receptor. Importantly, CCR8 promoted ILC2 homing to CCL8 deposits located within the airway epithelium (Puttur et al., 2019), thereby suggesting that this receptor may be a key regulator of ILC2s across different tissues. In contrast, $CCR9^{+}$ILC2s as well as $CCR8^{+}CCR9^{+}$ double positive ILC2s were found to be significantly higher in mLN compared to VATs. CCR9 is a gut homing receptor involved in migration of lymphocytes to the SI and subsequent distribution to other tissues (Wu et al., 2014). In line with our studies, $CCR9^{+}$ILC2s have been shown to be significantly high within lymphoid tissues including the mLN (Kim et al., 2015). In addition, others have reported of the uniform expression of CCR9 by ILC2s in the SI compared to a more heterogeneous expression of this receptor by ILC2s isolated from mesenteric ATs (Sasaki et al., 2019). Similarly, earlier reports had shown that migration of ILC2s to the SI was partly mediated by CCR9 (Hoyler et al., 2012), further highlighting the possible dispensability of this chemokine receptor in VAT ILC2 homing and function. Finally, in all three tissues examined within our study, a $CCR8^{-}CCR9^{-}$ double negative ILC2 population could also be identified, most evident in the mLN and omentum, leaving room to suggest of other chemokine receptors involved in ILC2 AT distribution and function. ILC2s indeed express a number of chemokine receptors that direct their tropism to SLOs and barrier surfaces. It is therefore plausible that some may make up this double negative population. Notably, CCR4 - albeit in the context of ILC2 homing to the lungs - was shown to mediate the chemotaxis of *in vitro* expanded ILC2s in response to CCL17/22, with *in vivo* experiments

confirming these results; owing to the inability of CCR4$^{-/-}$ ILC2s to migrate into inflamed lungs following allergen challenge (Knipfer et al., 2019). However, it is also likely that this double negative population contain other yet-to-be-identified ILC2 chemokine receptor subsets, and as such may require further experiments to decipher if this is the case. Nonetheless, these results have been able to corroborate previous findings from our group, and further reveal that these data are largely consistent within other VATs such as the omentum.

Over the years, ILC2s have continued to emerge as key immune cells that not only drive innate responses in various pathologies, but also initiate adaptive Th2 responses, mediated largely by their secretion of type 2 cytokines. In the intestinal tract, ILC2s interact via MHC II with antigen specific T cells leading to ILC2 proliferation and IL-13 production, a crosstalk that ensures efficient transition to T cell-mediated immunity during helminth infection (Oliphant et al., 2014b). Meanwhile, lung ILC2-derived IL-5 and IL-13 have been particularly described, and while these also mediate protective immunity against helminths such as to *Nippostrongylus brasiliensis (N. brasiliensis)* (Neill et al., 2010), as well viral infection (Gorski et al., 2013), they have also been shown to be major contributors of allergic airway inflammation and asthma (Halim et al., 2012, Klein Wolterink et al., 2012). Therefore, the dynamics of the ILC2 derived cytokines, IL-5 and IL-13 within VATs was investigated, again using mLN as controls, given their close anatomical localisation to ATs. At steady state considerably higher frequencies and expression (via MFI) of IL-5^{+}ILC2s was observed within the mesenteries and omentum, compared to the mLN. ILC2s are known to be endowed with unique functions, one of these being their ability to independently produce type 2 cytokines such as IL-5 (Moro et al., 2016). Such results therefore highlight VAT ILC2s as a major source of constitutive IL-5. Indeed, others have also described the critical role of ILC2-derived IL-5 in

sustaining AT homeostasis and preventing the development of obesity and insulin resistance (Molofsky et al., 2013). Similarly, during one of the initial descriptions of ILC2s, Moro and colleagues were able to reveal that ILC2s isolated from mesenteric FALCs produced high amounts of IL-5 and IL-13 following stimulation with PMA/ionomycin, and dominated in such production compared to CD4 T cells from spleen or mLN (Moro et al., 2010). In agreement with this, our results equally found that following *ex vivo* stimulation with PMA/ionomycin, significantly higher proportions of IL-13^{+}ILC2s were detected within the mesenteries and omentum, as part of the IL-5^{+}IL-13^{+} ILC2 population. Finally, IL-5^{+}IL-13^{+} double positive population were also observed to increase profoundly across all tissues, and appeared to be derived from the IL-5^{-}IL-13^{-} double negative ILC2 populations.

Therefore, through the characterisation of immune cell subsets within mesenteric and omental VAT FALCs, a tendency towards a type 2 milieu within these clusters has been observed, and is more prominent in the omentum, possibly as a consequence of the higher FALC content within this tissue. Data from immune profiling of ILC2s - one of the main immune populations enriched in FALCs - importantly validates previous work from our laboratory, and is consistent with other published studies, while also providing new information that furthers our understating of omental FALCs. Such steady state analysis therefore forms a foundation for this project, as it next seeks to understand the role of VAT FALCs during disease.

CHAPTER 4: IMMUNE RESPONSES IN PERITONEAL ADIPOSE TISSUES DURING HELMINTH INFECTION

4.1 Introduction

Helminth infections pose significant economical, medical and educational burdens to society; as one of the most prevalent infectious agents worldwide, they affect nearly a third of the global population (McSorley and Maizels, 2012). These parasites are capable of establishing long-term chronic infections in either their human or animal hosts, aided by their ability to manipulate host immune responses (M. Webb and D. Tait Wojno, 2017). As such, understanding their strategy of persistence as well as host-parasite interaction is necessary. Fortunately several animal models of helminth infection have been established and have highlighted how important type 2-dependent responses and pathways are in conferring protection (Reynolds et al., 2012).

While *N. brasiliensis* and *H. poly* are two of the most common models of infection studied, the former is not a natural parasite of the mice; neither does it represent a localised infection, owing to its systemic migration via the blood and across multiple tissues (Mohrs et al., 2005). Therefore this project focuses particularly on the intestinal helminths, *H. poly* and *S. mansoni* which are able to establish chronic infections in their host, and therefore provide natural experimental infection models that mirror the co-evolution of host-parasite interactions. Within FALCs, ILC2s are important – through their production of Th2 cytokines - in promoting early responses to *H. poly* at the local site of infection and within SLOs. As mentioned previously, IL-5 and IL-13 mediate eosinophil recruitment and goblet cell hyperplasia respectively, both of which are critical to helminth expulsion (M. Webb and D. Tait Wojno, 2017). Meanwhile ILC2-derived IL-4 drives Th2 differentiation and hence the development of adaptive immune responses (Pelly et al., 2016).

Owing to their lack of antigen specific receptors, ILCs become activated by responding to the cytokine milieu within their environment. ILC2s respond to epithelium derived IL-25, IL-33 and thymic stromal lymphopoietin (TSLP) (Eberl et al., 2015). IL-33 in particular is a nuclear associated cytokine, but can also be passively secreted during cell necrosis or tissue damage thereby functioning as an alarmin (Chan et al., 2019). Within our group we also observe IL-33 expression on FALC stromal cells (figure 4.6). Therefore upon its release, IL-33 can interact with its ST2 receptor expressed on a number of immune cells including Th2 cells, mast cells, ILC2s, and AT Tregs to potently induce Th2 cytokines (Molofsky et al., 2015). Notably, stimulation of ILC2s with IL-33 alone or in combination with IL-2 and IL-25 results in high (micrograms) amounts of IL-5 and IL-13 (Moro et al., 2010). In addition, IL-33 mRNA is increased in the mLN and SI lamina propria of *H. poly* infected mice, concomitant with increased number of ILC2s and IL-4/5/13 (Pelly et al., 2016). Meanwhile in *Trichuris muris* parasitic infection, early increases in caecal IL-33 mRNA are observed (Humphreys et al., 2008). Taken together, these highlight IL-33 as a central mediator across a spectrum of helminth infections and suggest that its early production at the site of infection can coordinate Th2 immunity via its action on responsive cells including ILC2s. Furthermore, the production of IL-5 and IL-13 by ILC2s in AT following *ex vivo* stimulation has been observed by us, as shown in chapter 3.3.3.

Whether ILC2s have a role in immune responses to *S. mansoni* infection remains largely unknown; there is also a need to investigate whether schistosomes are involved in ILC2 induction, be it directly or indirectly through tissue damage (Nausch and Mutapi, 2018). Previous reports have shown that gene expression levels of IL-33 are elevated in murine epidermis following percutaneous infection with *S. mansoni*, suggesting the likely activation

of IL-33 responsive cells such as ILC2s and Th2 cells (Bourke et al., 2015). However, others have shown that blocking IL-33 alone has no effect on the development and maintenance of type 2 cytokine driven pathology within the lungs and liver during acute and chronic *S. mansoni* infection; with a similar redundancy following IL-25 or TSLP blockade. Instead disrupting all three epithelial cytokines was found to impact Th2 pathology – albeit in a transient manner, owing to the significant reduction in IL-13-producing ILC2s within the mLNs, as well as in granuloma-associated eosinophils and hepatic fibrosis by 9 weeks post infection (Vannella et al., 2016). Such disparity therefore highlights the requirement for further studies, given the critical role of ILC2s in initiating Th2 responses as well as in wound healing during other gastrointestinal helminth infections (Costain et al., 2018). Nonetheless, more information exists on the impact of other type 2 immune cells during *S. mansoni*, namely CD4 Th2 cells, eosinophils and AAM which are needed for the development of granulomas that surround parasitic eggs following infection (Costain et al., 2018). These structures are particularly evident in the intestine and liver where eggs usually become trapped. In addition, it is well known that parasitic infections in general can modulate a number of host physiological pathways relating to metabolism and immune responses in specific tissues. In this regard *Schistosoma* infections along with *Schistosoma*-derived molecules are reported to affect the immune cell composition within WATs, most notably through the polarisation of immune cells to a type 2 phenotype, with studies particularly investigating this in the context of inflammatory disease and metabolic dysfunction (Tang et al., 2018). For instance, Hussaarts and colleagues were able to demonstrate that in high fat diet-induced obese mice, chronic infection with *S. mansoni*, resulted in improved insulin sensitivity, glucose uptake and reduced fat mass gain, likely mediated by the concomitant

increases in eosinophils, and AAM within the gonadal and mesenteric ATs (Hussaarts et al., 2015). Therefore while this highlights a role for schistosomes in improving metabolic function through its effect on AT immune cells, what is less clear is whether AT - and more specific to us - whether VAT FALCs can initiate or contribute to the developing immune responses during *Schistosoma* infection.

4.2 Investigating the Phenotype of Effector ILC2s during *Heligmosomoides polygyrus* Infection

The identification that ILC2s within the mesenteries and omentum expressed varying levels of CCR8 and CCR9 at homeostasis, resulting in the delineation of separate ILC2 subsets (chapter 3.3.1), led to the investigation of these differences in the context of infection using the helminth *H. poly*. In particular, we assessed whether proliferation following *H. poly* infection could be attributed to specific ILC2 subsets. As such, C57BL/6J mice were infected with either 200 *H. poly* L_3 larvae or PBS, with the mesenteries, omentum and mLN harvested 7 days post infection. Tissues were enzymatically digested to generate a single cell suspension, which was subsequently stained with antibodies for the detection of ILC2s via flow cytometry. Proliferation of total ILC2s within all tissues examined was first determined using the proliferation marker Ki67 (figure 4.1A). ILC2s were then divided into CCR8/9 subsets, and Ki67 expression within each of the subsets was evaluated (figure 4.1B).

The percentage of total ILC2s expressing Ki67 was observed to be higher in the mesenteries and omentum of infected mice compared to control mice, with a notable statistically significant increase in the mesenteries (figure 4.2A). However, no difference in ILC2 proliferation was observed in the mLN following infection (figure 4.2A).

Next the proliferative capacity of the individual ILC2 subsets based on CCR8 and CCR9 was determined. Within the mesenteries and omentum, all four subsets designated as $CCR8^+$; $CCR9^+$; $CCR8^+CCR9^+$ and $CCR8^-CCR9^-$, had higher proportions of $Ki67^+$ ILC2s following *H. poly* infection compared to PBS controls. These increases were statistically significant for $CCR9^+$; $CCR8^+CCR9^+$ and $CCR8^-CCR9^-$ ILC2s in the mesenteries, and for $CCR8^+$; $CCR9^+$; $CCR8^+CCR9^+$ ILC2s in the omentum (figure 4.2B). However, no single individual subset emerged as the most proliferative within these VATs. Additionally, there was no difference in $Ki67^+$ ILC2s amongst any of the subsets within the mLN post infection (figure 4.2B).

Figure 4.1: Gating strategies to identify Ki67 expression within ILC2 CCR8/CCR9 subsets

The mesenteries, omentum and mLN were isolated from C57BL/6J mice 7 days after oral gavage with either 200 *H. poly* L_3 larvae or PBS. Cells were isolated from tissues and proliferation of total ILC2s, as well as of ILC2 chemokine receptor subsets were assessed by flow cytometry as described in materials and methods. Representative FACS plots are shown, whereby n=9 for PBS, and n=9-10 for *H. poly,* across 4 independent experiments. Lineage (Lin) gate included CD3, CD5, B220, CD11b and CD11c.

a) FACS plots comparing Ki67 expression on total $GATA3^{+}CD3i^{-}$ ILC2s in mLN (top), mesenteries (middle) and omentum (bottom) between PBS and *H. poly* infected mice. Cells have been pre-gated on FSC and SSC followed by $liveCD45.2^{+}$.
b) FACS plots showing Ki67 expression within each ILC2 CCR8/CCR9 subset in indicated tissues. Cells have been pre-gated on FSC and SSC followed by $liveCD45.2^{+}Lin^{-}IL7Ra^{+}$ $GATA3^{+}CD3i^{-}$.

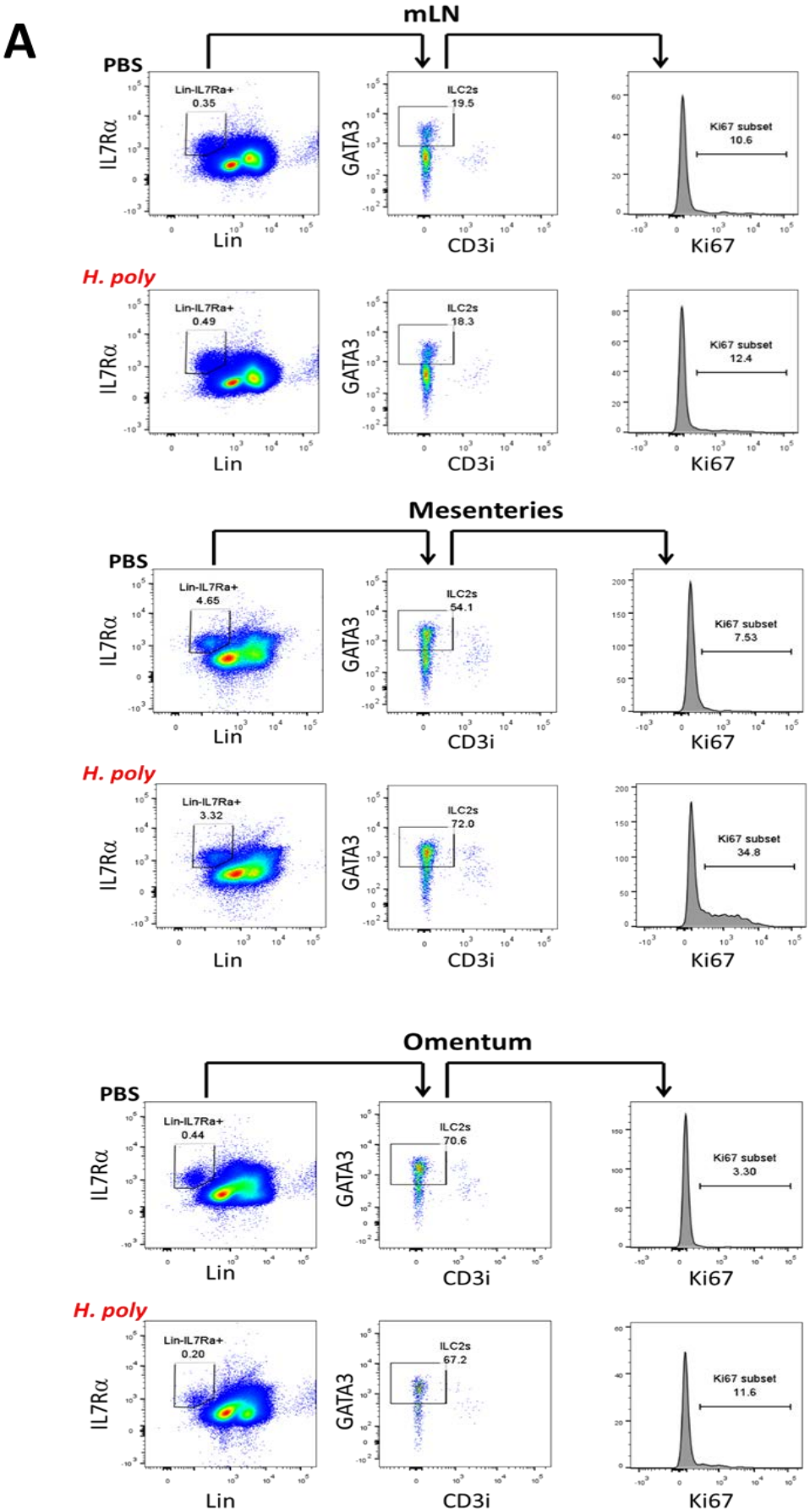
A
mLN
PBS
Lin-IL7Ra+
0.35
ILC2s
19.5
Ki67 subset
10.6
IL7Rα
Lin
GATA3
CD3i
Ki67
H. poly
Lin-IL7Ra+
0.49
ILC2s
18.3
Ki67 subset
12.4
Mesenteries
PBS
Lin-IL7Ra+
4.65
ILC2s
54.1
Ki67 subset
7.53
H. poly
Lin-IL7Ra+
3.32
ILC2s
72.0
Ki67 subset
34.8
Omentum
PBS
Lin-IL7Ra+
0.44
ILC2s
70.6
Ki67 subset
3.30
H. poly
Lin-IL7Ra+
0.20
ILC2s
67.2
Ki67 subset
11.6

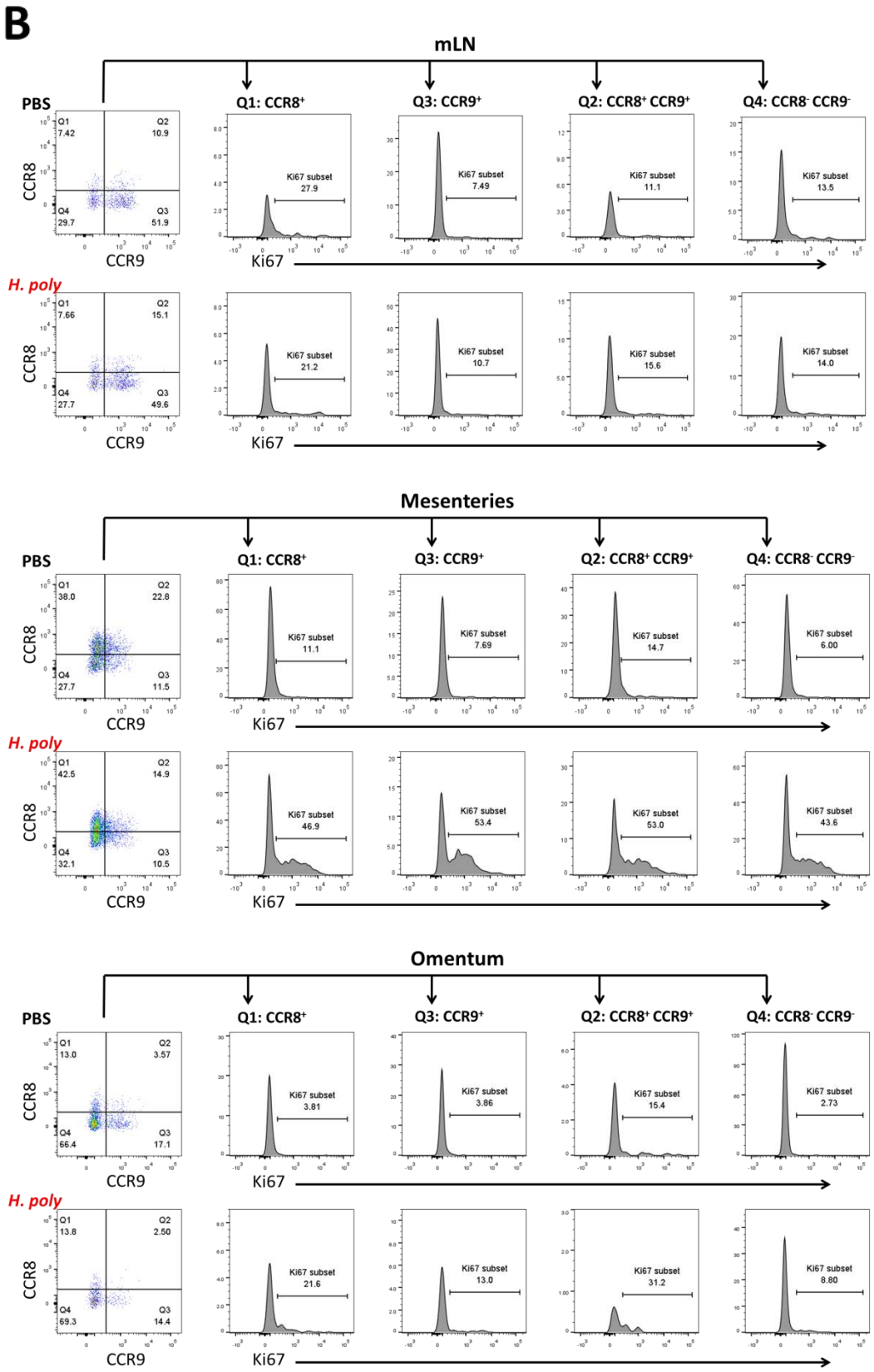
B
mLN
PBS
Q1: CCR8+
Q3: CCR9+
Q2: CCR8+ CCR9+
Q4: CCR8- CCR9-
CCR8
CCR9
Ki67
Ki67 subset 27.9
Ki67 subset 7.49
Ki67 subset 11.1
Ki67 subset 13.5
H. poly
Ki67 subset 21.2
Ki67 subset 10.7
Ki67 subset 15.6
Ki67 subset 14.0
Mesenteries
Ki67 subset 11.1
Ki67 subset 7.69
Ki67 subset 14.7
Ki67 subset 6.00
Ki67 subset 46.9
Ki67 subset 53.4
Ki67 subset 53.0
Ki67 subset 43.6
Omentum
Ki67 subset 3.81
Ki67 subset 3.86
Ki67 subset 15.4
Ki67 subset 2.73
Ki67 subset 21.6
Ki67 subset 13.0
Ki67 subset 31.2
Ki67 subset 8.80

Figure 4.1

Figure 4.2: Proliferation within ILC2 CCR8 and CCR9 subsets in visceral adipose tissues following *H. poly* infection

C57BL/6J mice received 200 *H. poly* L_3 larvae by oral gavage, while control groups received PBS. Cells from mLN, mesenteries and omentum were isolated as described in materials and methods. The difference in proliferation between ILC2 CCR8/CCR9 subsets following infection was assessed.

Data are representative of 4 independent experiments, with the following sample numbers: PBS (n=9), *H. poly* (n=9-10). Bars on the graph represent the median value. Statistical significance was determined using Kruskal-Wallis followed by Dunn's multiple comparisons test. *P<0.05, **P<0.01, ***P<0.001 and ****P<0.0001.

a) Graph showing the percentage of Ki67 on total ILC2s in mLN, mesenteries (Me) and omentum (Om) between PBS and *H. poly* infected mice.
b) Graph comparing the percentage of Ki67 expressed by $CCR8^+$; $CCR9^+$; $CCR8^+CCR9^+$ and $CCR8^-CCR9^-$ ILC2 subpopulations following *H. poly* infection in the mLN, mesenteries and omentum.

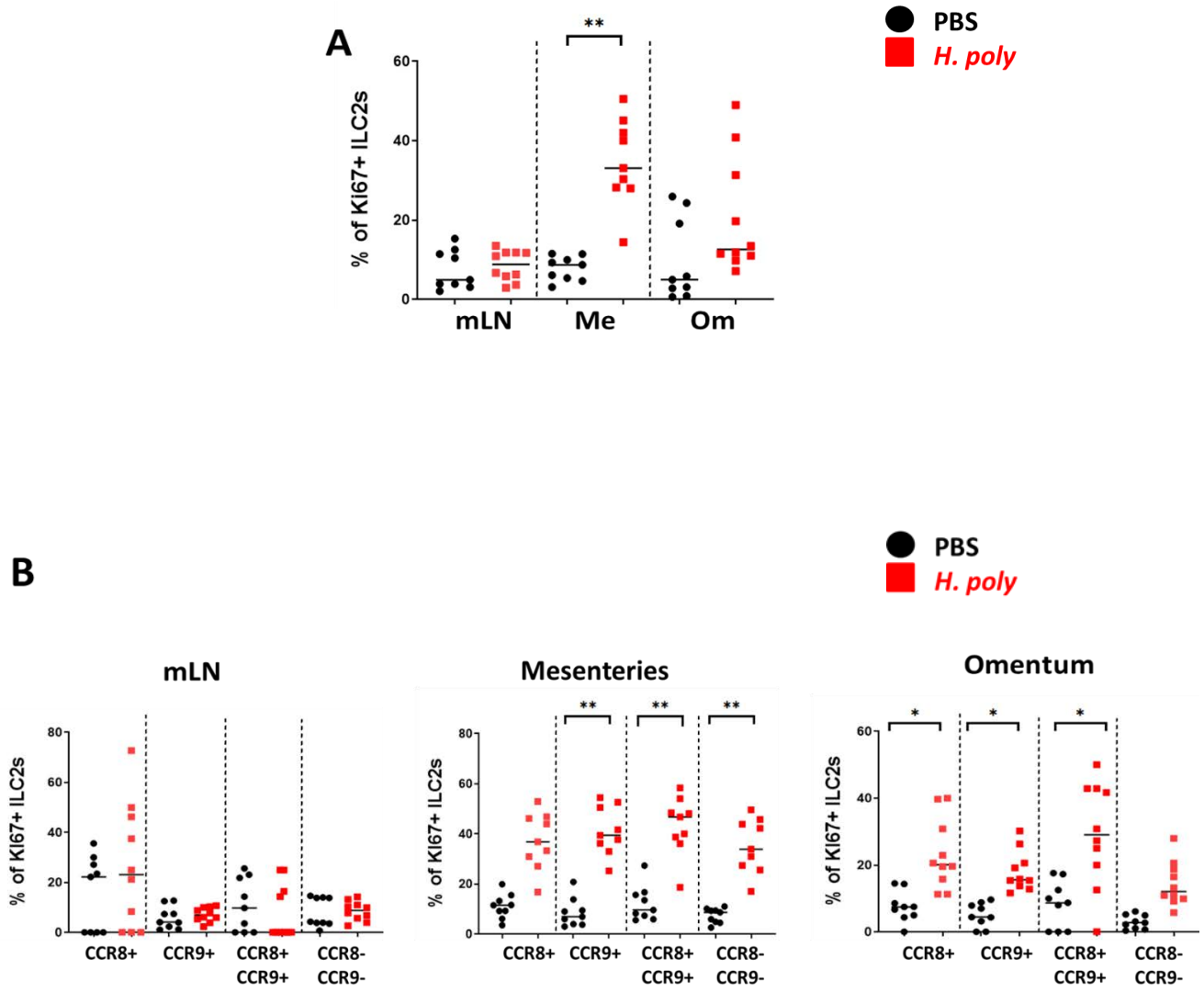
A
PBS
H. poly
% of Ki67+ ILC2s
mLN
Me
Om
B
mLN
Mesenteries
Omentum
CCR8+
CCR9+
CCR8+ CCR9+
CCR8- CCR9-

Figure 4.2

4.3 *In Vivo* Responses to *Heligmosomoides polygyrus* Infection

Following the observation that none of the individual ILC2 CCR8/9 subsets had a greater proliferative capacity upon *H. poly* infection, it was therefore decided to investigate ILC2 function as a whole, as opposed to the individual chemokine receptor subsets. ILC2s in the lamina propia of the SI had been reported as early as day 5 post *H. poly* infection to transcribe IL-4 mRNA as well as IL-4 protein that not only led to the recruitment of ILC2s to this tissue following infection, but also supported CD4 Th2 differentiation (Pelly et al., 2016). However, whether such immune cells located within VAT FALCs could also contribute to early IL-4 secretion in response to *H. poly* infection was unknown. As such to determine if VAT ILC2s were secreting IL-4 *in vivo*, IL-4-IRES-eGFP (B6.4get) mice were infected and IL-4-GFP expression on ILC2s (figure 4.3A) as well as on CD4 T cells (figure 4.3B) 7 days post infection was assessed. In addition, the activation status of these immune cells was determined via the expression of CD69 and CD44 (figure 4.3A-B). To preserve reporter signal ILC2s were identified as IL-7Ra^{+}Lin^{-}KLRG1^{+}CD25^{+} cells (Tait Wojno and Beamer, 2018). Following *H. poly*, a slight but non-statistically significant increase in *in vivo* IL-4 secretion by CD44^{+}ILC2s was observed in the mesenteries, with no difference found in other tissues examined (mLN, SI, omentum- figure 4.4A). However, there was a statistically significant increase in the normalised numbers of IL-4^{+}CD44^{+}CD4 T cells within the mesenteries, omentum and mLN (figure 4.5A); furthermore ILC2s within these tissues significantly upregulated their expression of the early activation marker CD69 post infection, compared to PBS controls (figure 4.4B).

Figure 4.3: Gating strategy to identify activation and *in vivo* IL-4 production by ILC2s and CD4 T cells

The mesenteries, omentum, mLN and SI were isolated from B6.4get mice 7 days after oral gavage with either 200 *H. poly* L_3 larvae or PBS. Cells were isolated from tissues; expression of IL-4-expressing GFP by ILC2s and CD4 T cells, as well as expression of activation markers CD44 and CD69 was assessed by flow cytometry as described in materials and methods. Representative FACS plots are shown, whereby n=8-10 for PBS, and n=8-9 for *H. poly*, across 3 independent experiments. Lineage (Lin) gate included CD3, CD5, B220, CD11b and CD11c.

a) FACS plots comparing IL-4-GFP expression from total $CD44^+$ILC2s, and CD69 expression from $KLRG1^+CD25^+$ILC2s in SI, mLN, mesenteries and omentum between PBS and *H. poly* infected B6.4get mice. Cells have been pre-gated on FSC and SSC followed by live$CD45.2^+$.
b) FACS plots comparing IL-4-GFP from total $CD44^+$CD4 T cells and CD69 expression from IL-$7Ra^+$CD4 T cells in SI, mLN, mesenteries and omentum between PBS and *H. poly* infected B6.4get mice. Cells have been pre-gated on FSC and SSC followed by live $CD45.2^+Lin^+$ IL-$7Ra^+$. (Lin+ gate is the same as shown in figure 4.3A).

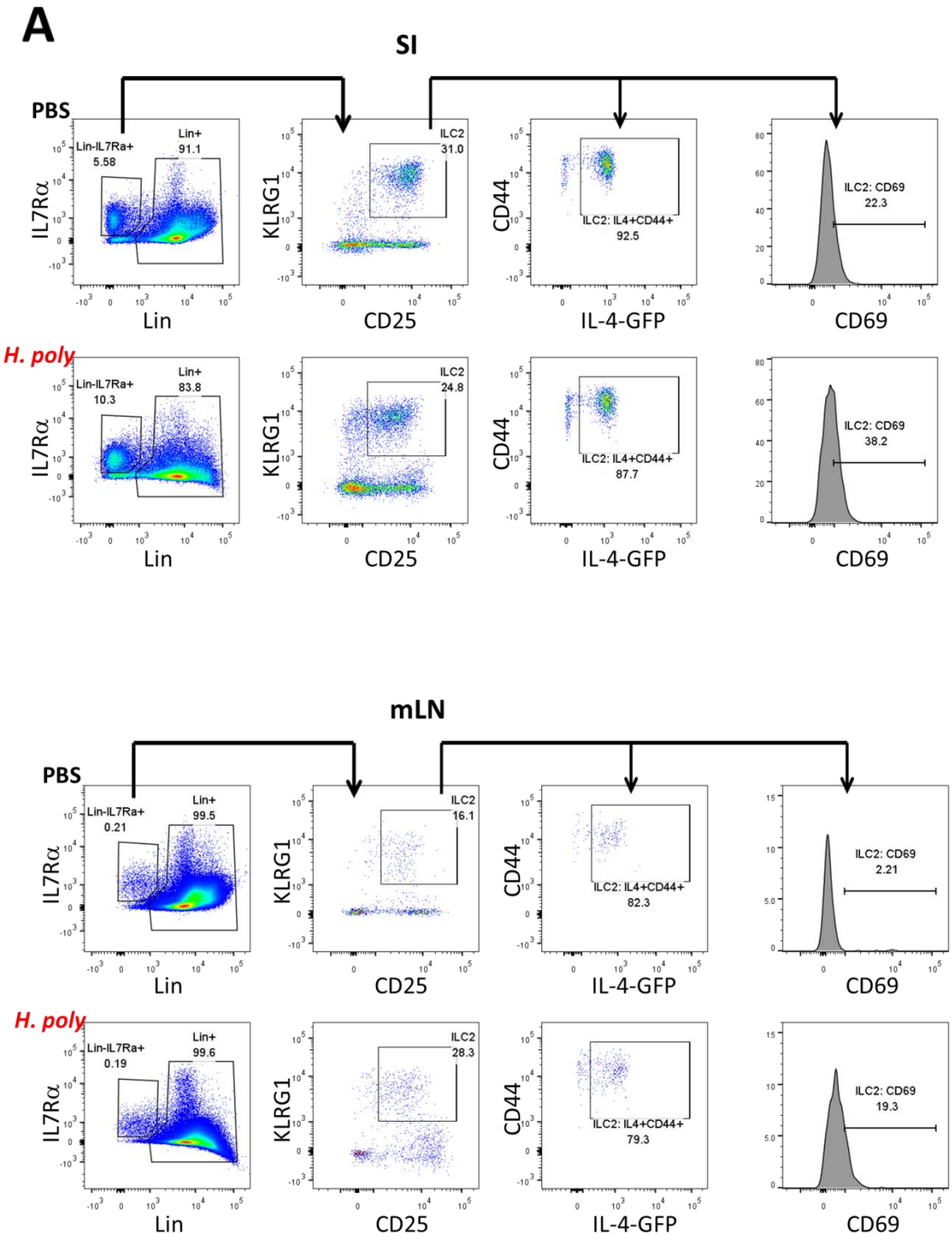
A
SI
PBS
Lin-IL7Ra+
5.58
Lin+
91.1
IL7Rα
Lin
ILC2
31.0
KLRG1
CD25
ILC2: IL4+CD44+
92.5
CD44
IL-4-GFP
ILC2: CD69
22.3
CD69
H. poly
Lin-IL7Ra+
10.3
Lin+
83.8
ILC2
24.8
ILC2: IL4+CD44+
87.7
ILC2: CD69
38.2
mLN
PBS
Lin-IL7Ra+
0.21
Lin+
99.5
ILC2
16.1
ILC2: IL4+CD44+
82.3
ILC2: CD69
2.21
H. poly
Lin-IL7Ra+
0.19
Lin+
99.6
ILC2
28.3
ILC2: IL4+CD44+
79.3
ILC2: CD69
19.3

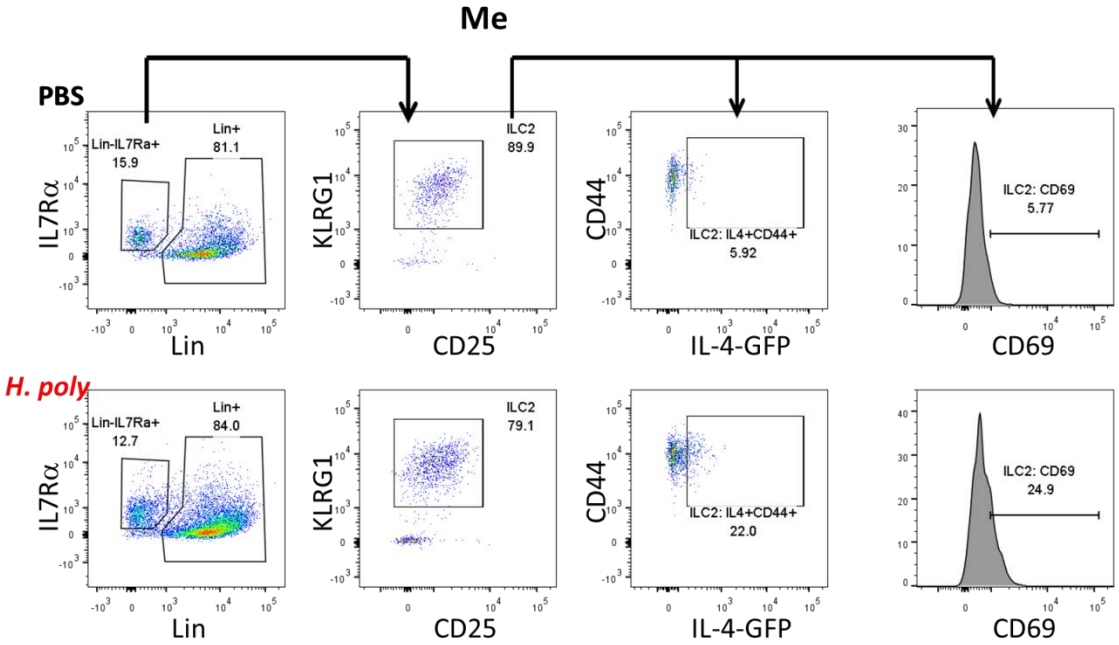
Me
PBS
Lin-IL7Ra+
15.9
Lin+
81.1
IL7Rα
Lin
ILC2
89.9
KLRG1
CD25
CD44
ILC2: IL4+CD44+
5.92
IL-4-GFP
ILC2: CD69
5.77
CD69
H. poly
Lin-IL7Ra+
12.7
Lin+
84.0
ILC2
79.1
ILC2: IL4+CD44+
22.0
ILC2: CD69
24.9

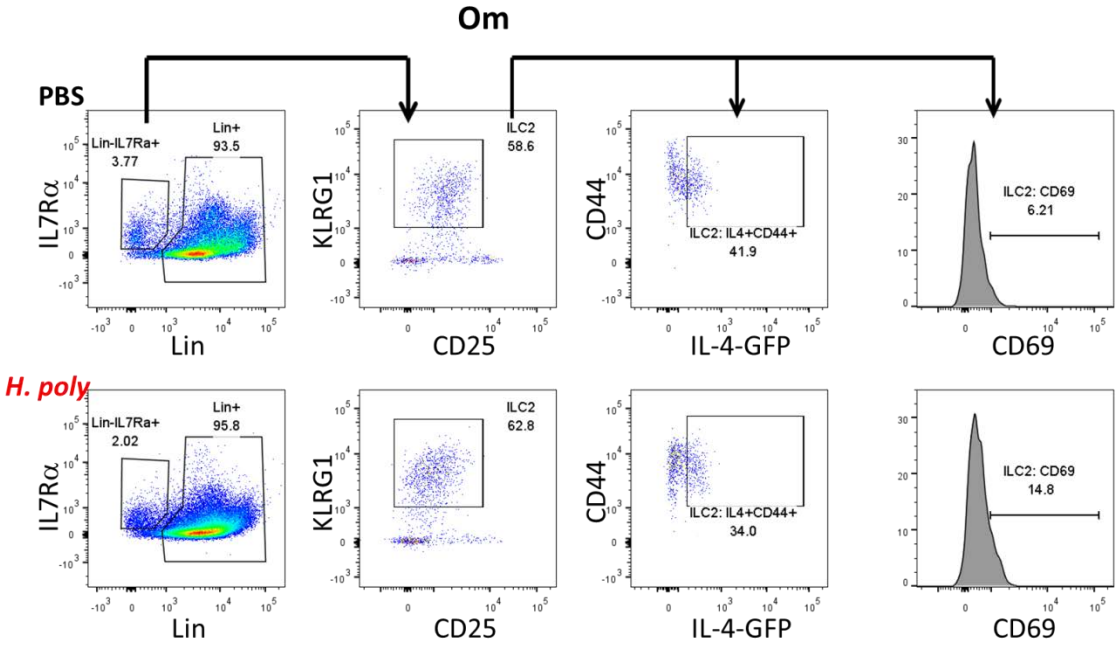
Om
PBS
Lin-IL7Ra+
3.77
Lin+
93.5
IL7Rα
Lin
ILC2
58.6
KLRG1
CD25
CD44
ILC2: IL4+CD44+
41.9
IL-4-GFP
ILC2: CD69
6.21
CD69
H. poly
Lin-IL7Ra+
2.02
Lin+
95.8
ILC2
62.8
ILC2: IL4+CD44+
34.0
ILC2: CD69
14.8

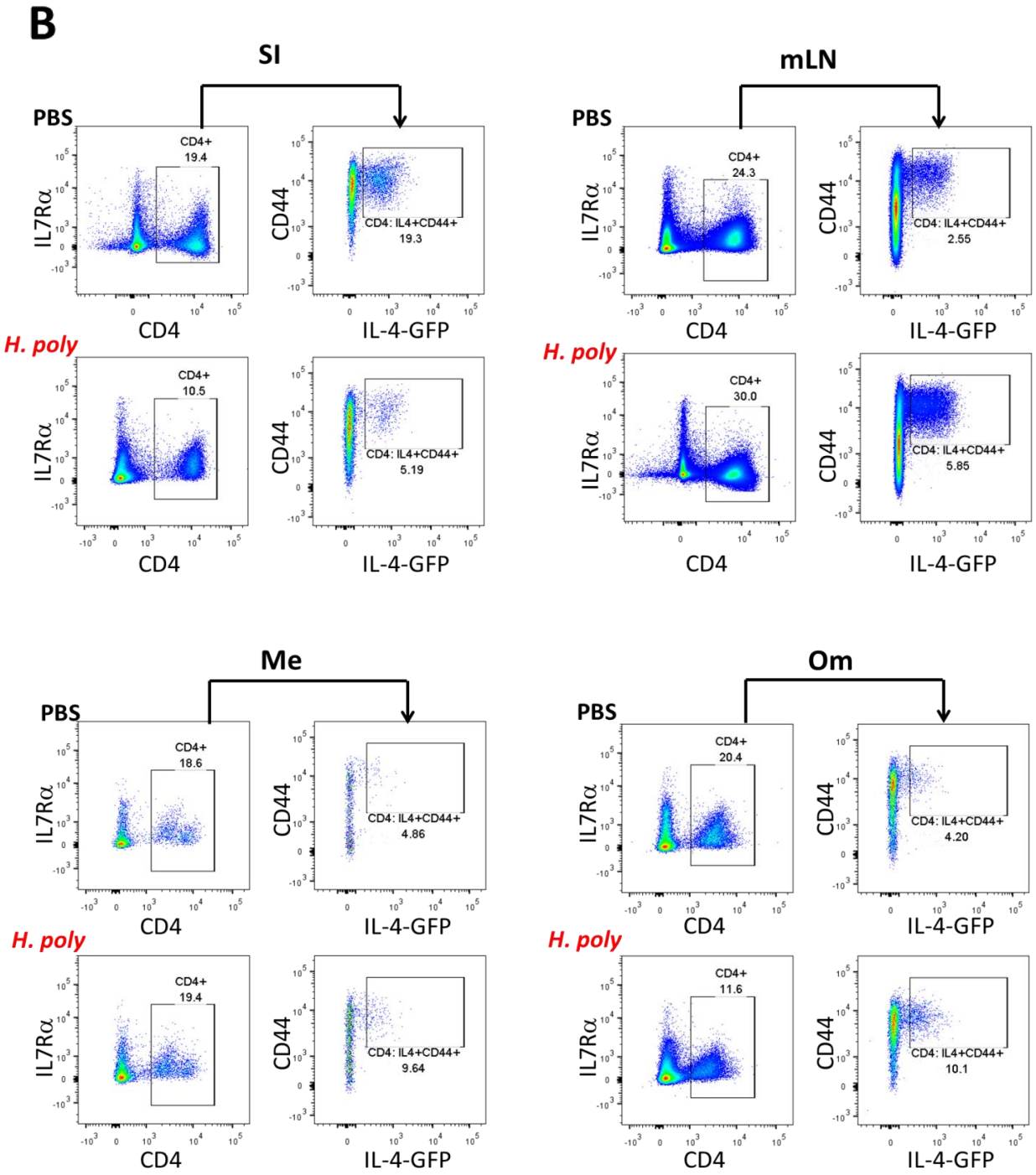
B
SI
mLN
Me
Om
PBS
H. poly
IL7Rα
CD4
CD44
IL-4-GFP
CD4+
19.4
CD4: IL4+CD44+
19.3
CD4+
10.5
CD4: IL4+CD44+
5.19
CD4+
24.3
CD4: IL4+CD44+
2.55
CD4+
30.0
CD4: IL4+CD44+
5.85
CD4+
18.6
CD4: IL4+CD44+
4.86
CD4+
19.4
CD4: IL4+CD44+
9.64
CD4+
20.4
CD4: IL4+CD44+
4.20
CD4+
11.6
CD4: IL4+CD44+
10.1

Figure 4.3

Figure 4.4: Assessing *in vivo* ILC2 responses in visceral adipose tissues of B6.4get mice following *H. poly* infection

B6.4get mice were administered 200 *H. poly* L_3 larvae by oral gavage, with control groups receiving PBS. Cells from mLN, mesenteries, omentum and SI were isolated as described in materials and methods. Total number of cells were normalised to weight of individual tissues and represented as number of cells per 100mg of tissue.

The effect of infection on adjusted number of $CD44^+$IL-4^+ILC2s, as well as expression (MFI) of CD69 on total ILC2s was assessed between PBS and *H. poly* infected mice.

Data are representative of 3 independent experiments with the following sample numbers: PBS (n=8-10), *H. poly* (n=8-9). Bars on the graph represent the median value. Statistical significance was determined using Unpaired students t test. *P<0.05, **P<0.01, ***P<0.001 and ****P<0.0001.

a) Graph comparing the adjusted number of $CD44^+$IL-4^+ILC2s per 100 mg tissue in SI, mLN, mesenteries and omentum between PBS and *H. poly* infected B6.4get mice.
b) Graph comparing the MFI of CD69 on ILC2s in SI, mLN, mesenteries and omentum between PBS and *H. poly* infected B6.4get mice.

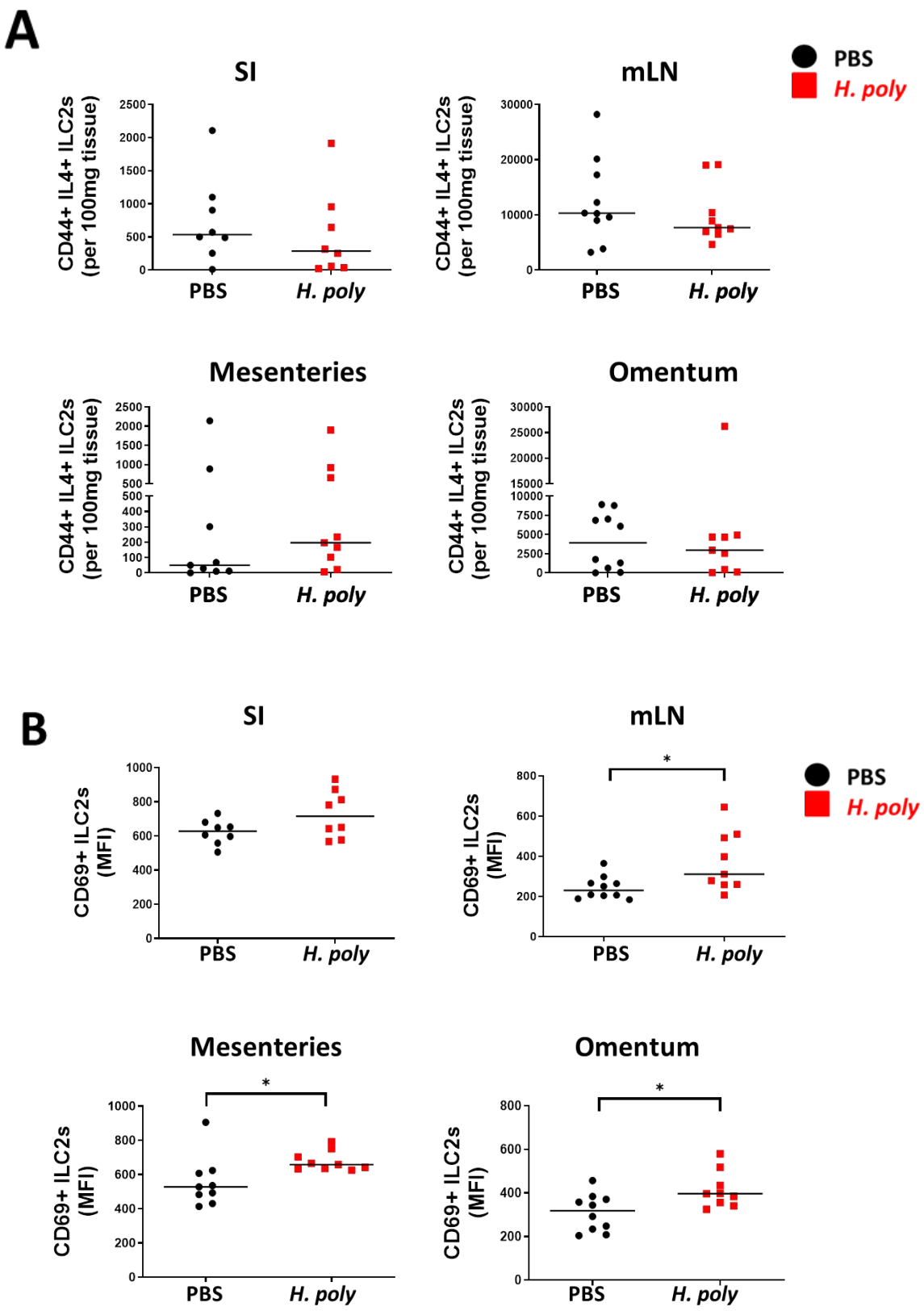
A
SI
mLN
Mesenteries
Omentum
CD44+ IL4+ ILC2s (per 100mg tissue)
PBS
H. poly
B
CD69+ ILC2s (MFI)
*

Figure 4.4

Figure 4.5: Assessing *in vivo* CD4 T cell responses in visceral adipose tissue of B6.4get mice following *H. poly* infection

B6.4get mice were administered 200 *H. poly* L_3 larvae by oral gavage, with control groups receiving PBS. Cells from mLN, mesenteries, omentum and SI were isolated as described in materials and methods. Total number of cells were normalised to weight of individual tissues and represented as number of cells per 100mg of tissue.

The effect of infection on adjusted number of $CD44^+IL\text{-}4^+CD4$ T cells was assessed between PBS and *H. poly* infected mice.

Data are representative of 3 independent experiments with the following sample numbers: PBS (n=8-10), *H. poly* (n=8-9). Bars on the graph represent the median value. Statistical significance was determined using Unpaired students t test. *$P<0.05$, **$P<0.01$, ***$P<0.001$ and ****$P<0.0001$.

a) Graph comparing the adjusted number of $CD44^+IL\text{-}4^+CD4$ T cells per 100mg tissue in the SI, mLN, mesenteries and omentum between PBS and *H. poly* infected B6.4get mice.

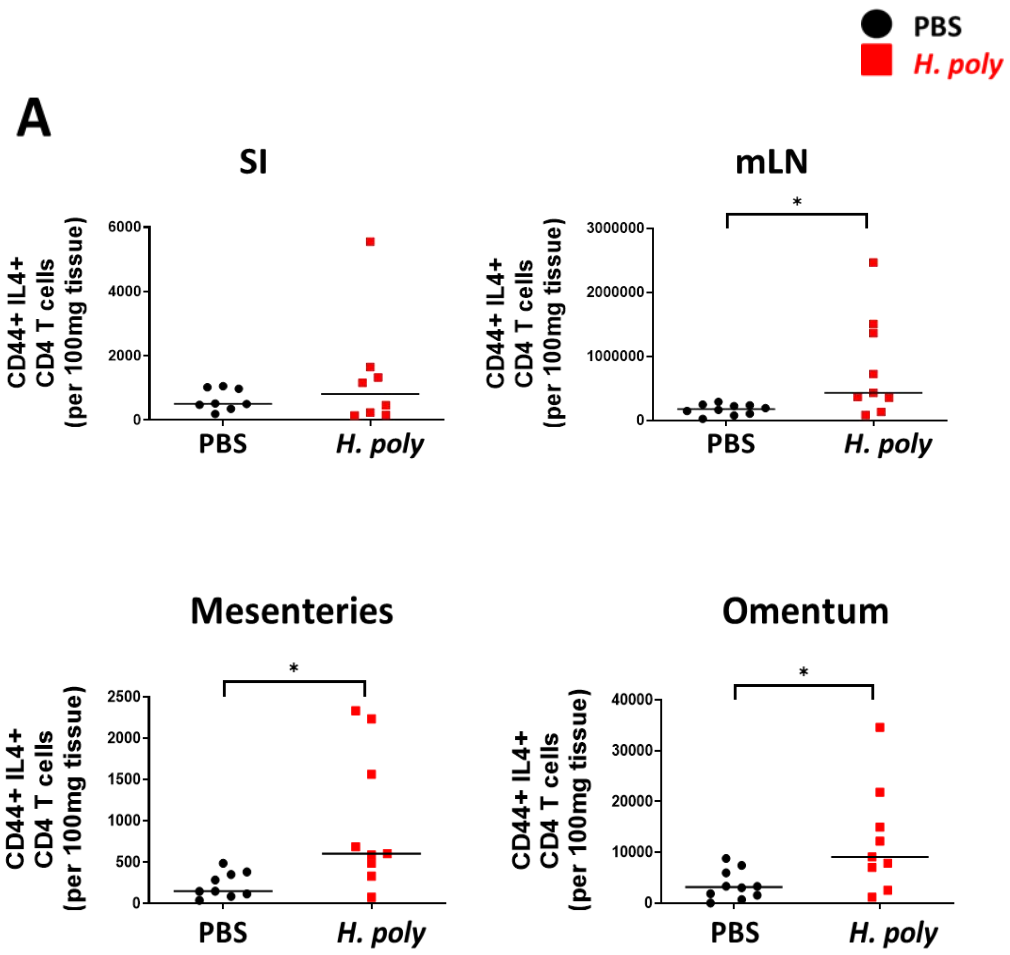
PBS
H. poly
A
SI
mLN
Mesenteries
Omentum
CD44+ IL4+
CD4 T cells
(per 100mg tissue)
PBS
H. poly
*

Figure 4.5

4.4 Investigating the Role of IL-33 in Mediating ILC2 and CD4 T Cell Responses within Visceral Adipose Tissues following *Heligmosomoides polygyrus* infection

IL-33 is known to be a potent inducer of type 2 responses, with important roles in homeostasis but also during infection and inflammation (Rostan et al., 2015). Signalling of this cytokine through ST2 expressed on ILC2s, induces IL-5 and IL-13 secretion that are involved in promoting the accumulation of AT Tregs, eosinophils and AAM, and the subsequent regulation of tissue homeostasis (Kolodin et al., 2015, Molofsky et al., 2013), as well as in the beiging of WAT (Brestoff et al., 2015, Lee et al., 2015). Meanwhile, early on during *H. poly* infection increased expression of IL-33 observed in the SI and mLN is suggested to initiate the cascade that leads to IL-4 production and subsequent priming of CD4 Th cells (Pelly et al., 2016). It was established in chapter 4.3, that ILC2s and CD4 T cells within the VATs examined could indeed become activated and functional during *H. poly* infection. Therefore given the importance of IL-33 in inducing type 2 responses within SLOs as well as at the site of infection, we investigated whether IL-33 was also required for ILC2 and CD4 T cell function within VATs during *H. poly* infection. Furthermore, proliferation and IL-5/IL-13 production was used as a measure of immune cell functionality having previously established that VAT ILC2s could significantly upregulate Ki67 post infection, as well as IL-5 and IL-13 following *ex vivo* stimulation - sections 4.2 and 3.3.3 respectively.

IL-33 expression was first identified in FALCs within the mesenteries and omentum via immunofluorescence staining. Using a knock-in reporter mouse expressing Citrine on one of the alleles of the *Il33* gene ($Il33^{+/Citrine}$), VATs were isolated, and antibody stained for the expression of CD4, CXCL13 and DAPI, with Citrine amplified using anti-GFP. This revealed the presence of three subsets of FALC stromal cells in both the mesenteries and omentum that

either singly expressed IL-33-Citrine (green) or CXCL13 (red), as well as double positive cells (yellow) – figure 4.6A.

Figure 4.6: IL-33 can be detected on FALC stromal cells using *Il33*$^{+/Citrine}$ reporter mice

The mesenteries and omentum were isolated from *Il33*$^{+/Citrine}$ mice, stained with primary and secondary antibodies for immunofluorescence, and counter stained with DAPI as described in materials and methods. Images were scanned using a confocal microscope.

a) Images showing representative FALC in mesenteries and omentum stained for CXCL13 (red), and CD4 (blue). Citrine - a reporter protein for IL-33 expression was detected using anti-GFP secondary antibody (green). Scale bar represents 50 µm. Images were taken at 25x.

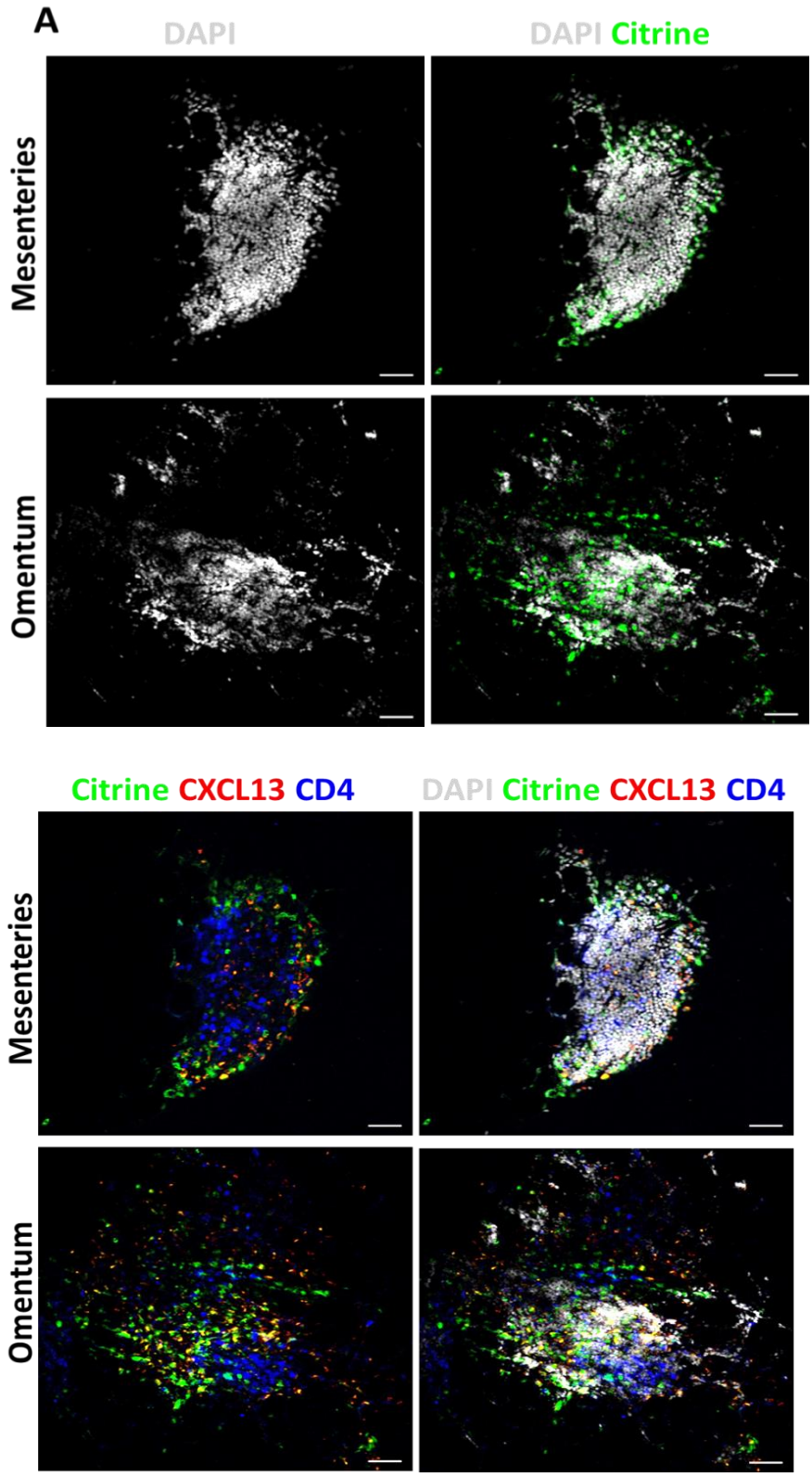
A
DAPI
DAPI Citrine
Mesenteries
Omentum
Citrine CXCL13 CD4
DAPI Citrine CXCL13 CD4
Mesenteries
Omentum

Figure 4.6

4.4.1 ILC2 responses within visceral adipose tissues of *Il33*$^{-/-}$ mice are not significantly affected following *H. poly* infection.

In order to understand the role of IL-33 in mediating immune responses within VATs following *H. poly*, WT and *Il33*$^{-/-}$ mice were infected with 200 *H. poly* L_3 worms. Proliferation by ILC2s, CD4 T cells and Tregs, as well as cytokine production by ILC2s and CD4 T cells was assessed 7 days post infection. Figure 4.7 A-C shows the gating strategy used in identifying these immune cells in WT and *Il33*$^{-/-}$ mice post infection.

Following infection, *H. poly* worms could be detected in the intestine of infected mice, with a trend towards reduced worm burden in *Il33*$^{-/-}$ mice compared to WT, though this was not found to be statistically significant (figure 4.8A). Next, the effect of infection on ILC2 responses in the absence of IL-33 was evaluated. Following *H. poly* infection, there was no significant difference in the total number of ILC2s within the mLN and VATs examined (figure 4.8B). However, and in line with our earlier experiments (as shown in figure 4.2A), the total number Ki67^{+}ILC2s within the mesenteries was found to increase significantly in WT but also in *Il33*$^{-/-}$ mice post infection (figure 4.8C). Nonetheless, total ILC2 numbers and ILC2 proliferation between WT and *Il33*$^{-/-}$ mice, across all three tissues was not significantly different (figure 4.8B-C). Similarly, total numbers of IL-5^{+}/IL-13^{+} producing ILC2s remained comparable between both mouse strains following infection (figure 4.8D).

Figure 4.7: Gating strategies to identify ILC2s, CD4 T cells and Tregs between WT and *Il33*$^{-/-}$ mice following *H. poly* infection

The mesenteries, omentum and mLN were isolated from WT and *Il33*$^{-/-}$ mice 7 days after oral gavage with either 200 *H. poly* L_3 larvae or PBS. Following isolation of cells from tissues, proliferation and cytokine expression by ILC2s and CD4 T cells was analysed by flow cytometry as described in materials and methods. Representative FACS plots are shown whereby n=6 for PBS and n=6-7 for *H. poly* across 5 independent experiments. Lineage (Lin) gate included CD3, CD5, B220, CD11b and CD11c.

a) FACS plots comparing Ki67 expression and cytokine production by GATA3^{+}CD3i^{-} ILC2s in mLN (top), mesenteries (middle) and omentum (bottom) between WT and *Il33*$^{-/-}$ *H. poly* infected mice. Cells have been pre-gated on FSC and SSC followed by liveCD45.2^{+}Lin^{-}IL-7Ra^{+}.
b) FACS plots comparing Ki67 expression and cytokine production by CD4^{+} T cells in mLN (top), mesenteries (middle) and omentum (bottom) between WT and *Il33*$^{-/-}$ *H. poly* infected mice. Cells have been pre-gated on FSC and SSC followed by liveCD45.2^{+}.
c) FACS plots comparing Ki67 expression by ST2^{-} and ST2^{+} Tregs in mLN (top), mesenteries (middle) and omentum (bottom) between WT and *Il33*$^{-/-}$ *H. poly* infected mice. Cells have been pre-gated on FSC and SSC followed by liveCD45.2^{+}CD3i^{+} CD4^{+}.

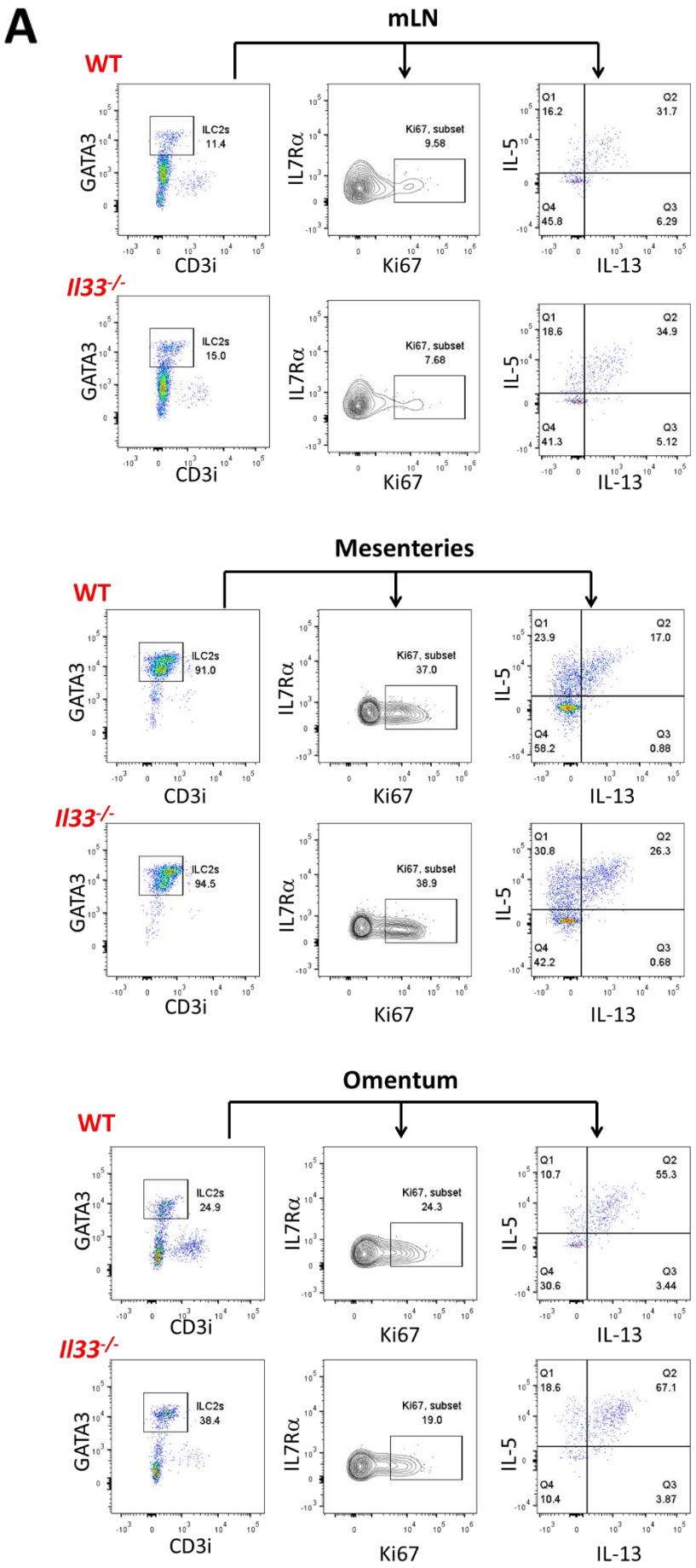
A
mLN
WT
GATA3
CD3i
ILC2s
11.4
IL7Rα
Ki67
Ki67, subset
9.58
IL-5
IL-13
Q1
16.2
Q2
31.7
Q4
45.8
Q3
6.29
Il33-/-
ILC2s
15.0
Ki67, subset
7.68
Q1
18.6
Q2
34.9
Q4
41.3
Q3
5.12
Mesenteries
WT
ILC2s
91.0
Ki67, subset
37.0
Q1
23.9
Q2
17.0
Q4
58.2
Q3
0.88
Il33-/-
ILC2s
94.5
Ki67, subset
38.9
Q1
30.8
Q2
26.3
Q4
42.2
Q3
0.68
Omentum
WT
ILC2s
24.9
Ki67, subset
24.3
Q1
10.7
Q2
55.3
Q4
30.6
Q3
3.44
Il33-/-
ILC2s
38.4
Ki67, subset
19.0
Q1
18.6
Q2
67.1
Q4
10.4
Q3
3.87

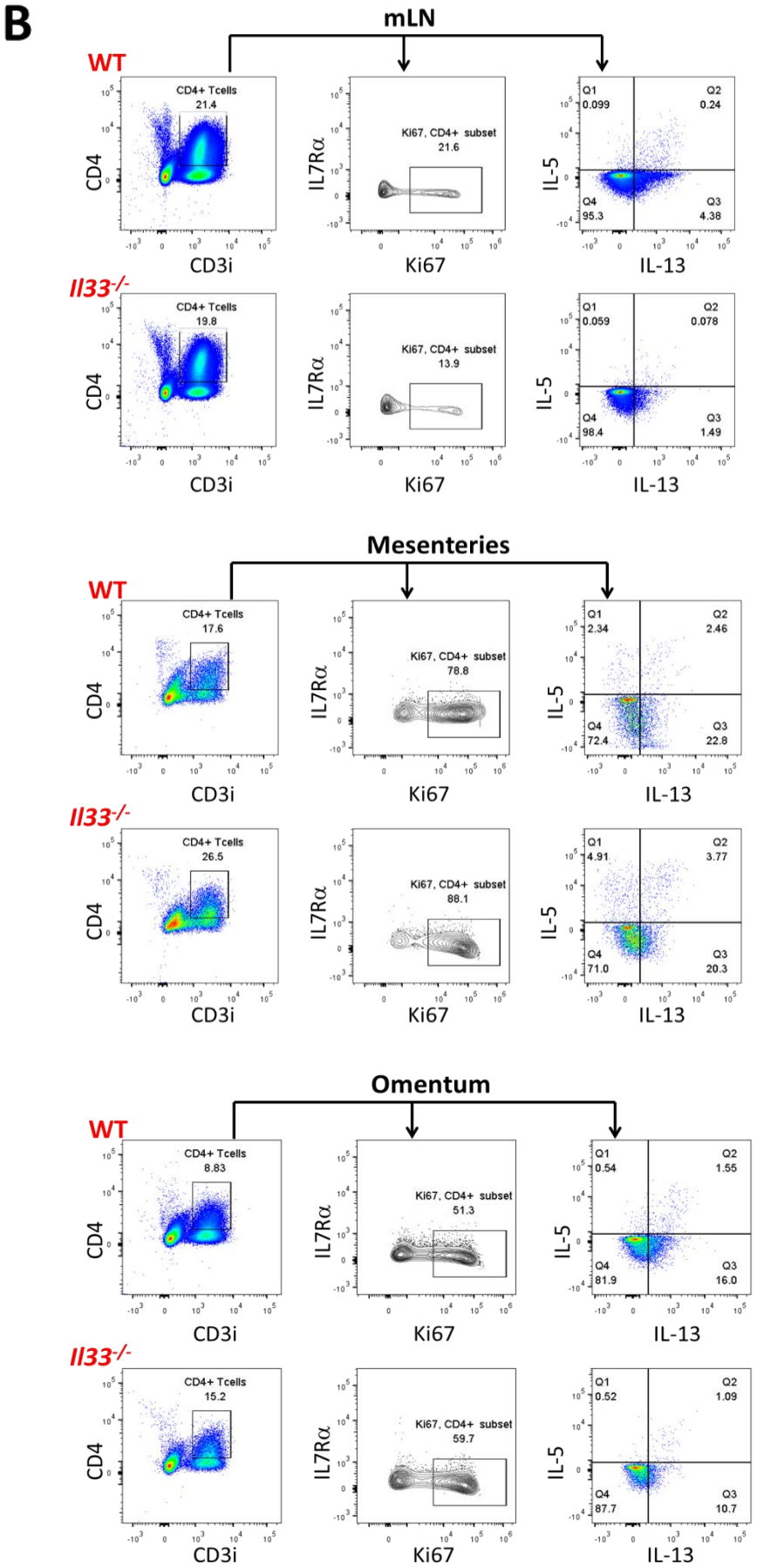
B
mLN
WT
CD4+ Tcells
21.4
Ki67, CD4+ subset
21.6
Q1
0.099
Q2
0.24
Q4
95.3
Q3
4.38
CD4
CD3i
IL7Rα
Ki67
IL-5
IL-13
Il33-/-
CD4+ Tcells
19.8
Ki67, CD4+ subset
13.9
Q1
0.059
Q2
0.078
Q4
98.4
Q3
1.49
Mesenteries
WT
CD4+ Tcells
17.6
Ki67, CD4+ subset
78.8
Q1
2.34
Q2
2.46
Q4
72.4
Q3
22.8
Il33-/-
CD4+ Tcells
26.5
Ki67, CD4+ subset
88.1
Q1
4.91
Q2
3.77
Q4
71.0
Q3
20.3
Omentum
WT
CD4+ Tcells
8.83
Ki67, CD4+ subset
51.3
Q1
0.54
Q2
1.55
Q4
81.9
Q3
16.0
Il33-/-
CD4+ Tcells
15.2
Ki67, CD4+ subset
59.7
Q1
0.52
Q2
1.09
Q4
87.7
Q3
10.7

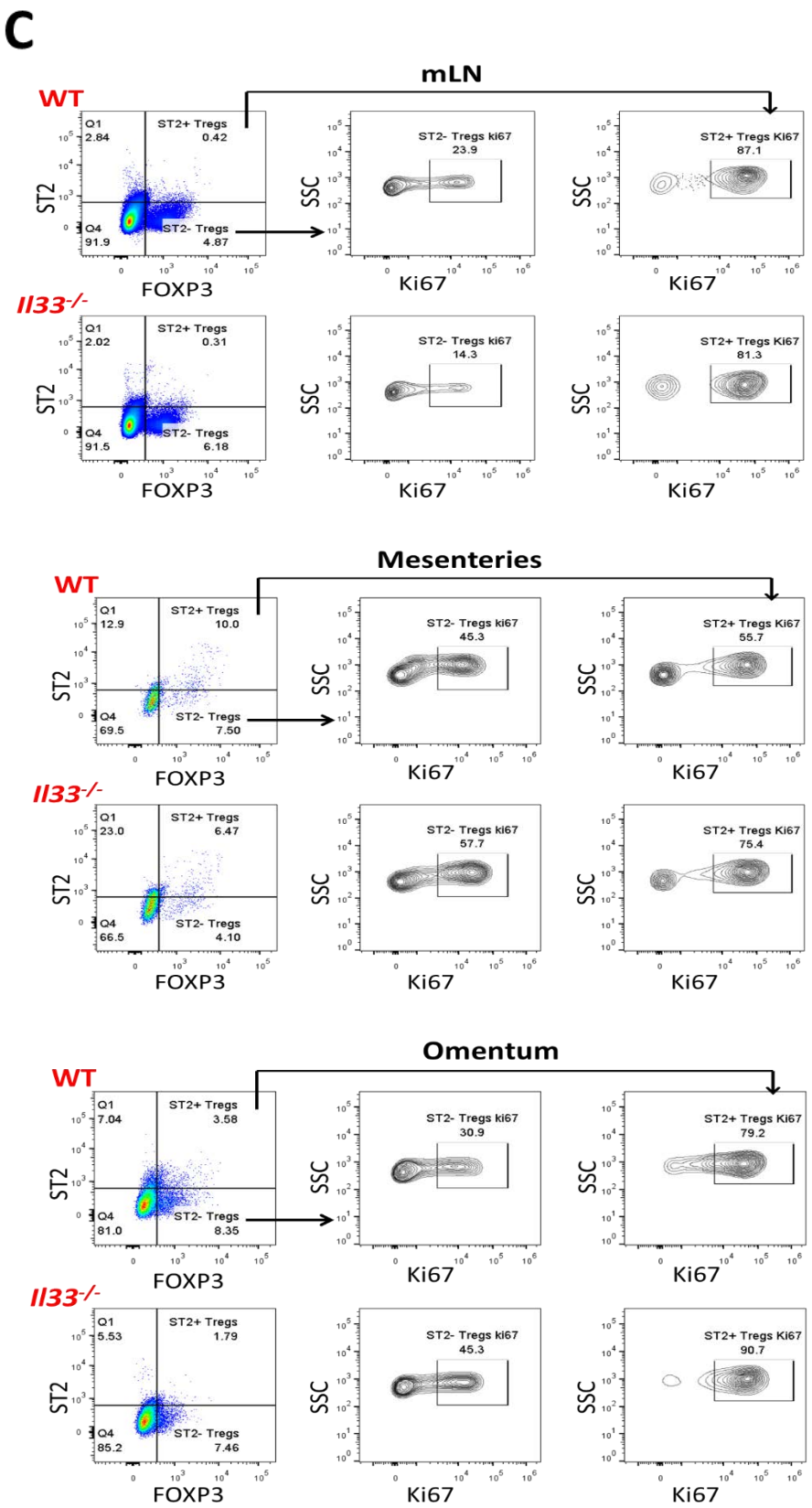
C
mLN
WT
Q1
2.84
ST2+ Tregs
0.42
Q4
91.9
ST2- Tregs
4.87
ST2- Tregs ki67
23.9
ST2+ Tregs Ki67
87.1
Il33-/-
Q1
2.02
ST2+ Tregs
0.31
Q4
91.5
ST2- Tregs
6.18
ST2- Tregs ki67
14.3
ST2+ Tregs Ki67
81.3
Mesenteries
WT
Q1
12.9
ST2+ Tregs
10.0
Q4
69.5
ST2- Tregs
7.50
ST2- Tregs ki67
45.3
ST2+ Tregs Ki67
55.7
Il33-/-
Q1
23.0
ST2+ Tregs
6.47
Q4
66.5
ST2- Tregs
4.10
ST2- Tregs ki67
57.7
ST2+ Tregs Ki67
75.4
Omentum
WT
Q1
7.04
ST2+ Tregs
3.58
Q4
81.0
ST2- Tregs
8.35
ST2- Tregs ki67
30.9
ST2+ Tregs Ki67
79.2
Il33-/-
Q1
5.53
ST2+ Tregs
1.79
Q4
85.2
ST2- Tregs
7.46
ST2- Tregs ki67
45.3
ST2+ Tregs Ki67
90.7
ST2
FOXP3
SSC
Ki67

Figure 4.7

Figure 4.8: Assessing ILC2 responses in visceral adipose tissues of *Il33*$^{-/-}$ mice following *H. poly* infection

WT and *Il33*$^{-/-}$ mice received 200 *H. poly* L_3 larvae by oral gavage, while control groups received PBS. Cells from mLN, mesenteries and omentum were isolated as described in materials and methods.

The effect of infection on total number of ILC2s and ILC2 proliferation was firstly assessed, followed by comparisons of ILC2 cytokine production between infected WT mice and infected *Il33*$^{-/-}$ mice.

Data are representative of 5 independent experiments, with the following sample numbers: PBS (n=6), *H. poly* (n=6-7). Bars on the graph represent the median value. Statistical significance was determined using Unpaired students t test. *P<0.05, **P<0.01, ***P<0.001 and ****P<0.0001.

a) Graph showing total number of worms enumerated from the intestine of WT and *Il33*$^{-/-}$ mice.
b) Graph showing the total number of ILC2s in mLN, mesenteries and omentum (left to right) of WT and *Il33*$^{-/-}$ mice.
c) Graph showing total number of Ki67^{+} ILC2s in mLN, mesenteries and omentum (left to right) of WT and *Il33*$^{-/-}$ mice.
d) Graph comparing the total number of IL-5^{+} / IL-13^{+} ILC2s in mLN, mesenteries and omentum (left to right), between WT and *Il33*$^{-/-}$ *H. poly* infected mice.

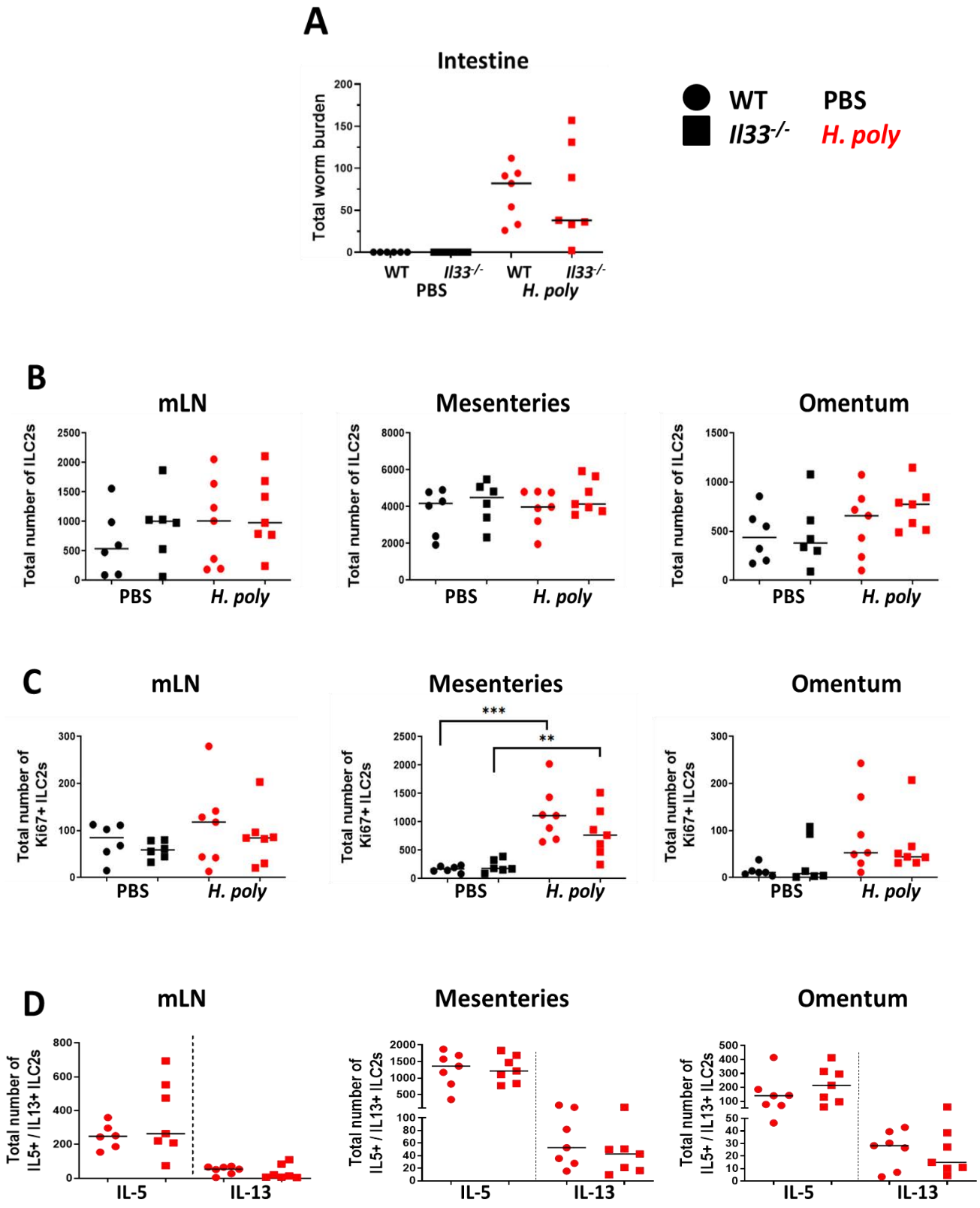
A
Intestine
Total worm burden
200
150
100
50
0
WT
Il33-/-
WT
Il33-/-
PBS
H. poly
WT
Il33-/-
PBS
H. poly
B
mLN
Mesenteries
Omentum
Total number of ILC2s
PBS
H. poly
C
mLN
Mesenteries
Omentum
Total number of Ki67+ ILC2s
***
**
PBS
H. poly
D
mLN
Mesenteries
Omentum
Total number of IL5+ / IL13+ ILC2s
IL-5
IL-13

Figure 4.8

4.4.2 CD4 T cell responses within visceral adipose tissues of *Il33*$^{-/-}$ mice are not significantly affected following *H. poly* infection

Given that ILC2s are involved in supporting Th2 cell differentiation, and any defects in ILC2 responses due to loss of IL-33 would have subsequent downstream consequences, the CD4 T cell compartment was evaluated simultaneously. As a mechanism of escape, *H. poly* modulates immune responses through the expansion of Tregs, which are observed to increase within lymphoid organs including the spleen and mLN following infection (Rausch et al., 2008). Further, subsets of Tregs expressing the IL-33 receptor, ST2, have been identified to accumulate within non-lymphoid tissues (Panduro et al., 2016), (denoted in our study as ST2^{+} Tregs). Therefore the accumulation of both ST2^{-} and ST2^{+} Tregs within VATs, following infection of *Il33*$^{-/-}$ mice with *H. poly* was also assessed.

The total number of CD4 T cells was found to be significantly higher in the mesenteries and omentum of *Il33*$^{-/-}$ infected mice compared to *Il33*$^{-/-}$ non-infected mice, but not in the mLN (figure 4.9A). While total CD4 T cells appeared to increase slightly in *Il33*$^{-/-}$ infected mice compared to WT infected mice in the mesenteries and omentum, this was not found to be statistically significant (figure 4.9A). Meanwhile within the mLN of both WT and *Il33*$^{-/-}$ mice, the total number of Ki67^{+} (i.e. proliferating) CD4 T cells was found to be significantly higher following infection. The same was observed in the mesenteries but only statistically significant in WT mice (figure 4.9B). Nonetheless, when comparing CD4 T cell proliferation between WT and *Il33*$^{-/-}$ mice following infection, no significant differences could be observed across all tissues (figure 4.9B). Similarly, numbers of IL-5^{+}/IL-13^{+} CD4 T cells were unaltered between both mouse strains following *H. poly* infection (figure 4.9C). Finally, although the numbers of proliferating ST2^{-} and ST2^{+} Tregs was significantly higher in the mesenteries and

omentum of *H. poly* infected mice compared to PBS controls, no difference in proliferation of both Treg subsets was found between WT and *Il33*$^{-/-}$ mice (figure 4.9D).

Figure 4.9: Assessing CD4 T cell responses in visceral adipose tissues of *Il33*$^{-/-}$ mice following *H. poly* infection

WT and *Il33*$^{-/-}$ mice received 200 *H. poly* L_3 larvae by oral gavage, with control groups receiving PBS. Cells from mLN, mesenteries and omentum were isolated as described in materials and methods.

The effect of infection on total number and proliferation of CD4 T cells (including Tregs) was firstly assessed, followed by comparisons of CD4 T cell cytokine production between infected WT mice and *Il33*$^{-/-}$ mice.

Data are representative of 5 independent experiments with the following sample numbers: PBS (n=6), *H. poly* (n=6-7). Bars on the graph represent the median value. Statistical significance was determined using Unpaired students t test. *P<0.05, **P<0.01, ***P<0.001 and ****P<0.0001.

a) Graph showing the total number of CD4 T cells in mLN, mesenteries and omentum (left to right) of WT and *Il33*$^{-/-}$ mice.
b) Graph showing total number of Ki67^{+}CD4 T cells in mLN, mesenteries and omentum (left to right) of WT and *Il33*$^{-/-}$ mice.
c) Graph comparing the total number of IL-5^{+} / IL-13^{+} CD4 T cells in mLN, mesenteries and omentum (left to right), between WT and *Il33*$^{-/-}$ mice following *H. poly* infection.
d) Graph showing total number of Ki67^{+}ST2^{-} and Ki67^{+}ST2^{+} Tregs in mLN, mesenteries and omentum (left to right) of WT and *Il33*$^{-/-}$ mice. Gating strategy for Tregs are shown in figure 4.7C

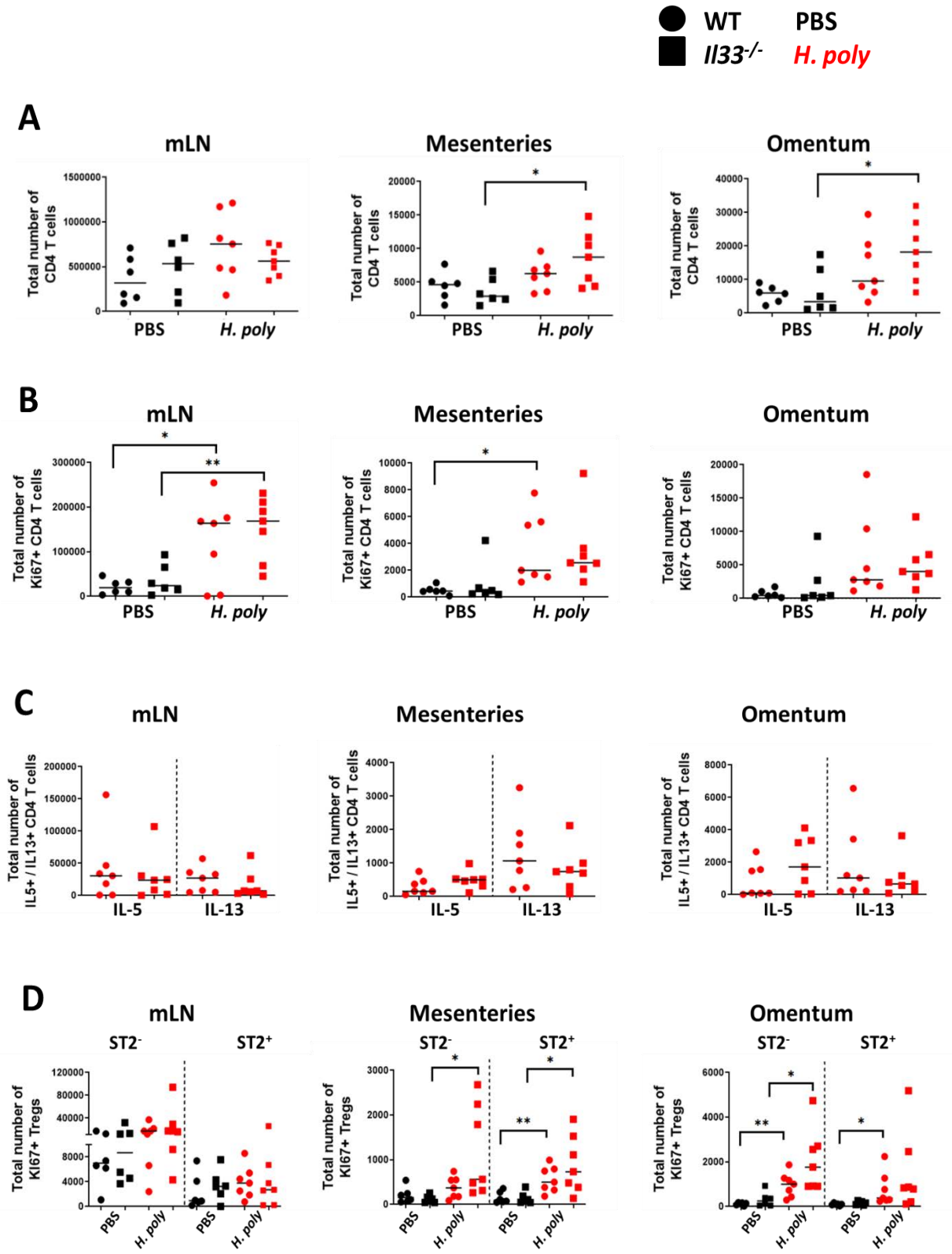
WT
PBS
Il33-/-
H. poly
A
mLN
Mesenteries
Omentum
Total number of CD4 T cells
PBS
H. poly
B
Total number of Ki67+ CD4 T cells
C
Total number of IL5+ / IL13+ CD4 T cells
IL-5
IL-13
D
ST2-
ST2+
Total number of Ki67+ Tregs

Figure 4.9

4.5 Investigating the Role of Visceral Adipose Tissues during *Schistosoma mansoni* infection

Given the fact that adult *S. mansoni* worms can migrate to and reside within the mesenteric vessels, where mature females can also lay their eggs (Costain et al., 2018), it is likely that mesenteric AT and surrounding VATs will be able to respond to such stimuli. To investigate this, WT C57BL/6J mice were infected with the larvae stage of *S. mansoni* also known as cercariae (cerc), at a physiological load of 40 cercs or a supra-infection of 180 cercs; the effect of infection on ILC2 and CD4 T cell responses within VATs as well as mLN was then analysed by flow cytometry 49 days after infection. Worms could be observed in the mesenteries of infected mice under a dissecting microscope (and to the naked eye); with 180 cerc (specified as *S. mansoni*_180 cerc) resulting in visibly more worms in the mesenteries compared to 40 cerc (*S. mansoni*_40 cerc). However, no worms were found in the omentum of either 40 or 180 cerc infected mice (figure 4.10A).

Figure 4.10: *S. mansoni* worms are visible within the mesenteric vasculature at D49 post infection

40 or 180 cercariae (cerc) of *S. mansoni* were placed on the abdomen of C57BL/6J mice in between 200 µl of pond water, for 30 min to allow absorption into mice as described in materials and methods. Mesenteries, omentum and mLN, were isolated from the mice at day 49 post infection. Tissues were visualised under a dissecting microscope for the presence of *S. mansoni* worms.

a) Representative images comparing the prevalence of *S. mansoni* worms (red arrows) in the mesenteries and omentum, between 40 cerc and 180 cerc infected mice, with tissue from non-infected mice as controls.

A
Non-infected
S. mansoni_
40 cerc
S. mansoni_
180 cerc
Mesenteries
Omentum

Figure 4.10

Next, mesenteric and omental ATs as well as the mLN were analysed for differences in ILC subsets (figure 4.11A) following infection with 40 cerc of parasitic larvae. A slight but non-significant increase in the normalised numbers of ILC1s (figure 4.11C; top) and a decrease in ILC3s (figure 4.11C; bottom), was observed in the mLN of infected mice compared to the non-infected group. Meanwhile, no difference in the numbers of ILC1s and ILC3s was found in the VATs examined (figure 4.11C). However, *S. mansoni*_40 cerc infected mice had significantly higher numbers of ILC2s in the mesenteries and omentum, but not in the mLN, compared to non-infected mice (figure 4.11C; middle). Subsequently, the proliferative and activation status of ILC2s in particular was examined (figure 4.11B). Across all tissues, *S. mansoni*_40 cerc infection resulted in a significant increase in the normalised numbers of proliferating ILC2s, identified as Ki67^{+}ILC2s (figure 4.11D). Additionally, in the mesenteries, the numbers of CD44^{+}ILC2s were significantly higher in infected mice compared to control groups (figure 4.11E). Similarly within the omentum, numbers of CD44^{+}CD69^{+} double positive ILC2s (figure 4.11E), as well as MHCII^{+}ILC2s (figure 4.11F) were significantly higher post infection. Finally, no difference in the numbers of CD44^{+} and/or CD69^{+} ILC2s was observed in the mLN; further, the numbers of MHCII^{+}ILC2s in the mLN tended to decrease following infection, though this did not reach statistical significance (figure 4.11F).

Figure 4.11: Assessing ILC2 responses in visceral adipose tissues following *S. mansoni* infection

40 cerc of *S. mansoni* were placed on the abdomen of WT C57BL/6J mice in between 200 µl of pond water, for 30 min to allow absorption into mice as described in materials and methods; non-infected mice were used as controls. Mesenteries, omentum and mLN were isolated from the mice at day 49 post infection to generate a single cell suspension. Total number of cells were normalised to weight of individual tissues and represented as number of cells per 100mg of tissue.

First, total ILC1, ILC2 and ILC3 subsets were analysed by flow cytometry. Next the effect of infection on adjusted number of proliferating (Ki67$^+$) ILC2s, as well as expression of a number of markers including CD69, CD44 and MHCII was assessed. Lineage (Lin) gate included CD3, CD5, B220, CD11b and CD11c.

Data are representative of 2 independent experiments with the following sample numbers: non-infected (n=6-7), *S. mansoni _40 cerc* (n=8). Bars on the graph represent the median value. Statistical significance was determined using Unpaired t test. *P<0.05, **P<0.01, ***P<0.001 and ****P<0.0001

a) FACS plots showing the identification of ILC subsets (ILC1, ILC2, ILC3) within mLN (top), mesenteries (middle) and omentum (bottom), between non-infected and *S. mansoni _4*0 cerc infected mice. Cells have been pre-gated on FSC and SSC followed by liveCD45.2$^+$.
b) FACS plots comparing Ki67, CD44, CD69 and MHCII expression by GATA3$^+$ILC2s in mLN (top), mesenteries (middle) and omentum (bottom) between non-infected and

S. mansoni _40 cerc infected mice. Cells have been pre-gated on FSC and SSC followed by live CD45.2^{+}Lin^{-}IL7Ra^{+}.

c) Graph comparing the adjusted number of ILC1s, ILC2s and ILC3s (top to bottom) per 100 mg tissue in the mLN, mesenteries and omentum (left to right), between non-infected and *S. mansoni*_40 cerc infected mice.

d) Graph comparing the adjusted number of Ki67^{+}ILC2s per 100 mg tissue in mLN, mesenteries and omentum (left to right) between non-infected and *S. mansoni*_40 cerc infected mice.

e) Graph comparing the adjusted number of CD44^{+}; CD69^{+} and CD69^{+}CD44^{+} ILC2s per 100 mg tissue in mLN, mesenteries and omentum (left to right) between PBS and *S. mansoni* _40 cerc infected mice.

f) Graph comparing the adjusted number of MHCII^{+}ILC2s per 100 mg tissue in mLN, mesenteries and omentum (left to right) between PBS and *S. mansoni* _40 cerc infected mice.

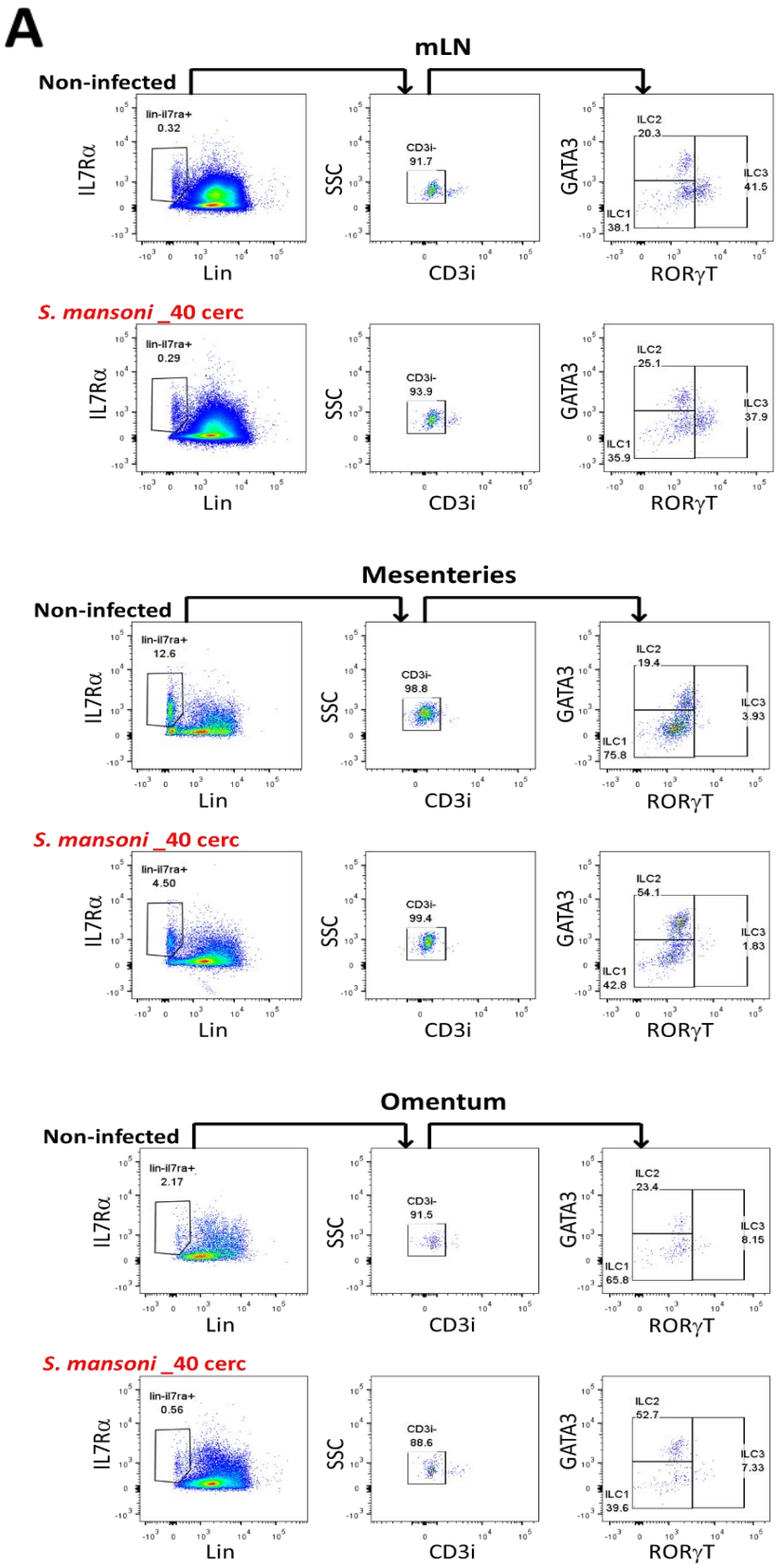
A
mLN
Non-infected
lin-il7ra+
0.32
CD3i-
91.7
ILC2
20.3
ILC3
41.5
ILC1
38.1
IL7Rα
Lin
SSC
CD3i
GATA3
RORγT
S. mansoni _40 cerc
lin-il7ra+
0.29
CD3i-
93.9
ILC2
25.1
ILC3
37.9
ILC1
35.9
Mesenteries
Non-infected
lin-il7ra+
12.6
CD3i-
98.8
ILC2
19.4
ILC3
3.93
ILC1
75.8
S. mansoni _40 cerc
lin-il7ra+
4.50
CD3i-
99.4
ILC2
54.1
ILC3
1.83
ILC1
42.8
Omentum
Non-infected
lin-il7ra+
2.17
CD3i-
91.5
ILC2
23.4
ILC3
8.15
ILC1
65.8
S. mansoni _40 cerc
lin-il7ra+
0.56
CD3i-
88.6
ILC2
52.7
ILC3
7.33
ILC1
39.6

B

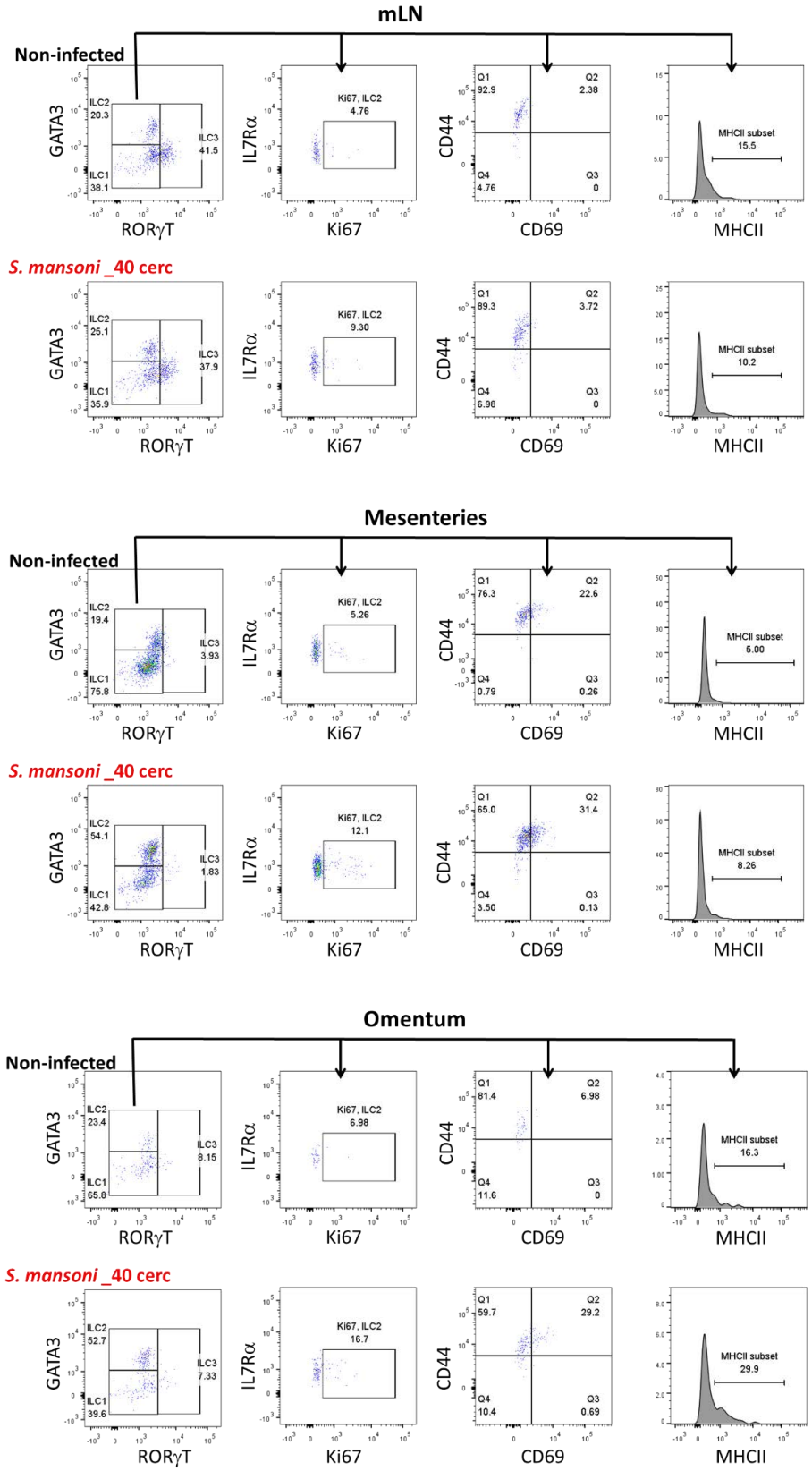
mLN
Non-infected
GATA3
RORγT
ILC2 20.3
ILC3 41.5
ILC1 38.1
IL7Rα
Ki67
Ki67, ILC2 4.76
CD44
CD69
Q1 92.9
Q2 2.38
Q4 4.76
Q3 0
MHCII
MHCII subset 15.5
S. mansoni _40 cerc
ILC2 25.1
ILC3 37.9
ILC1 35.9
Ki67, ILC2 9.30
Q1 89.3
Q2 3.72
Q4 6.98
Q3 0
MHCII subset 10.2
Mesenteries
Non-infected
ILC2 19.4
ILC3 3.93
ILC1 75.8
Ki67, ILC2 5.26
Q1 76.3
Q2 22.6
Q4 0.79
Q3 0.26
MHCII subset 5.00
S. mansoni _40 cerc
ILC2 54.1
ILC3 1.83
ILC1 42.8
Ki67, ILC2 12.1
Q1 65.0
Q2 31.4
Q4 3.50
Q3 0.13
MHCII subset 8.26
Omentum
Non-infected
ILC2 23.4
ILC3 8.15
ILC1 65.8
Ki67, ILC2 6.98
Q1 81.4
Q2 6.98
Q4 11.6
Q3 0
MHCII subset 16.3
S. mansoni _40 cerc
ILC2 52.7
ILC3 7.33
ILC1 39.6
Ki67, ILC2 16.7
Q1 59.7
Q2 29.2
Q4 10.4
Q3 0.69
MHCII subset 29.9

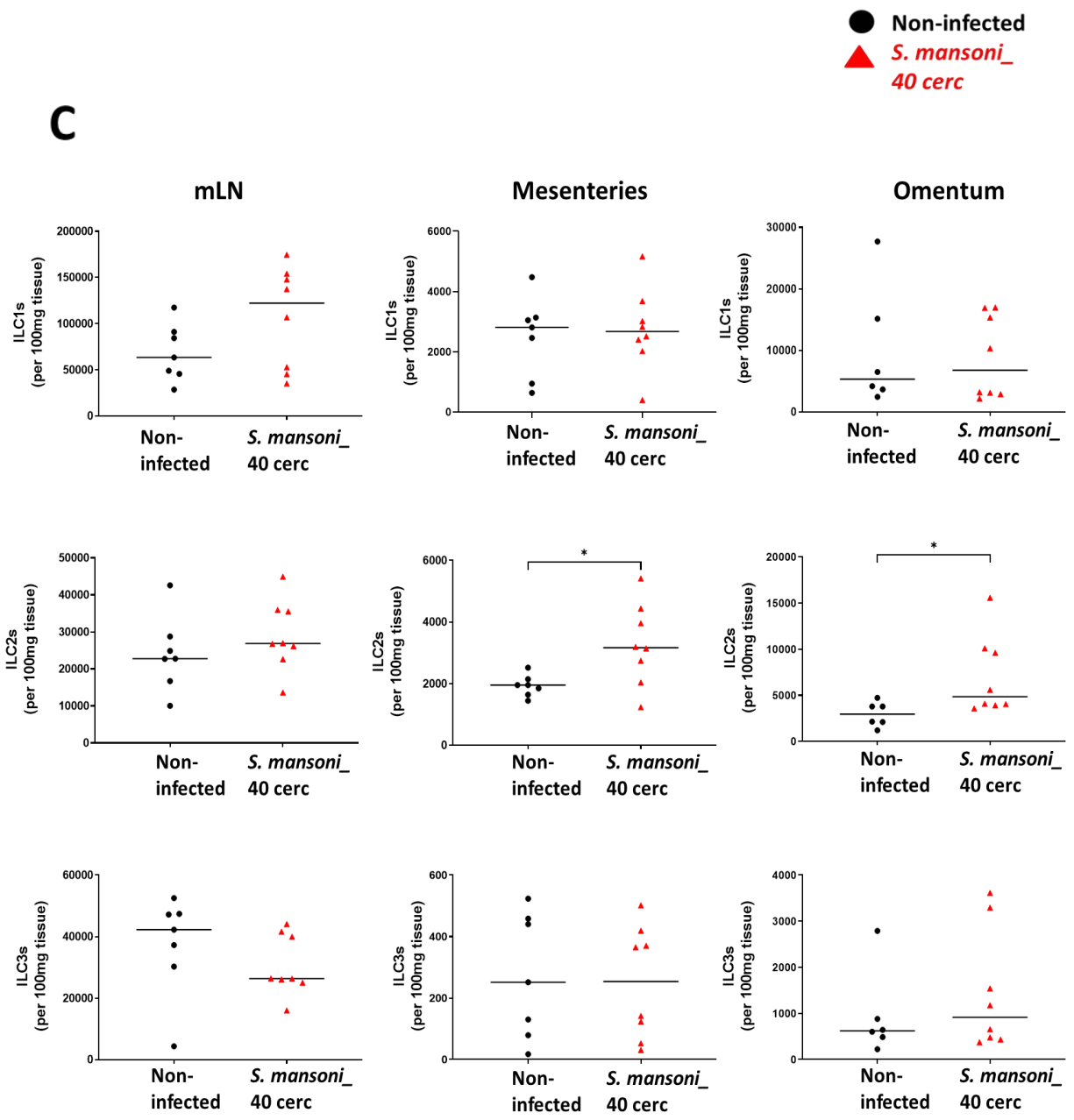
Non-infected
S. mansoni_ 40 cerc
C
mLN
Mesenteries
Omentum
ILC1s (per 100mg tissue)
ILC2s (per 100mg tissue)
ILC3s (per 100mg tissue)
Non-infected
S. mansoni_ 40 cerc
*

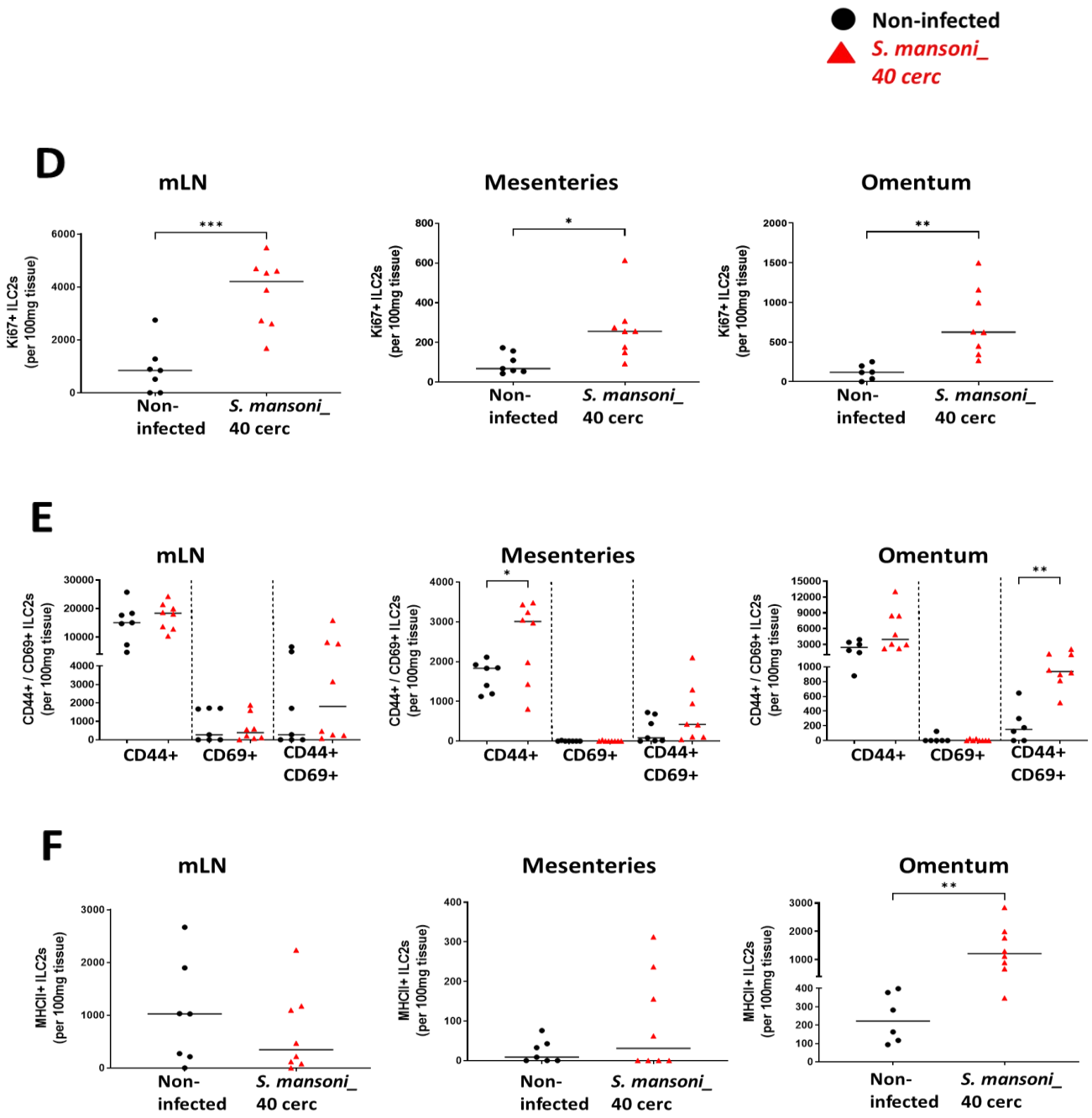
Non-infected
S. mansoni_ 40 cerc
D
mLN
Mesenteries
Omentum
Ki67+ ILC2s (per 100mg tissue)
Non-infected
S. mansoni_ 40 cerc
E
CD44+ / CD69+ ILC2s (per 100mg tissue)
CD44+
CD69+
CD44+ CD69+
F
MHCII+ ILC2s (per 100mg tissue)

Figure 4.11

While schistosomes induce a predominantly Th2 response, *S. mansoni* infection in particular can induce both Th1 and Th2 responses, depending on the stage of infection (Pearce and MacDonald, 2002). VAT FALCs were therefore assessed for the production of IFN-γ, IL-4/5/10/13 cytokines (figure 4.12A) following infection with 40 cercs of *S. mansoni* larvae. This resulted in a statistically significant reduction in normalised numbers of CD4, CD8 T cells and Tregs in the mLN (figure 4.12B-D). Although, the numbers of CD8 T cells in the omentum (figure 4.12C) and Tregs in the mesenteries (figure 4.12D) tended to increase slightly following infection, this was not statistically significant; neither were there any differences in CD4 T cells within these VATs between infected and non-infected mice (figure 4.12B). When assessing cytokine production, the proportion of IFN-γ^+CD8 T cells within the mesenteries, omentum and mLN of infected mice was greater than their non-infected counterparts – though this increase was most profound in the latter two tissues – figure 4.13A. Secondly, a significant reduction in IFN-γ^+CD4 T cells was also found in the mesenteries. Thirdly, while the mLN had significantly more IL-4$^+$, IL-5$^+$ and IL-13$^+$CD4 T cells after infection, such significant increase in Th2 cytokines was not observed in the mesenteries nor the omentum (figure 4.13B-C). However, when mice were infected with 180 cerc of *S. mansoni* larvae, CD4 T cells within these VATs were found to produce significantly higher amounts of IL-4/5/13 as shown in the appendix (figure 7.1A-B). Nonetheless, following infection with *S. mansoni*_40 cerc, the production of IL-10 by Tregs was observed to be significantly higher in the mLN and mesenteries, and also tended to increase in the omentum (figure 4.13D).

Figure 4.12: Analysis of T cell responses in visceral adipose tissues following *S. mansoni* infection

40 cerc of *S. mansoni* were placed on the abdomen of C57BL/6J WT mice in between 200 µl of pond water, for 30 min to allow absorption into mice as described in materials and methods; non-infected mice were used as controls. Mesenteries, omentum and mLN were isolated from the mice at day 49 post infection to generate a single cell suspension. The effect of infection on T cell subsets was analysed by flow cytometry. Total number of cells were normalised to weight of individual tissues and represented as number of cells per 100mg of tissue.

Data are representative of 2 independent experiments with the following sample numbers: non-infected (n=3-6), *S. mansoni_40cerc* (n=3-6). Bars on the graph represent the median value. Statistical significance was determined using Unpaired t test. *P<0.05, **P<0.01, ***P<0.001 and ****P<0.0001

a) Representative FACS plots showing the identification of CD4 T, CD8 T cells and Tregs, as well as cytokine production by these cells, in mLN (top) mesenteries (middle) and omentum (bottom) between non-infected and *S. mansoni*_40 cerc mice. Cells have been pre-gated on FSC and SSC followed by liveCD45.2^{+}CD3i^{+}.
b) Graph comparing the adjusted number of CD4 T cells per 100mg tissue in mLN, mesenteries and omentum (left to right) between non-infected and *S. mansoni*_40 cerc mice.
c) Graph comparing the adjusted number of CD8 T cells per 100mg tissue in mLN, mesenteries and omentum (left to right) between non-infected and *S. mansoni*_40 cerc mice.

d) Graph comparing the adjusted number of Tregs per 100mg tissue in mLN, mesenteries and omentum (left to right) between non-infected and *S. mansoni*_40 cerc mice.

A

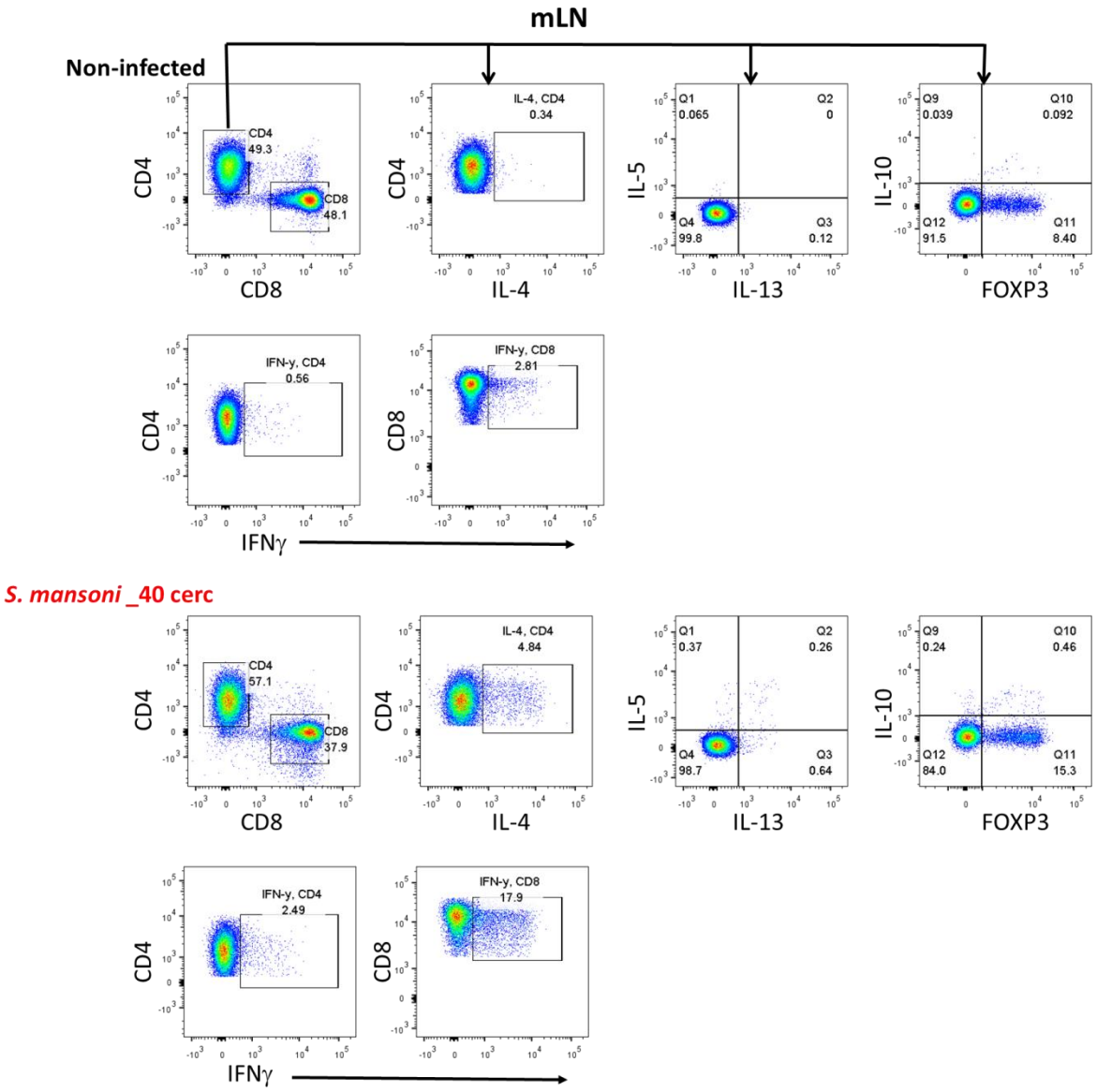
mLN
Non-infected
CD4
49.3
CD8
48.1
CD4
CD8
IL-4, CD4
0.34
CD4
IL-4
Q1
0.065
Q2
0
Q4
99.8
Q3
0.12
IL-5
IL-13
Q9
0.039
Q10
0.092
Q12
91.5
Q11
8.40
IL-10
FOXP3
IFN-y, CD4
0.56
CD4
IFN-y, CD8
2.81
CD8
IFNγ
S. mansoni _40 cerc
CD4
57.1
CD8
37.9
CD4
CD8
IL-4, CD4
4.84
CD4
IL-4
Q1
0.37
Q2
0.26
Q4
98.7
Q3
0.64
IL-5
IL-13
Q9
0.24
Q10
0.46
Q12
84.0
Q11
15.3
IL-10
FOXP3
IFN-y, CD4
2.49
CD4
IFN-y, CD8
17.9
CD8
IFNγ

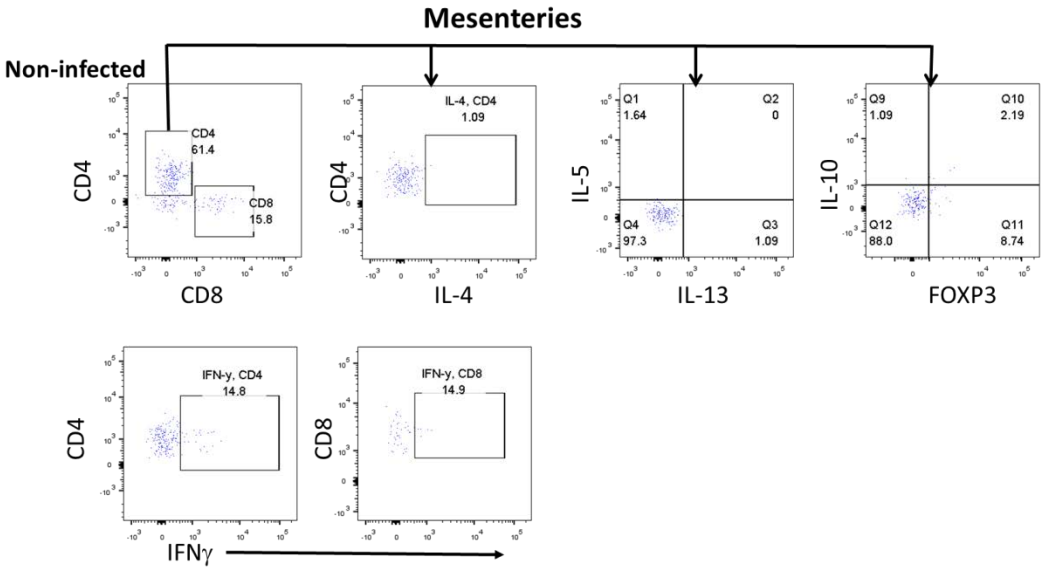

***S. mansoni* _40 cerc**

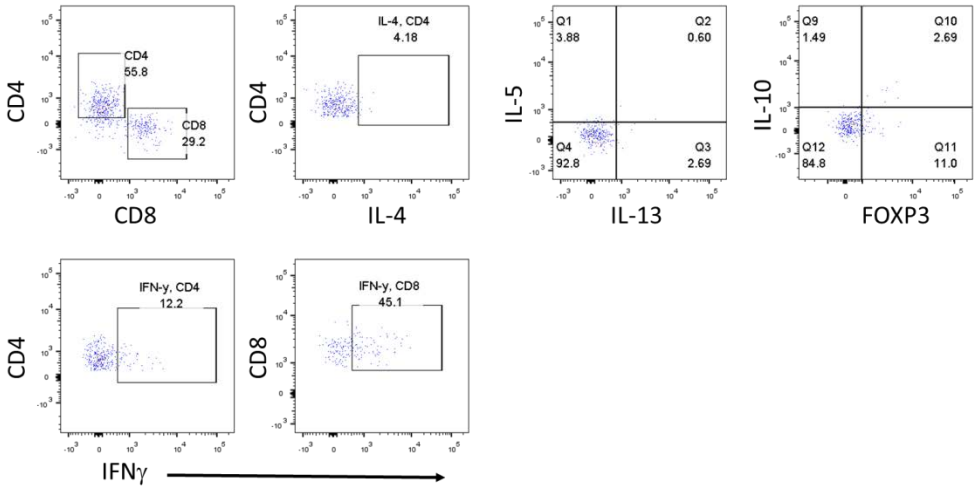

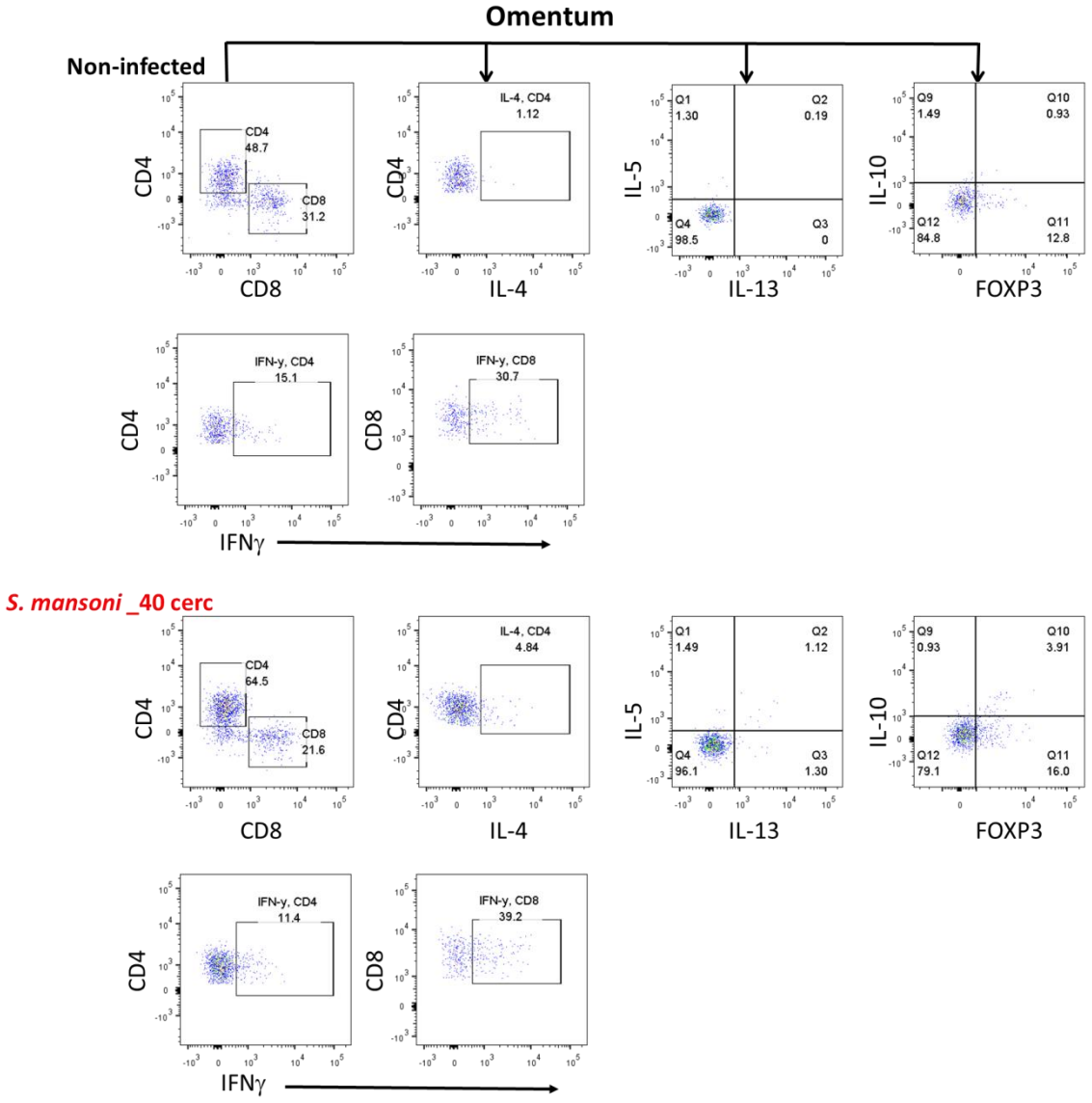
Omentum
Non-infected
CD4
48.7
CD8
31.2
CD4
CD8
IL-4, CD4
1.12
CD4
IL-4
Q1
1.30
Q2
0.19
Q4
98.5
Q3
0
IL-5
IL-13
Q9
1.49
Q10
0.93
Q12
84.8
Q11
12.8
IL-10
FOXP3
IFN-y, CD4
15.1
CD4
IFN-y, CD8
30.7
CD8
IFNγ
S. mansoni _40 cerc
CD4
64.5
CD8
21.6
CD4
CD8
IL-4, CD4
4.84
CD4
IL-4
Q1
1.49
Q2
1.12
Q4
96.1
Q3
1.30
IL-5
IL-13
Q9
0.93
Q10
3.91
Q12
79.1
Q11
16.0
IL-10
FOXP3
IFN-y, CD4
11.4
CD4
IFN-y, CD8
39.2
CD8
IFNγ

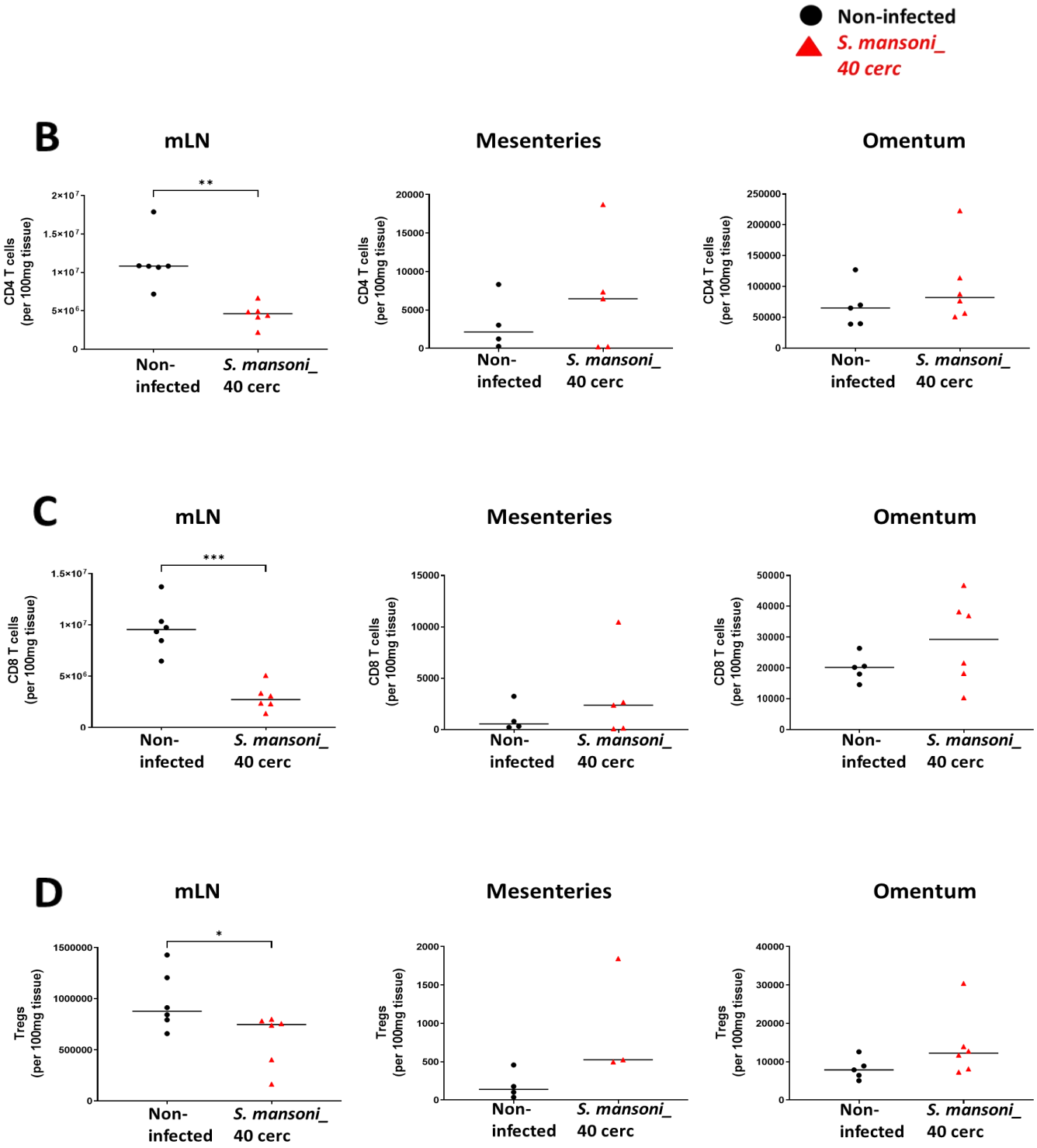
Non-infected
S. mansoni_ 40 cerc
B
mLN
Mesenteries
Omentum
CD4 T cells (per 100mg tissue)
**
C
CD8 T cells (per 100mg tissue)
***
D
Tregs (per 100mg tissue)
*
Non-infected
S. mansoni_ 40 cerc

Figure 4.12

Figure 4.13: Assessing cytokine profile of T cells in visceral adipose tissues following *S. mansoni* infection

40 cerc of *S. mansoni* were placed on the abdomen of WT C57BL/6J mice in between 200 µl of pond water, for 30 min to allow absorption into mice, with non-infected mice used as controls. The mesenteries, omentum and mLN were isolated 49 days post infection. A single cell suspension was generated and stimulated with PMA and ionomycin (P/I) as described in materials and methods, for the assessment of Th1 and Th2 cytokines by T cell subsets. Gating strategy is shown in figure 4.12A.

Data are representative of 2 independent experiments with the following sample numbers: non-infected (n=3-6), *S. mansoni*_40cer*c* (n=3-6). Bars on the graph represent the median value. Statistical significance was determined using Unpaired t test. *P<0.05, **P<0.01, ***P<0.001 and ****P<0.0001

a) Graph comparing the percentage of IFNγ^+ CD4 and CD8 T cells in mLN, mesenteries and omentum (left to right) between non-infected and *S. mansoni*_40 cerc infected mice.
b) Graph comparing the percentage of IL-4$^+$ CD4 T cells in mLN, mesenteries and omentum (left to right) between non-infected and *S. mansoni*_40 cerc infected mice.
c) Graph comparing the percentage of IL-5$^+$ and IL-13 $^+$ CD4 T cells in mLN, mesenteries and omentum (left to right) between non-infected and *S. mansoni* _40 cerc infected mice.
d) Graph comparing the percentage of IL-10$^+$ Tregs in mLN, mesenteries and omentum (left to right) between non-infected and *S. mansoni*_40 cerc infected mice.

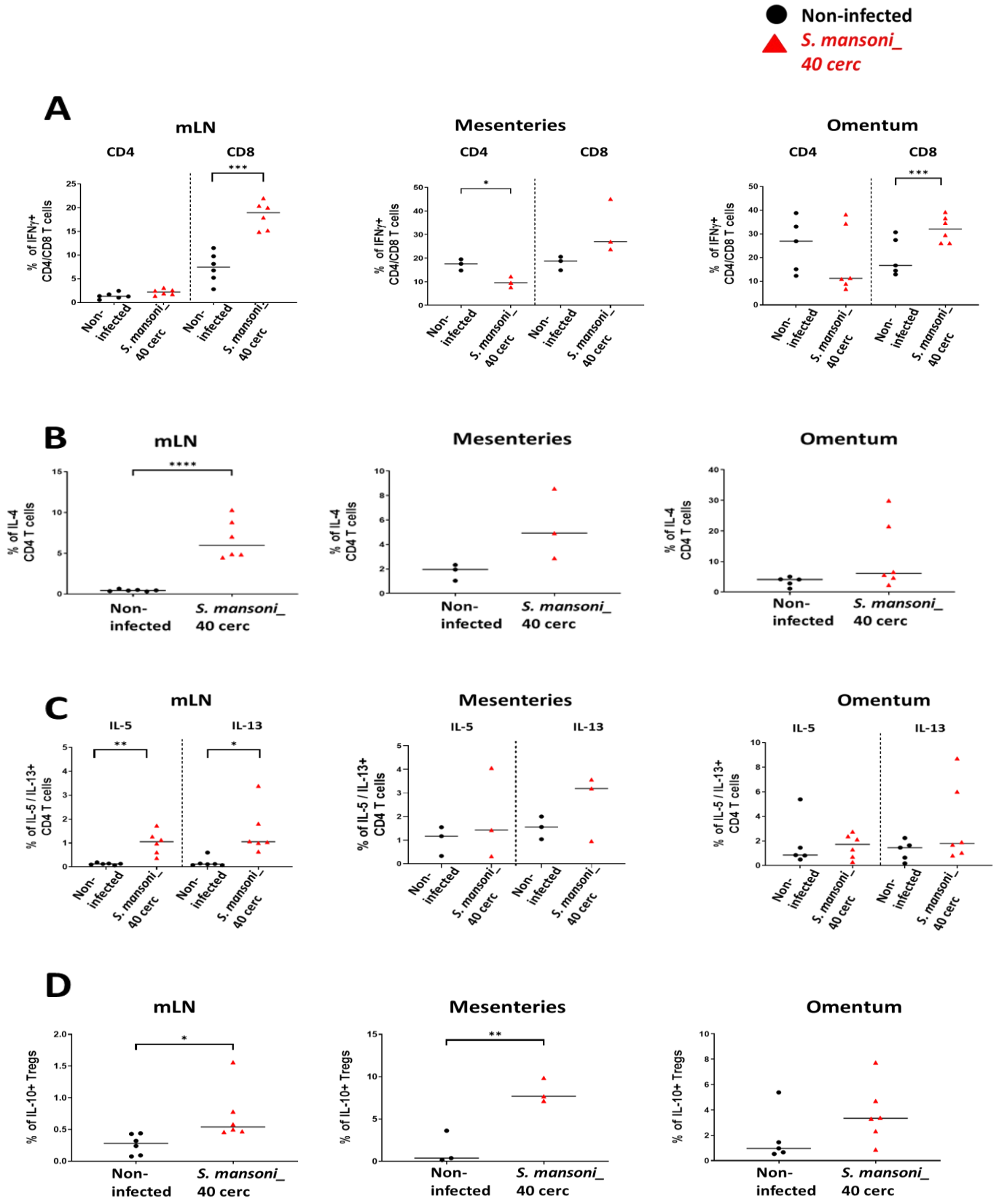
Non-infected
S. mansoni_ 40 cerc
A
mLN
Mesenteries
Omentum
CD4
CD8
% of IFNγ+ CD4/CD8 T cells
B
% of IL-4 CD4 T cells
C
IL-5
IL-13
% of IL-5 / IL-13+ CD4 T cells
D
% of IL-10+ Tregs

Figure 4.13

4.6 Summary

4.6.1 Immune Responses in Peritoneal Adipose Tissues during *H. Poly* Infection

Within the peritoneal cavity, VATs such as the mesenteries and omentum mediate immune protection against infection and inflammation through the presence of tertiary lymphoid structures, known as FALCs. These structures provide a compartmentalised, second line of defence for mucosal surfaces (Bénézech and Jackson-Jones, 2019), owing to their rich composition of both innate and adaptive immune cells. FALCs are particularly enriched in ILC2s (Moro et al., 2010), a widely dispersed innate effector cell population that was shown following its discovery to be integral in inducing type 2 immunity against helminth infections (Neill et al., 2010, Price et al., 2010). In chapter 3.3.1, it was determined that at steady state, VAT ILC2s could be characterised based on differential expression of chemokine receptors CCR8 and CCR9 which represent gut- and skin-homing receptors respectively. Therefore the next logical step was to assess these subsets further during tissue perturbation using the helminth *H. poly*, with the aim of establishing distinct ILC2 sub-populations that had specialised roles in mediating separate arms of the immune response following infection. For a suitable immune response to be initiated, adequate proliferation of lymphocytes is a necessary step that must occur in order to generate effector lymphocytes (Desforges et al., 2018); as such proliferation of total ILC2s as well as ILC2 CCR8/9 subsets was assessed following infection. Indeed, the proportion of total ILC2s proliferating within the VAT was found to be higher post infection, with the mesenteries showing more profound increases in ILC2 proliferation compared to the mLN and omentum. This thereby demonstrated evidence of immune activation provided by VAT FALCs and suggested a greater capacity of ILC2s in the mesenteries to respond compared to the other tissues examined. The latter may be

attributed to the close association and proximity of the mesenteries to the SI where adult *H. poly* parasites are located from their L_3 stage through to their maturation into adult worms (Mohrs et al., 2005). When ILC2 CCR8/9 subsets were evaluated individually, the disparity between VATs and mLN became even more apparent. ILC2 subsets within mLN did not appear to proliferate following infection, unlike in the mesenteries and omentum where proliferation could be observed equally across all ILC2 subsets. This thereby further alluded towards a preferential role of VATs in responding to intestinal infection, most likely due to abundance of ILC2s in VAT FALCs compared to other tissues - with the exception of the skin (Kim et al., 2016). Nonetheless, amongst the four identified ILC2 CCR8/9 subsets within the omentum and mesenteries, none appeared to stand out as the most proliferative. Although increased expression of CCR8 by ILC2s in mucosal tissues such as the lung has been observed by others, this was mainly evident during inflammation which directed ILC2 trafficking to inflamed lungs (Puttur et al., 2019). Meanwhile during *H. poly* infection, CCR7-dependent trafficking from the intestine into the mLN was shown for ILC3s, but not for ILC1 and ILC2 populations (Mackley et al., 2015). Instead, subsets of ILC2s derived in the intestine and induced by helminths or IL-25 known as inflammatory (iILC2s), could migrate following infection with *N. brasiliensis* to distal sites such as the lung in a manner that was dependent on the sphingosine 1-phosphate (S1P) receptor – also required for the egress of adaptive lymphocytes from SLOs (Huang et al., 2018a). Taken together, this suggests that staining for CCR8/9 may not be the most appropriate way to further dissect the phenotype of VAT ILC2s following *H. poly* infection. Furthermore, other reports recently revealed that the migration of mesenteric ILC2s to ATs during diet-induced obesity is consistent with their expression of CCR2 – a chemokine receptor reported to direct the recruitment of monocytes and

leukocytes into ATs (Sasaki et al., 2019), thereby alluding to a possible role of this receptor in other pathologies. Nonetheless, our data does highlight the proliferation of VAT ILC2s during *H. poly* infection and thus the likely involvement of VAT FALCs during a localised immune response.

Given the proliferative capacity of VAT ILC2s upon *H. poly* infection, their ability to respond functionally via cytokine production was evaluated next. Initial infection with *H. poly* induces a Th2 cytokine gene signature; IL-3, IL-5 and IL-9 mRNA are elevated in the Peyer's patches and mLN hours after infection, with IL-4 appearing 4 to 6 days later (Svetic et al., 1993). In addition, protein expression of these cytokines as well as of IL-10 and IL-13 within the spleen, mLN and lamina propria mononuclear cells have been reported (Reynolds et al., 2012). Nonetheless, IL-4 has been shown to be the most critical component of both primary and secondary *H. poly* infection due to its effects on the survival and physiology of parasites, including adult worm survival and fecundity, as well as contributing to elevated IgE levels associated with worm expulsion (Urban et al., 1991b). In addition, both CD4 T cells and ILC2s have been reported to be important cell populations involved in the regulation of such host protective immunity (Urban et al., 1991a, Pelly et al., 2016). Therefore, IL-4 secretion by VAT ILC2s and CD4 T cells was assessed using B6.4get mice. Compared to the mLN, SI and omentum, IL-4 production by VAT ILC2s tended to increase post infection in the mesenteries though this did not reach statistical significance, further highlighting this tissue as the dominant VAT responder during *H. poly* infection. However, no increase in ILC2-derived IL-4 was observed in the other tissues examined between control and infected mice.

Lymphocyte activation is usually accompanied by the upregulation of the surface marker CD69, thereby causing the retention of cells in peripheral tissues, while CD44 expression is

important in initiating effector responses within lymphocytes (Salimi et al., 2018). As such, the increased expression of CD69 observed on CD44^{+}ILC2s within VATs and mLN post infection suggested that while these cells were unable to significantly produce IL-4 at day 7 post infection, ILC2s within lymphoid and peritoneal tissues do display an activated phenotype. Nevertheless, these results pose further questions; could VAT ILC2s have secreted IL-4 much earlier than the time point analysed or was IL-4 yet to be secreted? However, others have noted the presence of IL-4 in the mLN 1 week after infection with *H. poly* and sometimes even earlier (Finney et al., 2007, Svetic et al., 1993), as well as the more recent study that ILC2s within SI could transcribe IL-4 as at 5 days after *H. poly* infection (Pelly et al., 2016). Additionally, ILC2s are known to dominate in early production of innate type 2 cytokines such as IL-5/IL-13 (Nausch and Mutapi, 2018). Taken together, it is therefore plausible to suggest that VAT ILC2s also secrete cytokines earlier on during *H. poly* infection which could help drive Th2 differentiation, and hence the induction of protective type 2 responses. Therefore, it will be useful to conduct further experiments analysing ILC2-IL-4 production before and after day 7 post infection with *H. poly* to reach more reliable conclusions on cytokine production by VAT ILC2s following.

Interestingly, rather than ILC2s, a large number of CD4 T cells within VATs and mLN were instead found to secret IL-4 following infection. Such accumulation of IL-4-expressing CD4 T cells in non-lymphoid tissues following *H. poly* infection has been shown by others (Mohrs et al., 2005). Using the bicistronic 4get IL-4 reporter mice, Mohrs and colleagues were able to track the systemic dissemination of Th2 cells as well as other innate cells after acute *H. poly* infection. Like our study, CD4^{+}/GFP^{+} Th2 cells increased significantly in all lymphoid organs, but also in non-lymphoid organs, most selectively in the peritoneal cavity albeit at 14 days

post infection, with peritoneal Th2 cells secreting more IL-4 than their mLN counterparts (Mohrs et al., 2005). Therefore, our results not only support the findings by Mohrs and colleagues but provide further information by revealing that the accumulation of activated and functional immune cells within peritoneal tissues can occur as early as 7 days after infection with *H. poly* and highlight the mesenteries and omentum as candidate sites for such accumulation.

All in all, these data help further our understanding of VAT FALCs in mediating immune responses during *H. poly* infection; they reveal that these clusters can act as depot sites, where immune cells are able to proliferate, become activated and (in the case of CD4 T cells) efficiently produce Th2 cytokines that are central to immunity against such helminth infections.

Having established a role for VAT FALCs in contributing to immune responses during *H. poly* infection, the immune mechanisms that might be involved in controlling these responses were investigated. As discussed previously, ILC2s mediate responses to parasitic infection, allergens and epithelial injury; their development and activation is orchestrated by a number of cytokines including IL-25, IL-33 and TSLP (Eberl et al., 2015). Of these, IL-33 potently induces type 2 responses, and can signal via ST2 which is highly expressed on ILC2s thus underpinning its involvement during helminth infection as well as allergic pathology (Molofsky et al., 2015). Given the fact that our group had access to *Il33*$^{-/-}$ (IL-33 deficient) mice - a kind gift from Professor A McKenzie, MRC LMB, Cambridge - these mice were therefore used to interrogate the role of IL-33 in mediating VAT ILC2 and CD4 T cell responses during *H. poly* infection.

Initial assessment of IL-33 expression in mesenteric and omental FALCs via immunofluorescence staining and confocal microscopy confirmed the presence of distinct subsets of FALC stromal cells that expressed either IL-33 or CXCL13 independently, but also the presence of double positive cells. CXCL13 is a chemokine that induces the migration of LTi cells to LN anlage during LN formation (van de Pavert et al., 2009). Additionally, it was shown by Bénézech and colleagues to be involved in the recruitment of B-cells to FALCs (Bénézech et al., 2015). Further, our imaging analysis showed that at steady state, IL-33 localised within the nucleus of FALC stromal cells. Therefore, while our observations were in line with previous reports, it also indicated a potential role of FALC stromal cells in coordinating immune responses to *H. poly,* given their expression of IL-33, but also the role of these lymphoid clusters as being sites of crosstalk between immune and stromal cells. During infection, migratory *H. poly* parasites penetrate the wall of SI, and mature into adults within the gut lumen (Reynolds et al., 2012). Indeed, intestinal worms were observed in WT and *Il33*$^{-/-}$ mice 7 days after administration of L_3 *H. poly* larvae, suggesting the establishment of infection. A slight though non-statistically significant decrease in total worm burden within the intestine of infected mice was observed in the absence of IL-33. Such a decrease would have suggested that loss of IL-33 was having a protective effect by limiting maturation and survival of adult worms. This contrasts with studies which have shown a requirement of IL-33 for helminth expulsion, owing to the significant increases in intestinal worms and worm length in IL-33 knock-out mice compared to WT (Hung et al., 2013). Nonetheless, the use of a different helminth – *N. brasiliensis* by Hung and colleagues may account for our conflicting results. Furthermore, loss of IL-33 did not seem to affect ILC2 numbers prior to, nor after infection; a result also shown by others particularly in the steady state (Mahlakoiv et al.,

2019). Similar to our earlier observations (section 4.2), ILC2s within the mesenteries showed significant increases in proliferation, both in WT and *Il33*$^{-/-}$ mice, with absence of IL-33 seeming to only result in a very modest, non-significant reduction in ILC2 proliferation. Expansion of CD4 T cells did however occur within the mesenteries and omentum of infected *Il33*$^{-/-}$ mice but not in WTs. Interestingly though not significant, numbers of CD4 T cells within these tissues were moderately higher in the absence of IL-33 following infection. While this result appeared to be consistent with the reduced worm burden found in *Il33*$^{-/-}$ mice – i.e. suggestive of a better immune response in the absence of IL-33 - no difference in the proliferation of CD4 T cells nor in their cytokine production, was observed between WT and *Il33*$^{-/-}$ mice. Nevertheless, the accumulation of CD4 T cells in VATs as well as their increased proliferation within mLN and mesenteries, once again highlights the fact that VAT CD4 T cells, and not necessarily VAT ILC2s seem to be the dominating immune cells at 7 days post infection, supported by the increased secretion of IL-4 by CD4 T cells demonstrated in previous experiments (section 4.3). Lastly, numbers of IL-5^{+} and IL-13^{+} ILC2 cells were also found to be comparable between WT and *Il33*$^{-/-}$ mice. IL-33 has been reported by others to orchestrate the initiation of ILC2 and subsequent CD4 T cell activation within the SI following tissue damage by *H. poly* (Pelly et al., 2016). In addition, defective ILC2 and to a lesser extent CD4 T cell derived IL-13 production in the lungs of *Il33*$^{-/-}$ mice, as well as reduced intestinal responses in ST2-deficient mice has been shown following *N. brasiliensis* and *Trichuris muris* infections respectively (Hung et al., 2013, Scalfone et al., 2013). As such, these studies along with data obtained in our experiments allude to IL-33 being more of a prerequisite to Th2 responses at primary sites of infection. Furthermore, its role in inducing immune responses at distal sites such as peritoneal cavities is likely restricted to certain helminth infections,

such as in the case of *N. brasiliensis*, where the induction of ILC2-derived IL-5 and IL-13, as well as the recruitment of eosinophils within mesenteric AT is demonstrated to be IL-33 dependent (Mahlakoiv et al., 2019).

To escape protective host immune responses, parasitic nematodes can exert immunomodulatory functions and *H. poly* is no exception. This helminth has been reported to dampen immune mechanisms that lead to its expulsion, by expanding numbers of Foxp3^{+} Tregs within SLOs (Grainger et al., 2010, Rausch et al., 2008). In addition, a subset of AT Tregs activated by IL-33 (i.e. FOXP3^{+}ST2^{+} Tregs; denoted as ST2^{+} for short) have been identified in lymphoid and non-lymphoid tissues, with a preferential enrichment within VATs (Panduro et al., 2016). The response of ST2^{-} (i.e. Foxp3^{+} ST2^{-}) and ST2^{+} Tregs within the mesenteries, omentum and mLN, as well as whether IL-33 was necessary for their expansion following infection was therefore assessed. Results revealed that neither ST2^{-} nor ST2^{+} Tregs in the mLN proliferated significantly following infection, likely caused by the disparity in data points across the assessed groups. However, profound increases in the proliferation of both Treg subsets within the mesenteries and omentum following *H. poly* was observed. Still, IL-33 appeared to be unessential for the proliferation of both Treg subsets, given the comparable numbers of Ki67^{+} cells between WT and *Il33*$^{-/-}$ mice. In line with this, Seide and colleagues found that under homeostatic conditions, the accumulation, as well as generation and maintenance of ST2^{+} Tregs was not dependent on IL-33 (Siede et al., 2016), with our studies further showing that this lack of IL-33 dependence holds true during *H. poly* infection.

As discussed above, VAT ILC2s, CD4 T cells as well as ST2^{-} and ST2^{+} Tregs proliferated significantly following *H. poly* infection, yet worms primarily infect the SI, suggesting the

possible recruitment of cells activated within the mLN, SI and/or FALCs in mesenteries and omentum. To address such question, ILC2 movement could be tracked using transgenic tools such as the photoconvertible fluorescence protein (Kaede) mice, which has proved useful in analysing the *in vivo* migration of cells across lymphoid as well as non-lymphoid organs (Tomura et al., 2008). By manipulating this system for use in our helminth model, SI can be exposed to violet light leading to expression of fluorescence in cells; mLN, mesenteries and omentum could then be harvested at the end of the study to assess the proportion of proliferating photoconverted Kaede cells in these tissues, thereby revealing if indeed cells emigrating from the SI are also localised to VATs.

4.6.2 Immune Responses in Peritoneal Adipose Tissues during *S. Mansoni* Infection

In collaboration with the group of Andrew MacDonald at the University of Manchester Innovation Centre, the role of VAT FALCs during helminth infection was investigated further using a second intestinal helminth – *S. mansoni.* Infection of WT C57BL/6J mice with 40 and 180 cerc of *S. mansoni* parasitic larvae resulted in trapping of adults in the mesenteries. Adult worms were obvious to the naked eye, with the presence of worms appearing proportional to parasitic load. This observation was not surprising given previous reports that the mesenteric veins were a preferred site of *S. mansoni* localisation, where worms could cause intestinal schistosomiasis (Costain et al., 2018, McManus et al., 2018). Although the enumeration of FALCs following 40 cerc of *S. mansoni* infection did not yield conclusive results due to few sample numbers and data variability across the samples, analysis of ILC subsets revealed that ILC2s within the mesenteries and omentum increased significantly following infection compared to ILC1s and ILC3s, thereby suggesting that VAT ILC2s were likely responding to *S. mansoni* infection and a preference for this subset compared to

ILC1/3s. As such, ILC2s were further assessed for their proliferative and activation status. Indeed, the proportion and number of proliferating ILC2s were significantly higher in the mesenteries and omentum (as well as mLN). Others have similarly reported of the accumulation of ILC2s in the WAT of mice following infection with *S. mansoni* in a mechanism dependent on IL-33. Briefly, infection with *Schistosoma mansoni* egg-derived ω1 (ω1) induced the release of IL-33 from adipocytes, that triggered downstream recruitment of IL-33 responsive cells including ILC2s, eosinophils and AAMs within peritoneal ATs (Hams et al., 2016).

Furthermore, ILC2s within the VATs showed an activated phenotype owing to the increased numbers of CD69^{+} and/or CD44^{+}ILC2s in the mesenteries and omentum – but not in the mLN following infection. Such proliferative and activated state of ILC2s was also observed in the *H. poly* model as discussed in 4.6.1, thereby highlighting a shared ILC2 phenotype during infection with different helminth parasites. MHC-II expression on ILC2s has been shown to be important in the development and polarisation of Th2 responses. *In vitro* co-culture experiments showed that in the presence of ILC2s, activated CD4 T cells produced enhanced Th2 cytokines including IL-4/5/13. More so, this was revealed to involve contact dependent mechanisms, whereby ILC2s could present peptide-antigen that induced CD4 T cell proliferation and Th2 polarisation (Mirchandani et al., 2014). Additionally, *in vivo* studies using *N. brasiliensis*, further showed that crosstalk between ILC2s and T cells was important for worm expulsion. Indeed, MHC-II expressing ILC2s interacted with antigen-specific T cells, to induce IL-2 production, leading to enhanced ILC2 proliferation and cytokine production (Oliphant et al., 2014a). As such, the increased numbers of MHC-II^{+}ILC2s observed in the omentum within our study may be indicative of the capacity of activated ILC2s within this

tissue to present *S. mansoni* larval antigens. Although adult worms were not seen in the omentum, it is possible that parasitic eggs could have migrated to and lodged in the omentum, thereby activating ILC2s within this tissue. Furthermore, the antigenic potential as well as the pathology of schistosomiasis results from the presence of eggs, rather than the worms, with eggs becoming trapped in a number of tissues during their transit to excretory organs (Wu and Halim, 2000). Therefore, while it is yet unclear whether the omentum is one of such tissues, the activation of immune cells (including CD4 T cells discussed below) within the omentum, provides some evidence that *S. mansoni* eggs may indeed have become trapped in this tissue. As such future experiments should ascertain this hypothesis via methods that have been reported by other groups, which include tissue digest protocols that enable eggs lodged in the liver and intestine to be counted while in suspension (Mukendi et al., 2021), as well as confocal laser scanning microscopy that allow direct visualisation of eggs within the gut (Holtfreter et al., 2011). These techniques could be adapted for use with VATs to confirm the presence of eggs in such tissues and their likely contribution to the Th2 responses observed in our study.

When analysing T cell responses, significant proportions of IFN-γ^+CD8 T cells were observed in the mLN, omentum, and to a lesser extent in the mesenteries. In addition, the numbers of CD8 T cells tended to increase, particularly in VATs. It is well reported that *S. mansoni* can elicit Th1 and Th2 responses; however, the activation of type 1 immune responses including Th1 IFN-γ production is stated to occur early in infection, in the first 3-5weeks (Pearce and MacDonald, 2002, Pearce et al., 1991). It was therefore surprising to see the persistence of such responses given that tissues were analysed 7 weeks post infection, as which point Th2 responses should be dominating. Furthermore, it is interesting to note that IFN-γ production

observed in our study was particularly by CD8s, rather than by CD4 T cells as has been reported by others (Hams et al., 2013a). Moreover, the proportion of IFN-γ^+CD4 T cells was found to decrease in the mesenteries. Additionally, earlier studies that investigated the effect of *S. mansoni* infection on type 1 cytokine (IFN-γ) production by CD8 T cells in the spleen further confirmed the dominance of this cytokine at day 28 post infection, with its levels diminishing by day 49, as a result of the emerging type 2 signature – namely IL-4-, IL-5- and IL-10-producing CD4 T cells (Fallon et al., 1998). In contrast, Pedras-Vasconcelos and colleagues reported that anti-CD3 stimulated splenic cells isolated from mice infected with *S. mansoni*, still secreted large amounts of IFN-γ even 8 weeks after infection compared to non-infected mice (Pedras-Vasconcelos and Pearce, 1996), thereby highlighting some exceptions to the Th1/Th2 divide of *S. mansoni* pathology – one that is echoed in this project.

Finally, while IL-4/5/13 secreting CD4 T cells were observed to significantly increase in the mLN post infection, this was not seen in the mesenteries or omentum, suggesting a disparity in CD4 T cell responses between VATs and SLOs. However, the proportion of IL-10-producing Tregs was found to increase across all tissues, with slight increases in the numbers of Tregs also found within the mesenteries and omentum. Elevated IL-10 has been reported to downregulate IFN-γ production during later stages of *S. mansoni* infection (Sher et al., 1991). Given the enhanced IFN-γ in the mLN and VATs observed in our study, it is therefore likely that the expansion of IL-10^+ Tregs in these tissues mediates a similar anti-inflammatory role. However as shown in supplementary figure 7.1 of the appendix, when mice were given a larger parasite burden of 180 cercs, enhanced Th2 responses were observed particularly in the omentum, thereby suggesting that VAT FALCs are more likely to respond to a supra-infection of *S. mansoni,* by expanding numbers of CD4 T cells, Tregs as well as the Th2

cytokines IL-4/5/10/13. As such, the magnitude of such responses within VATs is likely to be proportional, and dependent on the parasitic load.

Taken together, the results above therefore indicate that innate and adaptive immune cells in VAT FALCs can contribute to immune responses to helminth infections that primarily occur in the small intestine, by supporting immune cell interactions and proliferation, through the upregulation of canonical markers, and the predominant expression of Th2 cytokines. While such Th2 responses are favourable for the host during parasitic infection, a Th2 enviroment is generally considered to support and promote tumour growth in the context of cancer (Mantovani et al., 2008). As mentioned in the introduction (chapter 1.2), AT can exist in a pro-inflammatory (Th1) or anti-inflammatory (Th2) state with the latter typically found in healthy, lean individuals, suggesting that AT may be able to mediate diverse immune responses dependent on different disease contexts. As such, this study also set out to investigate the immune cell composition of VAT FALCs during metastatic tumour formation, how these tumours are supported within FALCs and whether their polarisation towards a pro-inflammatory state would be sufficient to initiate anti-tumour mechanisms.

CHAPTER 5: INVOLVEMENT OF FALCs IN PERITONEAL CANCER METASTASIS

5.1 Introduction

The peritoneal cavity is often the site for metastatic tumour formation, with advanced stages of ovarian, colon and gastric cancers topping the list (Desai and Moustarah, 2020). Within the peritoneal cavity, such metastatic tumours preferentially localise to omental and mesenteric FALCs/milky spots (Gerber et al., 2006). The presence of mesothelial cells, collagen fibres and angiogenic blood vessels within these immune clusters (Sorensen et al., 2009), provision of fatty acids through lipid metabolism (Nieman et al., 2011), and levels of secreted adipokines (Au-Yeung et al., 2020), have all been shown to mediate tumour cell homing, attachment and growth. Furthermore, under homeostatic conditions, omental FALCs are abundantly populated by type 2 immune cells including ILC2s, Tregs, eosinophils, iNKT cells and AAMs, (Meza-Perez and Randall, 2017), with such type 2 milieu also observed in mesenteric FALCs as revealed and further confirmed in this study (chapter 3.4). In addition, Th2 cytokines are also present; for instance, WAT resident multipotent stromal cells act as reservoirs for the potent Th2 inducer IL-33, that sustains adipose resident immune cells including ILC2s, consequently resulting in ILC2 derived IL-4 and IL-13 (Rana et al., 2019). Likewise, this project showed in chapter 3, significant production of IL-5 and IL-13 by ILC2s within the mesenteries and omentum following *ex vivo* stimulation. Together, these immune cells and cytokines can culminate in the polarisation of an anti-inflammatory or tolerogenic AT environment. While such immune cells are also important in the metabolic and homeostatic regulation of VATs (Molofsky et al., 2013, Hams et al., 2013b), it is well established that the balance between effector (pro-inflammatory) and tolerogenic (anti-inflammatory) responses can dictate the fate of tumours, with the latter often driving tumour-promoting functions (Mantovani et al., 2008, Balkwill et al., 2012). It is therefore

feasible to conceive why VAT FALCs make such favourable and suitable candidates for tumour colonisation. Indeed changes in the cellular composition of the omentum have been noted during ovarian metastasis, whereby the adipocytes – a major component of the omentum – was replaced by a combination of lymphocytes, macrophages and fibroblasts, as well as significant tumour-associated inflammation (Pearce et al., 2018). Furthermore, as stated in chapter 1.2, FALC stromal cells express several chemokines and cytokines, including IL-33. While IL-33 appeared to be dispensable for the generation of ILC2- and CD4 T cell-responses observed in this project during *H. poly* infection (chapter 4), its localisation within FALC stromal cells during tumour metastasis was additionally explored. Moreover, while the involvement of IL-33 and its cognate receptor, ST2, in cancer formation has been reported by different authors these have included both protective (O'Donnell et al., 2015) and detrimental (Liu et al., 2014, Zhang et al., 2017b) effects, as such a clear role for IL-33 in tumour progression remains elusive.

With colon and ovarian cancers amongst the leading causes of cancer related deaths (Fitzmaurice et al., 2018, Sorensen et al., 2009), it will be beneficial to elucidate further mechanisms that mediate and support tumour metastasis in FALCs. Therefore, the changes in immune cell populations within omental and mesenteric FALCs following tumour formation was investigated using syngeneic tumour models of colon cancer, and through the analysis of metastatic omental tissue from patients with HGSOC.

5.2 MC38 Murine Colon Cancer Model

Previous work within our group had observed that ip injection of MC38 colon cancer cells in mice resulted in tumour formation within mesenteric and omental FALCs. To gain insight

into the changes occurring within FALC immune cells in response to tumours, further experiments were conducted. Additionally, it had been reported that acute peritonitis triggered via zymosan resulted in *de novo* formation of FALCs, as shown by the marked increase in the number as well as size of FALCs in mesenteric ATs (Bénézech et al., 2015). Therefore, the responses between two groups of mice were evaluated: one administered PBS (PBS/MC38-GFP) and the other zymosan (to induce peritoneal inflammation - zymosan/MC38-GFP) at day 0, followed 3 days later by MC38 colon cancer cells. Mesenteric and omental VATs were then harvested 10 days later - figure 5.1A. Following two independent experiments, ip injection of PBS followed by MC38 led to 100% of mice developing metastatic tumours in FALCs as expected. Tumours were visible in both mesenteries and omentum often overtaking the whole tissue in the case of the omentum (figure 5.1A-B). However, only ~45% of mice in the zymosan/MC38 group developed tumours in their VAT FALCs (figure 5.1A-B).

Next the proportion of T cell subsets, including CD4, CD8 T cells and Tregs within the mesenteries and omentum was analysed between the two groups (figure 5.2A). Mesenteries and omentum isolated from zymosan/MC38 group displayed slightly higher proportions of CD4 T cells compared to PBS/MC38 group (figure 5.2B). While the proportion of CD8 T cells tended to decrease non-significantly in the two tissues within zymosan/MC38 group (figure 5.2C). Furthermore, mesenteric and omental FALCs within zymosan/MC38 mice were found to have statistically significantly lower proportions of Tregs compared to PBS/MC38 group (figure 5.2D), with the presence of Tregs within PBS/MC38 group confirmed via immunofluorescence staining – figure 5.2E. When cytokine production was assessed following *ex vivo* stimulation of single cell suspensions, no difference in IFN-γ production by

CD4 T, CD8 T, NK cells and iNKTs between PBS/MC38 and zymosan/MC38 could be observed in the mesenteries (Figure 5.2F-I). However omentum isolated from zymosan/MC38 group had significantly higher proportions of IFN-γ^+ CD4 T cells (figure 5.2F), and IFN-γ^+ NK cells (figure 5.2H), as well as a trend towards increased frequency of IFN-γ^+ iNKT cells (figure 5.2I).

Figure 5.1: Assessing the tumour burden within mesenteric and omental FALCs following MC38 injection

C57BL/6J WT mice were initially administered zymosan to induce peritoneal inflammation (D0), with control groups receiving PBS, followed 3 days later by intra-peritoneal (ip) injection of 5 x 10^5 GFP-tagged MC38 colon cancer cells (D3). Mesenteries and omentum were harvested 10 days post MC38 injection (D13) as described in material and methods. The effect of zymosan on total tumour burden was analysed by visualising tumours using a stereofluorescence microscope.

a) Schematic of MC38 colon cancer, showing timeline of injections and number of animals that developed tumours between PBS (PBS/MC38) and zymosan (zymosan/MC38) groups.
b) Immunofluorescence imaging of MC38-GFP tumours within mesenteric (left) and omental FALCs (right). White arrows indicate tumours. Images were taken at 7.97x.

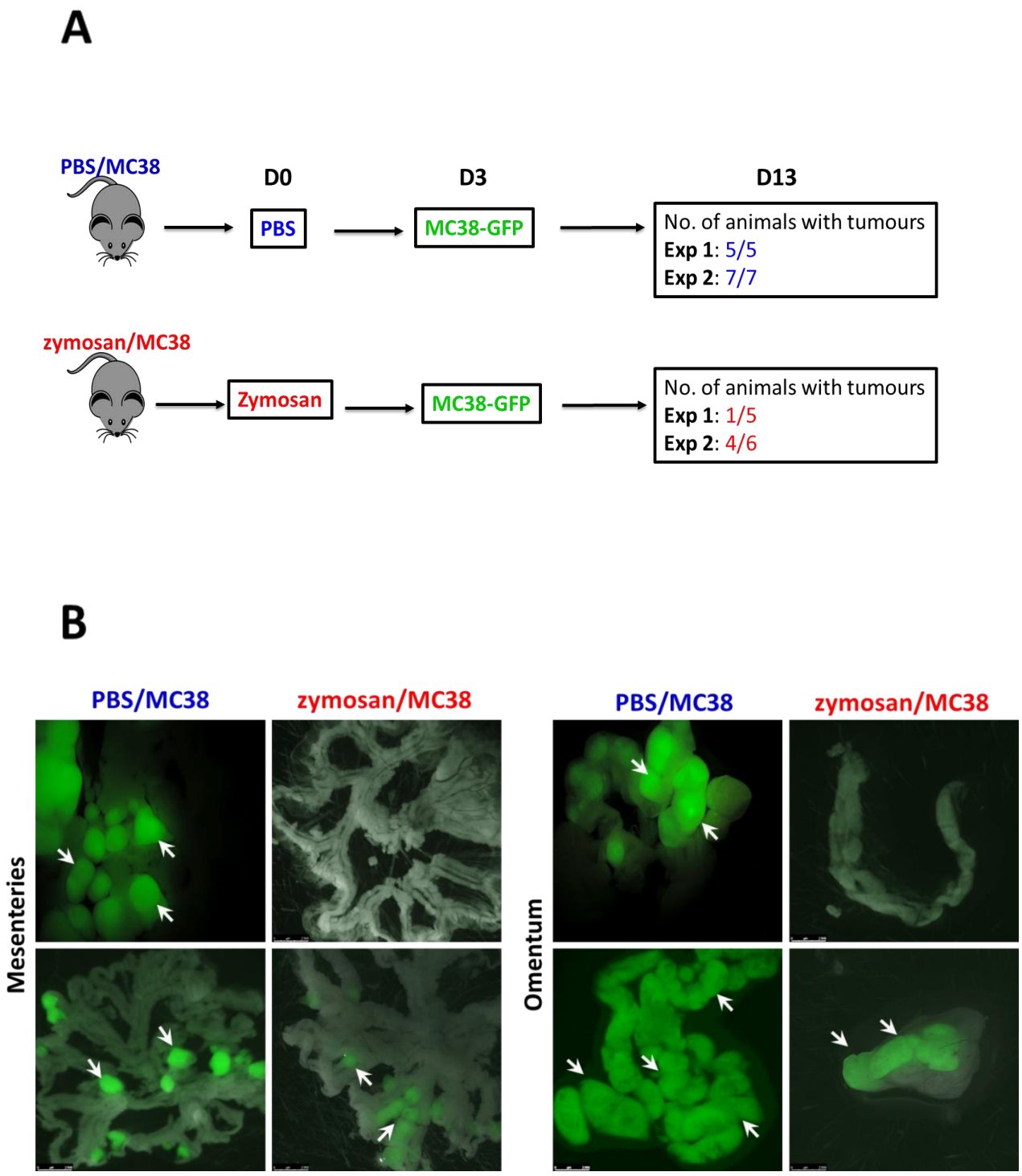
A
PBS/MC38
D0
D3
D13
PBS
MC38-GFP
No. of animals with tumours
Exp 1: 5/5
Exp 2: 7/7
zymosan/MC38
Zymosan
MC38-GFP
No. of animals with tumours
Exp 1: 1/5
Exp 2: 4/6
B
PBS/MC38
zymosan/MC38
PBS/MC38
zymosan/MC38
Mesenteries
Omentum

Figure 5.1

Figure 5.2: Analysis of lymphoid subsets in visceral adipose tissues following MC38 injection

The mesenteries and omentum were isolated from PBS/MC38 and zymosan/MC38 mice 10 days after ip injection with 5 x 10^5 GFP-tagged MC38 cancer cells (D13), as shown in the schematic in figure 5.1A. Following isolation of cells from tissues, the effect of zymosan on the proportion of lymphoid immune cell subsets as well as cytokine production by effector immune subsets was analysed by flow cytometry. The difference in Treg infiltration between the two groups was also confirmed by immunofluorescence staining.

Data are representative of a single independent experiment with the following sample numbers: PBS/MC38 (n=2-3), zymosan/MC38 (n=3). Bars on the graph represent the median value. Statistical significance was determined using Unpaired t test.*P<0.05, **P<0.01, ***P<0.001 and ****P<0.0001.

a) Representative FACS plots showing the proportion of CD4/CD8 T cells, NK cells, iNKTs and Tregs in mesenteries (top) and omentum (bottom) between PBS/MC38 and zymosan/MC38 mice. Cells have been pre-gated on FSC and SSC followed by live CD45.2$^+$.
b) Graph comparing the percentage of CD4 T cells in mesenteries and omentum (left to right) between PBS/MC38 and zymosan/MC38 mice.
c) Graph comparing the percentage of CD8 T cells in mesenteries and omentum (left to right) between PBS/MC38 and zymosan/MC38 mice.
d) Graph comparing the percentage of Tregs in mesenteries and omentum (left to right) between PBS/MC38 and zymosan/MC38 mice.

e) Confocal images comparing representative FALCs in mesenteries (top) and omentum (bottom) between PBS/MC38 and zymosan/MC38 mice. MC38 tumours (green); Foxp3 (red); CD4 (blue). Scale bar represents 50 µm. Images were taken at 40x. White arrows indicate Tregs.

f) Graph comparing the percentage of IFNγ^+ CD4 T cells in mesenteries and omentum (left to right) between PBS/MC38 and zymosan/MC38 mice.

g) Graph comparing the percentage of IFNγ^+ CD8 T cells in mesenteries and omentum (left to right) between PBS/MC38 and zymosan/MC38 mice.

h) Graph comparing the percentage of IFNγ^+ NK cells in mesenteries and omentum (left to right) between PBS/MC38 and zymosan/MC38 mice.

i) Graph comparing the percentage of IFNγ^+ iNKTs in mesenteries and omentum (left to right) between PBS/MC38 and zymosan/MC38 mice.

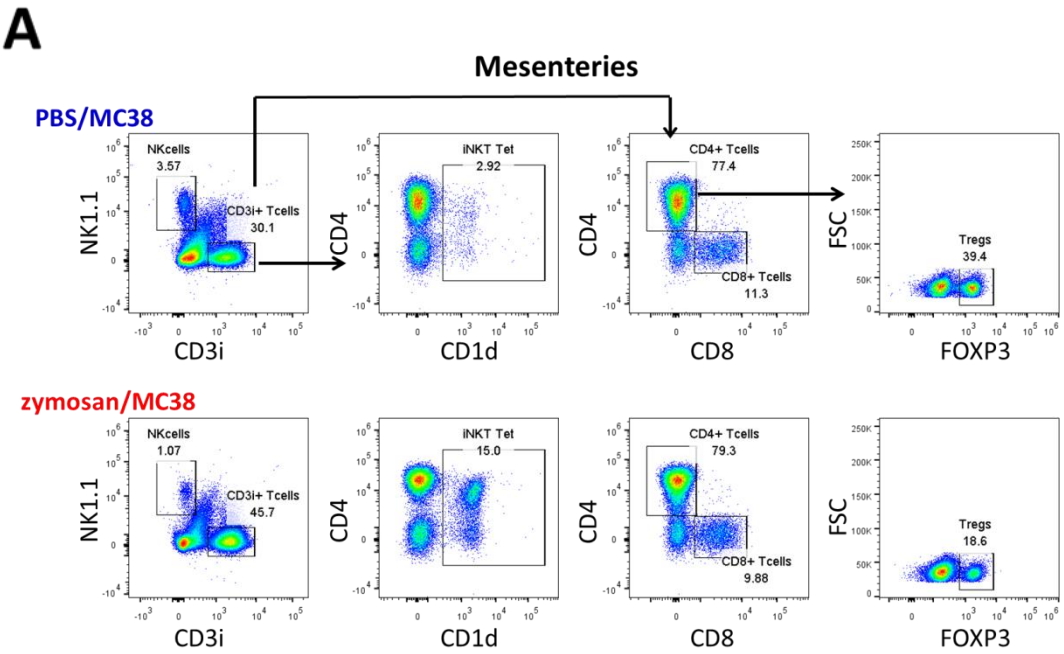
A
Mesenteries
PBS/MC38
NKcells
3.57
CD3i+ Tcells
30.1
NK1.1
CD3i
iNKT Tet
2.92
CD4
CD1d
CD4+ Tcells
77.4
CD8+ Tcells
11.3
CD4
CD8
Tregs
39.4
FSC
FOXP3
zymosan/MC38
NKcells
1.07
CD3i+ Tcells
45.7
NK1.1
CD3i
iNKT Tet
15.0
CD4
CD1d
CD4+ Tcells
79.3
CD8+ Tcells
9.88
CD4
CD8
Tregs
18.6
FSC
FOXP3

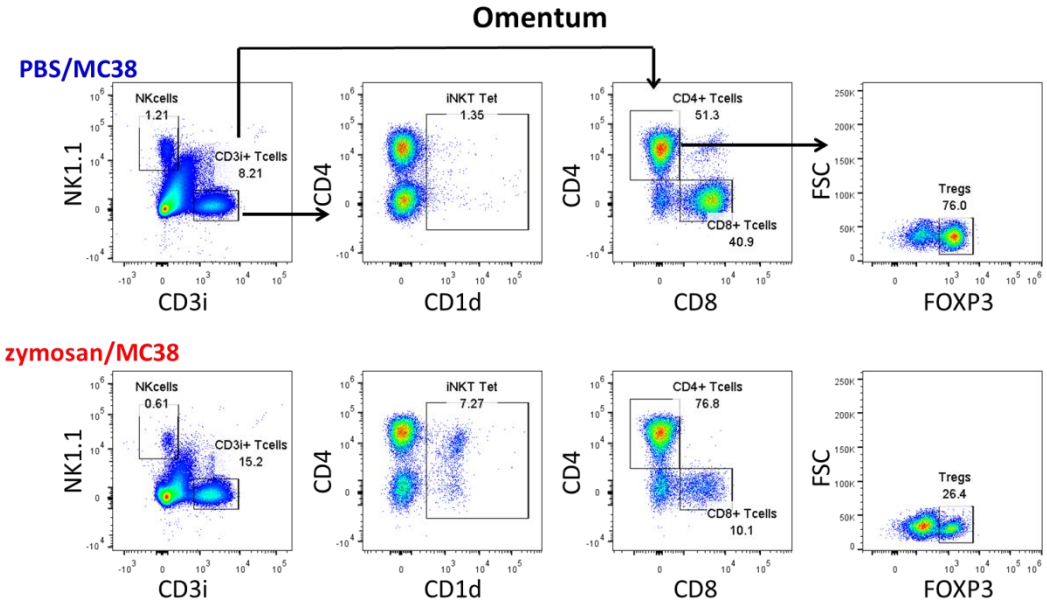
Omentum
PBS/MC38
NKcells
1.21
CD3i+ Tcells
8.21
NK1.1
CD3i
iNKT Tet
1.35
CD4
CD1d
CD4+ Tcells
51.3
CD8+ Tcells
40.9
CD4
CD8
Tregs
76.0
FSC
FOXP3
zymosan/MC38
NKcells
0.61
CD3i+ Tcells
15.2
NK1.1
CD3i
iNKT Tet
7.27
CD4
CD1d
CD4+ Tcells
76.8
CD8+ Tcells
10.1
CD4
CD8
Tregs
26.4
FSC
FOXP3

PBS/MC38
zymosan/MC38

B

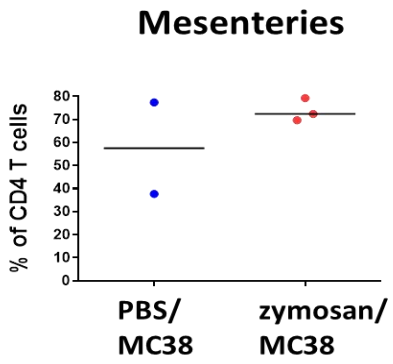

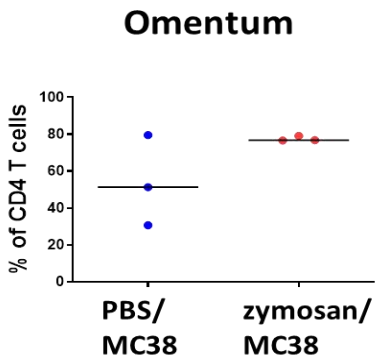

C

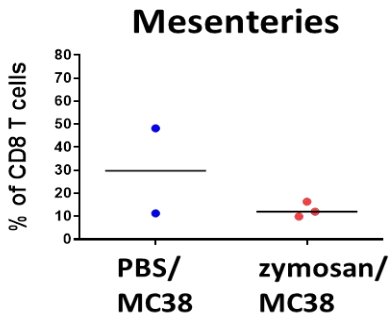

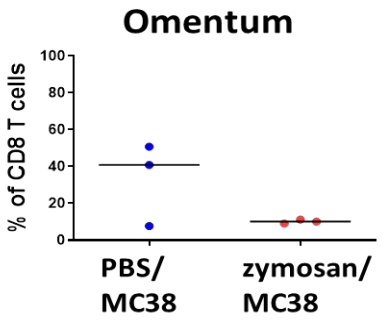

D

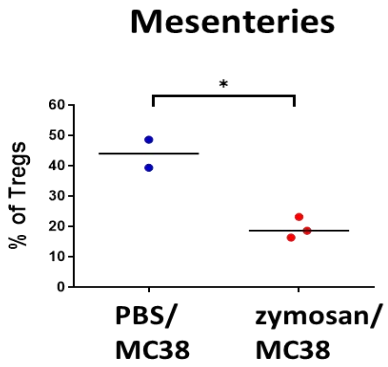

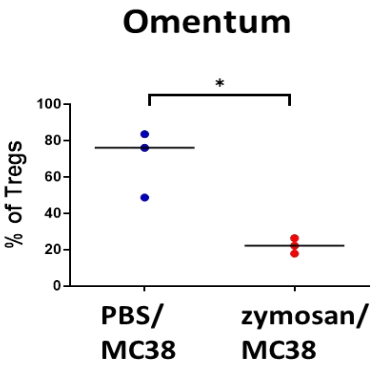

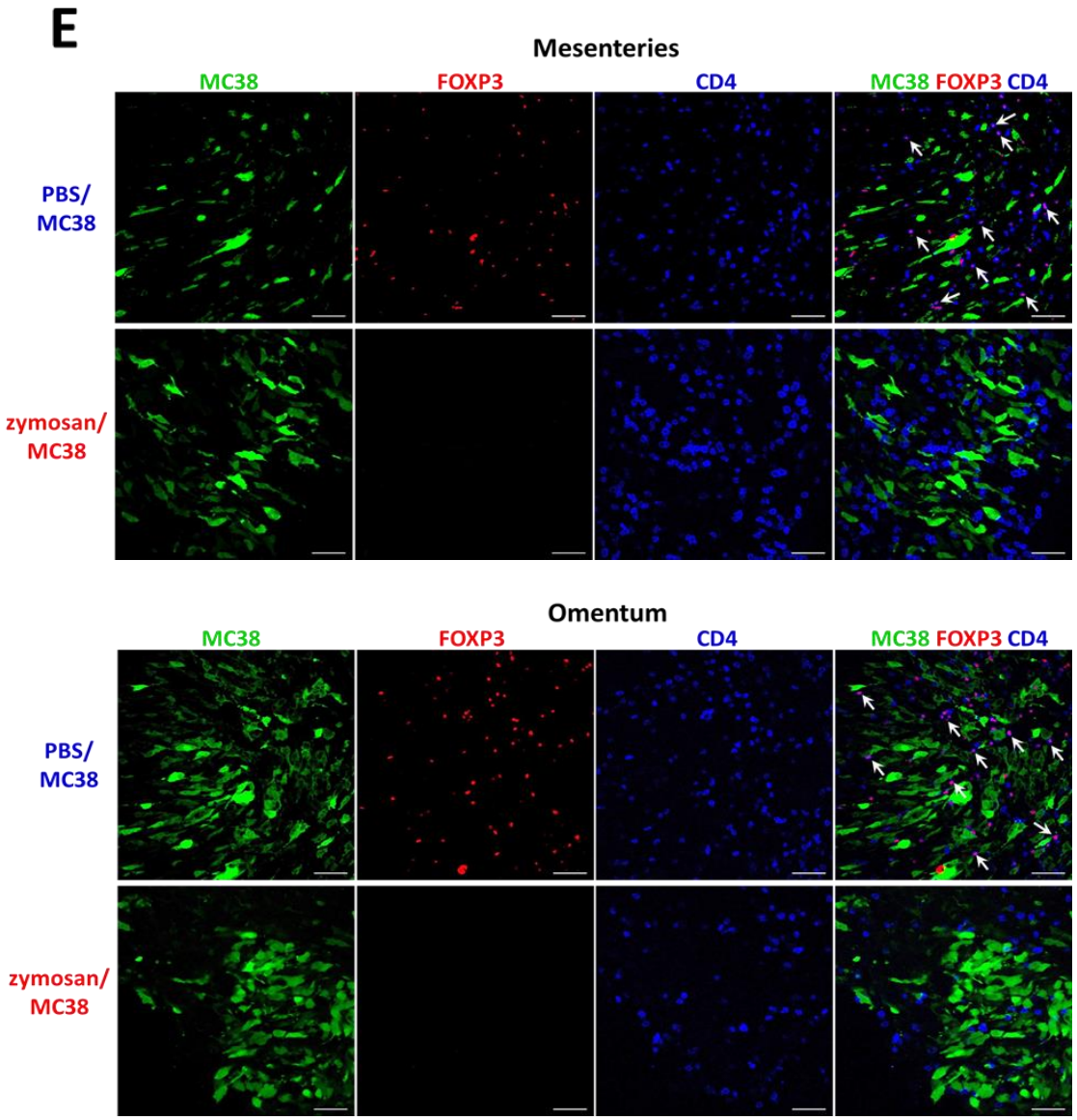
E
Mesenteries
MC38
FOXP3
CD4
MC38 FOXP3 CD4
PBS/
MC38
zymosan/
MC38
Omentum
MC38
FOXP3
CD4
MC38 FOXP3 CD4
PBS/
MC38
zymosan/
MC38

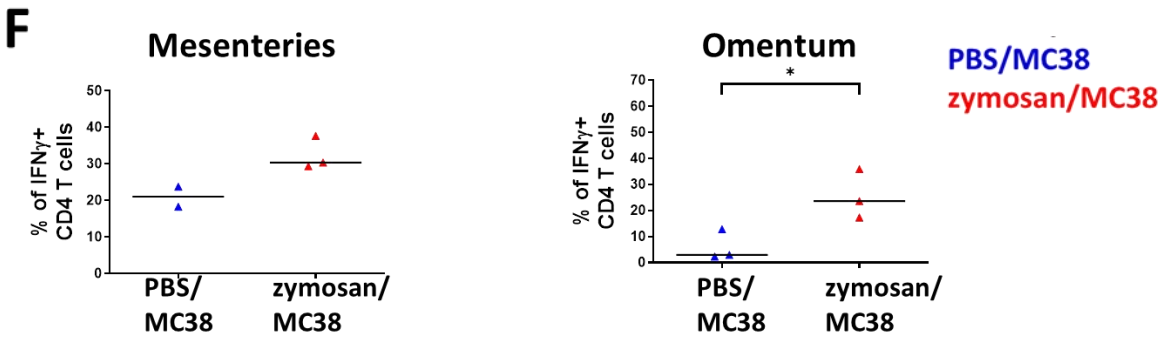
F
Mesenteries
% of IFNγ+
CD4 T cells
50
40
30
20
10
0
PBS/
MC38
zymosan/
MC38
Omentum
*
70
60
50
40
30
20
10
0
PBS/MC38
zymosan/MC38

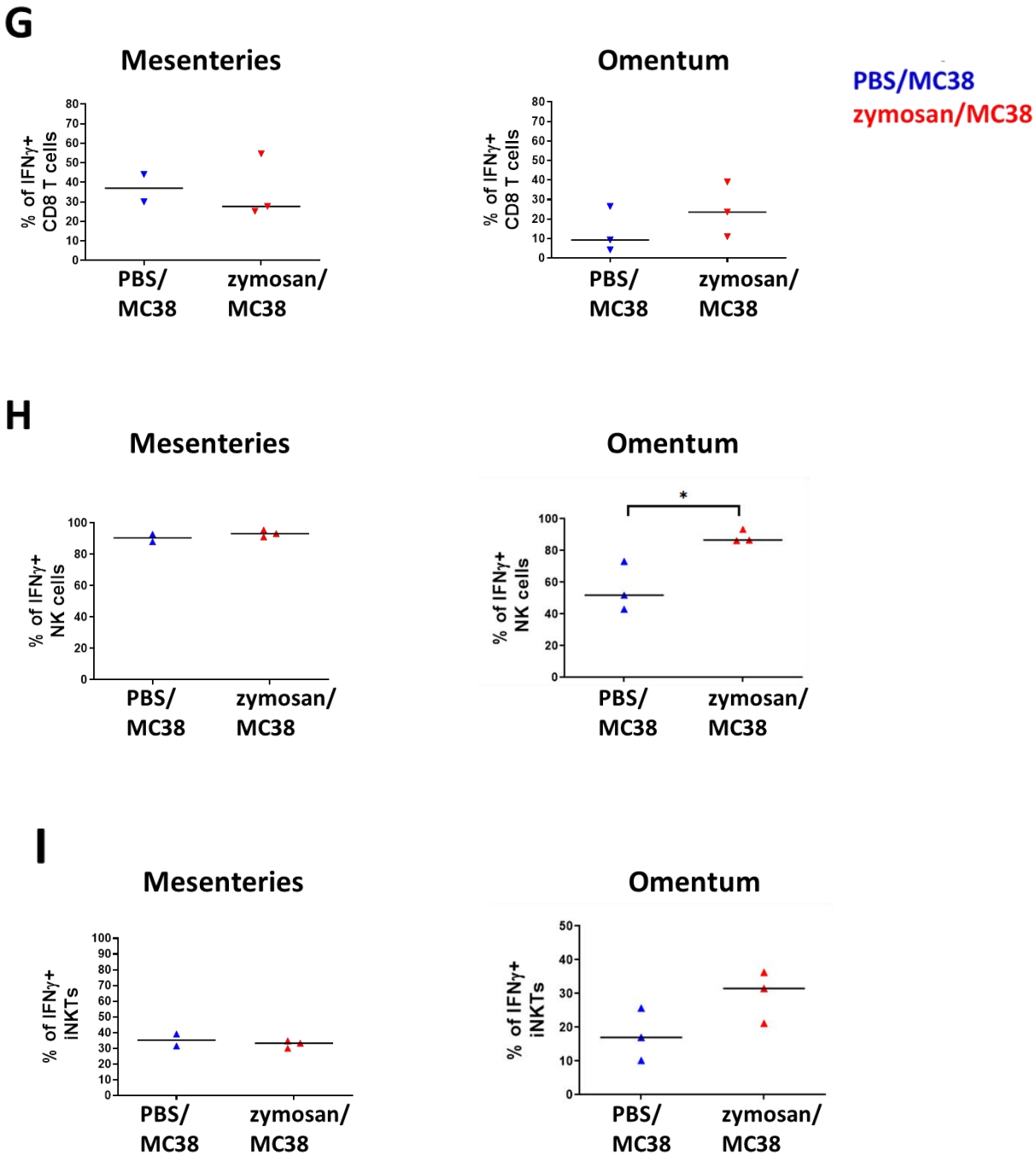
G
Mesenteries
Omentum
PBS/MC38
zymosan/MC38
% of IFNγ+ CD8 T cells
PBS/ MC38
zymosan/ MC38
H
Mesenteries
Omentum
% of IFNγ+ NK cells
*
I
Mesenteries
Omentum
% of IFNγ+ iNKTs

Figure 5.2

Zymosan particles can be recognised by myeloid cells through engagement between PAMPs and TLR leading to the engulfment of zymosan (Underhill, 2003). Coincidently, the expansion of FALCs in response to zymosan-induced peritoneal inflammation is reported to involve the recruitment of CD11b^{+} myeloid cells (Bénézech et al., 2015). Therefore the changes to the myeloid compartment of mesenteric and omental FALCs between PBS/MC38 and zymosan/MC38 groups, was also assessed – figure 5.3A, with the inclusion of a PBS only group that did not receive any tumour cells. Within the mesenteries, no significant difference in neutrophils, eosinophils and monocytes (figure 5.3B-D) was observed between PBS controls and PBS/MC38 mice, though macrophages (figure 5.3E) tended to increase; however the normalised number of neutrophils (figure 5.3B), monocytes (figure 5.3D) and macrophages (figure 5.3E) in the mesenteries was significantly higher in zymosan/MC38 group compared to PBS only mice. Secondly, compared to PBS only mice, a significantly higher number of neutrophils, eosinophils, monocytes and macrophages were present in omental FALCs of PBS/MC38 mice, with no difference observed between the PBS/MC38 and zymosan/MC38 groups – figure 5.3B-E.

With IL-33 being a potent inducer of type 2 immune responses, which as mentioned previously creates a favourable environment for tumours, we sought to determine whether any changes in this stromal cell cytokine could be observed within FALCs following tumour formation. Under steady state conditions, IL-33 is present within the nuclei of FALC stromal cells in both the mesenteries and omentum (figure 5.4A). Similarly immunofluorescence staining showed nuclear IL-33 expression in VATs from zymosan/MC38 groups, both in the presence (mesenteries) or absence of tumours (omentum) - figure 5.4B. In contrast, IL-33

was observed in the cytoplasm of FALC stromal cells within mesenteries and omentum isolated from PBS/MC38 mice (figure 5.4B).

Figure 5.3: Analysis of myeloid subsets in visceral adipose tissues following MC38 injection

C57BL/6J WT mice received zymosan or PBS as control, followed 3 days later by intra-peritoneal (ip) injection of 5 x 10^5 GFP-tagged MC38 colon cancer cells (D3). Cells from mesenteries and omentum were isolated as described in materials and methods.

The effect of zymosan on myeloid immune cell subsets including neutrophils, eosinophils, monocytes and macrophages, between PBS/MC38 and zymosan/MC38 mice was assessed. Total number of cells were normalised to weight of individual tissues and represented as number of cells per 100mg of tissue.

Data are representative of a single independent experiment with the following sample numbers: tumour-free (i.e. PBS only) (n=4), PBS/MC38 (n=5), zymosan/MC38 (n=3). Bars on the graph represent the median value. Statistical significance was determined using Kruskal-Wallis followed by Dunn's multiple comparisons test. *P<0.05, **P<0.01, ***P<0.001 and ****P<0.0001.

a) Representative FACS plots showing the proportion of neutrophils, eosinophils, monocytes and macrophages in, mesenteries (top) and omentum (bottom) between PBS/MC38 and zymosan/MC38 mice. Cells have been pre-gated on FSC and SSC followed by liveCD45.2$^+$Lin$^-$ CD11c$^-$CD11b$^+$. Lineage (Lin) gate included CD3, CD8, B220.

b) Graph comparing the adjusted number of neutrophils per 100 mg tissue in mesenteries and omentum (left to right) between PBS only, PBS/MC38 and zymosan/MC38 mice.

c) Graph comparing the adjusted number of eosinophils per 100 mg tissue in mesenteries and omentum (left to right) between PBS only, PBS/MC38 and zymosan/MC38 mice.

d) Graph comparing the adjusted number of monocytes per 100 mg tissue in mesenteries and omentum (left to right) between PBS only, PBS/MC38 and zymosan/MC38 mice.

e) Graph comparing the adjusted number of macrophages per 100 mg tissue in mesenteries and omentum (left to right) between PBS only, PBS/MC38 and zymosan/MC38 mice.

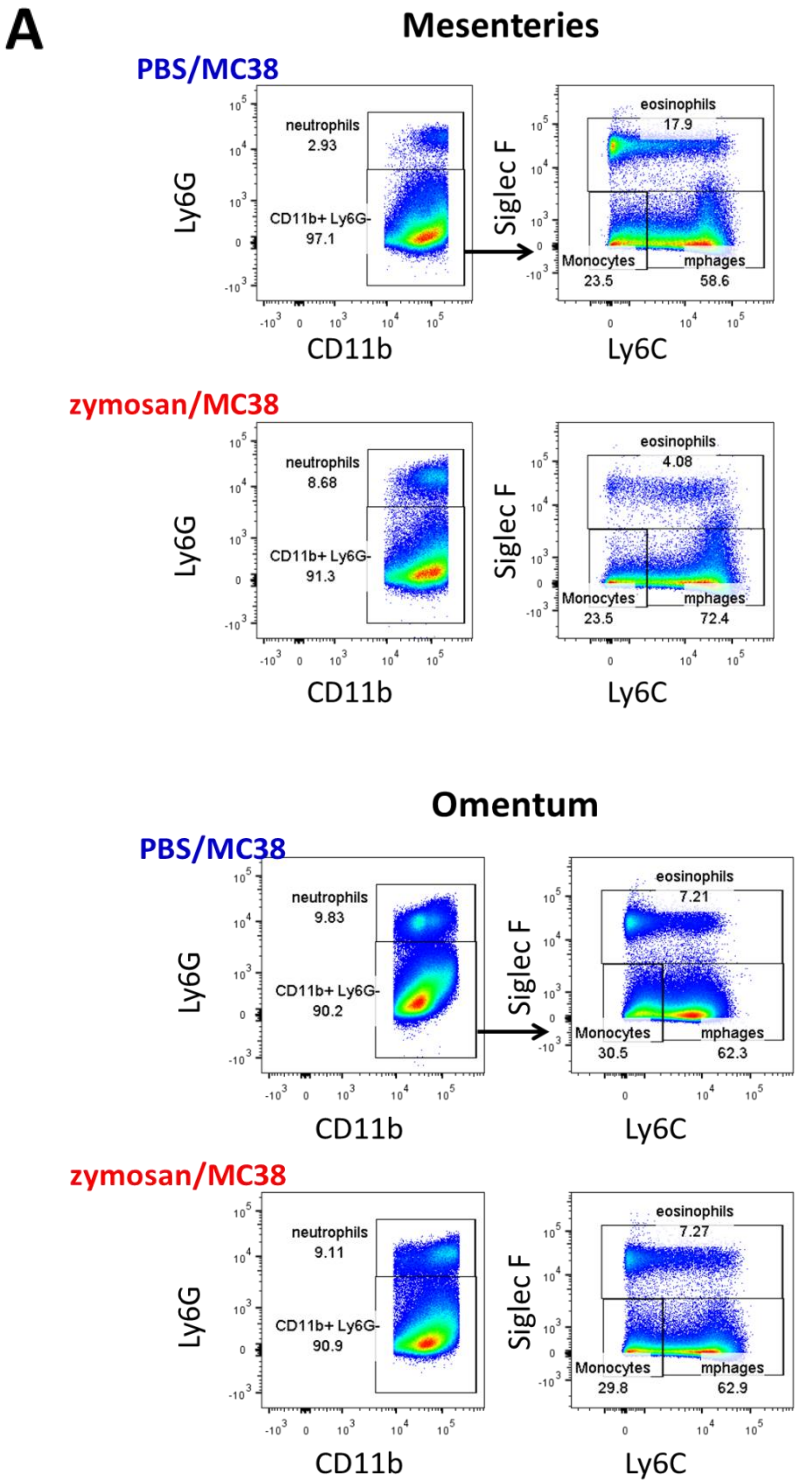
A
Mesenteries
PBS/MC38
neutrophils
2.93
CD11b+ Ly6G-
97.1
Ly6G
CD11b
eosinophils
17.9
Monocytes
23.5
mphages
58.6
Siglec F
Ly6C
zymosan/MC38
neutrophils
8.68
CD11b+ Ly6G-
91.3
eosinophils
4.08
Monocytes
23.5
mphages
72.4
Omentum
PBS/MC38
neutrophils
9.83
CD11b+ Ly6G-
90.2
eosinophils
7.21
Monocytes
30.5
mphages
62.3
zymosan/MC38
neutrophils
9.11
CD11b+ Ly6G-
90.9
eosinophils
7.27
Monocytes
29.8
mphages
62.9

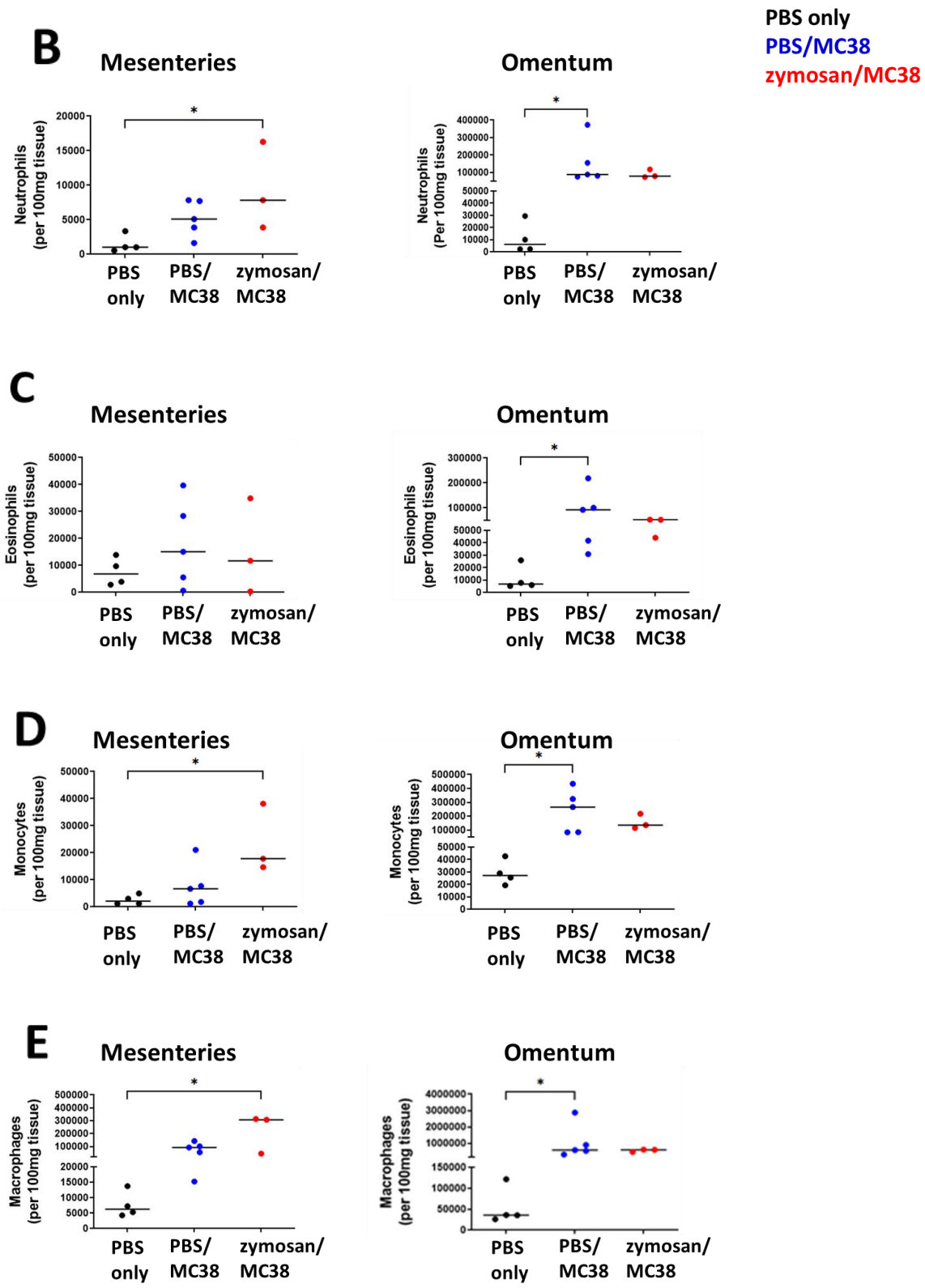
PBS only
PBS/MC38
zymosan/MC38
B
Mesenteries
Omentum
Neutrophils (per 100mg tissue)
Neutrophils (Per 100mg tissue)
C
Eosinophils (per 100mg tissue)
D
Monocytes (per 100mg tissue)
E
Macrophages (per 100mg tissue)
PBS only
PBS/ MC38
zymosan/ MC38

Figure 5.3

Figure 5.4: IL-33 is translocated to the cytoplasm of FALC stromal cells following MC38 injection

C57BL/6J WT mice were administered zymosan to induce peritoneal inflammation (D0), with control groups receiving PBS, followed 3 days later by intra-peritoneal (ip) injection of 5 x 10^5 GFP-tagged MC38 colon cancer cells (D3). Mesenteries and omentum were harvested 10 days post MC38 injection (D13), stained with primary and secondary antibodies for immunofluorescence, and counter stained with DAPI as described in materials and methods. Images were acquired using a confocal microscope.

a) Confocal images showing nuclear expression of IL-33 in mesenteric (top) and omental (bottom) FALCs under steady state conditions. CD45 (green); IL-33 (red). Scale bar represents 50 µm. Images were taken at 25x.
b) Confocal images showing representative FALCs in mesenteries (left) and omentum (right) comparing the expression of IL-33 (red) between PBS/MC38 and zymosan/MC38 mice. MC38 tumour expression was detected using anti-GFP secondary antibody (green). Scale bar represents 50 µm. Images were taken at 40x. White arrows indicate cytoplasmic IL-33 expression.

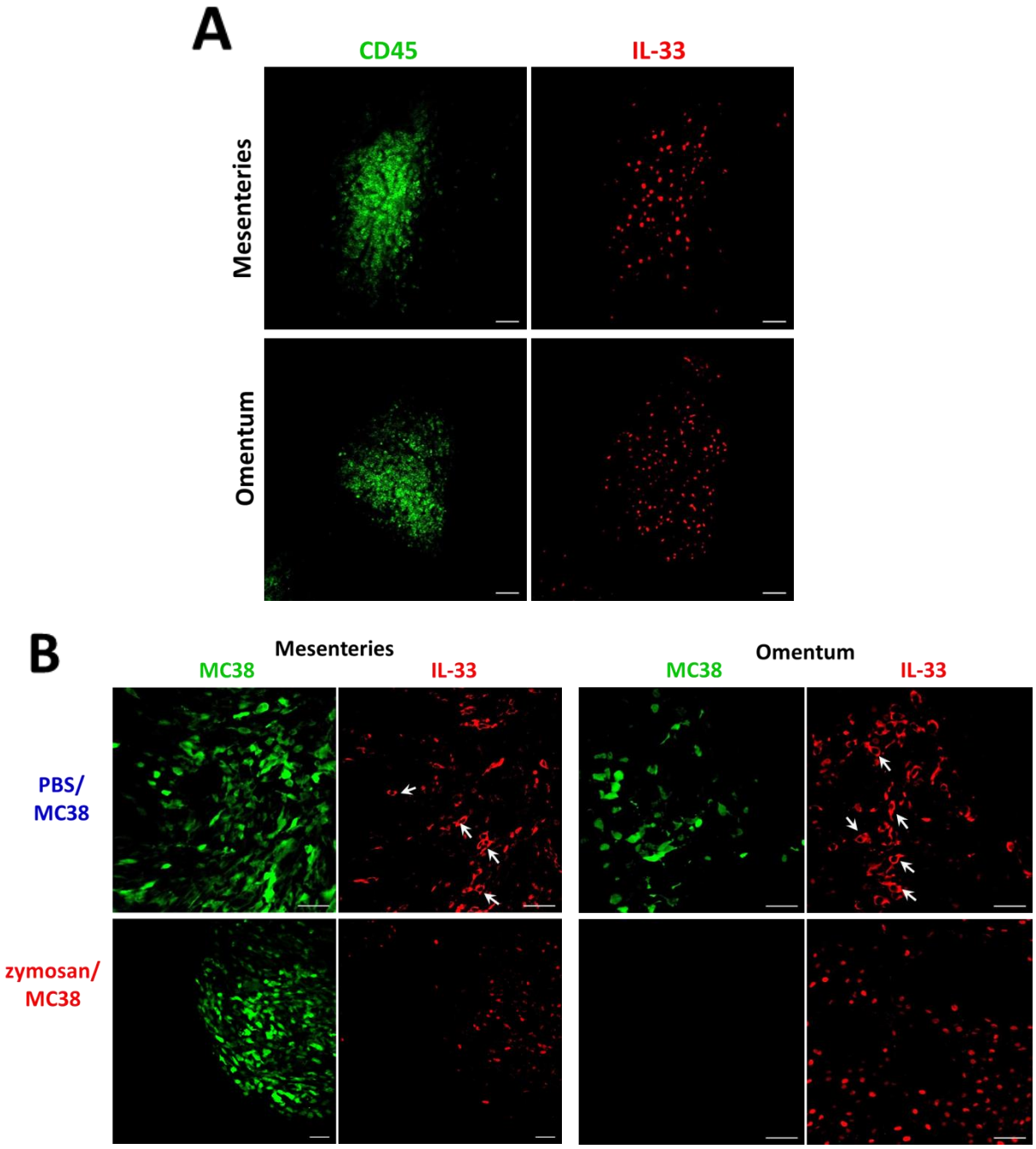
A
CD45
IL-33
Mesenteries
Omentum
B
Mesenteries
Omentum
MC38
IL-33
MC38
IL-33
PBS/
MC38
zymosan/
MC38

Figure 5.4

5.3 Human Cancer Metastasis – Ovarian Cancer

Having made the above observations in our murine model, equivalent analysis was conducted, investigating the immune profile of omental specimens collected from patients with metastatic and primary ovarian cancer. During tumorigenesis, ovarian carcinoma progresses from a slow growing borderline tumour to a well differentiated carcinoma (type I), or involves a genetically unstable and rapidly metastatic high grade serous carcinoma (type II) (Lengyel, 2010). The high grade serious subtype (HGSOC), often predominates in the clinical setting and accounts for a substantial proportion of mortalities from all forms of ovarian cancer (Lisio et al., 2019). This is largely due to the metastatic nature of HGSOC, with metastasis to the omentum and other abdominal organs such as the SI and retroperitoneal lymph nodes occurring during stage III of the disease. Advanced stages further encompass stage II where metastasis occurs to pelvic organs including the uterus, fallopian tube, rectum and bladder; and IV which goes beyond the peritoneal cavity to distant parenchymal organs such as the liver and lung (Bast et al., 2009, Motohara et al., 2019). Our analyses was therefore focused on metastatic omentum collected from stage III-IV HGSOC patients who either had primary debulking surgery only (denoted here as Met/NT), or delayed debulking surgery – i.e. had been administered neoadjuvant chemotherapy prior to surgery (denoted as Met/NACT), as well as healthy omentum controls.

The infiltration of CD4 T, CD8 T, NK cells and Tregs was first assessed (figure 5.5A); omentum from Met/NT patients contained significantly higher normalised numbers of CD4 and CD8 T cells (figure 5.5B), NK cells (figure 5.5C; left) and Tregs (figure 5.5C; right) compared to healthy omentum. However the numbers of these cells tended to reduce in omentum from Met/NACT patients (figure 5.5B-C). Additionally, the presence of Tregs in metastatic

omentum was further established by immunofluorescence staining, which confirmed the localisation of these cells within the omental FALCs (figure 5.5D). The production of IFN-γ, and IL-13, as well as expression of co-inhibitory molecule PD1 by T cell subsets was next investigated following *ex vivo* stimulation of cells isolated from human omentum (figure 5.6A-C). Compared to healthy tissue, omentum from Met/NT patients tended to have lower proportions of IFN-γ^+CD4 T cells and IFN-γ^+ NK cells; however the frequency of these IFN-γ producing cells was slightly higher in Met/NACT compared to Met/NT groups (figure 5.7A). Meanwhile, no statistically significant difference was observed in IFN-γ^+CD8s across all three groups (figure 5.7A). Furthermore, no significant difference was observed in the proportions of IL-13$^+$CD4 T cells between the three patient groups as shown in the appendix (figure 7.2A). However, compared to healthy omentum, the proportion of PD1-expressing CD4 T, CD8 T cells and Tregs tended to be slightly higher in the omentum of Met/NT patients, with no significant difference found between Met/NT and Met/NACT groups (figure 5.7B).

Figure 5.5: Analysis of lymphoid cell subsets in human metastatic omentum from high-grade serous ovarian cancer patients

Metastatic (and where possible healthy) omental samples were collected from patients with high-grade serous ovarian cancer (HGSOC) at City hospital, Birmingham, following informed consent according to the institutional tissue collection protocol. Samples included patients who had undergone neoadjuvant chemotherapy (NACT), as well as those who had not received treatment (NT) prior to surgery. Control samples were also supplemented via the collection of healthy omentum from the Human Biomaterials Resource Centre (HBRC). Tissues were digested to generate a single cell suspension as described in materials and methods.

The infiltration of lymphoid immune cell subsets including CD4 T, CD8 T, NK cells and Tregs, into metastatic omentum was assessed by flow cytometry and compared to healthy omental tissue. Total number of cells were normalised to weight of individual tissues and represented as number of cells per 100mg of tissue. Treg infiltration into the tissue was also confirmed by immunofluorescence staining.

Data are representative of 46 independent experiments with the following sample numbers: Healthy (n=25), Met/NT (n=11-12), Met/NACT (n=9). Bars on the graph represent the median value. Statistical significance was determined using Kruskal-Wallis followed by Dunn's multiple comparisons test. *P<0.05, **P<0.01, ***P<0.001 and ****P<0.0001.

a) Representative FACS plots showing the proportion of T cells, NK cells and Tregs between healthy (top) and metastatic human omentum (bottom). Cells have been pre-gated on FSC and SSC followed by live$CD45^+$.

b) Graph comparing the adjusted number of CD4 T and CD8 T cells (left to right) per 100 mg tissue, between healthy, Met/NT and Met/NACT human omentum. Met (Metastatic); NT (Not treated); NACT (Neoadjuvant Chemotherapy).

c) Graph comparing the adjusted number of NK cells and Tregs (left to right) per 100 mg tissue, between healthy, Met/NT and Met/NACT human omentum.

d) Confocal images showing staining for Tregs in representative FALCs between healthy and metastatic human omentum obtained from patients with HGSOC. CD45 (green); Foxp3 (blue); CD4 (red). Scale bar represents 50 µm. Images were taken at 40x. White arrows indicate Tregs.

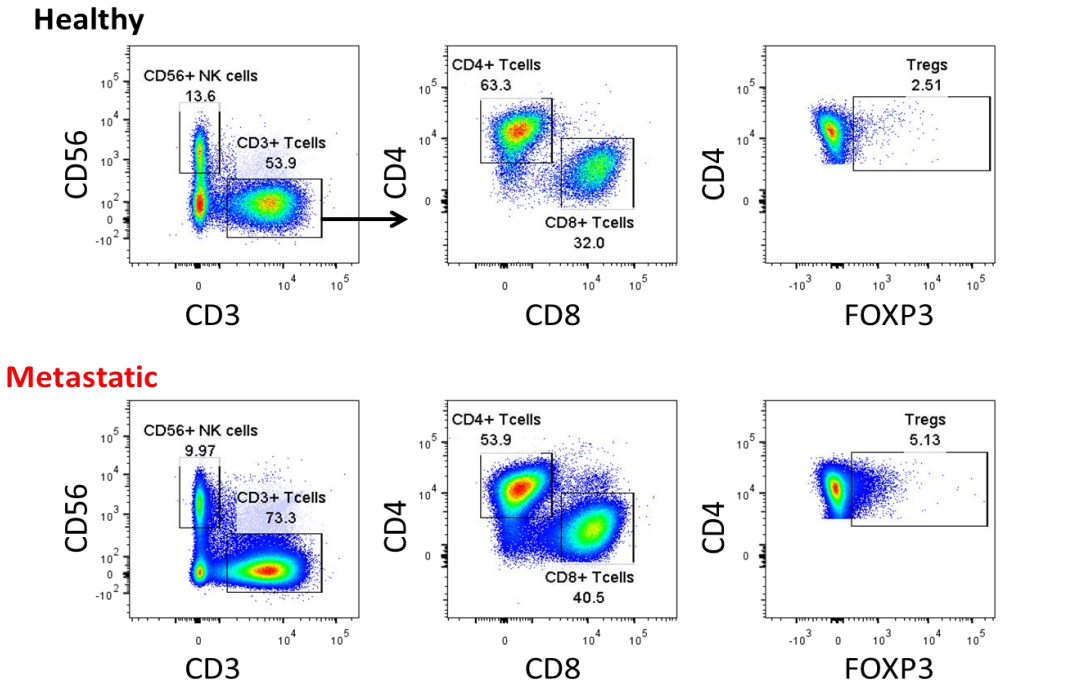
A
Healthy
CD56+ NK cells
13.6
CD3+ Tcells
53.9
CD56
CD3
CD4+ Tcells
63.3
CD8+ Tcells
32.0
CD4
CD8
Tregs
2.51
CD4
FOXP3
Metastatic
CD56+ NK cells
9.97
CD3+ Tcells
73.3
CD56
CD3
CD4+ Tcells
53.9
CD8+ Tcells
40.5
CD4
CD8
Tregs
5.13
CD4
FOXP3

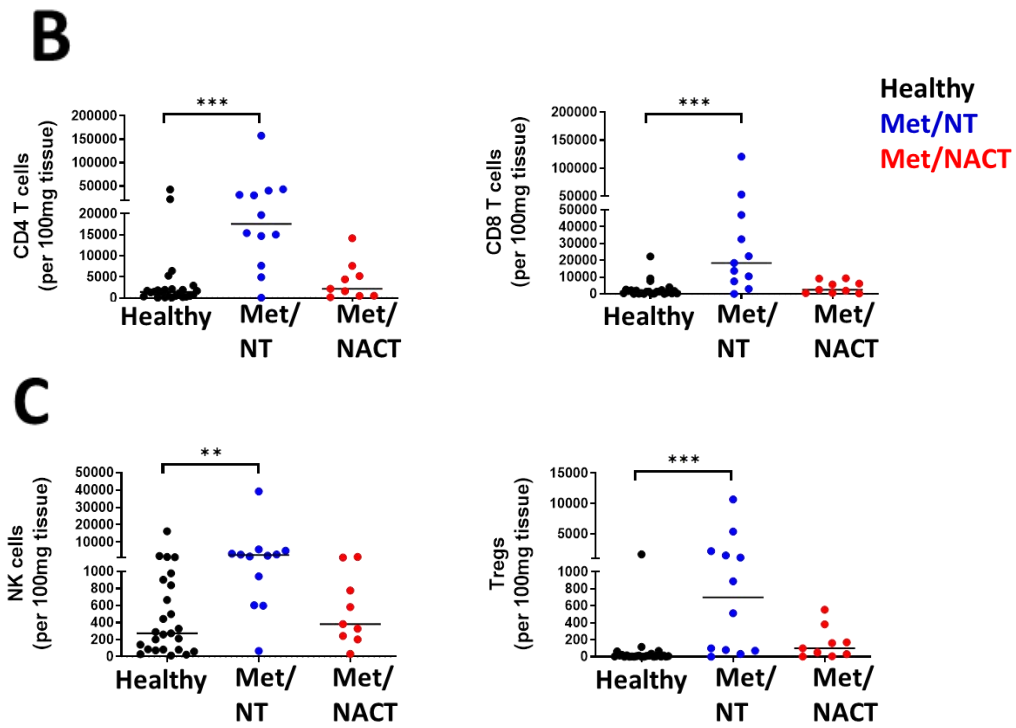
B
CD4 T cells
(per 100mg tissue)
***
Healthy
Met/
NT
Met/
NACT
CD8 T cells
(per 100mg tissue)
***
Healthy
Met/NT
Met/NACT
C
NK cells
(per 100mg tissue)
**
Tregs
(per 100mg tissue)
***

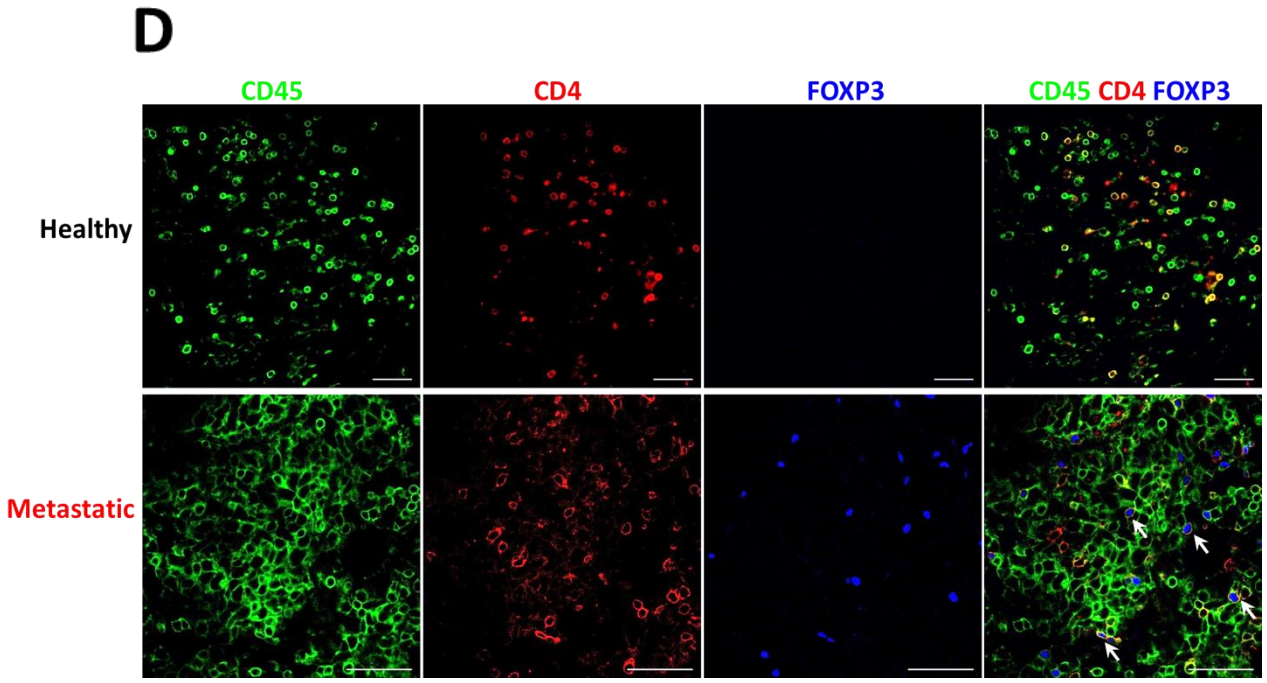

Figure 5.5

Figure 5.6: Gating strategy to identify cytokine and PD1 expression by lymphoid cell subsets in human metastatic omentum from high-grade serous ovarian cancer patients

Metastatic (and where possible healthy) omental samples were collected from patients with high-grade serous ovarian cancer (HGSOC) at City hospital, Birmingham, following informed consent according to the institutional tissue collection protocol. Samples included patients who had undergone neoadjuvant chemotherapy (NACT), as well as those who had not received treatment (NT) prior to surgery. Control samples were also supplemented via the collection of healthy omentum from the Human Biomaterials Resource Centre (HBRC). A single cell suspension was generated, and stimulated with PMA and ionomycin (P/I) as described in materials and methods, for the assessment of cytokine and PD1 expression by lymphoid subsets.

Data are representative of 38 independent experiments with the following sample numbers: Healthy (n=20), Met/NT (n=8-10), Met/NACT (n=6-8). Bars on the graph represent the median value. Statistical significance was determined using Kruskal-Wallis followed by Dunn's multiple comparisons test. *P<0.05, **P<0.01, ***P<0.001 and ****P<0.0001.

a) Representative FACS plots showing the expression of IL-13, IFNγ and PD1 by CD4 T cells, between healthy (top) and metastatic human omentum (bottom). Cells have been pre-gated on FSC and SSC followed by live$CD45^+CD56^-CD3^+$.
b) Representative FACS plots showing the expression of IFNγ and PD1 by CD8 T cells, between healthy (top) and metastatic human omentum (bottom). Cells have been pre-gated on FSC and SSC followed by live$CD45^+CD56^-CD3^+$.

c) Representative FACS plots showing the expression of IFNγ by NK cells, between healthy (top) and metastatic human omentum (bottom). Cells have been pre-gated on FSC and SSC followed by live$CD45^+$.

d) Representative FACS plots showing the expression of PD1 by Tregs, between healthy (top) and metastatic human omentum (bottom). Cells have been pre-gated on FSC and SSC followed by live$CD45^+CD3^-CD56^+CD8^-CD4^+$.

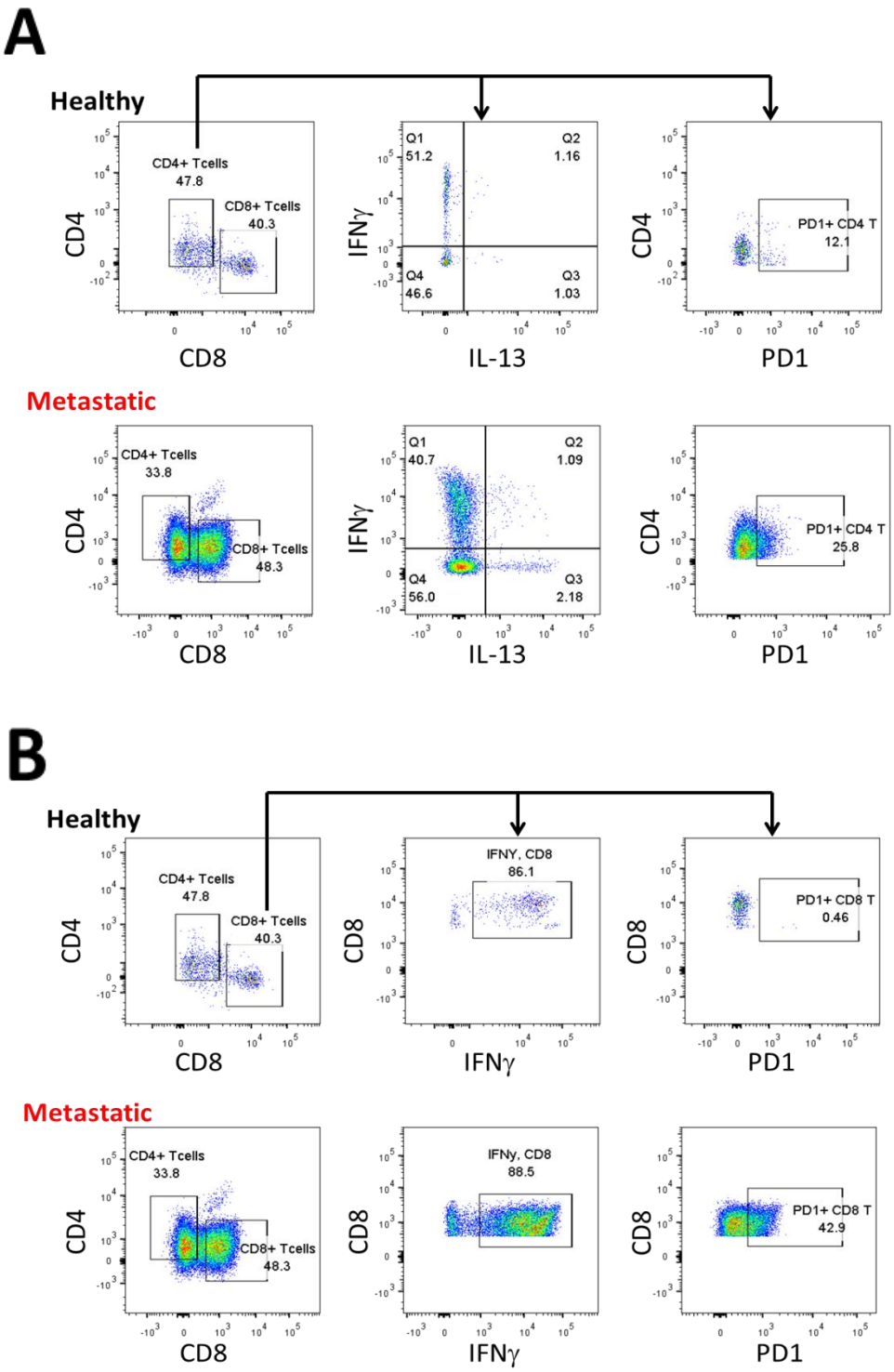
A
Healthy
CD4+ Tcells
47.8
CD8+ Tcells
40.3
CD4
CD8
Q1
51.2
Q2
1.16
Q4
46.6
Q3
1.03
IFNγ
IL-13
CD4
PD1+ CD4 T
12.1
PD1
Metastatic
CD4+ Tcells
33.8
CD8+ Tcells
48.3
CD4
CD8
Q1
40.7
Q2
1.09
Q4
56.0
Q3
2.18
IFNγ
IL-13
CD4
PD1+ CD4 T
25.8
PD1
B
Healthy
CD4+ Tcells
47.8
CD8+ Tcells
40.3
CD4
CD8
IFNY, CD8
86.1
CD8
IFNγ
CD8
PD1+ CD8 T
0.46
PD1
Metastatic
CD4+ Tcells
33.8
CD8+ Tcells
48.3
CD4
CD8
IFNy, CD8
88.5
CD8
IFNγ
CD8
PD1+ CD8 T
42.9
PD1

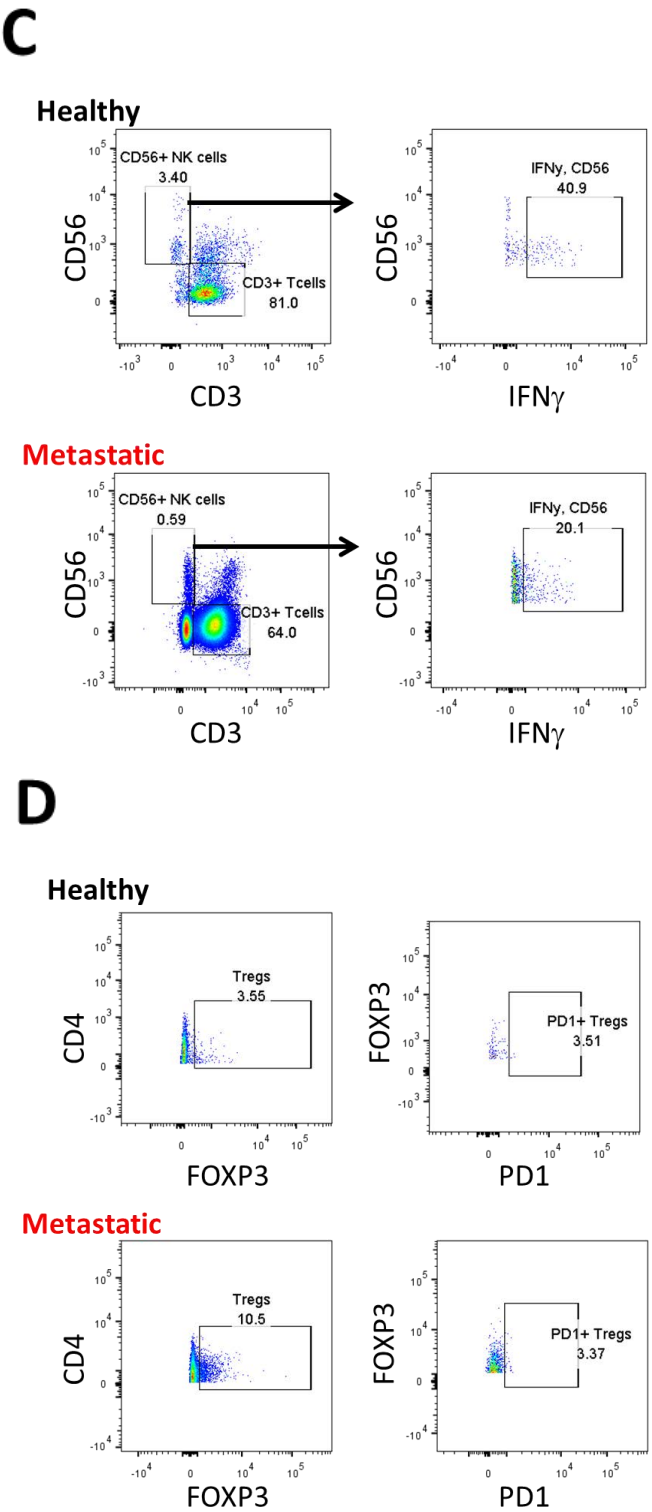
C
Healthy
CD56+ NK cells
3.40
CD3+ Tcells
81.0
CD56
CD3
IFNy, CD56
40.9
CD56
IFNγ
Metastatic
CD56+ NK cells
0.59
CD3+ Tcells
64.0
CD56
CD3
IFNy, CD56
20.1
CD56
IFNγ
D
Healthy
Tregs
3.55
CD4
FOXP3
PD1+ Tregs
3.51
FOXP3
PD1
Metastatic
Tregs
10.5
CD4
FOXP3
PD1+ Tregs
3.37
FOXP3
PD1

Figure 5.6

Figure 5.7: Assessing the cytokine production and PD1 expression of lymphoid cell subsets in human metastatic omentum from high-grade serous ovarian cancer patients

Metastatic (and where possible healthy) omental samples were collected from patients with high-grade serous ovarian cancer (HGSOC) at City hospital, Birmingham, following informed consent according to the institutional tissue collection protocol. Samples included patients who had undergone neoadjuvant chemotherapy (NACT), as well as those who had not received treatment (NT) prior to surgery. Control samples were also supplemented via the collection of healthy omentum from the Human Biomaterials Resource Centre (HBRC). A single cell suspension was generated, and stimulated with PMA and ionomycin (P/I) as described in materials and methods.

The difference in IFN-γ production as well as expression of co-inhibitory molecule PD1, by lymphoid immune cell subsets between healthy and metastatic human omentum was analysed by flow cytometry.

Data are representative of 38 independent experiments with the following sample numbers: Healthy (n=20), Met/NT (n=8-10), Met/NACT (n=6-8). Bars on the graph represent the median value. Statistical significance was determined using Kruskal-Wallis followed by Dunn's multiple comparisons test. *P<0.05, **P<0.01, ***P<0.001 and ****P<0.0001.

a) Graph comparing the percentage of IFNγ^+ CD4 T, CD8 T, and NK cells (left to right), between healthy, Met/NT and Met/NACT human omentum. Met (Metastatic); NT (Not treated); NACT (Neoadjuvant Chemotherapy).
b) Graph comparing the percentage of PD1$^+$ CD4 T, CD8 T and Tregs (left to right) between healthy, Met/NT and Met/NACT human omentum.

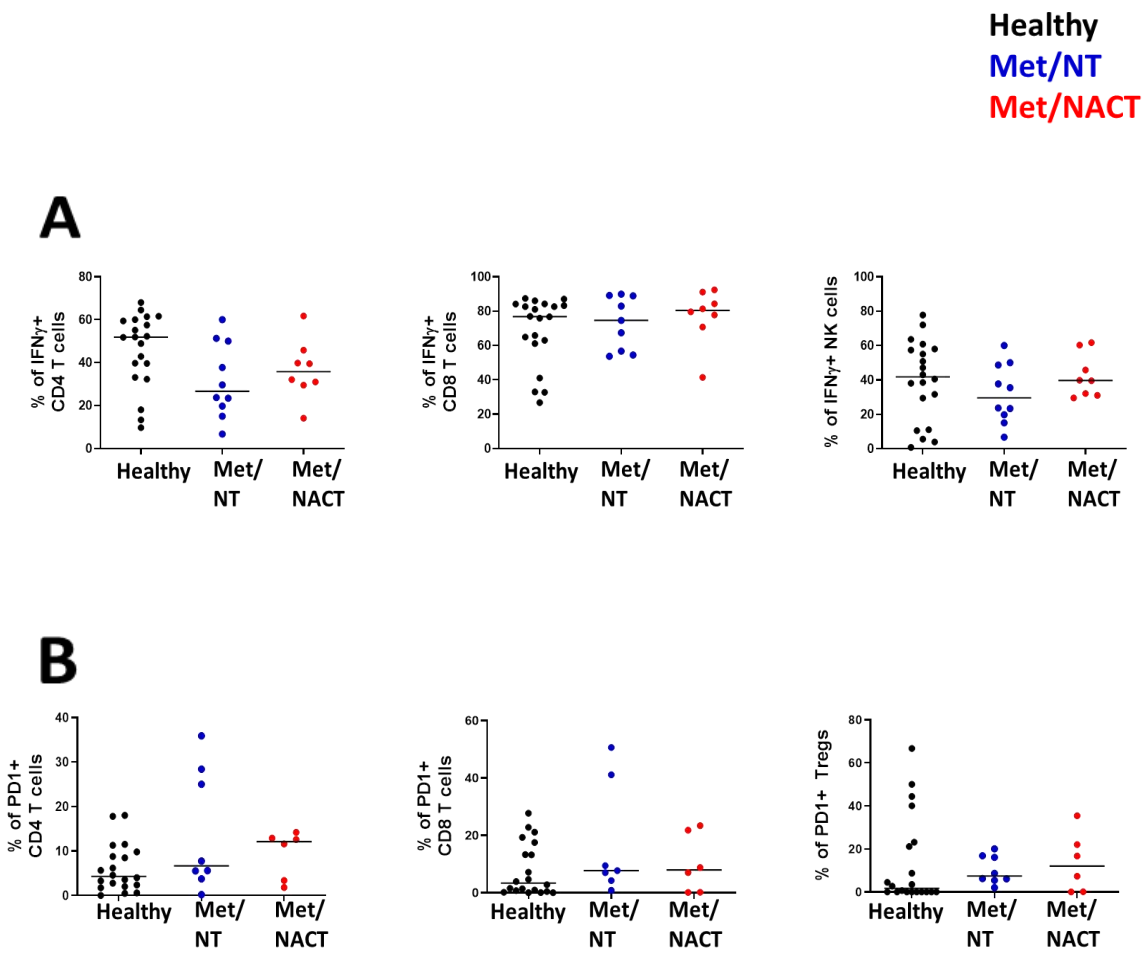
Healthy
Met/NT
Met/NACT
A
% of IFNγ+ CD4 T cells
% of IFNγ+ CD8 T cells
% of IFNγ+ NK cells
Healthy
Met/ NT
Met/ NACT
B
% of PD1+ CD4 T cells
% of PD1+ CD8 T cells
% of PD1+ Tregs

Figure 5.7

In adipose tissues, CD11c has been reported as a marker for macrophages with a pro-inflammatory, M1 phenotype (Cho et al., 2014), while CD206 is a common maker expressed by TAMs (M2 phenotype) (Balkwill et al., 2012). Using these two markers, the infiltration of macrophage subsets was also assessed. Furthermore a third macrophage subset emerged ($CD206^{+}CD11c^{+}$ denoted as M1/M2), which appeared to be enriched in metastatic omentum (figure 5.8A). Omentum from Met/NT patients contained significantly higher normalised numbers of M1 and M1/M2 subsets, with an increasing trend of M2s, compared to healthy omentum (figure 5.8B). However a significant reduction in the numbers of these macrophage subsets was observed in Met/NACT omentum compared to Met/NT groups (figure 5.8B). Finally, when expression of the PD1 ligand, PDL1 by the individual macrophage subsets was assessed (figure 5.9A), the proportion of $PDL1^{+}$M1 macrophages was significantly higher in the omentum of Met/NT patients compared to healthy omentum (figure 5.9B); similarly $PDL1^{+}$M2 and $PDL1^{+}$M1/M2 subsets also tended to be higher in the omentum of Met/NT patients (figure 5.9B). Although more patient samples will be needed to confirm this, omentum from Met/NACT groups began to show a reduced trend in the proportions of all three $PDL1^{+}$ macrophage subsets compared to omentum from Met/NT groups (figure 5.9B).

Figure 5.8: Analysis of macrophage subsets in human metastatic omentum from high-grade serous ovarian cancer patients

Metastatic (and where possible healthy) omental samples were collected from patients with high-grade serous ovarian cancer (HGSOC) at City hospital, Birmingham, following informed consent according to the institutional tissue collection protocol. Samples included patients who had undergone neoadjuvant chemotherapy (NACT), as well as those who had not received treatment (NT) prior to surgery. Control samples were also supplemented via the collection of healthy omentum from the Human Biomaterials Resource Centre (HBRC). Tissues were digested to generate a single cell suspension as described in materials and methods.

The infiltration of macrophages including $CD11c^+$ (M1), $CD206^+$ (M2), $CD11C^+CD206^+$ (M1/M2) subsets into metastatic omentum was assessed by flow cytometry and compared to healthy omental tissue. Total number of cells were normalised to weight of individual tissues and represented as number of cells per 100mg of tissue.

Data are representative of 50 independent experiments with the following sample numbers: Healthy (n=28), Met/NT (n=12), Met/NACT (n=10). Bars on the graph represent the median value. Statistical significance was determined using Kruskal-Wallis followed by Dunn's multiple comparisons test. *P<0.05, **P<0.01, ***P<0.001 and ****P<0.0001.

a) Representative FACS plots showing the proportion of $CD11c^+$ (M1), $CD206^+$ (M2), $CD11C^+CD206^+$ (M1/M2) macrophage subsets, between healthy (top) and metastatic human omentum (bottom). Cells have been pre-gated on FSC and SSC followed by $liveCD45^+Lin^-HLADR^+$. Lineage (Lin) gate included CD3, CD19 and CD56.

b) Graph comparing the adjusted number of $CD11c^+$ (M1; top left), $CD206^+$ (M2; top right), $CD11c^+CD206^+$ (M1/M2; bottom) macrophage subsets per 100 mg tissue, between healthy, Met/NT and Met/NACT omentum. Met (Metastatic); NT (Not treated); NACT (Neoadjuvant Chemotherapy).

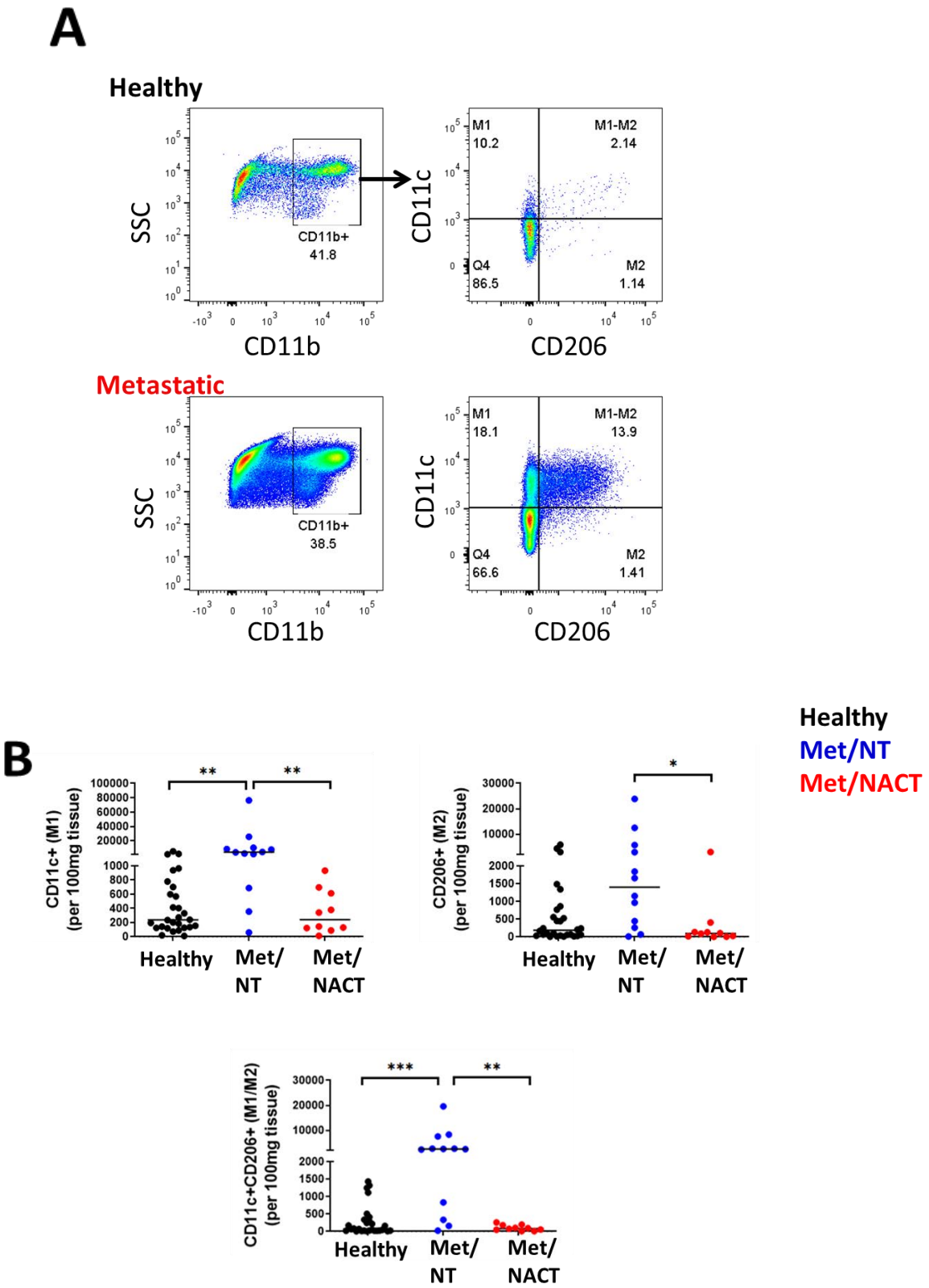
A
Healthy
SSC
CD11b
CD11b+
41.8
CD11c
CD206
M1
10.2
M1-M2
2.14
Q4
86.5
M2
1.14
Metastatic
CD11b+
38.5
M1
18.1
M1-M2
13.9
Q4
66.6
M2
1.41
B
Healthy
Met/NT
Met/NACT
CD11c+ (M1)
(per 100mg tissue)
CD206+ (M2)
(per 100mg tissue)
CD11c+CD206+ (M1/M2)
(per 100mg tissue)
Healthy
Met/
NT
Met/
NACT

Figure 5.8

Figure 5.9: Assessing PDL1 expression by macrophage subsets in human metastatic omentum from high-grade serous ovarian cancer patients

Metastatic (and where possible healthy) omental samples were collected from patients with high-grade serous ovarian cancer (HGSOC) at City hospital, Birmingham, following informed consent according to the institutional tissue collection protocol. Samples included patients who had undergone neoadjuvant chemotherapy (NACT), as well as those who had not received treatment (NT) prior to surgery. Control samples were also supplemented via the collection of healthy omentum from the Human Biomaterials Resource Centre (HBRC). Tissues were digested to generate a single cell suspension as described in materials and methods.

The difference in expression of the co-inhibitory molecule, PDL1 by macrophage subsets between healthy and metastatic human omentum was analysed by flow cytometry.

Data are representative of 25 independent experiments with the following sample numbers: Healthy (n=19), Met/NT (n=4), Met/NACT (n=2). Bars on the graph represent the median value. Statistical significance was determined using Kruskal-Wallis followed by Dunn's multiple comparisons test. *P<0.05, **P<0.01, ***P<0.001 and ****P<0.0001. Lineage (Lin) gate included CD3, CD19, CD56.

a) Representative FACS plots showing the expression of PDL1 by $CD11c^+$ (M1), $CD206^+$ (M2), $CD11C^+CD206^+$ (M1/M2) macrophage subsets, between healthy (top) and metastatic human omentum (bottom). Cells have been pre-gated on FSC and SSC followed by $liveCD45^+Lin^-HLADR^+CD11b^+$.

b) Graph comparing the percentage of PDL1^{+} M1, M2, and M1/M2 macrophage subsets (left to right), between healthy, Met/NT and Met/NACT human omentum. Met (Metastatic); NT (Not treated); NACT (Neoadjuvant Chemotherapy).

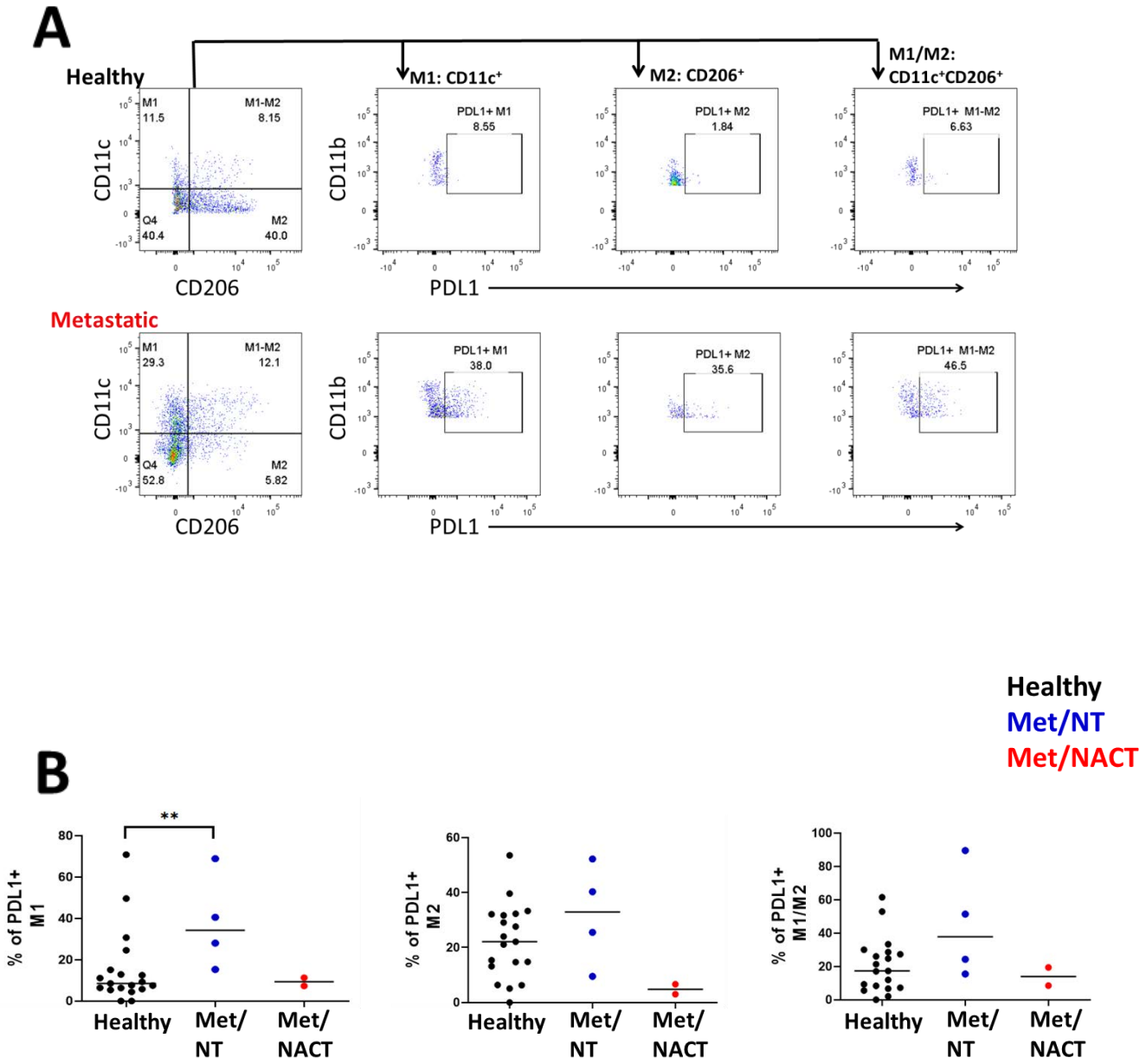
A
Healthy
M1: CD11c+
M2: CD206+
M1/M2:
CD11c+CD206+
M1
11.5
M1-M2
8.15
Q4
40.4
M2
40.0
CD11c
CD206
CD11b
PDL1+ M1
8.55
PDL1+ M2
1.84
PDL1+ M1-M2
6.63
PDL1
Metastatic
M1
29.3
M1-M2
12.1
Q4
52.8
M2
5.82
PDL1+ M1
38.0
PDL1+ M2
35.6
PDL1+ M1-M2
46.5
Healthy
Met/NT
Met/NACT
B
**
% of PDL1+ M1
% of PDL1+ M2
% of PDL1+ M1/M2
Healthy
Met/ NT
Met/ NACT

Figure 5.9

5.4 Summary

5.4.1 The immune landscape of metastatic tumours in visceral adipose tissues

Using the syngeneic MC38 colon tumour model which represents a metastatic grade III adenocarcinoma (Corbett et al., 1975), ip injection of PBS/MC38 cancer cells was shown to result in the localisation of tumours to omental and mesenteric FALCs. In a similar study, Shi and colleagues equally found that ip inoculation of C57BL/6J mice with MC38 resulted in the development of peritoneal carcinomatosis (i.e. the metastasis and deposition of colon cancer tumours to the peritoneal surface (McMullen et al., 2017)) within VATs, including the omentum, mesenteries and epididymal (gonadal) fat by day 15 post injection. Furthermore, tumour lesions were restricted to these ATs, owing to their absence in other visceral organs such as liver, spleen, kidney and lungs, even at later time-points in tumour development (Shi et al., 2019). Therefore together with our study, this confirms the preferential homing of such tumours to VATs, and further reveals this migration to be a rapid process that can occur as early as 10 days after inoculation as our study describes.

In contrast, reduced tumour burden – and in some cases, no tumours at all - was observed in the zymosan/MC38 groups. Zymosan is an insoluble polysaccharide found on the cell wall of yeast species, *Saccharomyces cerevisiae*, and contains β-1,3-glucan and mannan residues (Underhill, 2003). Importantly, zymosan activates the immune system through its recognition and phagocytosis by innate immune cells such as neutrophils, macrophages, monocytes and DCs, but can also elicit inflammatory responses mediated largely via the binding of zymosan particles to TLR2 and TLR6 (Frasnelli et al., 2005). These initial observations thereby suggested that the activation of immune cells in the peritoneal cavity by zymosan was sufficient to reduce metastatic tumour formation considerably. In a study

by Taghavi and colleagues, zymosan treatment was similarly found to result in a significant reduction in tumour weight in mice inoculated with the B16F10 melanoma cell line, compared to untreated groups (Taghavi et al., 2018), highlighting that zymosan may be able to attenuate tumour development across different cancer types. However, it was unclear whether zymosan could result in complete abolition of tumours in B16F10-innoculated mice as was observed in our study with MC38, thereby suggesting that the tumouricidal effects of this PAMP may be more lethal in certain cancers compared to others.

Upon analysis of immune cell recruitment, a notable difference in the frequency of Tregs between PBS/MC38 and zymosan/MC38 groups was observed, with PBS/MC38 mice displaying considerably more infiltrating Tregs in both mesenteric and omental FALCs. Tregs are well known to promote cancer progression through their production of suppressive cytokines IL-10, TGF-β and expression of co-inhibitory molecules such as CTLA4 that function to suppress anti-tumour activity (Chaudhary and Elkord, 2016). Given the fact that one of the tumour escape mechanisms initiated in MC38 tumour model is the expansion of immunosuppressive cells, in particular Tregs (Efremova et al., 2018), this suggests that the marked increase in Tregs observed in our study would facilitate the skewing of the FALC microenvironment by tumour cells to a more suppressive phenotype. Consistent with this notion, IL-33 was also observed to translocate to the cytoplasm of FALC stromal cells in PBS/MC38 but not zymosan/MC38 mice. During tissue injury or necrosis IL-33 can function as an alarmin; in this process IL-33 is excreted from the nucleus into the extracellular space where it can interact with ST2-expressing target cells, thereby inducing robust Th2 responses (Larsen et al., 2018). It is therefore likely that the cytoplasmic presence of IL-33 observed in PBS/MC38 mice resulted from tumour-induced tissue damage; in this scenario, IL-33 is likely

to cause the proliferation and activation of IL-33 responsive cells, including Tregs, further amplifying immunosuppression. Indeed, injection of MC38 into IL-33 transgenic mice has been reported to promote the proliferation of colon tumour cells by signalling through ST2 (Li et al., 2018). Meanwhile in $APC^{min/+}$ model of CRC (colorectal cancer), IL-33 led to the preferential proliferation and survival of an intra-tumour subset of $KLRG1^{+}GATA3^{+}$ Tregs (Meinicke et al., 2017). Other IL-33 responsive cells exists within VAT FALCs, a key one being ILC2s, which as discussed in previous chapters produce Th2 cytokines including IL-4/5/10/13 when activated (Molofsky et al., 2015). Such cytokines are generally known to facilitate tumour growth (Balkwill et al., 2012), and are capable of activating TAMs which promote almost all aspects of tumour progression (Bolli et al., 2017, Kiss et al., 2018). Furthermore, macrophages through their expression of ST2 can directly respond to IL-33, resulting in polarisation towards an M2 tumour promoting phenotype (Yang et al., 2013b). Notably, previous studies also using the MC38 murine model, showed that IL-33 facilitated macrophage recruitment and expression of PGE_2, leading to colon cancer stemness and enhanced tumorigenesis (Fang et al., 2017).

The reduced tumour burden observed in zymosan/MC38 mice coincided with significantly less Tregs in both VATs, but increased proportion of IFN-γ^{+}CD4 T, IFN-γ^{+}NK and to a lesser extent IFN-γ^{+}iNKT cells particularly within the omentum. The inflammatory response to zymosan is mainly orchestrated by TLR2 and TLR6 that function as a TLR2/TLR6 heterodimer (Underhill and Ozinsky, 2002). Upon ligand binding, nuclear factor kappa-B (NF-κB) is activated, resulting in the production of IL-1/6/8/18 and TNFα (Frasnelli et al., 2005, Underhill, 2003). Furthermore, Dectin-1, which recognises the β-glucan residues of zymosan has been reported to collaborate with TLR2 on macrophages and DCs, to enhance NF-κB

activation and mediate the production of IL-12 as well as TNFα (Gantner et al., 2003). IL-12 facilitates the recruitment and effector functions of NK cells, including the production of IFN-γ, which is further enhanced by cytokines including TNFα, IL-1 and IL-18 (Chaix et al., 2008, Paul and Lal, 2017), and in synergy with IL-33, IL-12 can induce IFN-γ production by iNKT cells (Reilly et al., 2010). It is therefore plausible that such zymosan-induced mechanisms could have resulted in IFN-γ production by NK and iNKTs observed within VATs of zymosan/MC38 mice; future experiments could confirm this by measuring levels of TNFα and IL-12 following zymosan injection. In agreement, the mesenteries and omentum of zymosan/MC38 mice were significantly infiltrated by macrophages, monocytes and neutrophils compared to PBS control; however the number of these zymosan targets were comparable between PBS/MC38 and zymosan/MC38 mice, which alluded to a possible difference in phenotype of these immune cells. As is widely recognised, macrophages can exist as distinct states; in its most simplistic form, classically activated macrophages (M1) respond to IFN-γ and LPS, to secret pro-inflammatory cytokines IL-6/12/ and TNF, while AAM (M2) secret anti-inflammatory cytokines such as IL-10, in response to IL-4 or IL-13 (Mantovani et al., 2004). While the former are associated with anti-tumour responses, macrophages with a M2-like phenotype often referred to as TAMs, support tumour development (Balkwill et al., 2012). Nonetheless, it is worth noting, that macrophage plasticity is becoming increasingly evident, with multiple 'shades' of macrophages observed to exist along a spectrum of M1-M2 phenotypes depending on their environmental cues and subsequent functions (Mantovani et al., 2004, Mosser and Edwards, 2008). Indeed early studies indicated that tumour infiltrating macrophages supported the growth and angiogenesis of colon tumours via the secretion of VEGF (Barbera-Guillem et al., 2002), while the presence of $CD68^+$ macrophages at the

tumour front correlated positively with patient prognosis and survival (Forssell et al., 2007). Similarly - though more controversial - neutrophils in the TME (or TANs) have been suggested to exhibit anti-tumor (N1) and pro-tumour (N2) properties (Fridlender et al., 2009). N1 neutrophils mediate anti-tumor and anti-metastatic activity via antibody-mediated cytotoxicity and activation of innate and adaptive immune responses, while N2 neutrophils promote tumour growth, dissemination, and metastasis via secretion of proangiogenic factors and ECM remodelling enzymes (Masucci et al., 2019). Taken together, it is likely that macrophages and neutrophils in zymosan/MC38 and PBS/MC38 mice are phenotypically and functionally different, possibly representing anti- and pro-tumour characteristics, respectively, as such further experiments should aim to address this hypothesis. Eosinophils are reported to constitute an abundant population within the TME, however, their contribution to tumour development is cancer dependent; in cervical cancer and Hodgkin's lymphoma eosinophil infiltration is associated with poor prognosis, however in gastric, oral, prostrate, breast and colon cancer they appear to have an anti-tumorigenic role (Varricchi et al., 2017). Within this study, a significantly higher number of eosinophils were observed in PBS/MC38 mice compared to PBS control groups, particularly in the omentum. Similar findings were reported by Arnold and colleagues who noted the considerable and early infiltration of eosinophils in the TME of C57BL/6J mice following MC38 inoculation. Interestingly, eosinophil depletion led to the formation of larger and heavier tumours at later points, indicating that the growth of MC38 tumours were dependent on the frequency of tumour infiltrating eosinophils (Arnold et al., 2020). Indeed previous studies *in vitro* have shown that eosinophils can induce the killing of Colo-205, a human colon cancer cell line; this was mediated by IL-18 which not only promoted

eosinophil-mediated cytotoxicity, but also enhanced the cell-to-cell contact between effector and tumour targets cells (Gatault et al., 2015). In the clinical setting, eosinophil infiltration in the stromal tissue is a favourable prognostic factor, with high tumour-stromal eosinophil score linked to reduced risk of all-cause and colon cancer deaths (Prizment et al., 2016). Therefore while this study shows that VATs can also be sites of eosinophil recruitment during MC38-induced colon cancer, the fact that tumours persisted within VAT FALCs even in the presence of such infiltrating eosinophils, could suggest that the abundance of other tumour promoting cells including Tregs and macrophages may dominate FALCs sufficiently enough to outcompete any anti-tumour activity of recruited eosinophils.

This project further analysed omental samples from patients with HGSOC – another cancer that commonly metastasise to the peritoneal cavity. Metastatic omentum of patients who had received no treatment (NT) prior to primary debulking surgery were abundantly infiltrated by CD4, CD8 T cells as well as NK cells, compared to healthy omentum or tissue isolated from NACT patients. Multiple studies have reported that the presence of TILs, including their number, type and location influences prognosis in several tumours (Galon et al., 2006, Galon et al., 2007, Hwang et al., 2012, Leffers et al., 2009). In ovarian cancer, intraepithelial $CD3^+$ and $CD8^+$ TILs were shown to be associated with favourable prognosis; $CD8^+$ TILs in particular were found to be more robust in predicting disease outcome (Hwang et al., 2012) and in addition with high CD8/Treg ratio, was also associated with improved survival (Sato et al., 2005). The prognostic influence of TILs in the omental metastases of patients with advanced stage ovarian cancer is also reported, with high numbers of $CD45RO^+$ memory T cells associated with increased survival (Leffers et al., 2009).

A considerable number of Tregs as well as three macrophage subsets: CD11c$^+$ (M1); CD206$^+$ (M2) and CD11c$^+$CD206$^+$ (M1/M2) was also observed in metastatic omentum of NT patients within our study. Treg accumulation has been demonstrated to be associated with poor overall as well as progression-free survival in ovarian cancer (Curiel et al., 2004, Wolf et al., 2005). Others have also reported of the abundance of CD25$^+$Foxp3$^+$Tregs in human omental metastases (as well as in primary ovarian tumours) compared to the peripheral blood, suggesting a preference for these suppressive cells in primary and secondary tumour sites (Kovacsovics-Bankowski et al., 2014). In the ovarian TME, macrophages (TAMs) are a major population of immune cells; however their behaviour can be shaped by their bidirectional interactions with the TME, resulting in either anti-tumorigenic M1-like or pro-tumorigenic M2-like phenotypes (Balkwill et al., 2012, Nowak and Klink, 2020). Furthermore, intra-tumoural TAM density is reported to increase with increasing ovarian cancer staging/grade, with the dominant TAM phenotype often determining patient prognosis (Zhang et al., 2014). As such patients with higher intra-islet and overall M1/M2 ratios are reported to have improved prognosis, longer overall survival as well as progression-free survival (Macciò et al., 2020, Zhang et al., 2014), highlighting the importance of M1 infiltration in driving a better disease outcome. Though our study observed increased numbers of M1 within the omentum of NT patients, assessment of PDL1 expression revealed that PDL1$^+$ M1 subsets were significantly higher in metastatic omentum compared to healthy tissue, further highlighting the omentum as a site of macrophage polarisation to more suppressive phenotypes by tumour cells. In line with this, metastatic omentum of NT patients also presented with increased M2 macrophages as well as an intermediate population that co-expressed CD11c and CD206, referred to as M1/M2. In addition, a recent study also revealed

that tissue-resident omental macrophages were required for the metastatic spread of ovarian cancer (Etzerodt et al., 2020). Using the ID8 murine model, cancer cells were observed to localise to FALCs and were in close association to a subset of $CD163^{+}Tim4^{+}$ expressing omental macrophages. Specific deletion of $CD163^{+}Tim4^{+}$ macrophages was enough to inhibit tumour progression, thereby confirming the role of tissue-resident macrophages in ovarian cancer invasiveness and in contributing to the role of the omentum as a pre-metastatic niche for such cancers (Etzerodt et al., 2020). Furthermore, Tregs and macrophages can inhibit the proliferation of other effector cells, alter their phenotype, but also induce suppressive activity within those cells (Ou et al., 2018). For example, the release of TGF-β and IL-10 can act directly on NK cells to reduce its cytotoxic functions, but also convert them into a pro-angiogenic phenotype that promotes metastatic spread (López-Soto et al., 2017). Interestingly our data detected reduced proportions of IFN-γ^{+} CD4 T and NK cells within the omentum of NT patients compared to healthy controls, suggestive of a poorly activated, anergic phenotype (Fridman et al., 2012). Similar observations were shown by Platonova and colleagues who found that in non-small cell lung cancer, intra-tumoural NK cells had reduced expression of a number of NK cell surface receptors leading to their inability to secret IFN-γ and stimulate degranulation (Platonova et al., 2011). It would therefore be useful for future work to asses receptor expression as well as other functional assays of NK cells isolated from metastatic omentum of ovarian cancer patients; notably tumour-associated NK cells from ovarian cancer patients are also shown by others to have reduced levels of activating receptors including DNAM-1, 2B4 and CD16, resulting in poor NK cell activation and targeting of tumour cells (Carlsten et al., 2009). Therefore such functional

defects appearing in metastatic sites would suggest their involvement in supporting omental metastasis.

Finally, CD4 T, CD8 T cells and Tregs in metastatic omentum from NT patients also expressed PD1, though this was highly variable, with some patients showing greater proportions of $PD1^+$ T cells compared to others, highlighting the heterogeneity between (and within) patients that can be observed during ovarian cancer (Kossaï et al., 2018). However, NACT was shown to result in a significant reduction in infiltration of Tregs as well as M1, M2 and M1/M2 subsets, in line with the notion that anti-tumour effects of chemotherapy can occur through a number of mechanisms, one being the depletion of immunosuppressive cells (Cubas et al., 2018). Taken together, these data therefore depict that the VAT FALC microenvironment which supports tumour metastases appears to be facilitated by the predominant anti-inflammatory milieu that is likely hijacked and augmented by tumour cells. Nonetheless, further questions remain to be addressed. In both the MC38 murine tumour model, as well as during HGSOC, Tregs were observed to accumulate in metastatic VATs, however the mechanism of such Treg infiltration was not investigated. Future studies could measure Treg proliferation through the expression of proliferative markers such as Ki67 as assessed in chapter 4.3. Alternatively, given the array of chemokine receptors expressed by Tregs, chemokine gradients may be involved. For instance, CCL28/ CCR10 axis induced as a result of tumour hypoxia is reported to promote Treg recruitment in ovarian cancer (Koyama and Nishikawa, 2021). Therefore, changes in gene expression of several chemokines expressed by tumour and stromal cells within metastatic VATs could be analysed by quantitative PCR (qPCR) or RNA sequencing, with protein confirmation via ELISA and/or immunohistochemistry. Upregulation of cognate receptors on Tregs within metastatic VATs

compared to control tissue (or zymosan treated mice in the case of MC38 tumour model) could then be analysed by flow cytometry. Such approaches may not only reveal useful therapeutic targets for controlling Treg accumulation during metastasis, but may also reveal other chemokines involved in promoting the immunosuppressive microenvironment observed within metastatic VATs. Conversely the inflammatory phenotype observed in zymosan/MC38-treated mice, as well as in Met/NACT patients during HGSOC involved NK and CD4 T cell activation as assessed by IFN-γ production. To further evaluate the functional role of these cells, killing assays could be conducted that test cytolytic activity. For example, by culturing tumour cells with NK cells isolated from both PBS/MC38 and zymosan/MC38 mice *in vitro*, tumour cells lysis and percentage of surviving cells between both groups could be measured. To supplement this, additional experiments could deplete NK cells *in vivo,* before the inoculation of mice with MC38 in the presence or absence of zymosan. Collectively these studies would be useful in understanding whether NK cells are involved in direct killing of tumour cells in this model, thereby suggesting that the reduction in tumour metastases observed may be the result of anti-tumour responses.

CHAPTER 6: DISCUSSION

AT is recognised as a metabolically dynamic organ that coordinates both physiological and metabolic roles. Primarily it functions to store fat and excess energy, but beyond this it also acts as an endocrine organ to produce a diverse array of biologically active compounds involved in maintaining tissue homeostasis (Coelho et al., 2013). Notably such metabolic functions are mediated mainly by WAT, and have been reported by a number of studies which also highlight the important role of immune cells within this tissue (Brestoff et al., 2015, Lee et al., 2015, Molofsky et al., 2013). WAT can be further divided based on its anatomical location, giving rise to subcutaneous and VATs. VATs are found particularly within the peritoneal cavity including the mesenteries, omentum (Lai and Leung, 2010, Ibrahim, 2010), and gonadal fat (Bjørndal et al., 2011). Such VATs have now been established to contain vascularised structures of innate and adaptive immune cells, as well as stromal cells – i.e. FALCs, which support localised immune responses against infection and inflammation within the peritoneal but also pleural cavities (Bénézech et al., 2015, Han et al., 2017, Jackson-Jones et al., 2016). Interestingly, FALCs appear to be a double-edged sword in other diseases. During cancer metastasis, in particular advanced stages of ovarian, colon and gastric cancers, these clusters become preferential sites for the localisation of metastatic tumours within the peritoneal cavity (Desai and Moustarah, 2020, Gerber et al., 2006). As such this project set out to investigate these opposing roles of VAT FALCs using *in vivo* models of helminth infection, and tumour metastasis as well as via the analysis of human metastatic samples from HGSOC.

To achieve these goals, the project began by characterising the immune cell composition within VATs during homeostasis. Initial enumeration of FALCs confirmed the heterogeneous presence of these clusters across the omentum, mesenteries and gonadal fat, with the latter

having the least number of FALCs as shown by others (Bénézech et al., 2015). As such, the mesenteries and omentum were the main focus of future experiments. One of the most notable observations was the predisposition of these tissues towards a type 2 milieu particularly within the omentum, owing to the enrichment of macrophages, CD4 T cells, B cells, iNKTs, $ST2^-$ and $ST2^+$ Tregs as well as cDC2s. Additionally, analysis of chemokine receptors governing the tissue distribution of ILC2s revealed the significant expression of CCR8 on VAT ILC2s compared to those isolated from mLN. Though CCR8 signalling is important during skin homing of Th2 cells and Tregs (Soler et al., 2006) and together with cognate ligands CCL1 and CCL8 is involved in the pathogenesis of type 2 related inflammatory diseases such as atopic dermatitis and asthma (Islam et al., 2011, Mikhak et al., 2009), CCR8 expression on mouse and human ILC2s have also been reported. Interestingly, analysis of genes preferentially expressed by ILC subsets across different vertebrate species revealed a number of conserved transcriptomic signatures for ILC2s one of them being *Ccr8* (Vivier et al., 2016), thereby suggesting the importance of this receptor in the regulation of ILC2 biology. Indeed, in the *in vitro* setting, accumulation as well as alarmin-induced ILC2 expansion and survival appears to be regulated by CCR8 (Knipfer et al., 2019). However, the observation of a $CCR8^-CCR9^-$ double negative ILC2 population, again particularly within the omentum suggested the likelihood of other chemokine receptors involved in the dynamics of VAT ILC2 distribution and as such function.

In line with the Th2 skewing of VAT FALCs, functional analysis using unperturbed Red5 reporter mice revealed the *in vivo* production of IL-5 by mesenteric and omental ILC2s and at greater proportions compared to ILC2s isolated from mLN. In response to signals from infected or injured tissues, ILC2s produce a number of cytokines including IL-4, IL-5, IL-9 and

IL-13 (Eberl et al., 2015, Artis and Spits, 2015), with IL-4, IL-5 and IL-13 involved in the protection against helminth infections as well as contributing to allergic inflammation (Fallon et al., 2006). Nonetheless, in the absence of stimuli, ILC2s were capable of producing type 2 cytokines which were involved in self renewal of B-1 cells (Moro et al., 2010). Such steady state IL-5 production therefore reveals VAT ILC2s to be primary sources of constitutive IL-5. Furthermore, *ex vivo* stimulation of ILC2s isolated from VAT FALCs led to significant production of IL-13 as well as IL-5^{+}IL-13^{+} ILC2s, thereby revealing the functional capabilities of VAT FALCs that were interrogated further during disease.

The role of VAT FALCs during helminth infection was therefore investigated using the intestinal helminths *H. poly* and *S. mansoni;* the latter was done in collaboration with the group of Andrew MacDonald at the University of Manchester who kindly carried out infections of the mice. Both of these helminths induce Th2 polarised responses (Finkelman et al., 1997), with *S. mansoni* capable of also inducing Th1 immunity (Pearce and MacDonald, 2002). Owing to previous reports that had shown the early expansion of ILC2s within the intestinal lamina propria and mLN during *H. poly* infection, that directed the differentiation of CD4 T cells towards Th2 immunity, (Pelly et al., 2016), VAT FALCs were equally analysed at early time points – day 7. In contrast, majority of analysis for *S. mansoni* infection was conducted at day 49 post infection as this was the main focus of our collaborators; nonetheless this coincided with the induction of Th2 responses which is reported to occur about 6-8 weeks during *S. mansoni* infection (Grzych et al., 1991), as such fitted with the theme of the project.

Interestingly, certain similarities were noted in immune responses within VAT FALCs between *H. poly* and *S. mansoni* infection. Firstly ILC2s were observed to undergo increased

proliferation following infection; additionally these cells displayed an activated phenotype as confirmed by CD44 and CD69 expression, as well as MHCII in *S. mansoni* infection. This thereby highlighted possible parallels in the function of ILC2s derived from VAT FALCs across these two gastrointestinal helminth infections, and also provided novel information on the induction of ILC2s by schistosomes, for which more extensive studies are reportedly required (Nausch and Mutapi, 2018). Future studies could aim to study the expansion of ILC2s at early time points following *S. mansoni* infection, given the ability of these cells to promote rapid and robust responses in other helminth infections, as seen in this project but also reported elsewhere (Hung et al., 2013, Huang et al., 2015, Pelly et al., 2016, Bouchery et al., 2019). When assessing CD4 T cell responses, while a considerable number of IL-4^{+}CD4 T cells was observed within the VATs and mLN following *H. poly* infection, Th2 responses within VATs following *S. mansoni* infection appeared to be dependent on parasitic load, with 180 cerc of parasitic larvae eliciting significantly more IL-4/5/13 production by CD4 T cells within the mesenteries and omentum compared to 40 cerc, thereby indicating that parasite-specific differences exists in VAT responses. Finally, the accumulation of ST2^{+} and ST2^{-} Tregs during *H. poly* infection, and IL-10^{+} Tregs during *S. mansoni* infection was also observed within VATs. This suggests that VAT FALCs are potential sites for the accumulation of regulatory cells that have the ability to control any immune dysregulation that may ensue from parasite-induced hyper-responsiveness, but to also mediate parasite survival as a result of immune suppression (White et al., 2020).

The role of IL-33 in contributing to VAT ILC2 and CD4 T cell responses was also assessed following *H. poly* infection. In our hands, lack of IL-33 did not appear to significantly impact ILC2 nor CD4 T responses within VAT FALCs and mLN. Previous studies showed that early

production of tissue-derived IL-33 as well as IL-25 and TSLP were reduced in mast cell deficient mice, leading to significantly impaired Th2 as well as anti-parasitic responses following *H. poly* infection (Hepworth et al., 2012). IL-25 which is expressed by intestinal epithelial cells is functionally related to IL-33 in that it is an epithelial derived cytokine that importantly drives the production of Th2-associated cytokines, and is also implicated in promoting type 2 immunity during gastrointestinal infections (Fort et al., 2001, Owyang et al., 2006). It is therefore possible that the lack of significant differences in the immune response to *H. poly* observed between IL-33 deficient and WT mice in our study could be due to compensatory mechanisms driven by other ILC2 activators. Notably, *H. poly* worm burden and faecal egg counts were shown to be elevated in mice lacking IL-25 but not those deficient in the IL-33 receptor, ST2, with IL-25 further demonstrated to be important for the expansion of ILC2s following infection (Zaiss et al., 2013). Moreover, IL-25 together with its receptor subunit IL-17RB were upregulated during primary *H. poly* infection, while in the absence of IL-25, host memory response and worm expulsion were impaired following a secondary challenge, with exogenous IL-25 restoring protective immunity (Pei et al., 2016). Collectively, these data thereby highlight the need for future experiments to define if any, the involvement of IL-25/TSLP in mediating VAT specific responses during intestinal helminth infections in the absence of IL-33.

As discussed above VAT FALCs were shown to be involved in mediating host immune responses to localised infection, however as this project has evidenced, they were also frequent sites for metastatic tumour formation including ovarian and colon cancers. *In vivo*, colon tumour cells were observed to migrate rapidly and specifically to omental and mesenteric FALCs. Lack of a basement membrane, the scarcity of mesothelial cells on milky

spots surfaces which enable tumour cell invasion, and the participation of the omentum in fluid drainage from the peritoneal cavity which increases the chance of passive attachment of tumour cells, have all been described as reasons for such preferential localisation to the omentum (Yeung et al., 2015). Furthermore *in vivo* studies using a number of ovarian cancer cell lines, revealed that milky spots/FALCs significantly enhanced the early lodging of tumour cells in peritoneal ATs with further studies confirming that conditioned medium from milky spot-containing ATs promoted tumour cell migration compared to conditioned medium from milky spot/FALC deficient tissues (Clark et al., 2013), with similar findings reported elsewhere (Etzerodt et al., 2020). This thereby suggests that other tissues that contain substantial amount of FALCs can become likely targets of tumour metastases. Indeed in our mouse model, the presence of colon tumour cells was also confirmed in the mesenteries. The cellular components of FALCs are also major players in tumour metastasis. Inoculation of mice with PBS/MC38 cancer cells induced the recruitment of Tregs and myeloid cells to omental and mesenteric FALCs. Analysis of omentum from patients with HGSOC corroborated our murine findings; similarly showing metastatic omentum from patients undergoing primary debulking surgery without any prior treatment to be heavily infiltrated by Tregs as well as macrophage subsets including $CD11c^{+}$ M1; $CD206^{+}$ M2 and double-positive M1/M2 population. Circulating monocytes can be recruited to the tumour site by different factors and differentiate into macrophage phenotypes depending on the stimuli. A recent study revealed that the ability of omental macrophages to promote the migration and colonization of ovarian cancer cells to the omentum was dependent on CCL6/23-CCR1 signalling. The chemokine ligands CCL6 and the human homolog CCL23 were reported to be significantly enriched on omental macrophages before and during tumour colonisation. The

expression of CCR1 was further shown to be associated with poorer prognosis; however, inhibition of this receptor on tumour derived tissues prevented CCL6 and CCL23 induced migration (Krishnan et al., 2020). Hybrid M1/M2 ($CD11C^{+}CD206^{+}$) macrophages have also been described in the obesity setting where they increase in obese AT and localise to crown aggregates (structures that surround necrotic adipocytes). Furthermore, hybrid M1/M2 macrophages were associated with insulin resistance, however displayed a more M1 surface phenotype (Wentworth et al., 2010). Meanwhile in renal cancer mixed CD11c/CD206 signature could be used as an independent factor in predicting patient outcome (Xu et al., 2014) suggesting a possible similar role in ovarian cancer that should be explored further. Data from our tumour model additionally revealed a possible role for IL-33 in promoting responses that may encourage cancer metastasis to FALCs, owing to the cytoplasmic presence of IL-33 in FALC stromal cells of PBS/MC38 mice. This alluded to the tumour-induced release of IL-33 and its likely impact on target cells. In human colorectal adenoma/carcinoma for example, ST2 and Foxp3 were significantly increased at the mRNA and cellular level in tumour tissues (Cui et al., 2020). Furthermore increased densities of ST2-positive cells not only correlated to Treg accumulation within the TME, but was also found to be associated with disease progression and lymph node metastasis (Cui et al., 2020), thereby supporting a role for IL-33-Treg crosstalk in promoting tumour invasion, with this project further revealing the likelihood of such crosstalk within VATs.

The analysis of metastatic omentum from patients receiving NACT revealed that this tissue was less infiltrated by Tregs and macrophage subsets compared to tissues from NT patients. Additionally, frequencies of IFN-γ^{+} CD4 T and NK cells, which had declined in metastatic omentum from NT patients, appeared to be restored in omentum from NACT patients –

though not to proportions found in healthy tissue. In our murine model, administration of zymosan prior to tumour cell inoculation similarly resulted in increased IFN-γ production by CD4 T, NK and iNKT cells within the omentum, which accompanied the reduction in tumour burden; as such, immune cells within VAT FALCs could be sources of pro-inflammatory cytokines that mediate anti-tumour immunity. Previous reports likewise showed that NACT could enhance host immune response during HGSOC, with omental biopsies from NACT responsive patients having increased Th1 genes, IFN-γ^+CD4 T cells, and fewer Tregs, compared to pre-NACT samples (Böhm et al., 2016). However, chemotherapeutic agents such as taxanes have also been reported to supress the cytotoxic functions of effector T and NK cells against ovarian cell lines *in vitro* (Chan and Yang, 2000). Interestingly, within our study, the number of CD4/8 T and NK cells tended to be lower in metastatic omentum isolated from NACT patients, thereby suggesting that the suppressive activity of chemotherapy could also occur in peripheral tissues. In support, Cubas and colleagues showed using the MC38 murine model, that the numbers of CD4 and CD8 T cells were significantly diminished in draining LNs but not in the tumour tissue following treatment with carboplatin (Cubas et al., 2018). Our study also observed that PD1$^+$ CD4/8 T cells and PD1$^+$ Tregs in metastatic omentum remained comparable between NACT and NT groups. Indeed, majority of cancer cytotoxic drugs also have the capacity to upregulate checkpoint molecules. 5-Fluorouracil used in colon cancer treatment can elevate PD-L1 expression on tumour cells (Bailly et al., 2020), while cisplatin upregulates PD-L1 expression on human ovarian cancer cell lines as well as in the *in vivo* setting (Grabosch et al., 2019). Furthermore, in the study by Bohm and colleagues, the anti-tumour effect of NACT on HGSOC was unfortunately hindered by the increased expression of immune checkpoint molecules

including PD1/L1 and CTLA4 within metastatic omental tissue (Böhm et al., 2016). Given the fact that omental metastasis has been linked to increased chemo-resistance and as such unfavourable prognosis in advanced stage ovarian cancer (Iwagoi et al., 2021), these studies as well as ours, continue to highlight the complex contribution of VATs to tumour metastasis and the impact of chemotherapy which can extend to peripheral tissues. Moreover, they echo the importance of combinatory chemo- and immunotherapies for such tumours, which have already begun to show promise in augmenting anti-tumour activity in such peritoneal cancers (Cubas et al., 2018, Yaghoubi et al., 2019).

In conclusion, this doctoral project has successfully characterised immune cell subsets within mesenteric and omental VAT FALCs, showing a type 2 cytokine environment within these clusters with differing implications for disease. During helminth infection VAT FALCs promote immune cell interactions, proliferation, activation, and expression of Th2 cytokines thereby contributing to immune responses within the host. In contrast, VAT FALCs supported the metastasis and survival of tumour cells to the peritoneal cavity. Significant infiltration of immunosuppressive cells into VATs was observed in both murine models of colon cancer and in human HGSOC; with the latter revealing the skewing of effector cells towards a less activated phenotype. Additionally, our murine model showed that prophylactic peritoneal inflammation by zymosan might be sufficient to prevent such tumour-induced immunosuppression. Collectively these data therefore highlight the paradoxical role of VAT FALCs during helminth infection and metastatic cancers, and suggest in the case of the latter, the potential to manipulate these clusters to induce anti-tumour responses. Nonetheless there were some limitations to our study. While the Red5 reporter mice clearly showed that ILC2s in VAT FALCs dominated in their production of IL-5 at steady state compared to ILC2s

isolated from mLN, such expression was considerably high, raising the concern of whether this reporter mice over-estimated the expression of the cytokine in these tissues. However, Red5 mice have been used by other groups that have also noted the spontaneous production of IL-5 by VAT ILC2s, also at striking proportions compared to other cytokines such as IL-4/IL-13 (Molofsky et al., 2013). Secondly, It had been previously shown that gene expression of *Il33* was elevated in the SI of *H. poly* infected mice, concomitant with type-2 responses as well as increase in ILC2s (Pelly et al., 2016), leading to the model of ILC2 activation following *H. poly* infection proposed by Pelly and colleagues as illustrated in figure 1.7. Part of this led to the investigation of the role of IL-33 in controlling VAT ILC2 and CD4 T cells responses following *H. poly* infection. However, it would have been beneficial prior to using the *Il33*$^{-/-}$ mice, to ascertain whether *H. poly* infection led to increased gene and/or protein expression of IL-33 (as well as other type 2 inducers) in VATs, either via real-time PCR or flow cytometry. This would have provided a stronger rationale for investigating IL-33 function and may have further revealed other immune cells within the VAT that might be influenced by IL-33. Finally, due to the MC38 murine model not being set up at Birmingham, most of these experiments were done at the laboratory of our collaborators in Switzerland, which prevented additional interrogation of initial results observed. For instance, as presented in this thesis, VATs isolated from PBS, PBS/MC38 and zymosan/MC38 mice showed interesting differences in their immune cell composition, however, would have benefitted from a more in-depth phenotyping of these immune subsets, in particular, assessing their co-stimulatory, suppressive, migratory and proliferative properties.

Given the limitations stated above the author will now discuss some areas for improvement and future studies. Firstly, the mechanisms that might be involved in controlling ILC2/CD4 T

cell responses within VATs during *H. poly* infection remain to be answered, given the fact that this study showed limited role for IL-33. As discussed previously other ILC2 activating cytokines such as IL-25 and TSLP have been reported to mediate immune responses to helminth infection (Pei et al., 2016, Zaiss et al., 2013). Interestingly, in a triple-deficient mice that lacked responsiveness to IL-33, IL-25 and TSLP, type 2 cytokine transcripts as well as the numbers of activated IL-5 expressing ILC2s were observed to be significantly reduced in several tissues, including the gonadal fat (Ricardo-Gonzalez et al., 2018). Furthermore, the parameters measured during *H. poly* infection focused largely on ILC2 and CD4 T cell responses; however, given the fact that IL-33 can activate a host of other immune cells, lack of the latter may have had an impact on such cells which this project did not investigate. Hashiguchi and colleagues for instance showed that eosinophils within gonadal AT could be directly activated by IL-33 as well as via an ILC-mediated pathway. Additionally, while blockage of IL-33Rα did not affect numbers of IL-5^{+}ILCs, numbers of eosinophils were significantly reduced (Hashiguchi et al., 2015). Meanwhile, macrophages have been reported to not only produce IL-5 and IL-13 following *in vitro* stimulation with IL-25/IL-33, but have also been found to be the dominant IL-13 producing cells following *H. poly* infection (Yang et al., 2013b, Smith et al., 2018). Therefore, the effect of *H. poly* on such cell types in the *Il33*$^{-/-}$ mice should also be investigated.

Secondly, given the expansion and proliferative capacity of VAT ILC2s as well as its upregulation of activation markers following *S. mansoni* infection, future experiments could further assess the functional activity of these cells by evaluating their cytokine producing capabilities as well as the mechanisms that govern this. Interestingly IL-33 has recently been found to be important in initiating, but not maintaining type 2 immunity within the intestinal

tissue during *S. mansoni* infection (Mukendi et al., 2021). Such findings would be worth corroborating within the context of VATs.

Thirdly, in our syngeneic tumour model, a number of myeloid cells including monocytes, macrophages, neutrophils and eosinophils were found to significantly infiltrate VATs both in PBS/MC38 and zymosan/MC38 mice – albeit to varying degrees. As such the combined or sequential depletion of these myeloid subsets would be useful in deciphering the role of each of them in the seeding of tumours cells within VATs. Furthermore, although we showed that tumour burden could be reduced following prophylactic administration of zymosan, a next key experiment would be to ascertain if the same effects are elicited therapeutically. Assuming tumour localisation to FALCs can be modulated by such therapeutic administration of zymosan and given the fact that this PAMP binds to TLR2/6 and Dectin-1 to elicit inflammatory responses, this would suggest a translational pathway via the use of PRR agonists as potential therapies for treating such metastatic cancers. Of date, three FDA-approved TLR ligands exists: Bacillus Calmette-Guérin (BCG), a TLR2/4 ligand approved for bladder cancer; TLR4 ligand monophosphoryl lipid A for human papillomavirus-induced cervical cancer; and the TLR7 agonist imiquimod, approved for basal cell carcinoma (Urban-Wojciuk et al., 2019). However, TLR engagement has been reported to have both pro- and anti-tumour effects. Although TLR5 signalling is associated with suppressing the growth of human colon cancer and causing tumour necrosis, TLR4 on the other hand is linked to prolonging tumour cell survival in mouse colon cancer models (Kaczanowska et al., 2013). Meanwhile TLR9 engagement on human ovarian cancer leads to increased tumour cell migration and invasion (Kaczanowska et al., 2013), highlighting the need for newer TLR agonists. Indeed, a newly designed glucomannan polysaccharide modified with acetyl groups

to a substitution degree of 1.8 (acGM-1.8) which specifically activated TLR2 with TLR6 acting as a co-receptor, was shown to induce macrophages to a pro-inflammatory state. Further, injection of acGM-1.8 intratumorally suppressed the growth of S180 sarcoma and B16 melanoma tumour models in mice (Feng et al., 2019). Such promising results therefore give hope for targeting this receptor pathway in other cancers.

Fourthly, immunofluorescence staining for IL-33 revealed this cytokine to be present in the cytoplasm of FALC stromal cells in tumours of PBS/MC38 mice, while remaining nucleic in zymosan/MC38 groups, as is also observed under steady state conditions, thereby alluding to the involvement of this cytokine in mediating tumour development. Nonetheless, IL-33 was not measured quantitatively between these groups, as such further approaches to assess IL-33 secretion following MC38 injection would prove beneficial in supporting immunofluorescence results. Additionally, *Il33*$^{-/-}$ mice could be a useful tool in assessing the impact of lack of IL-33 on tumour metastasis.

Finally, flow cytometry analyses of omental samples from patients with HGSOC showed the enrichment of a number of immune cells within metastatic omentum of NT patients, including CD4/CD8 T cells, Tregs, NK cells and macrophages. Though immunofluorescence staining confirmed the presence of Tregs within omental FALCs, it would also be advantageous to define the anatomic distribution of other cell subsets given the importance of immune cell location, density and functional orientation in influencing prognosis and treatment outcome (Fridman et al., 2012). Indeed, preparations to perform multiplex immunostaining of tissue from HGSOC patients had begun towards the end of my thesis, and will hopefully yield valuable insights of the immune landscape during such metastatic cancers.

CHAPTER 7: APPENDIX

7.1 The Role of Visceral Adipose Tissues during *Schistosoma Mansoni* Infection (See Chapter 4.5)

Figure 7.1: Assessing CD4 T cell responses in visceral adipose tissue of mice *following S. mansoni* infection

180 cercariae (cerc) of *S. mansoni* were placed on the abdomen of C57BL/6J WT mice in between 200 µl of pond water, for 30 min to allow absorption into mice, with non-infected mice used as controls. The mesenteries, omentum and mLN were isolated 49 days post infection. A single cell suspension was generated, and stimulated with PMA and ionomycin (P/I) as described in materials and methods, for the assessment of Th2 cytokines by CD4 T cells. The same gating strategy as shown in figure 4.12a was applied.

Data are representative of one independent experiment with the following sample numbers: non-infected (n=2-3), *S. mansoni*_180cer*c* (n=2-3). Bars on the graph represent the median value. Statistical significance was determined using Unpaired t test.**P*<0.05, ***P*<0.01, ****P*<0.001 and *****P*<0.0001

a) Graph comparing the percentage of IL-4^{+} CD4 T cells in mLN, mesenteries and omentum (left to right) between non-infected and *S. mansoni*_180 cerc infected mice.
b) Graph comparing the percentage of IL-5^{+} and IL-13^{+} CD4 T cells in mLN, mesenteries and omentum (left to right) between non-infected and *S. mansoni* _180 cerc infected mice.

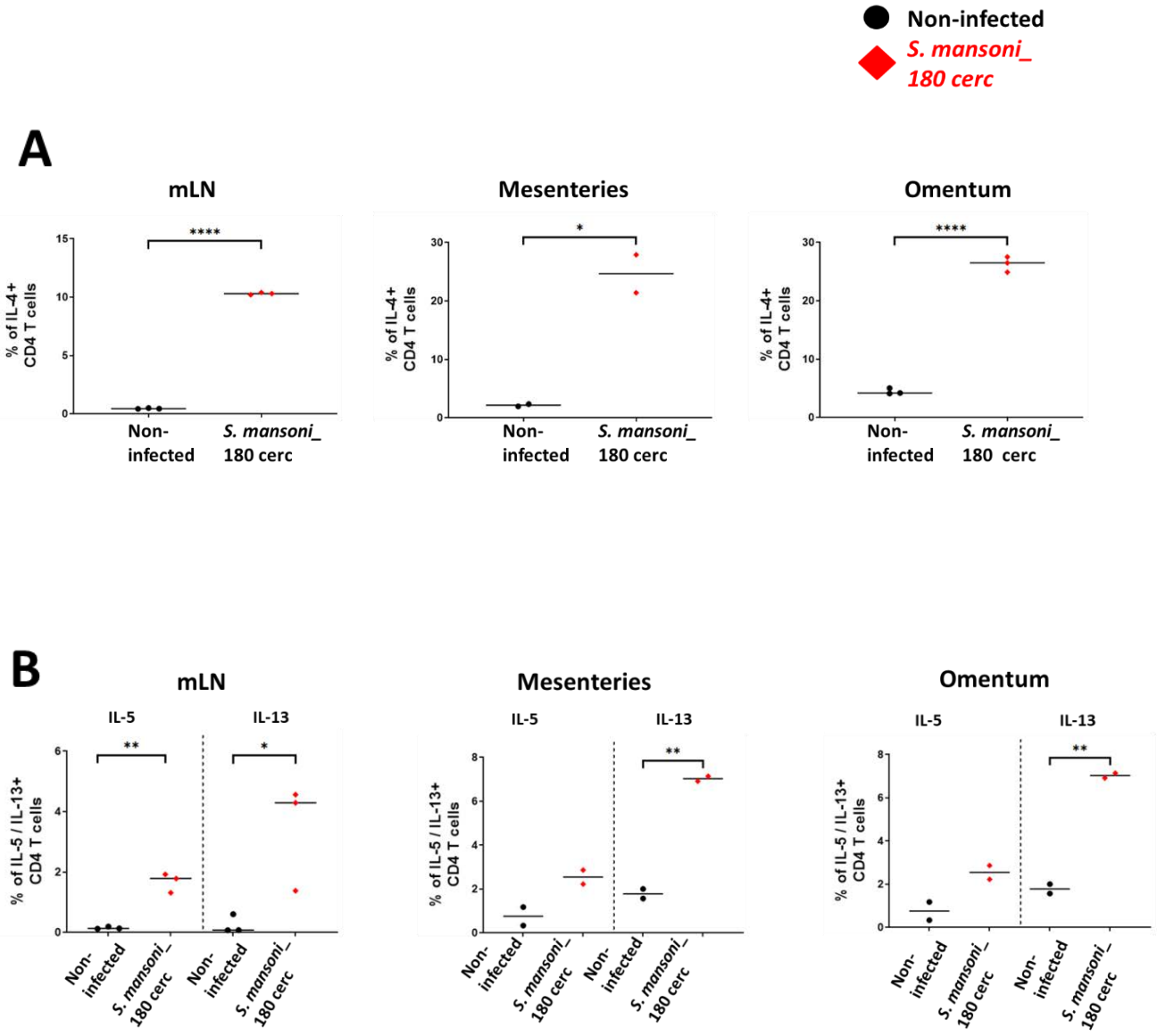
Non-infected
S. mansoni_ 180 cerc
A
mLN
Mesenteries
Omentum
% of IL-4+ CD4 T cells
****
*
Non-infected
S. mansoni_ 180 cerc
B
IL-5
IL-13
% of IL-5 / IL-13+ CD4 T cells
**
*

Figure 7.1

7.2 Peritoneal Cancer Metastasis (See Chapter 5.3)

Figure 7.2: Assessing IL-13 production by CD4 T cells in human metastatic omentum from high-grade serous ovarian cancer patients

Metastatic (and where possible healthy) omental samples were collected from patients with high-grade serous ovarian cancer (HGSOC) at City hospital, Birmingham, following informed consent according to the institutional tissue collection protocol. Samples included patients who had undergone neoadjuvant chemotherapy (NACT), as well as those who had not received treatment (NT) prior to surgery. Control samples were also supplemented via the collection of healthy omentum from the Human Biomaterials Resource Centre (HBRC). A single cell suspension was generated, and stimulated with PMA and ionomycin (P/I) as described in materials and methods.

The expression of IL-13 by CD4 T cells between healthy and metastatic human omentum were analysed by flow cytometry.

Data are representative of 25 independent experiments with the following sample numbers: Healthy (n=11), Met/NT (n=6), Met/NACT (n=8). Bars on the graph represent the median value. Statistical significance was determined using Kruskal-Wallis followed by Dunn's multiple comparisons test. *P<0.05, **P<0.01, ***P<0.001 and ****P<0.0001.

a) Graph comparing the percentage of IL-13^{+}CD4 T cells between healthy, Met/NT and Met/NACT human omentum. Met (Metastatic); NT (Not treated); NACT (Neoadjuvant Chemotherapy).

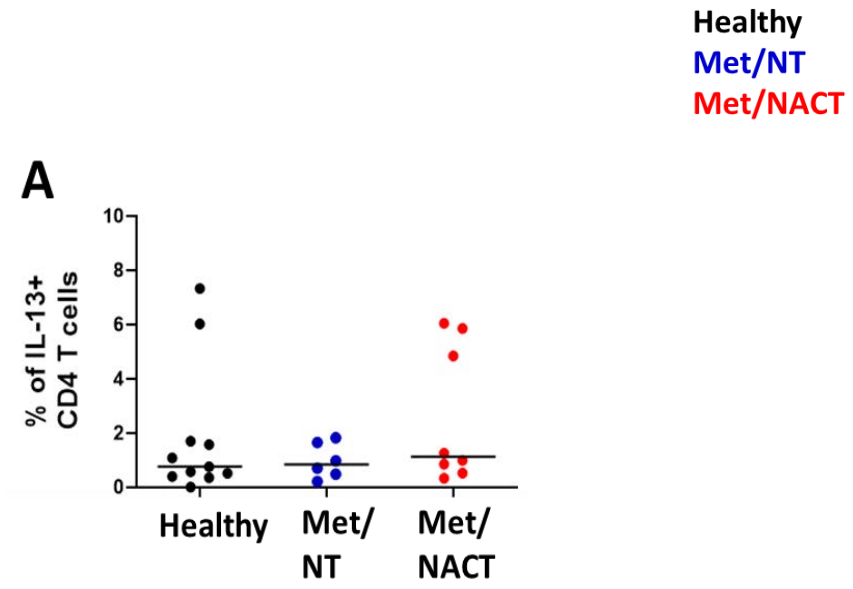
Healthy
Met/NT
Met/NACT
A
% of IL-13+ CD4 T cells
10
8
6
4
2
0
Healthy
Met/ NT
Met/ NACT

Figure 7.2

REFERENCES

Alexopoulos, N., Katritsis, D. and Raggi, P. (2014) 'Visceral adipose tissue as a source of inflammation and promoter of atherosclerosis', *Atherosclerosis,* 233(1), pp. 104-112.

Amarante-Mendes, G. P., Adjemian, S., Branco, L. M., Zanetti, L. C., Weinlich, R. and Bortoluci, K. R. (2018) 'Pattern Recognition Receptors and the Host Cell Death Molecular Machinery', *Frontiers in Immunology,* 9(2379).

Amemori, S., Ootani, A., Aoki, S., Fujise, T., Shimoda, R., Kakimoto, T., Shiraishi, R., Sakata, Y., Tsunada, S., Iwakiri, R. and Fujimoto, K. (2007) 'Adipocytes and preadipocytes promote the proliferation of colon cancer cells in vitro', *Am J Physiol Gastrointest Liver Physiol,* 292(3), pp. G923-9.

Aoyagi, T., Terracina, K. P., Raza, A. and Takabe, K. (2014) 'Current treatment options for colon cancer peritoneal carcinomatosis', *World journal of gastroenterology,* 20(35), pp. 12493-12500.

Araújo, M. I., de Jesus, A. R., Bacellar, O., Sabin, E., Pearce, E. and Carvalho, E. M. (1996) 'Evidence of a T helper type 2 activation in human schistosomiasis', *European Journal of Immunology,* 26(6), pp. 1399-1403.

Arnold, I. C., Artola-Boran, M., Gurtner, A., Bertram, K., Bauer, M., Frangez, Z., Becher, B., Kopf, M., Yousefi, S., Simon, H.-U., Tzankov, A. and Müller, A. (2020) 'The GM-CSF–IRF5 signaling axis in eosinophils promotes antitumor immunity through activation of type 1 T cell responses', *Journal of Experimental Medicine,* 217(12).

Artis, D. and Spits, H. (2015) 'The biology of innate lymphoid cells', *Nature,* 517(7534), pp. 293-301.

Au-Yeung, C.-L., Yeung, T.-L., Achreja, A., Zhao, H., Yip, K.-P., Kwan, S.-Y., Onstad, M., Sheng, J., Zhu, Y., Baluya, D. L., Co, N.-N., Rynne-Vidal, A., Schmandt, R., Anderson, M. L., Lu, K. H., Wong, S. T. C., Nagrath, D. and Mok, S. C. (2020) 'ITLN1 modulates invasive potential and metabolic reprogramming of ovarian cancer cells in omental microenvironment', *Nature Communications,* 11(1), pp. 3546.

Bailly, C., Thuru, X. and Quesnel, B. (2020) 'Combined cytotoxic chemotherapy and immunotherapy of cancer: modern times', *NAR Cancer,* 2(1).

Bal, S. M., Bernink, J. H., Nagasawa, M., Groot, J., Shikhagaie, M. M., Golebski, K., van Drunen, C. M., Lutter, R., Jonkers, R. E., Hombrink, P., Bruchard, M., Villaudy, J., Munneke, J. M., Fokkens, W., Erjefält, J. S., Spits, H. and Ros, X. R. (2016) 'IL-1β, IL-4 and IL-12 control the fate of group 2 innate lymphoid cells in human airway inflammation in the lungs', *Nature Immunology,* 17(6), pp. 636-645.

Balkwill, F. R., Capasso, M. and Hagemann, T. (2012) 'The tumor microenvironment at a glance', *Journal of Cell Science,* 125(23), pp. 5591-5596.

Barbera-Guillem, E., Nyhus, J. K., Wolford, C. C., Friece, C. R. and Sampsel, J. W. (2002) 'Vascular Endothelial Growth Factor Secretion by Tumor-infiltrating Macrophages Essentially Supports Tumor Angiogenesis, and IgG Immune Complexes Potentiate the Process', *Cancer Research,* 62(23), pp. 7042-7049.

Barnig, C., Cernadas, M., Dutile, S., Liu, X., Perrella, M. A., Kazani, S., Wechsler, M. E., Israel, E. and Levy, B. D. (2013) 'Lipoxin A4 regulates natural killer cell and type 2 innate lymphoid cell activation in asthma', *Science translational medicine,* 5(174), pp. 174ra26-174ra26.

Barone, F., Gardner, D. H., Nayar, S., Steinthal, N., Buckley, C. D. and Luther, S. A. (2016) 'Stromal Fibroblasts in Tertiary Lymphoid Structures: A Novel Target in Chronic Inflammation', *Front Immunol,* 7, pp. 477.

Barron, L. and Wynn, T. A. (2011) 'Macrophage activation governs schistosomiasis-induced inflammation and fibrosis', *European Journal of Immunology,* 41(9), pp. 2509-2514.

Bast, R. C., Hennessy, B. and Mills, G. B. (2009) 'The biology of ovarian cancer: new opportunities for translation', *Nature Reviews Cancer,* 9(6), pp. 415-428.

Batra, A., Heimesaat, M. M., Bereswill, S., Fischer, A., Glauben, R., Kunkel, D., Scheffold, A., Erben, U., Kühl, A., Loddenkemper, C., Lehr, H. A., Schumann, M., Schulzke, J. D., Zeitz, M. and Siegmund, B. (2012) 'Mesenteric fat—control site for bacterial translocation in colitis?', *Mucosal Immunology,* 5(5), pp. 580-591.

Bell, R. B., Feng, Z., Bifulco, C. B., Leidner, R., Weinberg, A. and Fox, B. A. (2018) '15 - Immunotherapy', in Bell, R.B., Fernandes, R.P. & Andersen, P.E. (eds.) *Oral, Head and Neck Oncology and Reconstructive Surgery*: Elsevier, pp. 314-340.

Bénézech, C. and Jackson-Jones, L. H. (2019) 'ILC2 Orchestration of Local Immune Function in Adipose Tissue', *Frontiers in Immunology,* 10(171).

Bénézech, C., Luu, N.-T., Walker, J. A., Kruglov, A. A., Loo, Y., Nakamura, K., Zhang, Y., Nayar, S., Jones, L. H., Flores-Langarica, A., McIntosh, A., Marshall, J., Barone, F., Besra, G., Miles, K., Allen, J. E., Gray, M., Kollias, G., Cunningham, A. F., Withers, D. R., Toellner, K. M., Jones, N. D., Veldhoen, M., Nedospasov, S. A., McKenzie, A. N. J. and Caamaño, J. H. (2015) 'Inflammation-induced formation of fat-associated lymphoid clusters', *Nature immunology,* 16(8), pp. 819-828.

Bénézech, C., Mader, E., Desanti, G., Khan, M., Nakamura, K., White, A., Ware, C. F., Anderson, G. and Caamaño, J. H. (2012) 'Lymphotoxin-β receptor signaling through NF-κB2-RelB pathway reprograms adipocyte precursors as lymph node stromal cells', *Immunity,* 37(4), pp. 721-734.

Berberich, S., Dähne, S., Schippers, A., Peters, T., Müller, W., Kremmer, E., Förster, R. and Pabst, O. (2008) 'Differential Molecular and Anatomical Basis for B Cell Migration into the Peritoneal Cavity and Omental Milky Spots', *The Journal of Immunology,* 180(4), pp. 2196-2203.

Berek, J. S., Kehoe, S. T., Kumar, L. and Friedlander, M. (2018) 'Cancer of the ovary, fallopian tube, and peritoneum', *Int J Gynaecol Obstet,* 143 Suppl 2, pp. 59-78.

Bernink, Jochem H., Krabbendam, L., Germar, K., de Jong, E., Gronke, K., Kofoed-Nielsen, M., Munneke, J. M., Hazenberg, Mette D., Villaudy, J., Buskens, Christianne J., Bemelman, Willem A., Diefenbach, A., Blom, B. and Spits, H. (2015) 'Interleukin-12 and -23 Control Plasticity of CD127+ Group 1 and Group 3 Innate Lymphoid Cells in the Intestinal Lamina Propria', *Immunity,* 43(1), pp. 146-160.

Bjørndal, B., Burri, L., Staalesen, V., Skorve, J. and Berge, R. K. (2011) 'Different Adipose Depots: Their Role in the Development of Metabolic Syndrome and Mitochondrial Response to Hypolipidemic Agents', *Journal of Obesity,* 2011, pp. 490650.

Böhm, S., Montfort, A., Pearce, O. M., Topping, J., Chakravarty, P., Everitt, G. L., Clear, A., McDermott, J. R., Ennis, D., Dowe, T., Fitzpatrick, A., Brockbank, E. C., Lawrence, A. C., Jeyarajah, A., Faruqi, A. Z., McNeish, I. A., Singh, N., Lockley, M. and Balkwill, F. R. (2016) 'Neoadjuvant Chemotherapy Modulates the Immune Microenvironment in Metastases of Tubo-Ovarian High-Grade Serous Carcinoma', *Clin Cancer Res,* 22(12), pp. 3025-36.

Bolli, E., Movahedi, K., Laoui, D. and Van Ginderachter, J. A. (2017) 'Novel insights in the regulation and function of macrophages in the tumor microenvironment', *Current Opinion in Oncology,* 29(1), pp. 55-61.

Bouchery, T., Le Gros, G. and Harris, N. (2019) 'ILC2s—Trailblazers in the Host Response Against Intestinal Helminths', *Frontiers in Immunology,* 10(623).

Bourke, C. D., Prendergast, C. T., Sanin, D. E., Oulton, T. E., Hall, R. J. and Mountford, A. P. (2015) 'Epidermal keratinocytes initiate wound healing and pro-inflammatory immune responses following percutaneous schistosome infection', *International journal for parasitology,* 45(4), pp. 215-224.

Bray, F., Ferlay, J., Soerjomataram, I., Siegel, R. L., Torre, L. A. and Jemal, A. (2018) 'Global cancer statistics 2018: GLOBOCAN estimates of incidence and mortality worldwide for 36 cancers in 185 countries', *CA: A Cancer Journal for Clinicians,* 68(6), pp. 394-424.

Brendolan, A. and Caamano, J. H. (2012) 'Mesenchymal cell differentiation during lymph node organogenesis', *Front Immunol,* 3, pp. 381.

Brenner, H., Kloor, M. and Pox, C. P. (2014) 'Colorectal cancer', *The Lancet,* 383(9927), pp. 1490-1502.

Brestoff, J. R., Kim, B. S., Saenz, S. A., Stine, R. R., Monticelli, L. A., Sonnenberg, G. F., Thome, J. J., Farber, D. L., Lutfy, K., Seale, P. and Artis, D. (2015) 'Group 2 innate lymphoid cells promote beiging of white adipose tissue and limit obesity', *Nature,* 519(7542), pp. 242-6.

Brubaker, S. W., Bonham, K. S., Zanoni, I. and Kagan, J. C. (2015) 'Innate immune pattern recognition: a cell biological perspective', *Annual review of immunology,* 33, pp. 257-290.

Buckley, C. D., Barone, F., Nayar, S., Bénézech, C. and Caamaño, J. (2015) 'Stromal Cells in Chronic Inflammation and Tertiary Lymphoid Organ Formation', *Annual Review of Immunology,* 33(1), pp. 715-745.

Buettner, M. and Lochner, M. (2016) 'Development and Function of Secondary and Tertiary Lymphoid Organs in the Small Intestine and the Colon', *Frontiers in Immunology,* 7(342).

Buscher, K., Wang, H., Zhang, X., Striewski, P., Wirth, B., Saggu, G., Lutke-Enking, S., Mayadas, T. N., Ley, K., Sorokin, L. and Song, J. (2016) 'Protection from septic peritonitis by rapid neutrophil recruitment through omental high endothelial venules', *Nat Commun,* 7, pp. 10828.

Cancel, J.-C., Crozat, K., Dalod, M. and Mattiuz, R. (2019) 'Are Conventional Type 1 Dendritic Cells Critical for Protective Antitumor Immunity and How?', *Frontiers in Immunology,* 10(9).

Cano, R. L. E. and Lopera, H. D. E. (2013) 'Chapter Five - Introduction to T and B lymphocytes', in Anaya JM, Shoenfeld Y & Rojas-Villarraga A (eds.) *Autoimmunity: From Bench to Bedside*. Colombia: El Rosario University Press.

Carlsten, M., Norell, H., Bryceson, Y. T., Poschke, I., Schedvins, K., Ljunggren, H.-G., Kiessling, R. and Malmberg, K.-J. (2009) 'Primary Human Tumor Cells Expressing CD155 Impair Tumor Targeting by Down-Regulating DNAM-1 on NK Cells', *The Journal of Immunology,* 183(8), pp. 4921-4930.

Castoldi, A., Naffah de Souza, C., Câmara, N. O. S. and Moraes-Vieira, P. M. (2016) 'The Macrophage Switch in Obesity Development', *Frontiers in Immunology,* 6(637).

Chaix, J., Tessmer, M. S., Hoebe, K., Fuséri, N., Ryffel, B., Dalod, M., Alexopoulou, L., Beutler, B., Brossay, L., Vivier, E. and Walzer, T. (2008) 'Cutting Edge: Priming of NK Cells by IL-18', *The Journal of Immunology,* 181(3), pp. 1627-1631.

Chalubinski, M., Luczak, E., Wojdan, K., Gorzelak-Pabis, P. and Broncel, M. (2016) 'Innate lymphoid cells type 2 – emerging immune regulators of obesity and atherosclerosis', *Immunology Letters,* 179, pp. 43-46.

Chan, B. C. L., Lam, C. W. K., Tam, L.-S. and Wong, C. K. (2019) 'IL33: Roles in Allergic Inflammation and Therapeutic Perspectives', *Frontiers in Immunology,* 10(364).

Chan, O. T. and Yang, L. X. (2000) 'The immunological effects of taxanes', *Cancer Immunol Immunother,* 49(4-5), pp. 181-5.

Chaplin, D. D. (2010) 'Overview of the immune response', *The Journal of allergy and clinical immunology,* 125(2 Suppl 2), pp. S3-S23.

Chau, Y.-Y., Bandiera, R., Serrels, A., Martínez-Estrada, O. M., Qing, W., Lee, M., Slight, J., Thornburn, A., Berry, R., McHaffie, S., Stimson, R. H., Walker, B. R., Chapuli, R. M., Schedl, A. and Hastie, N. (2014) 'Visceral and subcutaneous fat have different origins and evidence supports a mesothelial source', *Nature Cell Biology,* 16(4), pp. 367-375.

Chaudhary, B. and Elkord, E. (2016) 'Regulatory T Cells in the Tumor Microenvironment and Cancer Progression: Role and Therapeutic Targeting', *Vaccines,* 4(3), pp. 28.

Chea, S., Perchet, T., Petit, M., Verrier, T., Guy-Grand, D., Banchi, E.-G., Vosshenrich, C. A. J., Di Santo, J. P., Cumano, A. and Golub, R. (2016) 'Notch signaling in group 3 innate lymphoid cells modulates their plasticity', *Science Signaling,* 9(426), pp. ra45-ra45.

Cherrier, M., Sawa, S. and Eberl, G. (2012) 'Notch, Id2, and RORγt sequentially orchestrate the fetal development of lymphoid tissue inducer cells', *The Journal of experimental medicine,* 209(4), pp. 729-740.

Cho, K. W., Morris, D. L. and Lumeng, C. N. (2014) 'Flow cytometry analyses of adipose tissue macrophages', *Methods in enzymology,* 537, pp. 297-314.

Cinti, S., Mitchell, G., Barbatelli, G., Murano, I., Ceresi, E., Faloia, E., Wang, S., Fortier, M., Greenberg, A. S. and Obin, M. S. (2005) 'Adipocyte death defines macrophage localization and function in adipose tissue of obese mice and humans', *J Lipid Res,* 46(11), pp. 2347-55.

Clark, G. J., Angel, N., Kato, M., López, J. A., MacDonald, K., Vuckovic, S. and Hart, D. N. J. (2000) 'The role of dendritic cells in the innate immune system', *Microbes and Infection,* 2(3), pp. 257-272.

Clark, R., Krishnan, V., Schoof, M., Rodriguez, I., Theriault, B., Chekmareva, M. and Rinker-Schaeffer, C. (2013) 'Milky Spots Promote Ovarian Cancer Metastatic Colonization of Peritoneal Adipose in Experimental Models', *The American Journal of Pathology,* 183(2), pp. 576-591.

Coelho, M., Oliveira, T. and Fernandes, R. (2013) 'Biochemistry of adipose tissue: an endocrine organ', *Archives of medical science : AMS,* 9(2), pp. 191-200.

Coffey, J. C. and O'Leary, D. P. (2016) 'The mesentery: structure, function, and role in disease', *The Lancet Gastroenterology & Hepatology,* 1(3), pp. 238-247.

Colley, D. G. and Secor, W. E. (2014) 'Immunology of human schistosomiasis', *Parasite immunology,* 36(8), pp. 347-357.

Corbett, T. H., Griswold, D. P., Roberts, B. J., Peckham, J. C. and Schabel, F. M. (1975) 'Tumor Induction Relationships in Development of Transplantable Cancers of the Colon in Mice for Chemotherapy Assays, with a Note on Carcinogen Structure', *Cancer Research,* 35(9), pp. 2434-2439.

Costain, A. H., MacDonald, A. S. and Smits, H. H. (2018) 'Schistosome Egg Migration: Mechanisms, Pathogenesis and Host Immune Responses', *Frontiers in Immunology,* 9(3042).

Cruz-Migoni, S. and Caamaño, J. (2016) 'Fat-Associated Lymphoid Clusters in Inflammation and Immunity', *Frontiers in Immunology,* 7(612).

Cubas, R., Moskalenko, M., Cheung, J., Yang, M., McNamara, E., Xiong, H., Hoves, S., Ries, C. H., Kim, J. and Gould, S. (2018) 'Chemotherapy Combines Effectively with Anti–PD-L1 Treatment and Can Augment Antitumor Responses', *The Journal of Immunology*, pp. ji1800275.

Cui, G., Yuan, A., Li, Z., Goll, R. and Florholmen, J. (2020) 'ST2 and regulatory T cells in the colorectal adenoma/carcinoma microenvironment: implications for diseases progression and prognosis', *Scientific Reports,* 10(1), pp. 5892.

Culligan, K., Walsh, S., Dunne, C., Walsh, M., Ryan, S., Quondamatteo, F., Dockery, P. and Coffey, J. C. (2014) 'The mesocolon: a histological and electron microscopic characterization of the mesenteric attachment of the colon prior to and after surgical mobilization', *Ann Surg,* 260(6), pp. 1048-56.

Curiel, T. J., Coukos, G., Zou, L., Alvarez, X., Cheng, P., Mottram, P., Evdemon-Hogan, M., Conejo-Garcia, J. R., Zhang, L., Burow, M., Zhu, Y., Wei, S., Kryczek, I., Daniel, B., Gordon, A., Myers, L., Lackner, A., Disis, M. L., Knutson, K. L., Chen, L. and Zou, W. (2004) 'Specific recruitment of regulatory T cells in ovarian carcinoma fosters immune privilege and predicts reduced survival', *Nature Medicine,* 10(9), pp. 942-949.

de Jesus, A. R., Silva, A., Santana, L. B., Magalhaes, A., de Jesus, A. A., de Almeida, R. P., Rego, M. A., Burattini, M. N., Pearce, E. J. and Carvalho, E. M. (2002) 'Clinical and immunologic evaluation of 31 patients with acute schistosomiasis mansoni', *J Infect Dis,* 185(1), pp. 98-105.

De Larco, J. E., Wuertz, B. R. K. and Furcht, L. T. (2004) 'The Potential Role of Neutrophils in Promoting the Metastatic Phenotype of Tumors Releasing Interleukin-8', *Clinical Cancer Research,* 10(15), pp. 4895-4900.

Desai, J. P. and Moustarah, F. (2020) *Peritoneal Metastasis.* StatPearls Publishing, Treasure Island (FL).

Desforges, J.-P., Sonne, C., Dietz, R. and Levin, M. (2018) 'Chapter 12 - Immunotoxic Effects of Environmental Pollutants in Marine Mammals', in Fossi, M.C. & Panti, C. (eds.) *Marine Mammal Ecotoxicology*: Academic Press, pp. 321-343.

Diefenbach, A., Colonna, M. and Koyasu, S. (2014) 'Development, differentiation, and diversity of innate lymphoid cells', *Immunity,* 41(3), pp. 354-365.

Doherty, T. A. and Broide, D. H. (2018) 'Lipid regulation of group 2 innate lymphoid cell function: Moving beyond epithelial cytokines', *The Journal of allergy and clinical immunology,* 141(5), pp. 1587-1589.

Doherty, T. A., Khorram, N., Lund, S., Mehta, A. K., Croft, M. and Broide, D. H. (2013) 'Lung type 2 innate lymphoid cells express cysteinyl leukotriene receptor 1, which regulates TH2 cytokine production', *Journal of Allergy and Clinical Immunology,* 132(1), pp. 205-213.

Eberl, G., Colonna, M., Di Santo, J. P. and McKenzie, A. N. J. (2015) 'Innate lymphoid cells: A new paradigm in immunology', *Science,* 348(6237), pp. aaa6566.

Efremova, M., Rieder, D., Klepsch, V., Charoentong, P., Finotello, F., Hackl, H., Hermann-Kleiter, N., Löwer, M., Baier, G., Krogsdam, A. and Trajanoski, Z. (2018) 'Targeting immune checkpoints potentiates immunoediting and changes the dynamics of tumor evolution', *Nature communications,* 9(1), pp. 32-32.

Elewa, Y. H. A., Ichii, O., Takada, K., Nakamura, T., Masum, M. A. and Kon, Y. (2018) 'Histopathological Correlations between Mediastinal Fat-Associated Lymphoid Clusters and the Development of Lung Inflammation and Fibrosis following Bleomycin Administration in Mice', *Frontiers in Immunology,* 9(271).

Emanuela, F., Grazia, M., Marco de, R., Maria Paola, L., Giorgio, F. and Marco, B. (2012) 'Inflammation as a Link between Obesity and Metabolic Syndrome', *J Nutr Metab,* 2012, pp. 476380.

Etzerodt, A., Moulin, M., Doktor, T. K., Delfini, M., Mossadegh-Keller, N., Bajenoff, M., Sieweke, M. H., Moestrup, S. K., Auphan-Anezin, N. and Lawrence, T. (2020) 'Tissue-resident macrophages in omentum promote metastatic spread of ovarian cancer', *J Exp Med,* 217(4).

Fallon, P. G., Ballantyne, S. J., Mangan, N. E., Barlow, J. L., Dasvarma, A., Hewett, D. R., McIlgorm, A., Jolin, H. E. and McKenzie, A. N. (2006) 'Identification of an interleukin (IL)-25-dependent cell population that provides IL-4, IL-5, and IL-13 at the onset of helminth expulsion', *J Exp Med,* 203(4), pp. 1105-16.

Fallon, P. G., Richardson, E. J., McKenzie, G. J. and McKenzie, A. N. J. (2000) 'Schistosome Infection of Transgenic Mice Defines Distinct and Contrasting Pathogenic Roles for IL-4 and IL-13: IL-13 Is a Profibrotic Agent', *The Journal of Immunology,* 164(5), pp. 2585-2591.

Fallon, P. G., Smith, P. and Dunne, D. W. (1998) 'Type 1 and type 2 cytokine-producing mouse CD4+ and CD8+ T cells in acute Schistosoma mansoni infection', *European Journal of Immunology,* 28(4), pp. 1408-1416.

Fang, M., Li, Y., Huang, K., Qi, S., Zhang, J., Zgodzinski, W., Majewski, M., Wallner, G., Gozdz, S., Macek, P., Kowalik, A., Pasiarski, M., Grywalska, E., Vatan, L., Nagarsheth, N., Li, W., Zhao, L., Kryczek, I., Wang, G., Wang, Z., Zou, W. and Wang, L. (2017) 'IL33 Promotes Colon Cancer Cell Stemness via JNK Activation and Macrophage Recruitment', *Cancer Research,* 77(10), pp. 2735-2745.

Feng, Y., Mu, R., Wang, Z., Xing, P., Zhang, J., Dong, L. and Wang, C. (2019) 'A toll-like receptor agonist mimicking microbial signal to generate tumor-suppressive macrophages', *Nature Communications,* 10(1), pp. 2272.

Ferrante, A. (2007) 'Obesity-induced inflammation: A metabolic dialogue in the language of inflammation', *Journal of internal medicine,* 262, pp. 408-14.

Finkelman, F., Shea-Donohue, T., Goldhill, J., Sullivan, C., C. Morris, S., B. Madden, K. and Gause, W. (1997) *CYTOKINE REGULATION OF HOST DEFENSE AGAINST PARASITIC GASTROINTESTINAL NEMATODES:Lessons from Studies with Rodent Models*

Finney, C. A., Taylor, M. D., Wilson, M. S. and Maizels, R. M. (2007) 'Expansion and activation of CD4(+)CD25(+) regulatory T cells in Heligmosomoides polygyrus infection', *Eur J Immunol,* 37(7), pp. 1874-86.

Fitzmaurice, C., Naghavi, M. and Murray, C. J. L. (2018) 'Global Burden of Disease Cancer Collaboration. Global, Regional, and National Cancer Incidence, Mortality, Years of Life Lost, Years Lived With Disability, and Disability-Adjusted Life-Years for 29 Cancer Groups, 1990 to 2016.', *JAMA Oncology,* 4(11), pp. 1553-1568.

Flores Villanueva, P. O., Chikunguwo, S. M., Harris, T. S. and Stadecker, M. J. (1993) 'Role of IL-10 on antigen-presenting cell function for schistosomal egg-specific monoclonal T helper cell responses in vitro and in vivo', *The Journal of Immunology,* 151(6), pp. 3192-3198.

Forssell, J., Öberg, Å., Henriksson, M. L., Stenling, R., Jung, A. and Palmqvist, R. (2007) 'High Macrophage Infiltration along the Tumor Front Correlates with Improved Survival in Colon Cancer', *Clinical Cancer Research,* 13(5), pp. 1472-1479.

Fort, M. M., Cheung, J., Yen, D., Li, J., Zurawski, S. M., Lo, S., Menon, S., Clifford, T., Hunte, B., Lesley, R., Muchamuel, T., Hurst, S. D., Zurawski, G., Leach, M. W., Gorman, D. M. and Rennick, D. M. (2001) 'IL-25 induces IL-4, IL-5, and IL-13 and Th2-associated pathologies in vivo', *Immunity,* 15(6), pp. 985-95.

Fotopoulou, C., Hall, M., Cruickshank, D., Gabra, H., Ganesan, R., Hughes, C., Kehoe, S., Ledermann, J., Morrison, J., Naik, R., Rolland, P. and Sundar, S. (2017) 'British Gynaecological Cancer Society (BGCS) epithelial ovarian/fallopian tube/primary peritoneal cancer guidelines: recommendations for practice', *Eur J Obstet Gynecol Reprod Biol,* 213, pp. 123-139.

Frasnelli, M. E., Tarussio, D., Chobaz-Péclat, V., Busso, N. and So, A. (2005) 'TLR2 modulates inflammation in zymosan-induced arthritis in mice', *Arthritis research & therapy,* 7(2), pp. R370-R379.

Fridlender, Z. G., Sun, J., Kim, S., Kapoor, V., Cheng, G., Ling, L., Worthen, G. S. and Albelda, S. M. (2009) 'Polarization of Tumor-Associated Neutrophil Phenotype by TGF-β: “N1” versus “N2” TAN', *Cancer Cell,* 16(3), pp. 183-194.

Fridman, W. H., Pagès, F., Sautès-Fridman, C. and Galon, J. (2012) 'The immune contexture in human tumours: impact on clinical outcome', *Nature Reviews Cancer,* 12(4), pp. 298-306.

Galon, J., Costes, A., Sanchez-Cabo, F., Kirilovsky, A., Mlecnik, B., Lagorce-Pagès, C., Tosolini, M., Camus, M., Berger, A., Wind, P., Zinzindohoué, F., Bruneval, P., Cugnenc, P.-H., Trajanoski, Z., Fridman, W.-H. and Pagès, F. (2006) 'Type, Density, and Location of Immune Cells Within Human Colorectal Tumors Predict Clinical Outcome', *Science,* 313(5795), pp. 1960-1964.

Galon, J., Fridman, W.-H. and Pagès, F. (2007) 'The Adaptive Immunologic Microenvironment in Colorectal Cancer: A Novel Perspective', *Cancer Research,* 67(5), pp. 1883-1886.

Gantner, B. N., Simmons, R. M., Canavera, S. J., Akira, S. and Underhill, D. M. (2003) 'Collaborative induction of inflammatory responses by dectin-1 and Toll-like receptor 2', *The Journal of experimental medicine,* 197(9), pp. 1107-1117.

Gao, Y., Nish, Simone A., Jiang, R., Hou, L., Licona-Limón, P., Weinstein, Jason S., Zhao, H. and Medzhitov, R. (2013) 'Control of T Helper 2 Responses by Transcription Factor IRF4-Dependent Dendritic Cells', *Immunity,* 39(4), pp. 722-732.

Gatault, S., Delbeke, M., Driss, V., Sarazin, A., Dendooven, A., Kahn, J.-E., Lefèvre, G. and Capron, M. (2015) 'IL-18 Is Involved in Eosinophil-Mediated Tumoricidal Activity against a Colon Carcinoma Cell Line by Upregulating LFA-1 and ICAM-1', *The Journal of Immunology,* 195(5), pp. 2483-2492.

Gause, W. C., Urban, J. F. and Stadecker, M. J. (2003) 'The immune response to parasitic helminths: insights from murine models', *Trends in Immunology,* 24(5), pp. 269-277.

Gerber, S. A., Rybalko, V. Y., Bigelow, C. E., Lugade, A. A., Foster, T. H., Frelinger, J. G. and Lord, E. M. (2006) 'Preferential attachment of peritoneal tumor metastases to omental immune aggregates and possible role of a unique vascular microenvironment in metastatic survival and growth', *The American journal of pathology,* 169(5), pp. 1739-1752.

Gilbert, C. A. and Slingerland, J. M. (2013) 'Cytokines, obesity, and cancer: new insights on mechanisms linking obesity to cancer risk and progression', *Annu Rev Med,* 64, pp. 45-57.

Golebski, K., Ros, X. R., Nagasawa, M., van Tol, S., Heesters, B. A., Aglmous, H., Kradolfer, C. M. A., Shikhagaie, M. M., Seys, S., Hellings, P. W., van Drunen, C. M., Fokkens, W. J., Spits, H. and Bal, S. M. (2019) 'IL-1β, IL-23, and TGF-β drive plasticity of human ILC2s towards IL-17-producing ILCs in nasal inflammation', *Nature Communications,* 10(1), pp. 2162.

Gorski, S. A., Hahn, Y. S. and Braciale, T. J. (2013) 'Group 2 Innate Lymphoid Cell Production of IL-5 Is Regulated by NKT Cells during Influenza Virus Infection', *PLOS Pathogens,* 9(9), pp. e1003615.

Grabosch, S., Bulatovic, M., Zeng, F., Ma, T., Zhang, L., Ross, M., Brozick, J., Fang, Y., Tseng, G., Kim, E., Gambotto, A., Elishaev, E., P. Edwards, R. and Vlad, A. M. (2019) 'Cisplatin-induced immune modulation in ovarian cancer mouse models with distinct inflammation profiles', *Oncogene,* 38(13), pp. 2380-2393.

Grainger, J. R., Smith, K. A., Hewitson, J. P., McSorley, H. J., Harcus, Y., Filbey, K. J., Finney, C. A. M., Greenwood, E. J. D., Knox, D. P., Wilson, M. S., Belkaid, Y., Rudensky, A. Y. and Maizels, R. M. (2010) 'Helminth secretions induce de novo T cell Foxp3 expression and regulatory function through the TGF-β pathway', *The Journal of experimental medicine,* 207(11), pp. 2331-2341.

Greenberg, A. S. and Obin, M. S. (2006) 'Obesity and the role of adipose tissue in inflammation and metabolism', *Am J Clin Nutr,* 83(2), pp. 461s-465s.

Grossmann, M. E., Ray, A., Nkhata, K. J., Malakhov, D. A., Rogozina, O. P., Dogan, S. and Cleary, M. P. (2010) 'Obesity and breast cancer: status of leptin and adiponectin in pathological processes', *Cancer and Metastasis Reviews,* 29(4), pp. 641-653.

Grzych, J. M., Pearce, E., Cheever, A., Caulada, Z. A., Caspar, P., Heiny, S., Lewis, F. and Sher, A. (1991) 'Egg deposition is the major stimulus for the production of Th2 cytokines in murine schistosomiasis mansoni', *J Immunol,* 146(4), pp. 1322-7.

Guo, S. and Deng, C.-X. (2018) 'Effect of Stromal Cells in Tumor Microenvironment on Metastasis Initiation', *International journal of biological sciences,* 14(14), pp. 2083-2093.

Ha , S.-a., Tsuji , M., Suzuki , K., Meek , B., Yasuda , N., Kaisho , T. and Fagarasan , S. (2006) 'Regulation of B1 cell migration by signals through Toll-like receptors', *Journal of Experimental Medicine,* 203(11), pp. 2541-2550.

Halim, Timotheus Y. F., Krauß, Ramona H., Sun, Ann C. and Takei, F. (2012) 'Lung Natural Helper Cells Are a Critical Source of Th2 Cell-Type Cytokines in Protease Allergen-Induced Airway Inflammation', *Immunity,* 36(3), pp. 451-463.

Hams, E., Aviello, G. and Fallon, P. (2013a) 'The Schistosoma Granuloma: Friend or Foe?', *Frontiers in Immunology,* 4(89).

Hams, E., Bermingham, R., Wurlod, F. A., Hogan, A. E., O'Shea, D., Preston, R. J., Rodewald, H.-R., McKenzie, A. N. J. and Fallon, P. G. (2016) 'The helminth T2 RNase ω1 promotes metabolic homeostasis in an IL-33- and group 2 innate lymphoid cell-dependent mechanism', *The FASEB Journal,* 30(2), pp. 824-835.

Hams, E., Locksley, R. M., McKenzie, A. N. J. and Fallon, P. G. (2013b) 'Cutting Edge: IL-25 Elicits Innate Lymphoid Type 2 and Type II NKT Cells That Regulate Obesity in Mice', *The Journal of Immunology,* 191(11), pp. 5349-5353.

Han, S. J., Glatman Zaretsky, A., Andrade-Oliveira, V., Collins, N., Dzutsev, A., Shaik, J., Morais da Fonseca, D., Harrison, O. J., Tamoutounour, S., Byrd, A. L., Smelkinson, M., Bouladoux, N., Bliska, J. B., Brenchley, J. M., Brodsky, I. E. and Belkaid, Y. (2017) 'White Adipose Tissue Is a Reservoir for Memory T Cells and Promotes Protective Memory Responses to Infection', *Immunity,* 47(6), pp. 1154-1168 e6.

Hara, H., Ishihara, C., Takeuchi, A., Imanishi, T., Xue, L., Morris, S. W., Inui, M., Takai, T., Shibuya, A., Saijo, S., Iwakura, Y., Ohno, N., Koseki, H., Yoshida, H., Penninger, J. M. and Saito, T. (2007) 'The adaptor protein CARD9 is essential for the activation of myeloid cells through ITAM-associated and Toll-like receptors', *Nature Immunology,* 8(6), pp. 619-629.

Hardman, C. S., Panova, V. and McKenzie, A. N. (2013) 'IL-33 citrine reporter mice reveal the temporal and spatial expression of IL-33 during allergic lung inflammation', *Eur J Immunol,* 43(2), pp. 488-98.

Harms, M. and Seale, P. (2013) 'Brown and beige fat: development, function and therapeutic potential', *Nat Med,* 19(10), pp. 1252-63.

Hashiguchi, M., Kashiwakura, Y., Kojima, H., Kobayashi, A., Kanno, Y. and Kobata, T. (2015) 'IL-33 activates eosinophils of visceral adipose tissue both directly and via innate lymphoid cells', *Eur J Immunol,* 45(3), pp. 876-85.

Hazenberg, M. D. and Spits, H. (2014) 'Human innate lymphoid cells', *Blood,* 124(5), pp. 700-709.

He, Z., Chen, L., Souto, F. O., Canasto-Chibuque, C., Bongers, G., Deshpande, M., Harpaz, N., Ko, H. M., Kelley, K., Furtado, G. C. and Lira, S. A. (2017) 'Epithelial-derived IL-33 promotes intestinal tumorigenesis in Apc (Min/+) mice', *Sci Rep,* 7(1), pp. 5520.

Healy, J. and H Reznek, R. (1998) *The peritoneum, mesenteries and omenta: Normal anatomy and pathological processes.*

Hepworth, M. R., Daniłowicz-Luebert, E., Rausch, S., Metz, M., Klotz, C., Maurer, M. and Hartmann, S. (2012) 'Mast cells orchestrate type 2 immunity to helminths through regulation of tissue-derived cytokines', *Proceedings of the National Academy of Sciences of the United States of America,* 109(17), pp. 6644-6649.

Herbert, D. B. R., Hölscher, C., Mohrs, M., Arendse, B., Schwegmann, A., Radwanska, M., Leeto, M., Kirsch, R., Hall, P., Mossmann, H., Claussen, B., Förster, I. and Brombacher, F. (2004) 'Alternative Macrophage Activation Is Essential for Survival during Schistosomiasis and Downmodulates T Helper 1 Responses and Immunopathology', *Immunity,* 20(5), pp. 623-635.

Hirosue, S. and Dubrot, J. (2015) 'Modes of Antigen Presentation by Lymph Node Stromal Cells and Their Immunological Implications', *Frontiers in Immunology,* 6(446).

Hoffman, W., Lakkis, F. G. and Chalasani, G. (2016) 'B Cells, Antibodies, and More', *Clin J Am Soc Nephrol,* 11(1), pp. 137-54.

Holtfreter, M. C., Stachs, O., Reichard, M., Loebermann, M., Guthoff, R. F. and Reisinger, E. C. (2011) 'Confocal Laser Scanning Microscopy for Detection of Schistosoma mansoni Eggs in the Gut of Mice', *PLOS ONE,* 6(4), pp. e18799.

Hotamisligil, G., Shargill, N. and Spiegelman, B. (1993) 'Adipose expression of tumor necrosis factor-alpha: direct role in obesity-linked insulin resistance', *Science,* 259(5091), pp. 87-91.

Hotez, P. J., Brindley, P. J., Bethony, J. M., King, C. H., Pearce, E. J. and Jacobson, J. (2008) 'Helminth infections: the great neglected tropical diseases', *The Journal of clinical investigation,* 118(4), pp. 1311-1321.

Hotez, P. J., Bundy, D. A., Kathleen., B., Brooker, S., Drake, L., de Silva, N., Montresor, A., Engels, D., Jukes, M., Chitsulo, L., Chow, J., Laxminarayan, R., Michaud, C., Bethony, J., Correa-Oliveira, R., Shuhua, X., Fenwick, A. and Savioli, L. (2006) 'Helminth Infections: Soil-transmitted Helminth Infections and Schistosomiasis

', in Jamison, D., Breman, J. & Measham, A. (eds.) *Disease Control Priorities in Developing Countries.* 2nd edition ed. Washington (DC).

Hoyler, T., Klose, C. S., Souabni, A., Turqueti-Neves, A., Pfeifer, D., Rawlins, E. L., Voehringer, D., Busslinger, M. and Diefenbach, A. (2012) 'The transcription factor GATA-3 controls cell fate and maintenance of type 2 innate lymphoid cells', *Immunity,* 37(4), pp. 634-48.

Huang, Y., Guo, L., Qiu, J., Chen, X., Hu-Li, J., Siebenlist, U., Williamson, P. R., Urban, J. F., Jr. and Paul, W. E. (2015) 'IL-25-responsive, lineage-negative KLRG1(hi) cells are multipotential 'inflammatory' type 2 innate lymphoid cells', *Nat Immunol,* 16(2), pp. 161-9.

Huang, Y., Mao, K., Chen, X., Sun, M.-a., Kawabe, T., Li, W., Usher, N., Zhu, J., Urban, J. F., Paul, W. E. and Germain, R. N. (2018a) 'S1P-dependent interorgan trafficking of group 2 innate lymphoid cells supports host defense', *Science,* 359(6371), pp. 114-119.

Huang, Z., Yan, H., Chavan, D., Yuan, Z., Yang, X., Zhang, Y., Song, K. and Kong, B. (2018b) 'Effective treatment of a patient with stage IV ovarian cancer: A case report', *Oncology letters,* 15(1), pp. 588-591.

Hui, H. and Feng, T. (2018) 'Adipose Tissue as an Endocrine Organ'.

Humphreys, N. E., Xu, D., Hepworth, M. R., Liew, F. Y. and Grencis, R. K. (2008) 'IL-33, a Potent Inducer of Adaptive Immunity to Intestinal Nematodes', *The Journal of Immunology,* 180(4), pp. 2443-2449.

Hung, L.-Y., Lewkowich, I. P., Dawson, L. A., Downey, J., Yang, Y., Smith, D. E. and Herbert, D. B. R. (2013) 'IL-33 drives biphasic IL-13 production for noncanonical Type 2 immunity against hookworms', *Proceedings of the National Academy of Sciences,* 110(1), pp. 282-287.

Hussaarts, L., García-Tardón, N., van Beek, L., Heemskerk, M. M., Haeberlein, S., van der Zon, G. C., Ozir-Fazalalikhan, A., Berbée, J. F. P., van Dijk, K. W., van Harmelen, V., Yazdanbakhsh, M. and Guigas, B. (2015) 'Chronic helminth infection and helminth-derived egg antigens promote adipose tissue M2 macrophages and improve insulin sensitivity in obese mice', *The FASEB Journal,* 29(7), pp. 3027-3039.

Hwang, W.-T., Adams, S. F., Tahirovic, E., Hagemann, I. S. and Coukos, G. (2012) 'Prognostic significance of tumor-infiltrating T cells in ovarian cancer: A meta-analysis', *Gynecologic Oncology,* 124(2), pp. 192-198.

Ibrahim, M. M. (2010) 'Subcutaneous and visceral adipose tissue: structural and functional differences', *Obes Rev,* 11(1), pp. 11-8.

Islam, S. A., Chang, D. S., Colvin, R. A., Byrne, M. H., McCully, M. L., Moser, B., Lira, S. A., Charo, I. F. and Luster, A. D. (2011) 'Mouse CCL8, a CCR8 agonist, promotes atopic dermatitis by recruiting IL-5+ T(H)2 cells', *Nat Immunol,* 12(2), pp. 167-77.

Iwagoi, Y., Motohara, T., Hwang, S., Fujimoto, K., Ikeda, T. and Katabuchi, H. (2021) 'Omental metastasis as a predictive risk factor for unfavorable prognosis in patients with stage III–IV epithelial ovarian cancer', *International Journal of Clinical Oncology*.

Jackson-Jones, L. H. and Bénézech, C. (2018) 'Control of innate-like B cell location for compartmentalised IgM production', *Current Opinion in Immunology,* 50, pp. 9-13.

Jackson-Jones, L. H., Duncan, S. M., Magalhaes, M. S., Campbell, S. M., Maizels, R. M., McSorley, H. J., Allen, J. E. and Bénézech, C. (2016) 'Fat-associated lymphoid clusters control local IgM secretion during pleural infection and lung inflammation', *Nature Communications,* 7, pp. 12651.

Jackson-Jones, L. H., Smith, P., Magalhaes, M. S., Portman, J. R., Mylonas, K. J., Nixon, M., Henderson, B. E. P., Dobie, R., Henderson, N. C., Mole, D. J. and Bénézech, C. (2019) 'Neutrophils mediate the capture of peritoneal contaminants by fat-associated lymphoid clusters of the omentum', *bioRxiv*, pp. 774968.

Jankovic, D., Kullberg, M. C., Noben-Trauth, N., Caspar, P., Ward, J. M., Cheever, A. W., Paul, W. E. and Sher, A. (1999) 'Schistosome-Infected IL-4 Receptor Knockout (KO) Mice, in Contrast to IL-4 KO Mice, Fail to Develop Granulomatous Pathology While Maintaining the Same Lymphokine Expression Profile', *The Journal of Immunology,* 163(1), pp. 337-342.

Jiao, P., Chen, Q., Shah, S., Du, J., Tao, B., Tzameli, I., Yan, W. and Xu, H. (2009) 'Obesity-Related Upregulation of Monocyte Chemotactic Factors in Adipocytes', *Involvement of Nuclear Factor-κB and c-Jun NH₂-Terminal Kinase Pathways,* 58(1), pp. 104-115.

Johnston, C. J. C., Robertson, E., Harcus, Y., Grainger, J. R., Coakley, G., Smyth, D. J., McSorley, H. J. and Maizels, R. (2015) 'Cultivation of Heligmosomoides polygyrus: an immunomodulatory nematode parasite and its secreted products', *Journal of visualized experiments : JoVE,* (98), pp. e52412-e52412.

Jones, G. W., Hill, D. G. and Jones, S. A. (2016) 'Understanding Immune Cells in Tertiary Lymphoid Organ Development: It Is All Starting to Come Together', *Frontiers in immunology,* 7, pp. 401-401.

Jones, R., Cosway, E. J., Willis, C., White, A. J., Jenkinson, W. E., Fehling, H. J., Anderson, G. and Withers, D. R. (2018) 'Dynamic changes in intrathymic ILC populations during murine neonatal development', *European journal of immunology,* 48(9), pp. 1481-1491.

Kaczanowska, S., Joseph, A. M. and Davila, E. (2013) 'TLR agonists: our best frenemy in cancer immunotherapy', *Journal of leukocyte biology,* 93(6), pp. 847-863.

Kamizono, S., Duncan, G. S., Seidel, M. G., Morimoto, A., Hamada, K., Grosveld, G., Akashi, K., Lind, E. F., Haight, J. P., Ohashi, P. S., Look, A. T. and Mak, T. W. (2009) 'Nfil3/E4bp4 is required for the development and maturation of NK cells in vivo', *J Exp Med,* 206(13), pp. 2977-86.

Karagiannides, I. and Pothoulakis, C. (2008) 'Neuropeptides, Mesenteric Fat, and Intestinal Inflammation', *Annals of the New York Academy of Sciences,* 1144(1), pp. 127-135.

Kawasaki, T. and Kawai, T. (2014) 'Toll-Like Receptor Signaling Pathways', *Frontiers in Immunology,* 5(461).

Keating, A. (2006) 'Mesenchymal stromal cells', *Current opinion in hematology,* 13(6), pp. 419-425.

Kehoe, S., Hook, J., Nankivell, M., Jayson, G. C., Kitchener, H., Lopes, T., Luesley, D., Perren, T., Bannoo, S., Mascarenhas, M., Dobbs, S., Essapen, S., Twigg, J., Herod, J., McCluggage, G., Parmar, M. and Swart, A.-M. (2015) 'Primary chemotherapy versus primary surgery for newly diagnosed advanced ovarian cancer (CHORUS): an open-label, randomised, controlled, non-inferiority trial', *The Lancet,* 386(9990), pp. 249-257.

Kellie, S. and Al-Mansour, Z. (2017) 'Chapter Four - Overview of the Immune System', in Skwarczynski, M. & Toth, I. (eds.) *Micro and Nanotechnology in Vaccine Development*: William Andrew Publishing, pp. 63-81.

Kim, C. H., Hashimoto-Hill, S. and Kim, M. (2016) 'Migration and Tissue Tropism of Innate Lymphoid Cells', *Trends in Immunology,* 37(1), pp. 68-79.

Kim, Myung H., Taparowsky, Elizabeth J. and Kim, Chang H. (2015) 'Retinoic Acid Differentially Regulates the Migration of Innate Lymphoid Cell Subsets to the Gut', *Immunity,* 43(1), pp. 107-119.

King, C. L., Medhat, A., Malhotra, I., Nafeh, M., Helmy, A., Khaudary, J., Ibrahim, S., El-Sherbiny, M., Zaky, S., Stupi, R. J., Brustoski, K., Shehata, M. and Shata, M. T. (1996) 'Cytokine control of parasite-specific anergy in human urinary schistosomiasis. IL-10 modulates lymphocyte reactivity', *The Journal of Immunology,* 156(12), pp. 4715-4721.

Kiss, M., Van Gassen, S., Movahedi, K., Saeys, Y. and Laoui, D. (2018) 'Myeloid cell heterogeneity in cancer: not a single cell alike', *Cellular Immunology,* 330, pp. 188-201.

Klein Wolterink, R. G., Kleinjan, A., van Nimwegen, M., Bergen, I., de Bruijn, M., Levani, Y. and Hendriks, R. W. (2012) 'Pulmonary innate lymphoid cells are major producers of IL-5 and IL-13 in murine models of allergic asthma', *Eur J Immunol,* 42(5), pp. 1106-16.

Klose, C. S. N., Kiss, E. A., Schwierzeck, V., Ebert, K., Hoyler, T., d'Hargues, Y., Göppert, N., Croxford, A. L., Waisman, A., Tanriver, Y. and Diefenbach, A. (2013) 'A T-bet gradient controls the fate and function of CCR6−RORγt+ innate lymphoid cells', *Nature,* 494(7436), pp. 261-265.

Knipfer, L., Schulz-Kuhnt, A., Kindermann, M., Greif, V., Symowski, C., Voehringer, D., Neurath, M. F., Atreya, I. and Wirtz, S. (2019) 'A CCL1/CCR8-dependent feed-forward mechanism drives ILC2 functions in type 2–mediated inflammation', *Journal of Experimental Medicine,* 216(12), pp. 2763-2777.

Kolodin, D., van Panhuys, N., Li, C., Magnuson, A. M., Cipolletta, D., Miller, C. M., Wagers, A., Germain, R. N., Benoist, C. and Mathis, D. (2015) 'Antigen- and cytokine-driven accumulation of regulatory T cells in visceral adipose tissue of lean mice', *Cell Metab,* 21(4), pp. 543-57.

Koning, J. J. and Mebius, R. E. (2012) 'Interdependence of stromal and immune cells for lymph node function', *Trends Immunol,* 33(6), pp. 264-70.

Kossaï, M., Leary, A., Scoazec, J. Y. and Genestie, C. (2018) 'Ovarian Cancer: A Heterogeneous Disease', *Pathobiology,* 85(1-2), pp. 41-49.

Kovacsovics-Bankowski, M., Chisholm, L., Vercellini, J., Tucker, C. G., Montler, R., Haley, D., Newell, P., Ma, J., Tseng, P., Wolf, R., Vetto, J. T., Hammill, C., Hansen, P. and Weinberg, A. D. (2014) 'Detailed characterization of tumor infiltrating lymphocytes in two distinct human solid malignancies show phenotypic similarities', *Journal for immunotherapy of cancer,* 2(1), pp. 38-38.

Koyama, S. and Nishikawa, H. (2021) 'Mechanisms of regulatory T cell infiltration in tumors: implications for innovative immune precision therapies', *Journal for ImmunoTherapy of Cancer,* 9(7), pp. e002591.

Krishnan, V., Tallapragada, S., Schaar, B., Kamat, K., Chanana, A. M., Zhang, Y., Patel, S., Parkash, V., Rinker-Schaeffer, C., Folkins, A. K., Rankin, E. B. and Dorigo, O. (2020) 'Omental macrophages secrete chemokine ligands that promote ovarian cancer colonization of the omentum via CCR1', *Communications Biology,* 3(1), pp. 524.

Kufareva, I., Salanga, C. L. and Handel, T. M. (2015) 'Chemokine and chemokine receptor structure and interactions: implications for therapeutic strategies', *Immunol Cell Biol,* 93(4), pp. 372-83.

Kurnit, K. C., Fleming, G. F. and Lengyel, E. (2021) 'Updates and New Options in Advanced Epithelial Ovarian Cancer Treatment', *Obstetrics and gynecology,* 137(1), pp. 108-121.

Kurosaki, T., Kometani, K. and Ise, W. (2015) 'Memory B cells', *Nature Reviews Immunology,* 15(3), pp. 149-159.

Lai, K. N. and Leung, J. C. K. (2010) 'Peritoneal adipocytes and their role in inflammation during peritoneal dialysis', *Mediators of inflammation,* 2010, pp. 495416-495416.

Larsen, K. M., Minaya, M. K., Vaish, V. and Peña, M. M. O. (2018) 'The Role of IL-33/ST2 Pathway in Tumorigenesis', *International journal of molecular sciences,* 19(9), pp. 2676.

Lawler, J. (2009) 'Introduction to the tumour microenvironment review series', *Journal of cellular and molecular medicine,* 13(8A), pp. 1403-1404.

LeBien, T. W. and Tedder, T. F. (2008) 'B lymphocytes: how they develop and function', *Blood,* 112(5), pp. 1570-80.

Lee, J. S., Cella, M., McDonald, K. G., Garlanda, C., Kennedy, G. D., Nukaya, M., Mantovani, A., Kopan, R., Bradfield, C. A., Newberry, R. D. and Colonna, M. (2011) 'AHR drives the development of gut ILC22 cells and postnatal lymphoid tissues via pathways dependent on and independent of Notch', *Nature immunology,* 13(2), pp. 144-151.

Lee, M. W., Odegaard, J. I., Mukundan, L., Qiu, Y., Molofsky, A. B., Nussbaum, J. C., Yun, K., Locksley, R. M. and Chawla, A. (2015) 'Activated type 2 innate lymphoid cells regulate beige fat biogenesis', *Cell,* 160(1-2), pp. 74-87.

Lee, W., Ko, S.-Y., S. Mohamed, M., Kenny, H., Lengyel, E. and Naora, H. (2018) *Neutrophils facilitate ovarian cancer premetastatic niche formation in the omentum.*

Leffers, N., Gooden, M. J., de Jong, R. A., Hoogeboom, B. N., ten Hoor, K. A., Hollema, H., Boezen, H. M., van der Zee, A. G., Daemen, T. and Nijman, H. W. (2009) 'Prognostic significance of tumor-

infiltrating T-lymphocytes in primary and metastatic lesions of advanced stage ovarian cancer', *Cancer Immunol Immunother,* 58(3), pp. 449-59.

Lengyel, E. (2010) 'Ovarian Cancer Development and Metastasis', *The American Journal of Pathology,* 177(3), pp. 1053-1064.

Lengyel, E., Makowski, L., DiGiovanni, J. and Kolonin, M. G. (2018) 'Cancer as a Matter of Fat: The Crosstalk between Adipose Tissue and Tumors', *Trends in cancer,* 4(5), pp. 374-384.

Li, Y., Shi, J., Qi, S., Zhang, J., Peng, D., Chen, Z., Wang, G., Wang, Z. and Wang, L. (2018) 'IL-33 facilitates proliferation of colorectal cancer dependent on COX2/PGE2', *Journal of Experimental & Clinical Cancer Research,* 37(1), pp. 196.

Lisio, M.-A., Fu, L., Goyeneche, A., Gao, Z.-H. and Telleria, C. (2019) 'High-Grade Serous Ovarian Cancer: Basic Sciences, Clinical and Therapeutic Standpoints', *International journal of molecular sciences,* 20(4), pp. 952.

Litbarg, N. O., Gudehithlu, K. P., Sethupathi, P., Arruda, J. A. L., Dunea, G. and Singh, A. K. (2007) 'Activated omentum becomes rich in factors that promote healing and tissue regeneration', *Cell and Tissue Research,* 328(3), pp. 487-497.

Liu, X., Hansen, D. M., Timko, N. J., Zhu, Z., Ames, A., Qin, C., Nicholl, M. B., Bai, Q., Chen, X., Wakefield, M. R., West, G. and Fang, Y. (2019) 'Association between interleukin33 and ovarian cancer', *Oncol Rep,* 41(2), pp. 1045-1050.

Liu, X., Zhu, L., Lu, X., Bian, H., Wu, X., Yang, W. and Qin, Q. (2014) 'IL-33/ST2 pathway contributes to metastasis of human colorectal cancer', *Biochem Biophys Res Commun,* 453(3), pp. 486-92.

Lochner, M., Ohnmacht, C., Presley, L., Bruhns, P., Si-Tahar, M., Sawa, S. and Eberl, G. (2011) 'Microbiota-induced tertiary lymphoid tissues aggravate inflammatory disease in the absence of RORgamma t and LTi cells', *The Journal of experimental medicine,* 208(1), pp. 125-134.

Lopes Cardozo, A. M. F., Gupta, A., Koppe, M. J., Meijer, S., van Leeuwen, P. A. M., Beelen, R. J. H. and Bleichrodt, R. P. (2001) 'Metastatic pattern of CC531 colon carcinoma cells in the abdominal cavity: an experimental model of peritoneal carcinomatosis in rats', *European Journal of Surgical Oncology (EJSO),* 27(4), pp. 359-363.

López-Soto, A., Gonzalez, S., Smyth, M. J. and Galluzzi, L. (2017) 'Control of Metastasis by NK Cells', *Cancer Cell,* 32(2), pp. 135-154.

Luckheeram, R. V., Zhou, R., Verma, A. D. and Xia, B. (2012) 'CD4^{+}T cells: differentiation and functions', *Clinical & developmental immunology,* 2012, pp. 925135-925135.

Lumeng, C. N., Bodzin, J. L. and Saltiel, A. R. (2007) 'Obesity induces a phenotypic switch in adipose tissue macrophage polarization', *J Clin Invest,* 117(1), pp. 175-84.

Luo, L. and Liu, M. (2016) 'Adipose tissue in control of metabolism', *J Endocrinol,* 231(3), pp. R77-r99.

M. Webb, L. and D. Tait Wojno, E. (2017) 'The role of rare innate immune cells in Type 2 immune activation against parasitic helminths', *Parasitology* 144(10), pp. 1-14.

Macciò, A., Gramignano, G., Cherchi, M. C., Tanca, L., Melis, L. and Madeddu, C. (2020) 'Role of M1-polarized tumor-associated macrophages in the prognosis of advanced ovarian cancer patients', *Scientific Reports,* 10(1), pp. 6096.

Mackley, E. C., Houston, S., Marriott, C. L., Halford, E. E., Lucas, B., Cerovic, V., Filbey, K. J., Maizels, R. M., Hepworth, M. R., Sonnenberg, G. F., Milling, S. and Withers, D. R. (2015) 'CCR7-dependent trafficking of RORγ+ ILCs creates a unique microenvironment within mucosal draining lymph nodes', *Nature Communications,* 6(1), pp. 5862.

Mahlakoiv, T., Flamar, A. L., Johnston, L. K., Moriyama, S., Putzel, G. G., Bryce, P. J. and Artis, D. (2019) 'Stromal cells maintain immune cell homeostasis in adipose tissue via production of interleukin-33', *Sci Immunol,* 4(35).

Maizels, R. M., Hewitson, J. P. and Smith, K. A. (2012) 'Susceptibility and immunity to helminth parasites', *Current opinion in immunology,* 24(4), pp. 459-466.

Mantovani, A., Allavena, P., Sica, A. and Balkwill, F. (2008) 'Cancer-related inflammation', *Nature,* 454(7203), pp. 436-44.

Mantovani, A., Sica, A., Sozzani, S., Allavena, P., Vecchi, A. and Locati, M. (2004) 'The chemokine system in diverse forms of macrophage activation and polarization', *Trends Immunol,* 25(12), pp. 677-86.

Masucci, M. T., Minopoli, M. and Carriero, M. V. (2019) 'Tumor Associated Neutrophils. Their Role in Tumorigenesis, Metastasis, Prognosis and Therapy', *Frontiers in Oncology,* 9(1146).

McManus, D. P., Bergquist, R., Cai, P., Ranasinghe, S., Tebeje, B. M. and You, H. (2020) 'Schistosomiasis—from immunopathology to vaccines', *Seminars in Immunopathology*.

McManus, D. P., Dunne, D. W., Sacko, M., Utzinger, J., Vennervald, B. J. and Zhou, X.-N. (2018) 'Schistosomiasis', *Nature Reviews Disease Primers,* 4(1), pp. 13.

McMullen, J. R. W., Selleck, M., Wall, N. R. and Senthil, M. (2017) 'Peritoneal carcinomatosis: limits of diagnosis and the case for liquid biopsy', *Oncotarget,* 8(26), pp. 43481-43490.

McSorley, H. J. and Maizels, R. M. (2012) 'Helminth Infections and Host Immune Regulation', *Clinical Microbiology Reviews,* 25(4), pp. 585-608.

Medzhitov, R. and Janeway, C. A. (1997) 'Innate immunity: impact on the adaptive immune response', *Current Opinion in Immunology,* 9(1), pp. 4-9.

Meinicke, H., Bremser, A., Brack, M., Akeus, P., Pearson, C., Bullers, S., Hoffmeyer, K., Stemmler, M. P., Quiding-Järbrink, M. and Izcue, A. (2017) 'Tumour-associated changes in intestinal epithelial cells cause local accumulation of KLRG1+ GATA3+ regulatory T cells in mice', *Immunology,* 152(1), pp. 74-88.

Merlo, L. M. F. and Mandik-Nayak, L. (2013) 'Chapter 3 - Adaptive Immunity: B Cells and Antibodies', in Prendergast, G.C. & Jaffee, E.M. (eds.) *Cancer Immunotherapy (Second Edition)*. San Diego: Academic Press, pp. 25-40.

Meza-Perez, S. and Randall, T. D. (2017) 'Immunological Functions of the Omentum', *Trends Immunol,* 38(7), pp. 526-536.

Mikhak, Z., Fukui, M., Farsidjani, A., Medoff, B. D., Tager, A. M. and Luster, A. D. (2009) 'Contribution of CCR4 and CCR8 to antigen-specific TH2 cell trafficking in allergic pulmonary inflammation', *Journal of Allergy and Clinical Immunology,* 123(1), pp. 67-73.e3.

Mirchandani, A. S., Besnard, A.-G., Yip, E., Scott, C., Bain, C. C., Cerovic, V., Salmond, R. J. and Liew, F. Y. (2014) 'Type 2 Innate Lymphoid Cells Drive CD4⁺ Th2 Cell Responses', *The Journal of Immunology,* 192(5), pp. 2442-2448.

Mitsdoerffer, M. and Peters, A. (2016) 'Tertiary Lymphoid Organs in Central Nervous System Autoimmunity', *Frontiers in immunology,* 7, pp. 451-451.

Mogensen, T. H. (2009) 'Pathogen recognition and inflammatory signaling in innate immune defenses', *Clinical microbiology reviews,* 22(2), pp. 240-273.

Mohrs, K., Harris, D. P., Lund, F. E. and Mohrs, M. (2005) 'Systemic dissemination and persistence of Th2 and type 2 cells in response to infection with a strictly enteric nematode parasite', *J Immunol,* 175(8), pp. 5306-13.

Mohrs, M., Shinkai, K., Mohrs, K. and Locksley, R. M. (2001) 'Analysis of Type 2 Immunity In Vivo with a Bicistronic IL-4 Reporter', *Immunity,* 15(2), pp. 303-311.

Molofsky, A. B., Nussbaum, J. C., Liang, H. E., Van Dyken, S. J., Cheng, L. E., Mohapatra, A., Chawla, A. and Locksley, R. M. (2013) 'Innate lymphoid type 2 cells sustain visceral adipose tissue eosinophils and alternatively activated macrophages', *J Exp Med,* 210(3), pp. 535-49.

Molofsky, Ari B., Savage, Adam K. and Locksley, Richard M. (2015) 'Interleukin-33 in Tissue Homeostasis, Injury, and Inflammation', *Immunity,* 42(6), pp. 1005-1019.

Momenimovahed, Z., Tiznobaik, A., Taheri, S. and Salehiniya, H. (2019) 'Ovarian cancer in the world: epidemiology and risk factors', *International journal of women's health,* 11, pp. 287-299.

Moro, K., Ealey, K. N., Kabata, H. and Koyasu, S. (2015) 'Isolation and analysis of group 2 innate lymphoid cells in mice', *Nat Protoc,* 10(5), pp. 792-806.

Moro, K., Kabata, H., Tanabe, M., Koga, S., Takeno, N., Mochizuki, M., Fukunaga, K., Asano, K., Betsuyaku, T. and Koyasu, S. (2016) 'Interferon and IL-27 antagonize the function of group 2 innate lymphoid cells and type 2 innate immune responses', *Nature Immunology,* 17(1), pp. 76-86.

Moro, K., Yamada, T., Tanabe, M., Takeuchi, T., Ikawa, T., Kawamoto, H., Furusawa, J.-i., Ohtani, M., Fujii, H. and Koyasu, S. (2010) 'Innate production of TH2 cytokines by adipose tissue-associated c-Kit+Sca-1+ lymphoid cells', *Nature,* 463, pp. 540.

Mosser, D. M. and Edwards, J. P. (2008) 'Exploring the full spectrum of macrophage activation', *Nature reviews. Immunology,* 8(12), pp. 958-969.

Motohara, T., Masuda, K., Morotti, M., Zheng, Y., El-Sahhar, S., Chong, K. Y., Wietek, N., Alsaadi, A., Karaminejadranjbar, M., Hu, Z., Artibani, M., Gonzalez, L. S., Katabuchi, H., Saya, H. and Ahmed, A. A. (2019) 'An evolving story of the metastatic voyage of ovarian cancer cells: cellular and molecular orchestration of the adipose-rich metastatic microenvironment', *Oncogene,* 38(16), pp. 2885-2898.

Mukendi, J. P. K., Nakamura, R., Uematsu, S. and Hamano, S. (2021) 'Interleukin (IL)-33 is dispensable for Schistosoma mansoni worm maturation and the maintenance of egg-induced pathology in intestines of infected mice', *Parasites & Vectors,* 14(1), pp. 70.

Nakaya, Y., Lilue, J., Stavrou, S., Moran, E. A. and Ross, S. R. (2017) 'AIM2-Like Receptors Positively and Negatively Regulate the Interferon Response Induced by Cytosolic DNA', *mBio,* 8(4), pp. e00944-17.

Nausch, N. and Mutapi, F. (2018) 'Group 2 ILCs: A way of enhancing immune protection against human helminths?', *Parasite Immunol,* 40(2).

Neill, D. R., Wong, S. H., Bellosi, A., Flynn, R. J., Daly, M., Langford, T. K. A., Bucks, C., Kane, C. M., Fallon, P. G., Pannell, R., Jolin, H. E. and McKenzie, A. N. J. (2010) 'Nuocytes represent a new innate effector leukocyte that mediates type-2 immunity', *Nature,* 464(7293), pp. 1367-1370.

Nelwan, M. L. (2019) 'Schistosomiasis: Life Cycle, Diagnosis, and Control', *Current therapeutic research, clinical and experimental,* 91, pp. 5-9.

Neyt, K., Perros, F., GeurtsvanKessel, C. H., Hammad, H. and Lambrecht, B. N. (2012) 'Tertiary lymphoid organs in infection and autoimmunity', *Trends in Immunology,* 33(6), pp. 297-305.

Nieman, K. M., Kenny, H. A., Penicka, C. V., Ladanyi, A., Buell-Gutbrod, R., Zillhardt, M. R., Romero, I. L., Carey, M. S., Mills, G. B., Hotamisligil, G. S., Yamada, S. D., Peter, M. E., Gwin, K. and Lengyel, E. (2011) 'Adipocytes promote ovarian cancer metastasis and provide energy for rapid tumor growth', *Nature Medicine,* 17, pp. 1498.

Nowak, M. and Klink, M. (2020) 'The Role of Tumor-Associated Macrophages in the Progression and Chemoresistance of Ovarian Cancer', *Cells,* 9(5), pp. 1299.

Nussbaum, J. C., Van Dyken, S. J., von Moltke, J., Cheng, L. E., Mohapatra, A., Molofsky, A. B., Thornton, E. E., Krummel, M. F., Chawla, A., Liang, H.-E. and Locksley, R. M. (2013) 'Type 2 innate lymphoid cells control eosinophil homeostasis', *Nature,* 502(7470), pp. 245-248.

Nutten, S., Trottein, F., Gounni, A., Papin, J.-P., Capron, A. and Capron, M. (1997) 'From Allergy to Schistosomes: Role of Fc Receptors and Adhesion Molecules in Eosinophil Effector Function', *Memórias do Instituto Oswaldo Cruz,* 92 Suppl 2, pp. 9-14.

O'Donnell, C., Mahmoud, A., Keane, J., Murphy, C., White, D., Carey, S., O'Riordain, M., Bennett, M. W., Brint, E. and Houston, A. (2015) 'An antitumorigenic role for the IL-33 receptor, ST2L, in colon cancer', *British Journal Of Cancer,* 114, pp. 37.

Ohne, Y., Silver, J. S., Thompson-Snipes, L., Collet, M. A., Blanck, J. P., Cantarel, B. L., Copenhaver, A. M., Humbles, A. A. and Liu, Y.-J. (2016) 'IL-1 is a critical regulator of group 2 innate lymphoid cell function and plasticity', *Nature Immunology,* 17(6), pp. 646-655.

Oliphant, C. J., Hwang, Y. Y., Walker, J. A., Salimi, M., Wong, S. H., Brewer, J. M., Englezakis, A., Barlow, J. L., Hams, E., Scanlon, S. T., Ogg, G. S., Fallon, P. G. and McKenzie, A. N. J. (2014a) 'MHCII-mediated dialog between group 2 innate lymphoid cells and CD4(+) T cells potentiates type 2 immunity and promotes parasitic helminth expulsion', *Immunity,* 41(2), pp. 283-295.

Oliphant, Christopher J., Hwang, You Y., Walker, Jennifer A., Salimi, M., Wong, See H., Brewer, James M., Englezakis, A., Barlow, Jillian L., Hams, E., Scanlon, Seth T., Ogg, Graham S., Fallon, Padraic G. and McKenzie, Andrew N. J. (2014b) 'MHCII-Mediated Dialog between Group 2 Innate Lymphoid Cells and CD4+ T Cells Potentiates Type 2 Immunity and Promotes Parasitic Helminth Expulsion', *Immunity,* 41(2), pp. 283-295.

Ou, Y., Cannon, M. J. and Nakagawa, M. (2018) 'Regulatory T Cells in Gynecologic Cancer', *MOJ immunology,* 6(2), pp. 34-42.

Owyang, A. M., Zaph, C., Wilson, E. H., Guild, K. J., McClanahan, T., Miller, H. R., Cua, D. J., Goldschmidt, M., Hunter, C. A., Kastelein, R. A. and Artis, D. (2006) 'Interleukin 25 regulates type 2 cytokine-dependent immunity and limits chronic inflammation in the gastrointestinal tract', *J Exp Med,* 203(4), pp. 843-9.

Panduro, M., Benoist, C. and Mathis, D. (2016) 'Tissue Tregs', *Annual review of immunology,* 34, pp. 609-633.

Parkin, J. and Cohen, B. (2001) 'An overview of the immune system', *The Lancet,* 357(9270), pp. 1777-1789.

Pastille, E., Wasmer, M.-H., Adamczyk, A., Vu, V. P., Mager, L. F., Phuong, N. N. T., Palmieri, V., Simillion, C., Hansen, W., Kasper, S., Schuler, M., Muggli, B., McCoy, K. D., Buer, J., Zlobec, I., Westendorf, A. M. and Krebs, P. (2019) 'The IL-33/ST2 pathway shapes the regulatory T cell phenotype to promote intestinal cancer', *Mucosal Immunology,* 12(4), pp. 990-1003.

Paul, S. and Lal, G. (2017) 'The Molecular Mechanism of Natural Killer Cells Function and Its Importance in Cancer Immunotherapy', *Frontiers in Immunology,* 8(1124).

Pearce, E. J., Caspar, P., Grzych, J. M., Lewis, F. A. and Sher, A. (1991) 'Downregulation of Th1 cytokine production accompanies induction of Th2 responses by a parasitic helminth, Schistosoma mansoni', *J Exp Med,* 173(1), pp. 159-66.

Pearce, E. J. and MacDonald, A. S. (2002) 'The immunobiology of schistosomiasis', *Nature Reviews Immunology,* 2(7), pp. 499-511.

Pearce, O. M. T., Delaine-Smith, R. M., Maniati, E., Nichols, S., Wang, J., Böhm, S., Rajeeve, V., Ullah, D., Chakravarty, P., Jones, R. R., Montfort, A., Dowe, T., Gribben, J., Jones, J. L., Kocher, H. M., Serody, J. S., Vincent, B. G., Connelly, J., Brenton, J. D., Chelala, C., Cutillas, P. R., Lockley, M., Bessant, C., Knight, M. M. and Balkwill, F. R. (2018) 'Deconstruction of a Metastatic Tumor Microenvironment Reveals a Common Matrix Response in Human Cancers', *Cancer discovery,* 8(3), pp. 304-319.

Pedras-Vasconcelos, J. A. and Pearce, E. J. (1996) 'Type 1 CD8+ T cell responses during infection with the helminth Schistosoma mansoni', *The Journal of Immunology,* 157(7), pp. 3046-3053.

Pei, C., Zhao, C., Wang, A.-J., Fan, A. X., Grinchuk, V., Smith, A., Sun, R., Xie, Y., Lu, N., Urban, J. F., Shea-Donohue, T., Zhao, A. and Yang, Z. (2016) 'Critical Role for Interleukin-25 in Host Protective Th2 Memory Response against *Heligmosomoides polygyrus bakeri*', *Infection and Immunity,* 84(12), pp. 3328-3337.

Pelly, V. S., Kannan, Y., Coomes, S. M., Entwistle, L. J., Rückerl, D., Seddon, B., MacDonald, A. S., McKenzie, A. and Wilson, M. S. (2016) 'IL-4-producing ILC2s are required for the differentiation of TH2 cells following Heligmosomoides polygyrus infection', *Mucosal Immunology,* 9, pp. 1407.

Pennock, N., White, J., W Cross, E., E Cheney, E., A Tamburini, B. and Kedl, R. (2013) 'T cell responses: Naïve to memory and everything in between', *Advances in physiology education,* 37(4), pp. 273-83.

Platonova, S., Cherfils-Vicini, J., Damotte, D., Crozet, L., Vieillard, V., Validire, P., André, P., Dieu-Nosjean, M.-C., Alifano, M., Régnard, J.-F., Fridman, W.-H., Sautès-Fridman, C. and Cremer, I. (2011) 'Profound Coordinated Alterations of Intratumoral NK Cell Phenotype and Function in Lung Carcinoma', *Cancer Research,* 71(16), pp. 5412-5422.

Plitas, G. and Rudensky, A. Y. (2016) 'Regulatory T Cells: Differentiation and Function', *Cancer immunology research,* 4(9), pp. 721-725.

Pradeep, S., Kim, Seung W., Wu, Sherry Y., Nishimura, M., Chaluvally-Raghavan, P., Miyake, T., Pecot, Chad V., Kim, S.-J., Choi, Hyun J., Bischoff, Farideh Z., Mayer, Julie A., Huang, L., Nick, Alpa M., Hall, Carolyn S., Rodriguez-Aguayo, C., Zand, B., Dalton, Heather J., Arumugam, T., Lee, Ho J., Han, Hee D., Cho, Min S., Rupaimoole, R., Mangala, Lingegowda S., Sehgal, V., Oh, Sang C., Liu, J., Lee, J.-S., Coleman, Robert L., Ram, P., Lopez-Berestein, G., Fidler, Isaiah J. and Sood, Anil K. (2014) 'Hematogenous Metastasis of Ovarian Cancer: Rethinking Mode of Spread', *Cancer Cell,* 26(1), pp. 77-91.

Price, A. E., Liang, H. E., Sullivan, B. M., Reinhardt, R. L., Eisley, C. J., Erle, D. J. and Locksley, R. M. (2010) 'Systemically dispersed innate IL-13-expressing cells in type 2 immunity', *Proc Natl Acad Sci U S A,* 107(25), pp. 11489-94.

Prizment, A. E., Vierkant, R. A., Smyrk, T. C., Tillmans, L. S., Lee, J. J., Sriramarao, P., Nelson, H. H., Lynch, C. F., Thibodeau, S. N., Church, T. R., Cerhan, J. R., Anderson, K. E. and Limburg, P. J. (2016) 'Tumor eosinophil infiltration and improved survival of colorectal cancer patients: Iowa Women's Health Study', *Modern pathology : an official journal of the United States and Canadian Academy of Pathology, Inc,* 29(5), pp. 516-527.

Puttur, F., Denney, L., Gregory, L. G., Vuononvirta, J., Oliver, R., Entwistle, L. J., Walker, S. A., Headley, M. B., McGhee, E. J., Pease, J. E., Krummel, M. F., Carlin, L. M. and Lloyd, C. M. (2019) 'Pulmonary

environmental cues drive group 2 innate lymphoid cell dynamics in mice and humans', *Science Immunology,* 4(36), pp. eaav7638.

Rana, B. M. J., Jou, E., Barlow, J. L., Rodriguez-Rodriguez, N., Walker, J. A., Knox, C., Jolin, H. E., Hardman, C. S., Sivasubramaniam, M., Szeto, A., Cohen, E. S., Scott, I. C., Sleeman, M. A., Chidomere, C. I., Cruz Migoni, S., Caamano, J., Jorgensen, H. F., Carobbio, S., Vidal-Puig, A. and McKenzie, A. N. J. (2019) 'A stromal cell niche sustains ILC2-mediated type-2 conditioning in adipose tissue', *Journal of Experimental Medicine,* 216(9), pp. 1999-2009.

Randall, T. D., Carragher, D. M. and Rangel-Moreno, J. (2008) 'Development of secondary lymphoid organs', *Annual review of immunology,* 26, pp. 627-650.

Rangel-Moreno, J., Moyron-Quiroz, J. E., Carragher, D. M., Kusser, K., Hartson, L., Moquin, A. and Randall, T. D. (2009) 'Omental Milky Spots Develop in the Absence of Lymphoid Tissue-Inducer Cells and Support B and T Cell Responses to Peritoneal Antigens', *Immunity,* 30(5), pp. 731-743.

Rankin, L. C., Groom, J. R., Chopin, M., Herold, M. J., Walker, J. A., Mielke, L. A., McKenzie, A. N. J., Carotta, S., Nutt, S. L. and Belz, G. T. (2013) 'The transcription factor T-bet is essential for the development of NKp46+ innate lymphocytes via the Notch pathway', *Nature Immunology,* 14(4), pp. 389-395.

Rausch, S., Huehn, J., Kirchhoff, D., Rzepecka, J., Schnoeller, C., Pillai, S., Loddenkemper, C., Scheffold, A., Hamann, A., Lucius, R. and Hartmann, S. (2008) 'Functional Analysis of Effector and Regulatory T Cells in a Parasitic Nematode Infection', *Infection and Immunity,* 76(5), pp. 1908-1919.

Rawla, P., Sunkara, T. and Barsouk, A. (2019) 'Epidemiology of colorectal cancer: incidence, mortality, survival, and risk factors', *Przeglad gastroenterologiczny,* 14(2), pp. 89-103.

Reilly, E. C., Wands, J. R. and Brossay, L. (2010) 'Cytokine dependent and independent iNKT cell activation', *Cytokine,* 51(3), pp. 227-231.

Reynolds, L. A., Filbey, K. J. and Maizels, R. M. (2012) 'Immunity to the model intestinal helminth parasite Heligmosomoides polygyrus', *Seminars in immunopathology,* 34(6), pp. 829-846.

Ricardo-Gonzalez, R. R., Van Dyken, S. J., Schneider, C., Lee, J., Nussbaum, J. C., Liang, H.-E., Vaka, D., Eckalbar, W. L., Molofsky, A. B., Erle, D. J. and Locksley, R. M. (2018) 'Tissue signals imprint ILC2 identity with anticipatory function', *Nature Immunology,* 19(10), pp. 1093-1099.

Rostan, O., Arshad, M. I., Piquet-Pellorce, C., Robert-Gangneux, F., Gangneux, J.-P. and Samson, M. (2015) 'Crucial and Diverse Role of the Interleukin-33/ST2 Axis in Infectious Diseases', *Infection and Immunity,* 83(5), pp. 1738-1748.

Ruddle, N. H. and Akirav, E. M. (2009) 'Secondary Lymphoid Organs: Responding to Genetic and Environmental Cues in Ontogeny and the Immune Response', *The Journal of Immunology,* 183(4), pp. 2205-2212.

Saely, C. H., Geiger, K. and Drexel, H. (2012) 'Brown versus White Adipose Tissue: A Mini-Review', *Gerontology,* 58(1), pp. 15-23.

Saijo, S., Ikeda, S., Yamabe, K., Kakuta, S., Ishigame, H., Akitsu, A., Fujikado, N., Kusaka, T., Kubo, S., Chung, S.-h., Komatsu, R., Miura, N., Adachi, Y., Ohno, N., Shibuya, K., Yamamoto, N., Kawakami, K., Yamasaki, S., Saito, T., Akira, S. and Iwakura, Y. (2010) 'Dectin-2 Recognition of α-Mannans and Induction of Th17 Cell Differentiation Is Essential for Host Defense against Candida albicans', *Immunity,* 32(5), pp. 681-691.

Salimi, M., Barlow, J. L., Saunders, S. P., Xue, L., Gutowska-Owsiak, D., Wang, X., Huang, L.-C., Johnson, D., Scanlon, S. T., McKenzie, A. N. J., Fallon, P. G. and Ogg, G. S. (2013) 'A role for IL-25 and IL-33–driven type-2 innate lymphoid cells in atopic dermatitis', *Journal of Experimental Medicine,* 210(13), pp. 2939-2950.

Salimi, M., Wang, R., Yao, X., Li, X., Wang, X., Hu, Y., Chang, X., Fan, P., Dong, T. and Ogg, G. (2018) 'Activated innate lymphoid cell populations accumulate in human tumour tissues', *BMC cancer,* 18(1), pp. 341-341.

Sasaki, T., Moro, K., Kubota, T., Kubota, N., Kato, T., Ohno, H., Nakae, S., Saito, H. and Koyasu, S. (2019) 'Innate Lymphoid Cells in the Induction of Obesity', *Cell Reports,* 28(1), pp. 202-217.e7.

Sato, E., Olson, S. H., Ahn, J., Bundy, B., Nishikawa, H., Qian, F., Jungbluth, A. A., Frosina, D., Gnjatic, S., Ambrosone, C., Kepner, J., Odunsi, T., Ritter, G., Lele, S., Chen, Y.-T., Ohtani, H., Old, L. J. and Odunsi, K. (2005) 'Intraepithelial CD8+ tumor-infiltrating lymphocytes and a high CD8+regulatory T cell ratio are associated with favorable prognosis in ovarian cancer', *Proceedings of the National Academy of Sciences of the United States of America,* 102(51), pp. 18538-18543.

Scalfone, L. K., Nel, H. J., Gagliardo, L. F., Cameron, J. L., Al-Shokri, S., Leifer, C. A., Fallon, P. G. and Appleton, J. A. (2013) 'Participation of MyD88 and Interleukin-33 as Innate Drivers of Th2 Immunity to *Trichinella spiralis*', *Infection and Immunity,* 81(4), pp. 1354-1363.

Schipper, H. S., Prakken, B., Kalkhoven, E. and Boes, M. (2012) 'Adipose tissue-resident immune cells: key players in immunometabolism', *Trends Endocrinol Metab,* 23(8), pp. 407-15.

Seehus, C. R., Kadavallore, A., Torre, B. d. l., Yeckes, A. R., Wang, Y., Tang, J. and Kaye, J. (2017) 'Alternative activation generates IL-10 producing type 2 innate lymphoid cells', *Nature Communications,* 8(1), pp. 1900.

Seijkens, T., Kusters, P., Chatzigeorgiou, A., Chavakis, T. and Lutgens, E. (2014) 'Immune cell crosstalk in obesity: a key role for costimulation?', *Diabetes,* 63(12), pp. 3982-91.

Sekiya, A., Suzuki, S., Tanaka, A., Hattori, S., Shimizu, Y., Yoshikawa, N., Koya, Y., Kajiyama, H. and Kikkawa, F. (2019) 'Interleukin33 expression in ovarian cancer and its possible suppression of peritoneal carcinomatosis', *Int J Oncol,* 55(3), pp. 755-765.

Setiawan, T., Metwali, A., Blum, A. M., Ince, M. N., Urban, J. F., Jr., Elliott, D. E. and Weinstock, J. V. (2007) 'Heligmosomoides polygyrus promotes regulatory T-cell cytokine production in the murine normal distal intestine', *Infection and immunity,* 75(9), pp. 4655-4663.

Sher, A., Fiorentino, D., Caspar, P., Pearce, E. and Mosmann, T. (1991) 'Production of IL-10 by CD4+ T lymphocytes correlates with down-regulation of Th1 cytokine synthesis in helminth infection', *The Journal of Immunology,* 147(8), pp. 2713-2716.

Shi, R., Xiang, W., Kang, X., Zhang, L., Wang, J., Miao, H. and He, F. (2019) 'Alteration of Adaptive Immunity in a Colorectal Peritoneal Carcinomatosis Model', *Journal of Cancer,* 10(2), pp. 367-377.

Shuster, A., Patlas, M., Pinthus, J. H. and Mourtzakis, M. (2012) 'The clinical importance of visceral adiposity: a critical review of methods for visceral adipose tissue analysis', *The British journal of radiology,* 85(1009), pp. 1-10.

Siede, J., Fröhlich, A., Datsi, A., Hegazy, A. N., Varga, D. V., Holecska, V., Saito, H., Nakae, S. and Löhning, M. (2016) 'IL-33 Receptor-Expressing Regulatory T Cells Are Highly Activated, Th2 Biased and Suppress CD4 T Cell Proliferation through IL-10 and TGFβ Release', *PloS one,* 11(8), pp. e0161507-e0161507.

Silver, J. S., Kearley, J., Copenhaver, A. M., Sanden, C., Mori, M., Yu, L., Pritchard, G. H., Berlin, A. A., Hunter, C. A., Bowler, R., Erjefalt, J. S., Kolbeck, R. and Humbles, A. A. (2016) 'Inflammatory triggers associated with exacerbations of COPD orchestrate plasticity of group 2 innate lymphoid cells in the lungs', *Nature Immunology,* 17(6), pp. 626-635.

Smith, K. A., Löser, S., Varyani, F., Harcus, Y., McSorley, H. J., McKenzie, A. N. and Maizels, R. M. (2018) 'Concerted IL-25R and IL-4Rα signaling drive innate type 2 effector immunity for optimal helminth expulsion', *Elife,* 7.

Soler, D., Chapman, T. R., Poisson, L. R., Wang, L., Cote-Sierra, J., Ryan, M., McDonald, A., Badola, S., Fedyk, E., Coyle, A. J., Hodge, M. R. and Kolbeck, R. (2006) 'CCR8 Expression Identifies CD4 Memory T Cells Enriched for FOXP3+ Regulatory and Th2 Effector Lymphocytes', *The Journal of Immunology,* 177(10), pp. 6940-6951.

Sorensen, E. W., Gerber, S. A., Sedlacek, A. L., Rybalko, V. Y., Chan, W. M. and Lord, E. M. (2009) 'Omental immune aggregates and tumor metastasis within the peritoneal cavity', *Immunologic research,* 45(2-3), pp. 185-194.

Svetic, A., Madden, K. B., Zhou, X. D., Lu, P., Katona, I. M., Finkelman, F. D., Urban, J. F., Jr. and Gause, W. C. (1993) 'A primary intestinal helminthic infection rapidly induces a gut-associated elevation of Th2-associated cytokines and IL-3', *J Immunol,* 150(8 Pt 1), pp. 3434-41.

Tabuso, M., Homer-Vanniasinkam, S., Adya, R. and Arasaradnam, R. P. (2017) 'Role of tissue microenvironment resident adipocytes in colon cancer', *World journal of gastroenterology,* 23(32), pp. 5829-5835.

Taghavi, M., Mortaz, E., Khosravi, A., Vahedi, G., Folkerts, G., Varahram, M., Kazempour-Dizaji, M., Garssen, J. and Adcock, I. M. (2018) 'Zymosan attenuates melanoma growth progression, increases splenocyte proliferation and induces TLR-2/4 and TNF-α expression in mice', *Journal of Inflammation,* 15(1), pp. 5.

Tait Wojno, E. D. and Beamer, C. A. (2018) 'Isolation and Identification of Innate Lymphoid Cells (ILCs) for Immunotoxicity Testing', *Methods in molecular biology (Clifton, N.J.),* 1803, pp. 353-370.

Tang, C.-L., Liu, Z.-M., Gao, Y. R. and Xiong, F. (2018) 'Schistosoma Infection and Schistosoma-Derived Products Modulate the Immune Responses Associated with Protection against Type 2 Diabetes', *Frontiers in immunology,* 8, pp. 1990-1990.

Tomura, M., Yoshida, N., Tanaka, J., Karasawa, S., Miwa, Y., Miyawaki, A. and Kanagawa, O. (2008) 'Monitoring cellular movement in vivo with photoconvertible fluorescence protein "Kaede" transgenic mice', *Proceedings of the National Academy of Sciences of the United States of America,* 105(31), pp. 10871-10876.

Tong, X., Barbour, M., Hou, K., Gao, C., Cao, S., Zheng, J., Zhao, Y., Mu, R. and Jiang, H.-R. (2016) 'Interleukin-33 predicts poor prognosis and promotes ovarian cancer cell growth and metastasis through regulating ERK and JNK signaling pathways', *Molecular Oncology,* 10(1), pp. 113-125.

Tourniaire, F., Romier-Crouzet, B., Lee, J. H., Marcotorchino, J., Gouranton, E., Salles, J., Malezet, C., Astier, J., Darmon, P., Blouin, E., Walrand, S., Ye, J. and Landrier, J.-F. (2013) 'Chemokine Expression in Inflamed Adipose Tissue Is Mainly Mediated by NF-κB', *PLOS ONE,* 8(6), pp. e66515.

Underhill, D. (2003) 'Macrophage recognition of zymosan particles', *Journal of endotoxin research,* 9, pp. 176-80.

Underhill, D. M. and Ozinsky, A. (2002) 'Toll-like receptors: key mediators of microbe detection', *Current Opinion in Immunology,* 14(1), pp. 103-110.

Urban-Wojciuk, Z., Khan, M. M., Oyler, B. L., Fåhraeus, R., Marek-Trzonkowska, N., Nita-Lazar, A., Hupp, T. R. and Goodlett, D. R. (2019) 'The Role of TLRs in Anti-cancer Immunity and Tumor Rejection', *Frontiers in immunology,* 10, pp. 2388-2388.

Urban, J. F., Jr., Katona, I. M. and Finkelman, F. D. (1991a) 'Heligmosomoides polygyrus: CD4+ but not CD8+ T cells regulate the IgE response and protective immunity in mice', *Exp Parasitol,* 73(4), pp. 500-11.

Urban, J. F., Jr., Katona, I. M., Paul, W. E. and Finkelman, F. D. (1991b) 'Interleukin 4 is important in protective immunity to a gastrointestinal nematode infection in mice', *Proc Natl Acad Sci U S A,* 88(13), pp. 5513-7.

Urban, J. F., Jr., Maliszewski, C. R., Madden, K. B., Katona, I. M. and Finkelman, F. D. (1995) 'IL-4 treatment can cure established gastrointestinal nematode infections in immunocompetent and immunodeficient mice', *J Immunol,* 154(9), pp. 4675-84.

van Beek, L., van Klinken, J. B., Pronk, A. C. M., van Dam, A. D., Dirven, E., Rensen, P. C. N., Koning, F., Willems van Dijk, K. and van Harmelen, V. (2015) 'The limited storage capacity of gonadal adipose tissue directs the development of metabolic disorders in male C57Bl/6J mice', *Diabetologia,* 58(7), pp. 1601-1609.

van de Pavert, S. A., Olivier, B. J., Goverse, G., Vondenhoff, M. F., Greuter, M., Beke, P., Kusser, K., Hopken, U. E., Lipp, M., Niederreither, K., Blomhoff, R., Sitnik, K., Agace, W. W., Randall, T. D., de Jonge, W. J. and Mebius, R. E. (2009) 'Chemokine CXCL13 is essential for lymph node initiation and is induced by retinoic acid and neuronal stimulation', *Nat Immunol,* 10(11), pp. 1193-9.

van der Burg, M. E. (2001) 'Advanced ovarian cancer', *Curr Treat Options Oncol,* 2(2), pp. 109-18.

Van der Jeught, K., Xu, H.-C., Li, Y.-J., Lu, X.-B. and Ji, G. (2018) 'Drug resistance and new therapies in colorectal cancer', *World journal of gastroenterology,* 24(34), pp. 3834-3848.

Vannella, K. M., Ramalingam, T. R., Borthwick, L. A., Barron, L., Hart, K. M., Thompson, R. W., Kindrachuk, K. N., Cheever, A. W., White, S., Budelsky, A. L., Comeau, M. R., Smith, D. E. and Wynn, T. A. (2016) 'Combinatorial targeting of TSLP, IL-25, and IL-33 in type 2 cytokine–driven inflammation and fibrosis', *Science Translational Medicine,* 8(337), pp. 337ra65-337ra65.

Varricchi, G., Galdiero, M. R., Loffredo, S., Lucarini, V., Marone, G., Mattei, F., Marone, G. and Schiavoni, G. (2017) 'Eosinophils: The unsung heroes in cancer?', *Oncoimmunology,* 7(2), pp. e1393134-e1393134.

Venook, A. (2005) 'Critical evaluation of current treatments in metastatic colorectal cancer', *Oncologist,* 10(4), pp. 250-61.

Vergote, I., Tropé, C. G., Amant, F., Kristensen, G. B., Ehlen, T., Johnson, N., Verheijen, R. H. M., van der Burg, M. E. L., Lacave, A. J., Panici, P. B., Kenter, G. G., Casado, A., Mendiola, C., Coens, C., Verleye, L., Stuart, G. C. E., Pecorelli, S. and Reed, N. S. (2010) 'Neoadjuvant Chemotherapy or Primary Surgery in Stage IIIC or IV Ovarian Cancer', *New England Journal of Medicine,* 363(10), pp. 943-953.

Vivier, E., Artis, D., Colonna, M., Diefenbach, A., Di Santo, J. P., Eberl, G., Koyasu, S., Locksley, R. M., McKenzie, A. N. J., Mebius, R. E., Powrie, F. and Spits, H. (2018) 'Innate Lymphoid Cells: 10 Years On', *Cell,* 174(5), pp. 1054-1066.

Vivier, E., van de Pavert, S. A., Cooper, M. D. and Belz, G. T. (2016) 'The evolution of innate lymphoid cells', *Nature Immunology,* 17(7), pp. 790-794.

von Moltke, J., O'Leary, C. E., Barrett, N. A., Kanaoka, Y., Austen, K. F. and Locksley, R. M. (2016) 'Leukotrienes provide an NFAT-dependent signal that synergizes with IL-33 to activate ILC2s', *Journal of Experimental Medicine,* 214(1), pp. 27-37.

Von. Recklinghausen, F. (1863) 'Ueber Eiter- und Bindegewebskörperchen', *Archiv für pathologische Anatomie und Physiologie und für klinische Medicin,* 28(1), pp. 157-197.

Vonarbourg, C., Mortha, A., Bui, V. L., Hernandez, P. P., Kiss, E. A., Hoyler, T., Flach, M., Bengsch, B., Thimme, R., Hölscher, C., Hönig, M., Pannicke, U., Schwarz, K., Ware, C. F., Finke, D. and Diefenbach, A. (2010) 'Regulated Expression of Nuclear Receptor RORγt Confers Distinct Functional Fates to NK Cell Receptor-Expressing RORγt+ Innate Lymphocytes', *Immunity,* 33(5), pp. 736-751.

Wang, M., Zhao, J., Zhang, L., Wei, F., Lian, Y., Wu, Y., Gong, Z., Zhang, S., Zhou, J., Cao, K., Li, X., Xiong, W., Li, G., Zeng, Z. and Guo, C. (2017a) 'Role of tumor microenvironment in tumorigenesis', *Journal of Cancer,* 8(5), pp. 761-773.

Wang, S., Xia, P., Chen, Y., Qu, Y., Xiong, Z., Ye, B., Du, Y., Tian, Y., Yin, Z., Xu, Z. and Fan, Z. (2017b) 'Regulatory Innate Lymphoid Cells Control Innate Intestinal Inflammation', *Cell,* 171(1), pp. 201-216.e18.

Waugh, D. J. J. and Wilson, C. (2008) 'The Interleukin-8 Pathway in Cancer', *Clinical Cancer Research,* 14(21), pp. 6735-6741.

Wei, R., Liu, S., Min, L. and Zhu, S. (2020) 'Cellular and Extracellular Components in Tumor Microenvironment and Their Application in Early Diagnosis of Cancers', *Analytical Cellular Pathology,* 2020, pp. 1-13.

Wen, T. and Rothenberg, M. E. (2016) 'The Regulatory Function of Eosinophils', *Microbiology spectrum,* 4(5), pp. 10.1128/microbiolspec.MCHD-0020-2015.

Wentworth, J. M., Naselli, G., Brown, W. A., Doyle, L., Phipson, B., Smyth, G. K., Wabitsch, M., O'Brien, P. E. and Harrison, L. C. (2010) 'Pro-inflammatory CD11c+CD206+ adipose tissue macrophages are associated with insulin resistance in human obesity', *Diabetes,* 59(7), pp. 1648-56.

Wherry, E. J. and Masopust, D. (2016) 'Chapter 5 - Adaptive Immunity: Neutralizing, Eliminating, and Remembering for the Next Time', in Katze, M.G., Korth, M.J., Law, G.L. & Nathanson, N. (eds.) *Viral Pathogenesis (Third Edition)*. Boston: Academic Press, pp. 57-69.

White, M. P. J., McManus, C. M. and Maizels, R. M. (2020) 'Regulatory T-cells in helminth infection: induction, function and therapeutic potential', *Immunology,* 160(3), pp. 248-260.

Wikström, P., Lissbrant, I., Stattin, P., Egevad, L. and Bergh, A. (2002) *Endoglin (CDI05) is expressed on immature blood vessels and is a marker for survival in prostate cancer.*

Willinger, T. (2019) 'Metabolic Control of Innate Lymphoid Cell Migration', *Frontiers in immunology,* 10, pp. 2010-2010.

Withers, D. R. (2016) 'Innate lymphoid cell regulation of adaptive immunity', *Immunology,* 149(2), pp. 123-130.

Wolf, D., Wolf, A. M., Rumpold, H., Fiegl, H., Zeimet, A. G., Muller-Holzner, E., Deibl, M., Gastl, G., Gunsilius, E. and Marth, C. (2005) 'The Expression of the Regulatory T Cell–Specific Forkhead Box Transcription Factor FoxP3 Is Associated with Poor Prognosis in Ovarian Cancer', *Clinical Cancer Research,* 11(23), pp. 8326-8331.

Wu, G. Y. and Halim, M. H. (2000) 'Schistosomiasis: progress and problems', *World journal of gastroenterology,* 6(1), pp. 12-19.

Wu, J., Boström, P., Sparks, Lauren M., Ye, L., Choi, Jang H., Giang, A.-H., Khandekar, M., Virtanen, Kirsi A., Nuutila, P., Schaart, G., Huang, K., Tu, H., van Marken Lichtenbelt, Wouter D., Hoeks, J., Enerbäck, S., Schrauwen, P. and Spiegelman, Bruce M. (2012) 'Beige Adipocytes Are a Distinct Type of Thermogenic Fat Cell in Mouse and Human', *Cell,* 150(2), pp. 366-376.

Wu, W., Doan, N., Said, J., Karunasiri, D. and Pullarkat, S. T. (2014) 'Strong expression of chemokine receptor CCR9 in diffuse large B-cell lymphoma and follicular lymphoma strongly correlates with gastrointestinal involvement', *Hum Pathol,* 45(7), pp. 1451-8.

Wynn, T. A., Cheever, A. W., Williams, M. E., Hieny, S., Caspar, P., Kühn, R., Müller, W. and Sher, A. (1998) 'IL-10 Regulates Liver Pathology in Acute Murine Schistosomiasis mansoni But Is Not Required for Immune Down-Modulation of Chronic Disease', *The Journal of Immunology,* 160(9), pp. 4473-4480.

Xu, L., Zhu, Y., Chen, L., An, H., Zhang, W., Wang, G., Lin, Z. and Xu, J. (2014) 'Prognostic Value of Diametrically Polarized Tumor-Associated Macrophages in Renal Cell Carcinoma', *Annals of Surgical Oncology,* 21(9), pp. 3142-3150.

Yaghoubi, N., Soltani, A., Ghazvini, K., Hassanian, S. M. and Hashemy, S. I. (2019) 'PD-1/ PD-L1 blockade as a novel treatment for colorectal cancer', *Biomedicine & Pharmacotherapy,* 110, pp. 312-318.

Yanaba, K., Bouaziz, J. D., Haas, K. M., Poe, J. C., Fujimoto, M. and Tedder, T. F. (2008) 'A regulatory B cell subset with a unique CD1dhiCD5+ phenotype controls T cell-dependent inflammatory responses', *Immunity,* 28(5), pp. 639-50.

Yang, Q., Monticelli, Laurel A., Saenz, Steven A., Chi, Anthony W.-S., Sonnenberg, Gregory F., Tang, J., De Obaldia, Maria E., Bailis, W., Bryson, J. L., Toscano, K., Huang, J., Haczku, A., Pear, Warren S., Artis, D. and Bhandoola, A. (2013a) 'T Cell Factor 1 Is Required for Group 2 Innate Lymphoid Cell Generation', *Immunity,* 38(4), pp. 694-704.

Yang, Z., Grinchuk, V., Urban, J. F., Jr., Bohl, J., Sun, R., Notari, L., Yan, S., Ramalingam, T., Keegan, A. D., Wynn, T. A., Shea-Donohue, T. and Zhao, A. (2013b) 'Macrophages as IL-25/IL-33-responsive cells play an important role in the induction of type 2 immunity', *PLoS One,* 8(3), pp. e59441.

Yeung, T.-L., Leung, C. S., Yip, K.-P., Yeung, C. L. A., Wong, S. T. C. and Mok, S. C. (2015) 'Cellular and molecular processes in ovarian cancer metastasis. A Review in the Theme: Cell and Molecular Processes in Cancer Metastasis', *American Journal of Physiology-Cell Physiology,* 309(7), pp. C444-C456.

Yokota, Y., Mansouri, A., Mori, S., Sugawara, S., Adachi, S., Nishikawa, S. and Gruss, P. (1999) 'Development of peripheral lymphoid organs and natural killer cells depends on the helix-loop-helix inhibitor Id2', *Nature,* 397(6721), pp. 702-6.

Young, A. and Rea, D. (2000) 'ABC of colorectal cancer: treatment of advanced disease', *BMJ (Clinical research ed.),* 321(7271), pp. 1278-1281.

Zaiss, M. M., Maslowski, K. M., Mosconi, I., Guenat, N., Marsland, B. J. and Harris, N. L. (2013) 'IL-1β Suppresses Innate IL-25 and IL-33 Production and Maintains Helminth Chronicity.', *PLoS Pathog,* 9(8), pp. e1003531.

Zhang, K., Xu, X., Pasha, M. A., Siebel, C. W., Costello, A., Haczku, A., MacNamara, K., Liang, T., Zhu, J., Bhandoola, A., Maillard, I. and Yang, Q. (2017a) 'Cutting Edge: Notch Signaling Promotes the Plasticity of Group-2 Innate Lymphoid Cells', *The Journal of Immunology,* 198(5), pp. 1798-1803.

Zhang, M., He, Y., Sun, X., Li, Q., Wang, W., Zhao, A. and Di, W. (2014) 'A high M1/M2 ratio of tumor-associated macrophages is associated with extended survival in ovarian cancer patients', *Journal of Ovarian Research,* 7(1), pp. 19.

Zhang, Y., Davis, C., Shah, S., Hughes, D., Ryan, J. C., Altomare, D. and Peña, M. M. O. (2017b) 'IL-33 promotes growth and liver metastasis of colorectal cancer in mice by remodeling the tumor microenvironment and inducing angiogenesis', *Molecular Carcinogenesis,* 56(1), pp. 272-287.

Zhu, Z., Zhang, X., Guo, H., Fu, L., Pan, G. and Sun, Y. (2014) *CXCL13-CXCR5 axis promotes the growth and invasion of colon cancer cells via PI3K/AKT pathway.*